年 報
2017

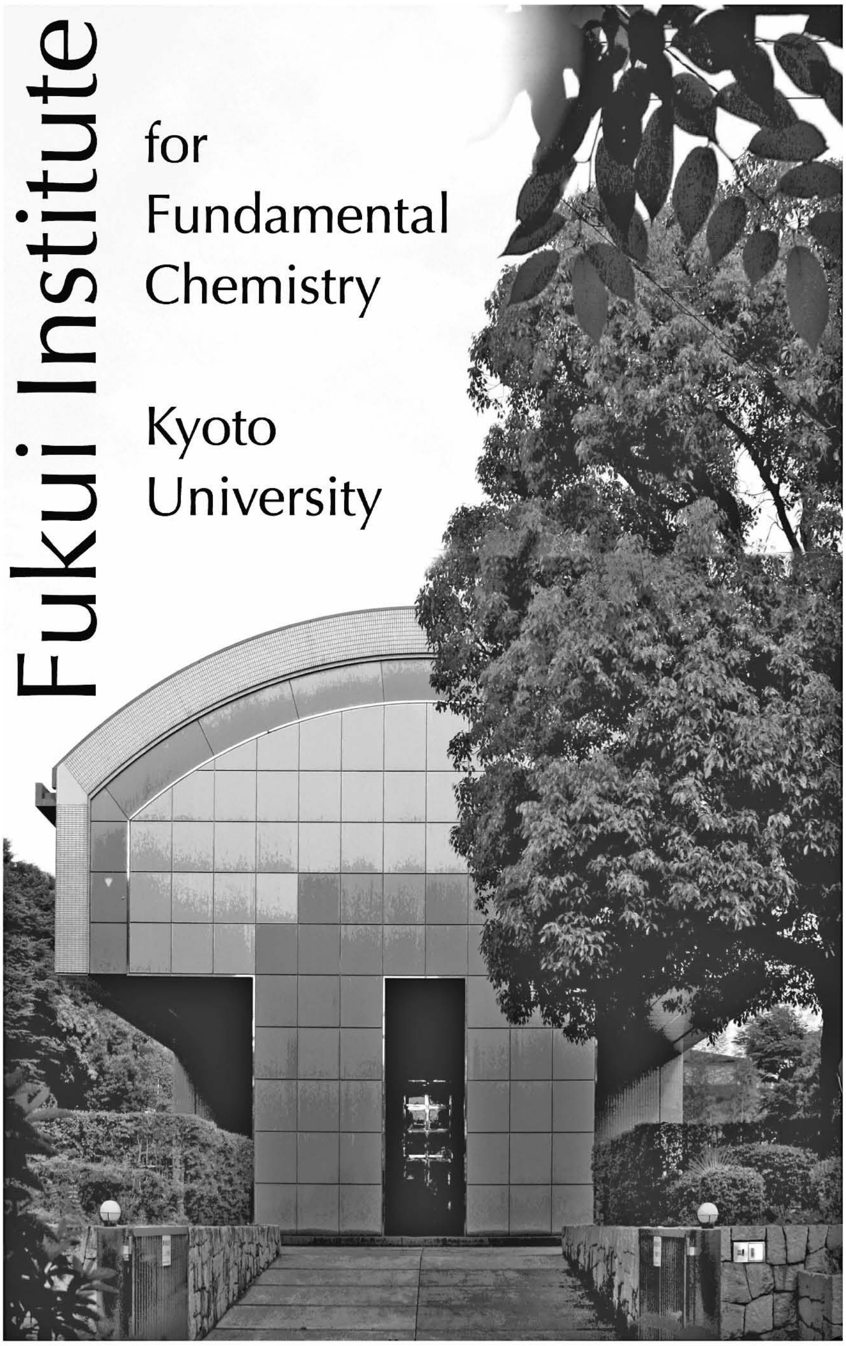

京都大学
福井謙一記念研究センター

はじめに

2017年度の京都大学福井謙一記念研究センターの活動をまとめた年報をお届けします。本センターは、京都大学本部構内の北、約1キロの高野川沿いの静かな住宅街に独立して位置しております。専任教員は理論研究部門と総合研究部門に1名ずつを持っているに過ぎませんが、センター長のほか副センター長とスーパーバイザーとして工学研究科、理学研究科、化学研究所所属の12名の教員にご協力頂いており、このメンバーが運営委員会を構成しています。そして優れた博士研究員に研究活動の機会を与える制度を持っており、若手研究者が国際的な雰囲気の中で日夜研究にいそしんでいます。福井センターフェローと呼ばれる博士研究員はセンターの雇用で、自分自身のアイデアで一定期間、自由闊達に研究できる身分を保証しています。

2017年度は本センターにとりまして大きな出来事がありました。2017年11月27日、FIFCリサーチフェローとしてご活躍であった諸熊奎治先生（分子科学研究所名誉教授）が、83年間の研究者人生を全うされました。本センターでは、2006年9月に福井謙一記念研究部第一のリサーチリーダーとして諸熊奎治先生を米国エモリー大学から招聘しました。諸熊先生は、2012年にシニアリサーチフェローに就任され、この年の11月には、複雑分子系の理論研究の発展に多大な貢献をしたとして、文化功労者の顕彰を受けられました。また、2015年からはFIFCリサーチフェローとして研究ならびに若手人材育成にご尽力頂き、逝去されるほぼ3週間前まで、活発な研究活動を展開してこられました。諸熊先生は理論化学・計算化学の領域で多くの学術的業績を挙げられるとともに、我が国の量子化学の分野を牽引され、多数の研究者を育成されました。謹んでご冥福をお祈り申し上げます。

本センターでは、上記の諸熊奎治先生の招聘ののち、2009年度に福井謙一記念研究部第二を設置し、名古屋大学名誉教授（前副学長）の大峯巖先生をリサーチリーダーとして招聘し、研究体制を拡大しました。なお、大峯先生は2010年4月に分子科学研究所長に転出されました。その後任として、2011年4月に京都大学物質—細胞統合システム拠点（iCeMS）特任教授の榊　茂好先生を研究部第二のリサーチリーダーとして招聘しました。榊先生は、遷移金属化合物や類縁化合物に関する研究で顕著な業績を挙げておられ、現在はd電子複合系の理論化学に関する研究を推進しておられます。

2012年にはシニアリサーチフェローとして永瀬茂先生（分子科学研究所名誉教授）を招聘しました。永瀬先生は、望む構造、物性、機能を持つ分子を自在に組み立てて思うように反応させる理論と計算およびコンピューター

シミュレーションの開発において顕著な業績を挙げられました。2015年からはFIFCリサーチフェローとして高周期典型元素と遷移金属元素化学種の理論化学に関する研究を進めておられます。同じ年に、シニアリサーチフェローとして田中一義先生（京都大学名誉教授）を招聘しました。田中一義先生は導電性や磁性を有する有機化合物など量子機能材料に関する物理化学的研究において優れた多くの業績を挙げておられ、現在は元素ブロックを有する分子・高分子の理論化学に関する研究を展開されています。さらに、2016年には、化学反応電子動力学の基礎理論研究において著名な高塚和夫先生（東京大学名誉教授）をリサーチリーダーとして招聘しました。センターでは非断熱電子動力学理論による化学反応の解析に関する研究を推進しておられます。

2018年2月には理論研究部門の専任教授として、佐藤徹先生が着任されました。佐藤徹先生は振電相互作用に関する研究、特に動的ヤーンテラー効果や振電相互作用を解析・制御する振電相互作用密度を用いた有機EL素子などの機能性分子材料の理論設計を行っています。佐藤徹先生の研究室は、工学研究科分子工学専攻の協力講座（分子材料科学講座　電子物性化学分野）としても位置付けられ、大学院生、学部4回生が配属されて、研究を進めています。

私達は、センターが若手研究者の登竜門となることを期待しています。実際に、センターの博士研究員であった多くの方々が、現在、国内外の大学、研究機関で活躍しておられます。2016年には、化学の将来の発展のために若手研究者の育成の大切さを説いておられた福井博士の遺志を汲み、基礎化学・理論化学の分野で顕著な研究業績を挙げた若手研究者を顕彰する「福井謙一奨励賞」を創設しました。2017年は、第2回福井謙一奨励賞が、「第一原理波動関数理論の固体への展開：量子化学と固体電子論の融合」に関する成果が評価された大阪大学大学院理学研究科の越智正之博士に授与されました。

当センターの歴史を簡単にご紹介します。ご承知のように故福井謙一京都大学名誉教授はフロンティア軌道理論を提案したご功績により、1981年にわが国で最初のノーベル化学賞を受賞されました。福井先生が京都大学ご退官後に研究を続けられるため、京都市と産業界などのご支援で1985年に財団法人「基礎化学研究所」が設立されました。専任研究員数名の規模でしたが、研究のレベルは高く、当時の研究員は、東京大学、名古屋大学、分子科学研究所の教授になるなど、理論化学分野でトップクラスの研究者として活躍しています。この基礎化学研究所は1998年の福井先生のご逝去の後、2002年に本学に寄贈され、福井謙一記念研究センターとなり、現在に至っております。京都大学の部局となった後、森島　績、中辻　博、榊　茂好、田中　功、田中一義、

赤木和夫の各先生にセンター長としてご指導を頂きました。

本センターは、国際活動も活発で、2005年よりチェコおよびスロバキアと理論化学・計算化学シンポジウムを定期的に開催しております。2011年には国内外（主にドイツ、東欧、中国、韓国）から第一線の研究者を招き、第1回福井センター理論化学・計算化学国際シンポジウムを開催しました。こうした国際連携活動をさらに活性化するという観点から、2016年2月に国際学術連携研究室（2016年12月に国際連携インターディシプリナリー研究推進室と改組）を設置し、その運営上必要となるコーディネーター役として、特定助教1名を配置しました。本センターは、今後も、理論化学・計算化学分野におけるわが国の研究拠点の役割を果たし、国際連携活動を展開して行きたいと考えております。

また、例年初冬に福井センターシンポジウムを開催しており、国内外のトップクラスの研究者による特別講演、運営委員の講演、並びに京都大学内外からのポスター発表を行っております。研究発表のレベルは高く、特別講演に来られた講師からも毎年高い評価を得ております。

さらに社会貢献活動の一環として、2011年が福井先生のノーベル化学賞受賞30周年にあたるため、これを節目として本センター玄関ロビーに先生ゆかりの文物の展示コーナーを設置しました。コーナーでは先生が使用された机、椅子、ノーベル賞メダル・賞状（複製）、研究ノート・メモ、写真などを展示し、常設展示として一般に公開しています。

加えて、福井謙一先生の生誕百年にあたる2018年に開催のメモリアルシンポジウム、記念式典、サテライトシンポジウム、京大総合博物館での記念展に向けて、2017年には福井謙一生誕百年記念事業実施委員会を中心に準備を進めました。

本センターは、上述のように規模は大きくありませんが、研究活動は極めて活発です。今後も、京都大学あるいは国内外との共同研究を積極的に進めて行きたいと考えております。とくに実験科学者との共同研究は重要であり、そのような連携研究をさらに活発化したいと考えております。

この年報により、本センターの活動に興味をお持ち頂ければ幸甚です。そして、それが共同研究の契機となり、時間をかけて大きな成果に結実していくことを念願しています。最後になりましたが、本センターの順調な活動はひとえに工学研究科、理学研究科、化学研究所のご協力、ご援助の賜物であり、ここに心から御礼申し上げる次第です。

2019年2月

京都大学福井謙一記念研究センター長

田中勝久

目　　次

Ⅰ　専任教員・スーパーバイザー

Ⅱ　博士研究員等

Ⅲ　研究広報活動

Ⅳ　研究業績

Ⅴ　資料

（本冊子は下記アドレス(URL)にて、ウェブ上でも閲覧いただけます。
http://www.fukui.kyoto-u.ac.jp/wp-content/themes/fifc/pdf/AnnualReport2017.pdf）

Ⅰ　専任教員・スーパーバイザー

１．教員組織

平成２９年度

職名		氏名	備考
センター長		田中 勝久	工学研究科材料化学専攻
副センター長		谷村 吉隆	理学研究科化学専攻
副センター長		佐藤 啓文	工学研究科分子工学専攻
副センター長		(欠員中)	
協議員	工学研究科長	北村 隆行	工学研究科機械理工学専攻
	理学研究科長	平野 丈夫	理学研究科生物科学専攻
	化学研究所長	時任 宣博	化学研究所物質創製化学研究系
総合研究部門 スーパーバイザー	教授	古賀 毅	工学研究科高分子化学専攻
	教授	跡見 晴幸	工学研究科合成・生物化学専攻
	教授	佐々 真一	理学研究科物理学・宇宙物理学専攻
	教授	山本 潤	理学研究科物理学・宇宙物理学専攻
	教授	渡辺 宏	化学研究所分子レオロジー
理論研究部門 スーパーバイザー	教授	田中 功	工学研究科材料工学専攻
	教授	田中 庸裕	工学研究科分子工学専攻
	教授	山本 量一	工学研究科化学工学専攻
	教授	高田 彰二	理学研究科生物科学専攻
	教授	林 重彦	理学研究科化学専攻
総合研究部門	准教授	(欠員中)	
理論研究部門	教授	佐藤 徹	専任：平成 30. 2. 1 － (工学研究科分子工学専攻協力講座)
国際連携インターディシプリナリー研究推進室	特定助教	西本 佳央	専任
諸熊グループ	FIFC リサーチフェロー	諸熊 奎治	研究員
永瀬グループ	FIFC リサーチフェロー	永瀬 茂	研究員
榊グループ	シニアリサーチフェロー	榊 茂好	研究員
田中グループ	シニアリサーチフェロー	田中 一義	研究員
高塚グループ	リサーチリーダー	高塚 和夫	研究員
榊グループ	研究員	北浦 和夫	研究員

２．教員プロフィール

(1) センター長

【氏名】	田中 勝久 （たなか かつひさ）
【職名】	教授
【所属】	工学研究科 材料化学専攻
【研究室】	桂キャンパス A3 クラスター 018
【直通電話】	075-383-2801
【FAX】	075-383-2420
【電子メールアドレス】	tanaka@dipole7.kuic.kyoto-u.ac.jp
【ホームページ】	http://dipole7.kuic.kyoto-u.ac.jp/
【研究分野】	無機固体化学
【現在の研究課題】	新規酸化物固体の合成と磁気的・誘電的・光学的性質
【研究内容キーワード】	酸化物、磁気的性質、誘電的性質、光学的性質
【学歴】	1984年3月 京都大学工学部工業化学科卒業 1986年3月 京都大学大学院工学研究科工業化学専攻修士課程修了
【学位】	1991年3月 京都大学工学博士
【略歴】	1986年4月 三重大学工学部助手 1989年4月 京都大学工学部助手 1999年7月 京都工芸繊維大学工芸学部助教授 2004年4月 京都大学大学院工学研究科教授
【所属学会】	日本セラミックス協会、日本化学会、応用物理学会、日本物理学会、粉体粉末冶金協会、日本材料学会、日本金属学会、Materials Research Society、Optical Society of America
【学会活動】	日本セラミックス協会理事、粉体粉末冶金協会理事
【主な著書、学術論文】 （過去5年以内）	1. H. Akamatsu, K. Fujita, T. Kuge, A. S. Gupta, A. Togo, S. Lei, F. Xue, G. Stone, J. M Rondinelli, L. Chen, I. Tanaka, V. Gopalan, and K. Tanaka, “Inversion symmetry breaking by oxygen octahedral rotations in Ruddlesden-Popper $NaRETiO_4$ family”, *Physical Review Letters* **112** (2014) 187602-1-5. 2. M. Nishijima, T. Ootani, Y. Kamimura, T. Sueki, S. Esaki, S. Murai, K. Fujita, K. Tanaka, K. Ohira, Y. Koyama, and I. Tanaka, “Accelerated discovery of cathode materials with prolonged cycle life for lithium-ion battery”, *Nature Communications* **5** (2014) 4553-1-7. 3. T. Kawamoto, K. Fujita, I. Yamada, T. Matoba, S. J. Kim, P. Gao, X. Pan, S. D. Findlay, C. Tassel, H. Kageyama, A. J. Studer, J. Hester, T. Irifune, H. Akamatsu, and K. Tanaka, “Room-temperature polar ferromagnet $ScFeO_3$ transformed from a high-pressure orthorhombic perovskite phase”, *Journal of the American Chemical Society* **136** (2014) 15291-15299. 4. T. Yajima, F. Takeiri, K. Aidzu, H. Akamatsu, K. Fujita, M. Ohkura, W. Yoshimune, S. Lei, V. Gopalan, K. Tanaka, C. M. Brown, M. A. Green, T. Yamamoto, Y.i Kobayashi, and H. Kageyama, “A labile hydride strategy to synthesize heavily nitridized $BaTiO_3$”, *Nature Chemistry* **7** (2015) 1017-1023. 5. K. Fujita, T. Kawamoto, I. Yamada, O. Hernandez, N. Hayashi, H. Akamatsu, W. Lafargue-Dit-Hauret, X. Rocquefelte, M. Fukuzumi, P. Manuel, A. J. Studer, C. Knee, and K. Tanaka, “$LiNbO_3$-type $InFeO_3$: Room-temperature polar magnet without second-order Jahn-Teller active ions”, *Chemistry of Materials* **28** (2016) 6644-6655. 6. Y. Nakatsuka, K. Pollok, T. Wieduwilt, F. Langenhorst, M. A. Schmidt, K. Fujita, S. Murai, K. Tanaka, and L. Wondraczek, “Giant Faraday rotation through Fe^{0}_{n} states in superparamagnetic FeO-SiO_2 vitreous films”, *Advanced Science* (2017) 1600299-1-6. 7. T. Sawai, Y. Yamaguchi, N. Kitamura, T. Date, S. Konishi, K. Taga, and K. Tanaka, “Pulse-based electron spin transient nutation measurement of $BaTiO_3$ fine particle: Identification of controversial signal around g=2.00”, *Applied Physics Letters* **112** (2018) 202902-1-4.
【学術関係の受賞など】	The Australasian Ceramic Society/Ceramic Society of Japan (ACS/CJS) Joint Ceramic Award（1997年）、日本セラミックス協会学術賞（2005年）、Award of the Outstanding Papers Published in the JCerSJ in 2013（2013年）

⑵ 副センター長

【氏名】	谷村　吉隆　(たにむら　よしたか)
【職名】	教授
【所属】	京都大学大学院理学研究科化学専攻
【研究室】	京都大学理学部 6 号館北棟 256 号室
【直通電話】	075-753-4017
【FAX】	075-753-4018
【電子メールアドレス】	tanimura@kuchem.kyoto-u.ac.jp
【ホームページ】	http://theochem.kuchem.kyoto-u.ac.jp
【研究分野】	化学物理理論
【現在の研究課題】	非線形光学応答
【研究内容キーワード】	統計物理学
【最終学歴】	1989 年 3 月　慶應義塾大学物理学専攻博士課程修了
【学位】	1989 年 3 月　博士号取得（慶応義塾大学）
【略歴】	1994 年 4 月　分子科学研究所理論研究系　助教授 総合研究大学院数物化学研究科　助教授（併任） 1998 年 4 月　京都大学大学院理学研究科　助教授（併任） 2003 年 6 月　京都大学大学院理学研究科　教授
【在外研究歴】	1989 年 6 月　イリノイ大学・シャンペン校　ベックマン研究所・研究員 1991 年 9 月　ロチェスター大学化学科　博士研究員
【所属学会】	日本物理学会、日本化学会、分子科学会、アメリカ化学会、アメリカ物理学会
【主な著書、学術論文】（過去 5 年以内）	1. Y. Tanimura, Real-Time and Imaginary-Time Quantum Hierarchal Fokker-Planck Equations, *J. Chem, Phys* **142**, 144110 [20 pages](2015). 2. H. Ito and Y. Tanimura, Simulating two-dimensional infrared-Raman and Raman spectroscopies for intermolecular and intramolecular modes of liquid water, *J. Chem. Phys.* **144** 074201 [16 pages] (2016). [JCP Editors’ Picks] 3. A. Kato and Y. Tanimura, Quantum Heat Current under Non-perturbative and Non-Markovian Conditions: Applications to Heat Machines, *J. Chem. Phys.* **145**, 224105 (2016) [JCP Editors’ Picks] 4. K. Nakamura and Y. Tanimura, Hierarchical Schrödinger Equations of Motion for Open Quantum Dynamic, *Phys. Rev. A* **98**, 012109 (2018) 5. Y. Iwamoto and Y. Tanimura, Linear Absorption Spectrum of a Quantum Two-Dimensional Rotator Calculated using a Rotationally Invariant System-Bath Hamiltonian, *J. Chem. Phys.* **149**, 084110 [8 page] (2018)
【学術関係の受賞など】	2002 年　分子科学研究奨励森野基金 2012 年　フンボルト賞（ドイツ） 2015 年　アメリカ物理学会フェロー

【氏名】	佐藤　啓文（さとう　ひろふみ）
【職名】	教授
【所属】	工学研究科分子工学専攻
【研究室】	A4 棟 026
【直通電話】	075-383-2548
【FAX】	075-383-2799
【電子メールアドレス】	hirofumi@moleng.kyoto-u.ac.jp
【ホームページ】	http://www.riron.moleng.kyoto-u.ac.jp/
【研究分野】	理論化学・量子化学・統計力学
【現在の研究課題】	理論化学・物理化学
【研究内容キーワード】	化学反応・自己集合・溶媒和
【学歴】	1996 年 5 月 京都大学理学研究科化学専攻博士後期課程修了
【学位】	1996 年 5 月 京都大学博士（理学）
【略歴】	1996 年 8 月 岡崎国立共同研究機構分子科学研究所助手、2002 年 5 月京都大学工学研究科講師、2004 年 5 月京都大学工学研究科助教授、2010 年 7 月京都大学工学研究科教授
【在外研究歴】	2004 年 6 月－2004 年 12 月 連合王国 Oxford 大学 PTCL 訪問研究員（Paul A. Madden 教授）
【所属学会】	日本化学会、分子科学会、理論化学研究会、溶液化学研究会、イオン液体研究会–
【学会活動】	日本化学会　理論化学・情報化学・計算化学ディビジョン幹事（2011 年–）、副主査（2015 年–） 理論化学研究会　第三期世話人（2009 年－2018 年） 分子科学会　幹事（2012 年－2013 年）、運営委員（2012 年－2016 年，2018 年–） 溶液化学研究会　運営委員（2015 年–）
【主な著書、学術論文】 （過去 5 年以内）	1. Yoshihiro Matsumura, Satoru Iuchi, Shuichi Hiraoka, and Hirofumi Sato, “Chiral effects on the final step of an octahedron-shaped coordination capsule self-assembly” *Phys. Chem. Chem. Phys.,* **20**, 7383-7386 (2018). 2. Hisashi Okumura, Masahiro Higashi, Yuichiro Yoshida, Hirofumi Sato, and Ryo Akiyama, “Theoretical approaches for dynamical ordering of biomolecular systems” *BBA General Subject,* **1862**, 212-228 (2018). 3. Maxim Shishkin, Shinichi Kumakura, Syuhei Sato, Kei Kubota, Shinichi Komaba, and Hirofumi Sato, “Unraveling the Role of Doping in Selective Stabilization of $NaMnO_2$ Polymorphs: Combined Theoretical and Experimental Study” *Chem. Materials,* **30**, 1257 (2018). 4. Kento Kasahara and Hirofumi Sato, “Dynamics theory for molecular liquids based on an interaction site model” *Phys. Chem. Chem. Phys.* **19**, 27917-27929 (2017). 5. Hirofumi Sato, “A modern solvation theory: quantum chemistry and statistical chemistry” *Phys. Chem. Chem. Phys.* **15**(20), 7450-7465 (2013).
【学術関係の受賞など】	日本化学会・進歩賞（2002年） 分子構造総合討論会奨励賞（2006年） 公益信託分子科学研究奨励森野基金（2008年） 溶液化学研究会学術賞（2009年）

⑶ スーパーバイザー

【氏名】	古賀　毅（こが　つよし）
【職名】	教授
【所属】	工学研究科　高分子化学専攻
【研究室】	桂キャンパス　A3 棟 115 号室
【直通電話】	075-383-2705
【FAX】	075-383-2706
【電子メールアドレス】	tkoga@phys.polym.kyoto-u.ac.jp
【ホームページ】	http://www.phys.polym.kyoto-u.ac.jp
【研究分野】	高分子系の統計力学・計算科学
【現在の研究課題】	高分子系の構造形成とダイナミクス
【研究内容キーワード】	高分子・ゲル・レオロジー
【学歴】	1993 年 3 月九州大学大学院理学研究科物理学専攻博士後期課程修了
【学位】	1993 年 3 月九州大学博士（理学）
【略歴】	1993 年 4 月日本学術振興会特別研究員，1994 年 4 月新技術事業団 ERATO 橋本相分離構造プロジェクト研究員，1998 年 5 月京都大学工学研究科助手，2009 年 4 月京都大学工学研究科准教授，2012 年 8 月京都大学工学研究科教授
【所属学会】	高分子学会，日本レオロジー学会，The American Chemical Society
【学会活動】	2016.6-2018.5: 高分子学会理事 2014.5- 現在 : 高分子学会関西支部常任幹事
【主な著書、学術論文】 （過去 5 年以内）	1. Theoretical study of inclusion complex formation of cyclodextrin and single polymer chain, T. Furuya, T. Koga, *POLYMER*, **131**, 193-201 (2017) 2. Physical gelation of supramolecular hydrogels cross-linked by metal-ligand interactions: Dynamic light scattering and microrheological studies, H. Ozaki, T. Indei, T. Koga, T. Narita, *POLYMER*, **128**, 363-372 (2017) 3. Network Formation and Mechanical Properties of Telechelic Associating Polymers with Fixed Junction Multiplicity, H. Ozaki, T. Koga, *MACROMOLECULAR THEORY AND SIMULATIONS*, **26**, 1600076 (2017) 4. Statistical Thermodynamic Theory of Heat-Induced Gelation of Aqueous Methylated Polyrotaxane Solutions, H. Kojima, T. Koga, *MACROMOLECULES*, **49**, 7015-7024 (2016) 5. Theoretical Study of Network Formation and Mechanical Properties of Physical Gels with a Well-Defined Junction Structure, H. Ozaki, T. Koga, *JOURNAL OF PHYSICAL CHEMISTRY B*, **120**, 7745-7753 (2016)

【氏名】	跡見　晴幸　（あとみ　はるゆき）
【職名】	教授
【所属】	工学研究科　合成・生物化学専攻
【研究室】	桂キャンパス A4 棟 217 号室
【直通電話】	075-383-2777
【FAX】	075-383-2778
【電子メールアドレス】	atomi@sbchem.kyoto-u.ac.jp
【ホームページ】	http://www.sbchem.kyoto-u.ac.jp/atomi-lab/en/
【研究分野】	応用微生物学･応用生物化学、基礎ゲノム科学、生体関連化学、生物･生体工学、生物系、構造生物化学
【現在の研究課題】	アーキアや極限環境微生物の代謝生理
【研究内容キーワード】	微生物、微生物代謝、生合成、アーキア、極限環境微生物、ゲノム、超好熱菌、炭酸固定、遺伝子発現制御、合成生物学
【最終学歴】	1992 年 3 月京都大学大学院工学研究科工業化学専攻博士課程単位認定退学
【学位】	1992 年 3 月工学博士（京都大学）
【略歴】	1992 年 4 月京都大学工学部工業化学科助手、1997 年 5 月京都大学大学院工学研究科合成･生物化学専攻助教授､2009 年 3 月京都大学大学院工学研究科合成･生物化学専攻教授
【在外研究歴】	1994 年 4 月 ~1995 年 9 月ドイツ Stuttgart 大学　博士研究員
【所属学会】	生物工学会、日本化学会、農芸化学会、ゲノム微生物学会、環境バイオテクノロジー学会、極限環境生物学会、生化学会、酵素工学研究会、バイオインダストリー協会、分子生物学会、マリンバイオテクノロジー学会、日本アーキア研究会、International Society for Extremophiles、American Society for Microbiology
【学会活動】	酵素工学研究会 会長、日本化学会バイオテクノロジー部会 部会長、 日本生物工学会 理事、ゲノム微生物学会 評議員、環境バイオテクノロジー学会 理事、日本アーキア研究会 幹事、極限環境生物学会 幹事 International Society for Extremophiles　Vice-president
【主な著書、学術論文】（過去 5 年以内）	1. Nagata R, Fujihashi M, Sato T, Atomi H, Miki K. “Identification of a pyrophosphate-dependent kinase and its donor selectivity determinants”, *Nature Commun*. **9**, 1765, (2018). 2. Nunoura T, Chikaraishi Y, Izaki R, Suwa T, Sato T, Harada T, Mori K, Kato Y, Miyazaki M, Shimamura S, Yanagawa K, Shuto A, Ohkouchi N, Fujita N, Takaki Y, Atomi H, Takai K. “A primordial and reversible TCA cycle in a facultatively chemolithoautotrophic thermophile”, *Science* **359**, 559-563, (2018). 3. Zheng RC, Hachisuka SI, Tomita H, Imanaka T, Zheng YG, Nishiyama M, Atomi H. “An ornithine *ω*-aminotransferase required for growth in the absence of exogenous proline in the archaeon Thermococcus kodakarensis”. *J. Biol. Chem*. **293**, 3625-3636, (2018). 4. Makino Y, Sato T, Kawamura H, Hachisuka SI, Takeno R, Imanaka T, Atomi H. “An archaeal ADP-dependent serine kinase involved in cysteine biosynthesis and serine metabolism”, *Nature Commun*. **7**, 13446, (2016). 5. Aono R, Sato T, Imanaka T, Atomi H. “A pentose bisphosphate pathway for nucleoside degradation in Archaea”, *Nature Chem. Biol*. **11**(5):355-360, 2015. 6. Watanabe S, Kawashima T, Nishitani Y, Kanai T, Wada T, Inaba K, Atomi H, Imanaka T, Miki K. “Structural basis of a Ni acquisition cycle for [NiFe] hydrogenase by Ni-metallochaperone HypA and its enhancer”. *Proc. Natl. Acad. Sci. USA* **112**(25), 7701-7706, (2015). 7. Tominaga T, Watanabe S, Matsumi R, Atomi H, Imanaka T, Miki K. “Crystal structures of the carbamoylated and cyanated forms of HypE for [NiFe] hydrogenase maturation”. *Proc. Natl. Acad. Sci. USA*. **110**, 20485-20490, (2013).
【学術関係の受賞など】	極限環境微生物学会　研究奨励賞（2004年）

【氏名】	佐々　真一　（ささ　しんいち）
【職名】	教授
【所属】	京都大学　大学院理学研究科　物理学宇宙物理学専攻
【研究室】	理学部5号館　424号室
【直通電話】	075-753-3743
【FAX】	075-753-3819
【電子メールアドレス】	sasa@scphys.kyoto-u.ac.jp
【ホームページ】	http://www.ton.scphys.kyoto-u.ac.jp/nonlinear/sasa/member_j.html
【研究分野】	統計物理学
【現在の研究課題】	マクロダイナミクスの創発
【研究内容キーワード】	エントロピー、ダイナミクス、統計力学
【学歴】	1991年3月 京都大学大学院理学研究科博士後期課程物理学第一専攻修了
【学位】	1991年3月 理学博士　（京都大学）
【略歴】	1991年4月 京都大学理学部助手、1994年8月 東京大学大学院総合文化研究科助教授、2007年4月 東京大学大学院総合文化研究科准教授、2009年4月 東京大学大学院総合研究科教授、2012年11月 京都大学大学院理学研究科教授
【在外研究歴】	1995.9- 1996.8 米国イリノイ大学　客員研究准教授
【所属学会】	日本物理学会
【学会活動】	2017.4-2018.3 日本物理学会領域11代表
【主な著書、学術論文】（過去5年以内）	1. Liquid-gas transitions in steady heat conduction, Naoko Nakagawa, Shin-ichi Sasa, *Phys. Rev. Lett.* **119**, 260602/1-6(2017) 2. Thermodynamic entropy as a Noether invariant, S.-I. Sasa, Yuki Yokokura, *Phys. Rev. Lett* **116** 140601/1-140601/6（2016） 3. Replica symmetry breaking in trajectories of a driven Brownian particle, Masahiko Ueda, S.-I. Sasa, *Phys. Rev. Lett* **115** 080605/1-080605/5（2015） 4. Derivation of Hydrodynamics from the Hamiltonian Description of Particle Systems, S.-I. Sasa, *Phys. Rev. Lett* **112** 100602/1-100602/5（2014） 5. Computation of large deviation statistics via iterative measurement-and-feedback procedure, T. Nemoto, S.-I. Sasa, *Phys. Rev. Lett* **112** 090602/1-090602/5（2014）

【氏名】	山本　潤　（やまもと　じゅん）
【職名】	教授
【所属】	大学院理学研究科　物理学・宇宙物理学専攻
【研究室】	理学研究科 5 号館 218 号室
【直通電話】	075-753-3788
【FAX】	075-753-3788
【電子メールアドレス】	junyama@scphys.kyoto-u.ac.jp
【ホームページ】	http://softmatter.scphys.kyoto-u.ac.jp/
【研究分野】	ソフトマター物理学
【現在の研究課題】	超界面とソフトマター
【研究内容キーワード】	ダイナミクス、揺らぎ、粘弾性
【学歴】	1987 年 7 月東京大学大学院工学系研究科物理工学専攻博士課程中退
【学位】	1990 年 6 月工学博士（東京大学）
【略歴】	1987 年 8 月東京大学工学部物理工学科助手、1991 年 6 月東京大学生産技術研究所助手、1999 年 10 月 ERATO 横山液晶微界面プロジェクト GL、2005 年 8 月京都大学大学院理学研究科教授
【所属学会】	日本物理学会、日本液晶学会
【学会活動】	2015 年日本物理学会京都支部長、2014~2016 年日本液晶学会財務理事
【学会活動】	2015.5-2017.5: 日本レオロジー学会 会長 2016.8-2020.8: President, The International Committee on Rheology 2011.3- 現在 : Associate Editor of Macromolecules (ACS)
【主な著書、学術論文】（過去 5 年以内）	1. K. Hata, Y. Takanishi, I. Nishiyama and J. Yamamoto, Softening of twist elasticity in the swollen smectic C liquid crystal, *Euro. Phys. Lett.* **120**, 56001(5P) (2017). 2. S. Bono, Y. Takanishi and J. Yamamoto, Effects of layer order on the mobility of mesogenic molecules in SmA liquid-crystalline emulsions, *Europhys. Lett.,* **113**, 56004 (5P) (2016). 3. E. Gorecka, N. Vaupotič, A. Zep, D. Pociecha, J. Yoshioka, J. Yamamoto, and H. Takezoe, A Twist-Bend Nematic (NTB)Phase of Chiral Materials, *Angew. Chem.* **127**, (2015) 10293 –10297. 4. Y. Kimoto, A. Nishizawa, Y. Takanishi, A. Yoshizawa and J. Yamamoto, Layer modulated smectic-C phase in liquid crystals with a terminal hydroxyl group, *Phys. Rev. E,* **89**, 042503 (2014). 5. Y. Uchida, Y. Takanishi and J. Yamamoto, Controlled Fabrication and Photonic Structure of Cholesteric Liquid Crystalline Shells, *Adv. Mat.,* **25** (2013) 3234-3237.
【学術関係の受賞など】	2015 年日本液晶学会業績賞

【氏名】	渡辺　宏　（わたなべ　ひろし）
【職名】	教授
【所属】	京都大学化学研究所
【研究室】	化学研究所本館 N542-C
【直通電話】	0774-38-3135
【FAX】	0774-38-3139
【電子メールアドレス】	hiroshi@scl.kyoto-u.ac.jp
【ホームページ】	http://rheology.minority.jp/jp/
【研究分野】	分子レオロジー
【現在の研究課題】	高分子ダイナミクス
【研究内容キーワード】	絡み合い，動的不均一性，粗視化
【最終学歴】	1985. 3 月 大阪大学　理学博士
【学位】	阪大理博
【略歴】	1983.4-1994.7: 大阪大学理学研究科　助手 1994.8-2002.12: 京都大学化学研究所　助教授 2003.1: 京都大学化学研究所　教授
【在外研究歴】	1987.4-1989.3: 米国 Minnesota 大学化学工学科　博士研究員
【所属学会】	日本レオロジー学会 ; The Society of Rheology (USA); The Korean Society of Rheology; The American Chemical Society; The American Physical Society
【学会活動】	2015.5-2017.5: 日本レオロジー学会 会長 2016.8-2020.8: President, The International Committee on Rheology 2011.3- 現在 : Associate Editor of Macromolecules (ACS)
【主な著書、学術論文】（過去 5 年以内）	1. K. I. S. Mongcopa, M. Tyagi, J. P. Mailoa, G. Samsonidze, B. Kozinsky, S. A. Mullin, D. A. Gribble, H. Watanabe and N. P. Balsara, "Relationship between Segmental Dynamics Measured by Quasi-Elastic Neutron Scattering and Conductivity in Polymer Electrolytes", *ACS Macro Lett.,* **7**, 504-508 (2018). 2. H. Watanabe, Y. Matsumiya, and Y. Kwon, "Dynamics of Rouse Chains undergoing Head-to-Head Association and Dissociation: Difference between Dielectric and Viscoelastic Relaxation", *J. Rheol.,* **61**, 1151-1170 (2017). 3. Y. Doi, A. Matsumoto, T. Inoue, T. Iwamoto, A. Takano, Y. Matsushita, Y. Takahashi, and H. Watanabe, "Re-examination of terminal relaxation behavior of high-molecular-weight ring polystyrene melts", *Rheol. Acta,* **56**, 567-581 (2017). 4. O. M. Kwon, H. Watanabe, K. H. Ahn, and S. J. Lee, "Interplay between structure and property of graphene nanoplatelet networks formed by an electric field in a poly(lactic acid) matrix", *J. Rheol.,* **61**, 291-303 (2017)

	5. Y. Matsumiya, H. Watanabe, O. Urakawa, and T. Inoue, "Experimental Test for Viscoelastic Relaxation of Polyisoprene Undergoing Monofunctional Head-to-Head Association and Dissociation", *Macromolecules,* **49**, 7088-7095 (2016). 6. S. Ankiewicz, H. Orbey, H. Watanabe, H. Lentzakis, and J. Dealy, On the use of continuous relaxation spectra to characterize model polymers", *J. Rheol.,* **60**, 1115-1120 (2016) 7. Y. Matsumiya and H. Watanabe, "Nonlinear Stress Relaxation of Miscible Polyisoprene/Poly(p-tert-butyl Styrene) Blends in Pseudo-monodisperse State", *Macromolecules*, **49**, 4544-4556 (2016). 8. Youngdon Kwon, Yumi Matsumiya, and Hiroshi Wtanabe, Viscoelastic and Orientational Relaxation of Linear and Ring Rouse Chains undergoing Reversible End-Association and Dissociation", *Macromolecules*, **49**, 3593-3607 (2016). 9. Y. Matsumiya, N. Rakkapao, and H. Watanabe, "Entanglement Length in Miscible Blends of cis-Polyisoprene and Poly(p-tert-butylstyrene)", *Macromolecules*, **48**, 7889-7908 (2015). 10. K. Timachova, H. Watanabe, and N. P. Balsara, "Effect of molecular weight and salt concentration on ion transport and the transference number in polymer electrolytes", *Macromolecules*, **48**, 7882-7888 (2015). 11. H. Watanabe, Y. Matsumiya , Y. Masubuchi ,O. Urakawa, and T. Inoue, "Viscoelastic Relaxation of Rouse Chains undergoing Head-to-Head Association and Dissociation: Motional Coupling through Chemical Equilibrium", *Macromolecules*, **48**, 3014–3030 (2015). 12. Y. Masubuchi and H. Watanabe, "Origin of Stress Overshoot under Start-up Shear in Primitive Chain Network Simulation", *ACS MACRO Letters,* **3**, 1183-1186 (2014). 3, 1183-1186 13. E. van Ruymbeke, V. Shchetnikava, Y. Matsumiya, and H. Watanabe, "Dynamic dilution effect in binary blends of linear polymers with well-separated molecular weights", *Macromolecules*, **47**, 7653-7665 (2014). 14. Y. Matsumiya, Y. Masubuchi, T. Inoue, O. Urakawa, C.-Y. Liu, E. van Ruymbeke, and H. Watanabe, "Dielectric and Viscoelastic Behavior of Star-branched Polyisoprene: Two Coarse-Grained Length Scales in Dynamic Tube Dilation", *Macromolecules*, **47**, 7637-7652 (2014). 15. Y. Masubuchi, Y. Matsumiya, and H. Watanabe,"Test of orientation/stretch-induced reduction of friction via primitive chain network simulations for polystyrene, polyisoprene and poly-n-buthylacrylate", *Macromolecules*, **47**, 6768-6775 (2014). 16. Y. Masubuchi, Y. Matsumiya, H. Watanabe, G. Marrucci, and G. Ianniruberto, "Primitive Chain Network Simulations for Pom-pom Polymers in Uniaxial Elongational Flows", *Macromolecules*, **47**, 3511-3519 (2014). 17. K. Horio, T.Uneyama, Y. Matsumiya, Y.Masubuchi, and H.Watanabe, "Rheo-Dielectric Responses of Entangled cis-Polyisoprene under Uniform Steady Shear and LAOS", *Macromolecules*, **47**, 246-255 (2014).
【学術関係の受賞など】	2008.5: 高分子学会賞 2012.5: 日本レオロジー学会賞 2015.10: Bingham Award, The Society of Rheology (USA).

【氏名】	田中　功　（たなか　いさお）
【職名】	教授
【所属】	工学研究科　材料工学専攻
【研究室】	吉田キャンパス　工学部物理系校舎　量子材料学研究室
【直通電話】	075-753-5465
【FAX】	075-753-5447
【電子メールアドレス】	tanaka@cms.MTL.kyoto-u.ac.jp
【ホームページ】	http://cms.mtl.kyoto-u.ac.jp/tanaka.html
【研究分野】	材料科学
【現在の研究課題】	計算材料科学，構造材料科学，材料情報学，エネルギー材料科学
【研究内容キーワード】	量子材料設計，第一原理計算，材料ｲﾝﾌｫﾏﾃｨｸｽ，ｾﾗﾐｯｸｽ科学，電子分光
【最終学歴】	1987 年 3 月 大阪大学大学院基礎工学研究科物理系専攻博士後期課程修了
【学位】	1987 年 3 月 大阪大学工学博士
【略歴】	1987 年 4 月 日本学術振興会特別研究員 (PD)、1987 年 6 月 大阪大学産業科学研究所・助手、1993 年 4 月 京都大学工学部・助手、1996 年 5 月 京都大学大学院エネルギー科学研究科・助教授、2001 年 7 月 京都大学大学院工学研究科・助教授、2003 年 12 月 京都大学大学院工学研究科・教授
【在外研究歴】	1992 年 4 月－1993 年 3 月 ドイツ マックスプランク金属研究所・客員研究員（アレキサンダー・フォン・フンボルト財団奨学研究員）
【所属学会】	日本金属学会、日本セラミックス協会、日本鉄鋼協会，応用物理学会、American Ceramic Society、Materials Research Society
【学会活動】	Journal of American Ceramics Society フェロー・編集委員、World Academy of Ceramics 会員
【主な著書、学術論文】（過去 5 年以内）	1 A. Seko, H. Hayashi, H. Kashima & I. Tanaka. Matrix- and tensor-based recommender systems for the discovery of currently unknown inorganic compounds. *Physical Review Materials* **2**, 013805, (2018). 2 Y. Ikeda, R. Körmann, B. Dutta, A. Carreras. A. Seko, J. Neugebauer & I. Tanaka. Temperature-dependent phonon spectra of magnetic random solid solutions. *npj Computational Materials* **4**, 7, (2018). 3 K. Shitara, T. Moriasa, A. Sumitani, A. Seko, H. Hayashi, Y. Koyama, R. Huang, D. L. Han, H. Moriwake & I. Tanaka. First-Principles Selection of Solute Elements for Er-Stabilized Bi_2O_3 Oxide-Ion Conductor with Improved Long-Term Stability at Moderate Temperatures. *Chemistry of Materials* **29**, 3763 (2017). 4 H. Hayashi, S. Katayama, T. Komura, Y. Hinuma, T. Yokoyama, K. Mibu, F. Oba & I. Tanaka. Discovery of a Novel Sn(II)-Based Oxide beta-SnMoO4 for Daylight-Driven Photocatalysis. *Advanced Science* **4**, 1600246 (2017). 5 Y. Hinuma, T. Hatakeyama, Y. Kumagai, Lee A. Burton, H. Sato, Y. Muraba, S. Iimura, H. Hiramatsu, I. Tanaka, H. Hosono & F. Oba. Discovery of earth-abundant nitride semiconductors by computational screening and high-pressure synthesis. *Nature Communications* **7**, 11962, (2016)
【学術関係の受賞など】	本多フロンティア賞（2018 年） ドイツ政府　　ﾌｨﾘｯﾌﾟ・ﾌﾗﾝﾂ・ﾌｫﾝ・ｼﾞｰﾎﾞﾙﾄ賞（2008 年） 米国ｾﾗﾐｯｸｽ学会　ﾘﾁｬｰﾄﾞ・ﾌﾙﾗｰｽ賞（2004 年）

【氏名】	田中　庸裕　（たなか　つねひろ）
【職名】	教授
【所属】	工学研究科　分子工学専攻
【研究室】	桂キャンパス A4 棟 126 号室
【直通電話】	075-383-2558
【FAX】	075-383-2561
【電子メールアドレス】	tanakat@moleng.kyoto-u.ac.jp
【ホームページ】	http://www.moleng.kyoto-u.ac.jp/~moleng_04/
【研究分野】	触媒化学・固体物理化学
【現在の研究課題】	固体と接触したナノ粒子・光触媒による人工光合成
【研究内容キーワード】	元素戦略・ナノ粒子・X 線分光法
【学歴】	1987 年 3 月 京都大学工学研究科博士後期課程修了
【学位】	1987 年 7 月 京都大学工学博士
【略歴】	1987 年 10 月 北海道大学理学部助手，1990 年 4 月 京都大学工学部助手，1997 年 7 月 京都大学工学研究科助教授，2004 年 同教授
【所属学会】	触媒学会，日本化学会，石油学会，アメリカ化学会，日本 XAFS 研究会，英国王立化学会
【主な著書、学術論文】（過去 5 年以内）	1. Dynamic Behavior of Rh Species in Rh/Al$_2$O$_3$ Model Catalyst during Three-Way Catalytic Reaction: An Operando X ray Absorption Spectroscopy Study, H.Asakura, S. Hosokawa, T. Tanaka et al., *J. Am. Chem. Soc.,* 2018, **140**, 176-184. 2. Efficient Photocatalytic Carbon Monoxide Production from Ammonia and Carbon Dioxide by the Aid of Artificial Photosynthesis, Z. Huang, K. Teramura, H. Asakura, S. Hosokawa, T. Tanaka, *Chemical Science,* 2017, **8,** 5797-5801. 3. Strong Metal-Support Interaction between Pt and SiO$_2$ Following High-Temperature Reduction: A Catalytic Interface for Propane Dehydrogenation, L. Deng, H. Miura, T. Shishido, S. Hosokawa, K. Teramura, T. Tanaka, *Chemical Communications,* 2017, **53**, 6937-6940. 4. Thermally Stable Single Atom Pt/m-Al$_2$O$_3$ for the Selective Hydrogenation and CO Oxidation, Z. Zhang, Y. Zhu, H. Asakura, B. Zhang, J. Zhang, M. Zhou, Y. Han, T. Tanaka, A.-Q. Wang, T. Zhang, N. Yan, *Nature Communications*, 2017, 8:16100. 5. Which is an Intermediate Species for Photocatalytic Conversion of CO$_2$ by H$_2$O as the Electron Donor: CO$_2$ Molecule, Carbonic Acid, Bicarbonate, or Carbonate Ions?, K. Teramura, K. Hori, Y. Terao, Z. Huan, S. Iguchi, Z. Wang, H. Asakura, S. Hosokawa, T. Tanaka, *J. Phys. Chem. C,* 2017, **121**, 8711-8721. 6. Visible Light-Induced Water Splitting in an Aqueous Suspension of a Plasmonic Au/TiO$_2$ Photocatalyst with Metal Co-Catalysts, A. Tanaka, K. Teramura, S. Hosokawa, H.Kominami, T. Tanaka, *Chemical Science,* 2017, **8**, 2574-2580. 7. Promoter Effect of Pd Species on Mn Oxide Catalysts Supported on Rare-Earth-Iron Mixed Oxide, S. Hosokawa, R. Tada, T. Shibano, S. Matsumoto, K. Teramura, T. Tanaka, *Catalysis Science & Technology,* 2016, **6**, 7868-7874. 8. Investigation on Electrochemical and Photoelectrochemical Properties of Ni-Al LDH Photocatalyst, S. Iguchi, S. Kikkawa, K. Teramura, S. Hosokawa, T. Tanaka, *Phys. Chem. Chem. Phys.,* 2016, **18**, 13811-13819. 9. Popping of Graphene Oxide: Application in Preparing Metal Nanoparticle Catalysts, Y. Gao, Xi Chen, J. Zhang, H. Asakura, T. Tanaka, K. Teramura, D. Ma, N. Yan, *Advanced Materials,* 2015, **27**, 4688-4694.

【氏名】	山本　量一　（やまもと　りょういち）
【職名】	教授
【所属】	工学研究科　化学工学専攻
【研究室】	桂キャンパス　A棟118号室
【直通電話】	075-383-2661
【FAX】	075-383-2651
【電子メールアドレス】	ryoichi@cheme.kyoto-u.ac.jp
【ホームページ】	http://www-tph.cheme.kyoto-u.ac.jp/
【研究分野】	ソフトマター／アクティブマターの計算科学
【現在の研究課題】	生体組織の物理モデリング／自己泳動する微生物のシミュレーション
【研究内容キーワード】	ソフトマター、アクティブマター、シミュレーション、移動現象
【最終学歴】	1992年3月 神戸大学大学院 工学研究科修士課程化学工学専攻修了
【学位】	1996年3月 博士（工学）京都大学
【略歴】	1994年9月 神戸大学大学院自然科学研究科物質科学専攻助手、1996年3月 京都大学大学院理学研究科物理学・宇宙物理学専攻助手、2000年1月 同講師、2004年10月 京都大学大学院工学研究科化学工学専攻助教授、2007年4月 同准教授、2008年10月 同教授
【在外研究歴】	2000年9月 -2001年8月 英国ケンブリッジ大学化学教室（J-P. Hansen 教授）（文部省在外研究員（若手））
【所属学会】	日本物理学会、化学工学会、分子シミュレーション研究会
【学会活動】	化学工学会理事
【主な著書、学術論文】 （過去5年以内）	1. C. Shih, J.J. Molina, and R. Yamamoto, Inter-particle force between two colloidal particles in an oscillating electric field, Soft Matter, in print. 2. N. Oyama, K. Teshigawara, J. J. Molina, R. Yamamoto, and T. Taniguchi, Hydrodynamic synchronization of externally driven colloids, *Phys. Rev. E* **97**, 032611 (2018). 3. S. K. Schnyder, J. J. Molina, Y. Tanaka, and R. Yamamoto, Collective motion of cells crawling on a substrate: roles of cell shape and contact inhibition, *Sci. Rep.* **7**, 5163 (2017). 4. J. J. Molina, K. Otomura, H. Shiba, H. Kobayashi, M. Sano, and R. Yamamoto, Rheological evaluation of colloidal dispersions using the smooth profile method: formulation and applications, *J. Fluid Mech.* **792**, 590-619 (2016). 5. N. Oyama, J. J. Molina, and R. Yamamoto, Purely hydrodynamic origin for swarming of swimming particles, *Phys. Rev. E* **93**, 043114 (2016). 6. S. Yasuda and R. Yamamoto, Synchronized molecular dynamics simulation via macroscopic heat and momentum transfer: an application to polymer lubrication, *Phys. Rev. X* **4**, 041011 (2014). 7. H. Mizuno and R. Yamamoto, General constitutive model for supercooled liquids: Anomalous transverse wave propagation, *Phys. Rev. Lett.* **110**, 095901 (2013). 8. J. J. Molina, Y. Nakayama, and R. Yamamoto, Hydrodynamic interactions of self-propelled swimmers, *Soft Matter* **9**, 4923-4936 (2013).
【学術関係の受賞など】	2007年1月 ホソカワ研究奨励賞、2002年12月 分子シミュレーション研究会学術賞

【氏名】	高田　彰二　（たかだ　しょうじ）
【職名】	教授
【所属】	理学研究科　生物科学専攻　生物物理学教室
【研究室】	理学部 1 号館 205 号室
【直通電話】	075-753-4220
【FAX】	075-753-4222
【電子メールアドレス】	takada@biophys.kyoto-u.ac.jp
【ホームページ】	http://theory.biophys.kyoto-u.ac.jp
【研究分野】	理論生物物理学
【現在の研究課題】	生体分子の構造機能についての理論およびコンピュータシミュレーション研究
【研究内容キーワード】	タンパク質フォールディング、分子モーター、遺伝子動態、生体分子モデリング
【最終学歴】	1991年9月 総合研究大学院大学数物科学研究科機能分子科学専攻博士後期課程退学
【学位】	1994年3月 理学博士（総合研究大学院大学）
【略歴】	1991年～1995年 岡崎国立共同研究機構技官（分子科学研究所）、1995年～1998年 日本学術振興会研究員（イリノイ大学化学科）、1998年～2001年 神戸大学理学部化学科講師、2001年～2007年 同助教授、2007年～2013年 京都大学理学研究科生物科学専攻生物物理教室准教授、2013年 同教授。
【在外研究歴】	1995年5月－1998年3月　米国イリノイ大学化学科（日本学術振興会研究員）
【所属学会】	日本生物物理学会
【学会活動】	日本生物物理学会副会長
【主な著書、学術論文】 （過去5年以内）	1. M. Shimizu, Y. Noguchi, Y. Sakiyama, H. Kawakami, T. Katayama*, S. Takada*, Near-atomic structural model for bacterial DNA replication initiation complex and its functional insights, *Proc. Nat. Acad. Sci. USA,* **113**: E8021-E8030, 2016 2. C. Tan, T. Terakawa, S. Takada*, Dynamic Coupling among Protein Binding, Sliding, and DNA Bending Revealed by Molecular Dynamics, *JACS.,* **138**: 8512-8522, 2016 3. S. Takada*, R. Kanada, C. Tan, T. Terakawa, W. Li, H. Kenzaki, Modeling Structural Dynamics of Biomolecular Complexes by Coarse-Grained Molecular Simulations, *Acc. Chem. Res.,* **48**: 3026-3035, 2015 4. W. Li, W. Wang, and S. Takada, Energy landscape views for interplays among folding, binding, and allostery of calmodulin domain, *Proc. Nat. Acad. Sci. USA,* **111**: 10550-10555, 2014. 5. M.J.McGrath, I.F.Kuo, S.Hayashi, and S.Takada, ATP hydrolysis mechanism in kinesin studied by combined quantum-mechanical molecular-mechanical metadynamics, *JACS,* **103**: 8908-8919, 2013. 6. X.Yao, N.Kimura, S.Murakami, and S.Takada, Drug Uptake Pathways of Multidrug Transporter AcrB Studied by Molecular Simulations and Site-Directed Mutagenesis Experiments, *JACS,* **135**: 7474-7485, 2013. 7. T.Terakawa, H.Kenzaki, & S.Takada, p53 searches on DNA by rotation-uncoupled sliding at C-terminal tails and restricted hopping of core domains , *JACS,* **134**: 14555-14562, 2012.

【氏名】	林　重彦　（はやし　しげひこ）
【職名】	教授
【所属】	理学研究科　化学専攻
【研究室】	理学研究科 6 号館 154 号室
【直通電話】	075-753-4006
【FAX】	075-753-4000
【電子メールアドレス】	hayashig@kuchem.kyoto-u.ac.jp
【ホームページ】	http://kuchem.kyoto-u.ac.jp/riron/hayashig
【研究分野】	理論化学・生物物理学
【現在の研究課題】	タンパク質分子機能の理論的研究
【研究内容キーワード】	タンパク質機能・分子シミュレーション
【学歴】	1997 年 11 月　京都大学大学院理学研究科化学専攻博士課程修了
【学位】	1997 年 11 月　博士（理学）（京都大学）
【略歴】	1998 年 4 月 日本学術振興会特別研究員（名古屋大学）、2000 年 4 月 米国イリノイ大学ベックマン研究所博士研究員、2003 年 6 月 京都大学福井謙一記念研究センター博士研究員、2003 年 10 月 科学技術振興機構さきがけ研究員、2005 年 5 月 京都大学大学院理学研究科准教授、2013 年 7 月 同教授
【所属学会】	分子科学会、生物物理学会、蛋白質科学会、日本化学会
【主な著書、学術論文】 （過去 5 年以内）	1. Atomistic modeling of alternating access of a mitochondrial ADP/ATP membrane transporter with molecular simulations. Koichi Tamura and Shigehiko Hayashi*, *PLOS ONE,* **12**, e0181489 (2017). 2. Photoactivation intermediates of a G-protein coupled receptor rhodopsin investigated by a hybrid molecular simulation. Motoshi Kamiya and Shigehiko Hayashi*, *J. Phys. Chem. B,* **121**, 3842-3852 (2017). 3. Molecular mechanism of wide photoabsorption spectral shifts of color variants of human cellular retinol binding protein II. Cheng Cheng, Motoshi Kamiya, Yoshihiro Uchida, Shigehiko Hayashi*, *J. Am. Chem. Soc.,* **137**, 13362-13370 (2015) 4. Atomistic design of microbial opsin-based blue-shifted optogenetics tools. Hideaki E. Kato, Motoshi Kamiya, Seiya Sugo, Jumpei Ito, Reiya Taniguchi, Ayaka Orito, Kunio Hirata, Ayumu Inutsuka, Akihiro Yamanaka, Andres D. Maturana, Ryuichiro Ishitani, Yuki Sudo, Shigehiko Hayashi*, and Osamu Nureki*, *Nat. Commun.,* **6**, 7177 (2015) 5. Molecular mechanism of ATP hydrolysis in F1-ATPase revealed by molecular simulations and single molecule observations. Shigehiko Hayashi*, et al., *J. Am. Chem. Soc.,* **134**, 8447-8454 (2012) 6. Crucial role of protein flexibility in formation of a stable reaction transition state in an α -amylase catalysis. Kosugi Takahiro and Shigehiko Hayashi*. *J. Am. Chem. Soc.,* **134**, 7045-7055 (2012)

⑷ 専任教員

【氏名】	佐藤　徹　（さとう　とおる）
【職名】	教授
【所属】	理論研究部門
【研究室】	210
【直通電話】	075-711-7849
【電子メールアドレス】	tsato@fukui.kyoto-u.ac.jp
【ホームページ】	準備中
【研究分野】	理論化学
【現在の研究課題】	振電相互作用理論、機能性分子の理論設計
【研究内容キーワード】	振電相互作用，有機 EL，Jahn-Teller 効果
【学歴】	平成 9 年 3 月　京都大学大学院工学研究科 分子工学専攻博士後期課程修了
【学位】	博士（工学）
【略歴】	平成 9 年 4 月　日本学術振興会特別研究員（PD）（財団法人基礎化学研究所） 平成 10 年 1 月　京都大学大学院工学研究科分子工学専攻助手 平成 15 年 10 月 文部科学省在外研究員（若手）（ルーヴァンカトリック大学） 平成 16 年 3 月　京都大学福井謙一記念研究センター理論研究部門助教授 平成 23 年 1 月　京都大学大学院工学研究科分子工学専攻准教授 平成 30 年 2 月　京都大学福井謙一記念研究センター理論研究部門教授 現在に至る
【所属学会】	日本コンピュータ化学会，日本化学会，フラーレン・ナノチューブ・グラフェン学会 , 日本物理学会，応用物理学会，有機 EL 討論会
【学会活動】	Jahn-Teller Steering Committee (2009-)
【主な著書、学術論文】（過去 5 年以内）	1. “Fluorescence via Reverse Intersystem Crossing from Higher Triplet States in a Bisanthracene Derivative”, Tohru Sato*, Rika Hayashi, Naoki Haruta, Yong-Jin Pu, *Sci. Rep.* **7** 4820 1-9 (2017). 2. “Thermodynamical vibronic coupling constant and density: Chemical potential and vibronic coupling in reactions”, Tohru Sato*, Naoki Haruta, and Kazuyoshi Tanaka, *Chem. Phys. Lett.* **652**, 157-161 (2016). 3. “A Light-Emitting Mechanism for Organic Light-Emitting Diodes: Molecular Design for Inverted Singlet-Triplet Structure and Symmetry-Controlled Thermally Activated Delayed Fluorescence”, Tohru Sato*, Motoyuki Uejima, Kazuyoshi Tanaka, Hironori Kaji, and Chihaya Adachi, *J. Mater. Chem. C* **3**, 870-878 (2015). 4. “Quantum Yield in Blue-Emitting Anthracene Derivatives: Vibronic Coupling Density and Transition Dipole Moment Density”, Motoyuki Uejima, Tohru Sato*, Daisuke Yokoyama, Kazuyoshi Tanaka, and Jong-Wook Park, *Phys. Chem. Chem. Phys.* **16**, 14244-14256 (2014) . 5. "Jahn-Teller Instability of Icosahedral [W@Au12]—", Tohru Sato*, Erwin Lijnen, Arnout Ceulemans, *J. Chem. Theo. Comput.* **10**, 613-622 (2014).
【学術関係の受賞など】	2016 年度日本コンピュータ化学会学会賞 平成 23 年 3 月 欧州委員会 Erasumus Mundus Scholar

【氏名】	西本　佳央（にしもと　よしお）
【職名】	特定助教
【所属】	京都大学福井謙一記念研究センター
【研究室】	福井謙一記念研究センター 208
【直通電話】	075-711-7894
【電子メールアドレス】	nishimoto.yoshio@fukui.kyoto-u.ac.jp
【研究分野】	理論化学・計算化学
【現在の研究課題】	大規模量子化学計算・エネルギー高次微分
【研究内容キーワード】	密度汎関数強束縛法・フラグメント分子軌道法・エネルギー微分
【学歴】	2015年3月　名古屋大学大学院理学研究科博士課程（後期課程）物質理学専攻修了
【学位】	2015年3月　博士（理学）（名古屋大学）
【略歴】	2015年4月　京都大学福井謙一記念研究センター・福井センターフェロー 2016年12月　京都大学福井謙一記念研究センター・特定助教
【所属学会】	日本化学会・理論化学研究会・分子科学会
【主な著書、学術論文】（過去5年以内）	1. Nishimoto, Y.; Fedorov, D. G. “Adaptive frozen orbital treatment for the fragment molecular orbital method combined with density-functional tight-binding”, *J. Chem. Phys.* 2018, **148**, 064115. 2. Kitoh-Nishioka, H.; Welke, K.; Nishimoto, Y.; Fedorov, D. G.; Irle, S. “Multi-Scale Simulations on Charge Transport in Covalent Organic Frameworks: Including Dynamics of Transfer Integrals from FMO-DFTB/LCMO”, *J. Phys. Chem. C* 2017, **121**, 17712–17726. 3. Nishimoto, Y.; Kondo, H.; Yamaguchi, K.; Yokogawa, D.; Yamaguchi, J.; Itami, K.; Irle, S. “Theoretical Elucidation of Potential Enantioselectivity in a Pd-Catalyzed Aromatic C–H Coupling Reaction”, *J. Org. Chem.* 2017, **82**, 4900–4906. 4. Nishimoto, Y. “Analytic Hyperpolarizability and Polarizability Derivative with Fractional Occupation Numbers for Large Extended Systems”, *J. Chem. Phys.* 2017, **146**. 084101. 5. Nishimoto, Y.; Fedorov, D. G. “Three-body expansion of the fragment molecular orbital method combined with density-functional tight-binding”, *J. Comput. Chem.* 2017, **38**, 406–418.
【学術関係の受賞など】	日本学術振興会特別研究員（DC1）　2012.4-2015.3

⑸ FIFC リサーチフェロー

【氏名】	永瀬　茂（ながせ　しげる）
【職名】	FIFC リサーチフェロー
【所属】	福井謙一記念研究センター
【研究室】	104 室
【直通電話】	075-711-7792
【FAX】	075-711-4757
【電子メールアドレス】	nagase@fukui.kyoto-u.ac.jp, nagase@ims.ac.jp
【ホームページ】	http://www.fukui.kyoto-u.ac.jp/
【研究分野】	理論化学・計算化学
【現在の研究課題】	元素の特性とナノ構造を利用した分子開発の理論と計算
【研究内容キーワード】	高周期典型元素、遷移金属、ナノカーボン、機能性分子
【最終学歴】	1975 年 3 月 大阪大学大学院基礎工学研究科博士課修了
【学位】	1975 年 3 月 工学博士（大阪大学）
【略歴】	ロチェスター大学博士研究員、オハイオ州立大学博士研究員、分子科学研究所技官を経て、1980 年 4 月 横浜国立大学助教授、1991 年 4 月 同教授、1995 年 4 月 東京都立大学教授、2001 年 4 月 分子科学研究所教授、総合研究大学院大学教授、20012 年 3 月 同名誉教授、2012 年 4 月 京都大学福井謙一記念研究センターシニアリサーチフェロー、2015 年 4 月 同 FIFC リサーチフェロー
【所属学会】	日本化学会、分子科学会、ケイ素化学協会、アメリカ化学会
【主な著書、学術論文】 （過去 5 年以内）	1. X. Lu, L. Feng, T. Akasaka, and S. Nagase, Current Statues and Future Developments of Endohedral Metallofullerenes, *Chem. Soc. Rev.,* **41**, 7723-7760 (2012). 2. S. Nagase, Multiple Bonds between Lead Atoms and Short Bonds between Transition Metals, *Pure Appl. Chem.,* **85**, 649-659 (2013). 3. X. Lu, T. Akasaka, and S. Nagase, Carbide Cluster Metallofullerenes: Structure, Properties, and Possible Origin, *Acc. Chem. Res.,* **46**, 1627-1635 (2013). 4. M. Yamada, T. Akasaka, and S. Nagase, Carbene Additions to Fullerenes, *Chem. Rev.,* **113**, 7209-7264 (2013). 5. S. Nagase, Theory and Calculations of Molecules Containing Heavier Main Group Elements and Fullerenes Encaging Transition Metals: Interplay with Experiment, *Bull. Chem. Soc. Jpn., (Award Accounts),* **87**, 167-195 (2014). 6. J. –D. Guo, D. J. Liptrot, S. Nagase, and P. P. Power, The Multiple Bonding in Heavier Group 14 Element Alkene Analogues is Stabilized Mainly by Dispersion Force Effects, *Chem. Sci.* **6**, 6235-6244 (2015). 7. 赤阪健，山田道夫，前田優，永瀬茂，化学の要点シリーズ 17「フラーレンの化学」（日本化学会編），共立出版 (2016).
【学術関係の受賞など】	2012 年 文部科学大臣表彰科学技術賞（研究部門）、2012 年 福井メダル (Asia-Pacific Association of Theoretical & Computational Chemists) 、2013 年 日本化学会賞

⑹ シニアリサーチフェロー

【氏名】	榊　茂好　（さかき　しげよし）
【職名】	シニアリサーチフェロー
【所属】	福井謙一記念研究センター・福井謙一記念研究部第2
【研究室】	303
【直通電話】	075-711-7907
【FAX】	075-781-4757
【電子メールアドレス】	sakaki.shigeyoshi.47e@st.kyoto-u.ac.jp
【ホームページ】	http://www.users.iimc.kyoto-u.ac.jp/~z59354/
【研究分野】	理論化学・計算化学
【現在の研究課題】	遷移金属元素を含む複合電子系の構造、電子状態、反応過程の理論化学
【研究内容キーワード】	電子状態・遷移金属錯体・反応解析・触媒作用・金属微粒子
【学歴】	1974年3月　京都大学工学研究科燃料化学専攻博士課程単位取得退学
【学位】	1974年11月　工学博士（京都大学）
【略歴】	1975年4月 熊本大学工学部助手、1982年1月 同助教授、1990年4月 同教授を経て、2002年4月より京都大学工学研究科教授、2010年3月 定年、現在に至る。
【所属学会】	日本化学会、触媒学会、近畿化学協会、ケイ素化学協会、錯体化学会
【主な著書、学術論文】 （過去5年以内）	1. Theoretical Study of One-Electron Oxidized Mn(III)– and Ni(II)–Salen Complexes: Localized vs Delocalized Ground and Excited States in Solution, S. Aono, M. Nakagaki, T. Kurahashi, H. Fujii, and S. Sakaki, *J. Chem. Theory Comput.,* **10**, 1062-1073 (2014). 2. How Can We Understand Au_8 Cores and Entangled Ligands of Selenolate- and Thiolate-Protected Gold Nanoclusters $\mathrm{Au}_{24}(\mathrm{ER})_{20}$ and $\mathrm{Au}_{20}(\mathrm{ER})_{16}$ (E = Se, S; R = Ph, Me)? A Theoretical Study, N. Takagi, K. Ishimura, M. Matsui, R. Fukuda, T. Matsui, T. Nakajima, M. Ehara, and S. Sakaki, *J. Am. Chem. Soc.,* **137**, 8593-8602 (2015). 3. CASPT2 study of inverse sandwich-type dinuclear 3d transition metal complexes of ethylene and dinitrogen molecules: similarities and differences in geometry, electronic structure, and spin multiplicity, M. Nakagaki and S. Sakaki, Phys. *Chem. Chem. Phys.,* **17**, 16294-16305 (2015). 4. Theoretical and Computational Study of a Complex System Consisting of Transition Metal Element(s): How to Understand and Predict Its Geometry, Bonding Nature, Molecular Property, and Reaction Behavior, S. Sakaki, *Bull. Chem. Soc. Jpn.,* **88**, 889-938 (2015). 5. Theoretical Study of Hydrogenation Catalysis of Phosphorus Compound and Prediction of Catalyst with High Activity and Wide Application Scope, G. Zeng, S. Maeda, T. Taketsugu, S. Sakaki, *ACS Cat.,* **6**, 4859-4870 (2016). 6. Catalytic Hydrogenation of Carbon Dioxide with Ammonia-Borane by Pincer-Type Phosphorus Compounds: Theoretical Prediction, GX. Zeng, S. Maeda, T. Taketsugu, S. Sakaki, *J. Am. Chem. Soc.,* **138**, 13481-13484 (2016). 7. Mo − Mo Quintuple Bond is Highly Reactive in H-H, C-H, and O-H σ-Bond Cleavages Be-cause of the Polarized Electronic Structure in Transition State, Y. Chen, S. Sakaki, *Inorg. Chem.,* **56**, 4011-4020 (2017). 8. Theoretical study of one-electron-oxidized salen complexes of group 7 (Mn(III), Tc(III), and Re(III)) and group 10 metals (Ni(II), Pd(II), and Pt(II)) with the 3D-RISM-GMC-QDPT method: localized vs. delocalized ground and excited states in solution, S. Aono, M. Nakagaki, S. Sakaki, *Phys. Chem. Chem. Phys.,* **19**, 16831-16849 (2017). 9. How to Control Inversion vs. Retention Transmetallation between $\mathrm{Pd}^{\mathrm{II}}$-Phenyl and Cu^{I}-Alkyl Complexes: Theoretical Insight, H. Zheng, K. Semba, Y. Nakao, S. Sakaki, *J. Am. Chem. Soc.,* **139**, 14065-14076 (2017).
【学術関係の受賞など】	第1回分子科学会賞（2009年9月）　第66回日本化学会賞（2014年3月） Fukui Medal（2015; from APATCC）

【氏名】	田中　一義　（たなか　かずよし）
【職名】	シニアリサーチフェロー
【所属】	福井謙一記念研究センター
【研究室】	福井謙一記念研究センター 206
【直通電話】	075-711-7867
【FAX】	075-781-4757
【電子メールアドレス】	ktanaka@moleng.kyoto-u.ac.jp
【ホームページ】	http://www.fukui.kyoto-u.ac.jp/members_ja
【研究分野】	物理化学、量子化学
【現在の研究課題】	元素ブロックを有する分子、高分子の理論化学
【研究内容キーワード】	分子・高分子の電子物性、量子機能材料、量子統計力学
【学歴】	1978 年 3 月　京都大学工学研究科石油化学専攻博士課程修了
【学位】	1978 年 3 月　工学博士（京都大学）
【略歴】	1979 年 6 月 米国エナージー・コンバージョン・デバイシズ社リサーチケミスト、1981 年 12 月 京都大学工学部助手、1988 年 12 月　同　助教授、1996 年 11 月 京都大学大学院工学研究科教授、2012 年 4 月 京都大学福井謙一記念研究センター長併任、2015 年 4 月 京都大学名誉教授ならびに京都大学福井謙一記念研究センターシニアリサーチフェロー
【所属学会】	日本化学会・日本物理学会・高分子学会
【主な著書、学術論文】 （過去 5 年以内）	1. 統計力学入門　化学者の視点から（単著，化学同人，2014） 2. Carbon Nanotubes and Graphene（共編著，Elsevier Science，2014） 3. 元素ブロック材料の基礎と実用化のための理論化学,「中條善樹監修 , 元素ブロック高分子−有機・無機ハイブリッド材料の新概念−」（共著，シーエムシー，2015） 4. ボール物理化学 第 2 版（上）（監訳ならびに共訳，化学同人，2015） 5. ボール物理化学 第 2 版（下）（監訳ならびに共訳，化学同人，2016） （以上著書） 1. 量子化学計算による有機 EL 電荷輸送材料の解析（共著）月刊ディスプレイ，**19**, No. 9, 49-52 (2013). 2. 福井先生の未完のテーマ －生命の起源への化学的試論（単著）化学 **68**, No. 11, 19-22 (2013). 3. スズ版グラフェン“スタネン”がつくられた！（単著）化学 **71**, No. 1, 21-26 (2016). 4. 元素ブロックの機能発現・電子化物を与える無機元素ブロック（共著）　セラミックス，**51**, No. 11, 739-742 (2016). 5. 2016 年ノーベル賞を読み解く　物理学賞　さまざまな可能性を秘めたエキゾチックな状態とは？（単著）　化学，**71**, No. 12, 24-27 (2016). 6. 化学つれづれ草　第一回　理屈っぽい化学？（単著）化学 **72**, No. 5, 55 (2017). 7. 化学つれづれ草　第二回　福井研究室の日常（単著）化学 **72**, No. 6, 31 (2017). 8. 化学つれづれ草　第三回　博士課程 考（単著）化学 **72**, No. 7, 29 (2017). 9. 化学つれづれ草　第四回　米国のベンチャー企業（単著）化学 **72**, No. 8, 27 (2017). 10. 化学つれづれ草　第五回　米国の研究資金事情（単著）化学 **72**, No. 9, 18 (2017). 11. 化学つれづれ草　第六回　日本の大学と研究資金（単著）化学 **72**, No. 10, 29 (2017). 12. 化学つれづれ草　第七回　妄想と基礎研究資金（単著）化学 **72**, No. 11, 46 (2017). 13. 化学つれづれ草　第八回　企業と大学の研究（単著）化学 **72**, No. 12, 28 (2017). 14. 化学つれづれ草　第九回　オリジナルな研究（単著）化学 **73**, No. 1, 59 (2018).

15. 化学つれづれ草　第十回　理論化学と計算化学（単著）化学 **73**, No. 2, 29 (2018).
16. 化学つれづれ草　第十一回　分割統治と化学（単著）化学 **73**, No. 3, 24 (2018).

（以上和文総説）

1. Meta-Para-Linked Octaaza[18]cyclophanes and Their Polycationic States (D. Sakamaki, A. Ito, K. Furukawa, T. Kato, and K. Tanaka) *J. Org. Chem.,* **78**, 2947-2956 (2013).
2. Vibronic Couplings in Cycloadditions to Fullerenes (N. Haruta, T. Sato, N. Iwahara, and K. Tanaka) *J. Phys. C: Conf. Ser.,* **428**, 012003 1-7 (2013).
3. Vibronic Coupling Density and Related Concepts (T. Sato, M. Uejima, N. Iwahara, N. Haruta, K. Shizu, and K. Tanaka) *J. Phys. C: Conf. Ser.,* **428**, 012010 1-19 (2013).
4. Vibronically Induced Activation Mechanism in Photocatalysis of Highly Dispersed Vanadium Oxide Supported on Silica, V_2O_5/SiO_2: Evidence in Phosphorescence Spectra (N. Iwahara, T. Sato, K. Tanaka, and T. Tanaka) *Chem. Phys. Lett.,* **584**, 63-66 (2013).
5. Reaction Mechanism in the Mechanochemical Synthesis of Dibenzophenazine: Application of Vibronic Coupling Density Analysis (N. Haruta, T. Sato, K. Tanaka, and M. Baron) *Tetrahedron Lett.*, **54**, 5920-5923 (2013).
6. Redox Modulation of para-Phenylenediamine by Substituted Nitronyl Nitroxide Groups and Their Spin States (A. Ito, R. Kurata, D. Sakamaki, S. Yano, Y. Kono, Y. Nakano, K. Furukawa, T. Kato, and K. Tanaka) *J. Phys. Chem. A,* **117**, 12858-12867 (2013).
7. Vibronic Couplings in C60 Derivatives for Organic Photovoltaics (N. Iwahara, T. Sato, K. Tanaka, and H. Kaji) *Chem. Phys. Lett.,* **590**, 169-174 (2013).
8. Preparation of D-A Polymer with Disilanobithiophene as New Donor Component and Application to High-voltage Bulk Heterojunction Polymer Solar Cell (J. Ohshita, M. Nakashima, D. Tanaka, Y. Morihara, H. Fueno, and K. Tanaka) *Polym. Chem.,* **5**, 346-349 (2014).
9. Enhancement of Fluorescence in Anthracene by Chlorination: Vibronic Coupling and Transition Dipole Moment Density Analysis (M. Uejima, T. Sato, K. Tanaka, and H. Kaji) *Chem. Phys.*, **430**, 47-55 (2014).
10. Pseudo Jahn-Teller Origin of Distortion in [6]Cycloparaphenylene (Y. Kameoka, T. Sato, T. Koyama, K. Tanaka, and T. Kato) *Chem. Phys. Lett.,* **598**, 69-74 (2014).
11. Highly Coplanar (E)-1,2-Di(1-naphthyl)disilene Involving a Distinct CH-π Interaction with the Perpendicularly Oriented Protecting Eind Group (M. Kobayashi, N. Hayakawa, K. Nakabayashi, T. Matsuo, D. Hashizume, H. Fueno, K. Tanaka, and K. Tamao) *Chem. Lett.,* **43**, 432-434 (2014).
12. A Designed Fluorescent Anthracene Derivative: Theory, Calculation, Synthesis, and Characterization (M. Uejima, T. Sato, M. Detani, A. Wakamiya, F. Suzuki, H. Suzuki, T. Fukushima, K. Tanaka, Y. Murata, C. Adachi, and H. Kaji) *Chem. Phys. Lett.,* **602**, 80-83 (2014).
13. Quantum Yield in Blue-Emitting Anthracene Derivatives: Vibronic Coupling Density and Transition Dipole Moment Density (M. Uejima, T. Sato, D. Yokoyama, K. Tanaka, and J. –W. Park) *Phys. Chem. Chem. Phys.,* **16**, 14244-14256 (2014).
14. Synthesis and Polymerization of a para-Disubstituted T8-caged Hexaisobutyl-POSS Monomer (T. Maegawa, Y. Irie, H. Fueno, K. Tanaka, and K. Naka) *Chem. Lett.,* **43**, 1532-1534 (2014).
15. An Isolable Diborane(4) Compound with Terminal B-H Bonds: Structural Characteristics and Electronic Properties (Y. Shoji, S. Kaneda, H. Fueno, K. Tanaka, K. Tamao, D. Hashizume, and T. Matsuo) *Chem. Lett.,* **43**, 1587-1589 (2014).
16. Electronic Structure of Tetraaza[1.1.1.1]o, p, o, p-Cyclophane and Its Oxidized States (D. Sakamaki, A. Ito, T. Matsumoto, and K. Tanaka) *RSC Adv.,* **4**, 39476-39483 (2014).

17. Synthesis of Conjugated Polymers Containing Gallium Atoms and Evaluation of Conju gation through Four-Coordinate Gallium Atoms (T. Matsumoto, Y. Onishi, K. Tanaka, H. Fueno, K. Tanaka, and Y. Chujo) *Chem. Commun.,* **50**, 15740-15743 (2014).
18. Reactivity of Endohedral Metallofullerene $La_2@C_{80}$ in Nucleophilic and Electrophilic Attacks: Vibronic Coupling Density Approach (N. Haruta, T. Sato, and K. Tanaka) *J. Org. Chem.,* **80**, 141-147 (2014).
19. Fluorescent Triphenylamine Derivative: Theoretical Design Based on Reduced Vibronic Coupling (Y. Kameoka, M. Uebe, A. Ito, T. Sato, and K. Tanaka) *Chem. Phys. Lett.,* **615**, 44-49 (2015).
20. A Light-Emitting Mechanism for Organic Light-Emitting Diodes: Molecular Design for Inverted Singlet-Triplet Structure and Symmetry-Controlled Thermally Activated Delayed Fluorescence (T. Sato, M. Uejima, K. Tanaka, H. Kaji, and C. Adachi) *J. Mater. Chem. C,* **3**, 870-878 (2015).
21. Enhanced Electroluminescence from a Thermally Activated Delayed-Fluorescence Emitter by Suppressing Nonradiative Decay (K. Shizu, M. Uejima, H. Nomura, T. Sato, K. Tanaka, H. Kaji, and C. Adachi) *Phys. Rev. Appl.,* **3**, 014001 1-7 (2015).
22. Strategy for Designing Electron Donors for Thermally Activated Delayed Fluorescence Emitters (K. Shizu, H. Tanaka, M. Uejima, T. Sato, K. Tanaka, H. Kaji, and C. Adachi) *J. Phys. Chem., C,* **119**, 1291-1297 (2015).
23. Reactivity Index for Diels-Alder Cycloadditions to Large Polycyclic Aromatic Hydrocarbons Using Vibronic Coupling Density (N. Haruta, T. Sato, and K. Tanaka) *Tetrahedron Lett.,* **56**, 590-594 (2015).
24. Synthesis and Characterization of Heterofluorenes Containing Four-coordinated Group 13 Elements: Theoretical and Experimental Analyses and Comparison of Structures, Optical Properties and Electronic States (T. Matsumoto, K. Tanaka, K. Tanaka, and Y. Chujo) *Dalton Trans.,* **44**, 8697-8707 (2015).
25. Luminescent Coordination Glass: Remarkable Morphological Strategy for Assembled Eu (III) Complexes (Y. Hirai, T. Nakanishi, Y. Kitagawa, K. Fushimi, T. Seki, H. Ito, H. Fueno, K. Tanaka, T. Satoh, and Y. Hasegawa) *Inorg. Chem.,* **54**, 4364-4370 (2015).
26. Multiscale Simulation of Charge Transport in a Host Material, N, N’-Dicarbazole-3,5-benzene (mCP), for Organic Light-Emitting Diodes (F. Suzuki, K. Shizu, H. Kawaguchi, S. Furukawa, T. Sato, K. Tanaka, and H. Kaji) *J. Mater. Chem. C,* **3**, 5549-5555 (2015).
27. A Triphenylamine with Two Phenoxy Radicals Having Unusual Bonding Patters and a Closed-Shell Electronic State (D. Sakamaki, S. Yano, T. Kobashi S. Seki, T. Kurahashi, S. Matsubara, A. Ito, and K. Tanaka) *Angew. Chem. Int. Ed.,* **54**, 8267-8270 (2015).
28. New Tris- and Pentakis-Fused Donors Containing Extended Tetrathiafulvalenes: New Positive Electrode Materials for Reachargeable Batteries (S. Iwamoto, Y. Inatomi, D. Ogi, S. Shibayama, Y. Murakami, M. Kato, K. Takahashi, K. Tanaka, N. Hojo, and Y. Misaki) *Beilstein J. Org. Chem.,* **11**, 1136-1147 (2015).
29. Fluorescence Enhancement of Non-Fluorescent Triphenylamine: A Recipe to Utilize Carborane Cluster Substituents (M. Uebe, A. Ito, Y. Kameoka, T. Sato, and K. Tanaka) *Chem. Phys. Lett.,* **633**, 190-194 (2015).
30. Highly Efficient Blue Electroluminescence Using Delayed-Fluorescence Emitters with Large Overlap Density between Luminescent and Ground States (K. Shizu, H. Noda, H. Tanaka, M. Taneda, M. Uejima, T. Sato, K. Tanaka, H. Kaji, and C. Adachi) *J. Phys. Chem. C,* **119**, 26283-26289 (2015).
31. para-Bisvinylhexaisobutyl-Substituted T_8 Caged Monomer: Synthesis and Hydrosilylation Polymerization (T. Maegawa, Y. Irie, H. Imoto, H. Fueno, K. Tanaka, and K. Naka) *Polym. Chem.,* **6**, 7500-7504 (2015).
32. Coplanar Oligo(p-phenylenedisilenylene)s as Si=Si Analogues of Oligo(p-phenylenevinylene)s: Evidence for Extended π-Conjugation through the Carbon-Silicon π-Frameworks (L. Li, T. Matsuo, D. Hashizume, H. Fueno, K. Tanaka, and K. Tamao) *J. Am. Chem. Soc.,* **137**, 15026-15035 (2015).

33. Isolation and Characterization of Persistent Radical Cation and Dication of 2,7-Bis(dianisylamino)pyrene (R. Kurata, K. Tanaka, and A. Ito) *J. Org. Chem.,* **81**, 137-145 (2016).
34. (Z)-1,2-Di(1-pyrenyl)disilene: Synthesis, Structure, and Intramolecular Charge-Transfer Emission (M. Kobayashi, N. Hayakawa, T. Matsuo, B. Li, T. Fukunaga, D. Hashizume, H. Fueno, K. Tanaka, and K. Tamao) *J. Am. Chem. Soc.,* **138**, 758-761 (2016).
35. Synthesis and Characterization of 6,13-Diamino-Substituted Pentacenes (A. Ito, M. Uebe, K. Takahashi, H. Ishikawa, D. Sakamaki, H. Sato, T. Matsumoto, and K. Tanaka) *Chem. Eur. J.,* **22**, 2165-2170 (2016).
36. O_2-Triggered Directional Switching of Photocurrent in Self-Assembled Monolayer Composed of Porphyrin- and Fullerene-Terminated Helical Peptides on Gold (H. Uji, K. Tanaka, and S. Kimura) *J. Phys. Chem. C,* **120**, 3684-3689 (2016).
37. Synthesis and Magnetic Properties of Linear Two-coordinate Monomeric Diaryliron(II) Complexes Bearing Fused-ring Bulky “Rind” Groups (S. Goda, M. Nikai, M. Ito, D. Hashizume, K. Tamao, A. Okazawa, N. Kojima, H. Fueno, K. Tanaka, Y. Kobayahsi, and T. Matsuo) *Chem. Lett.,* **45**, 634-636 (2016).
38. Thermodynamical Vibronic Coupling Constant and Density: Chemical Potential and Vibronic Coupling in Reactions (T. Sato, N. Haruta, and K. Tanaka) *Chem. Phys. Lett.,* **652**, 157-161 (2016).
39. Color Tuning of Alternating Conjugated Polymers Composed of Pentaazaphenanthrene by Modulating Their Unique Electronic Structures Involving Isolated-LUMOs (H. Watanabe, M. Hirose, K. Tanaka, K. Tanaka, and Y. Chujo) *Polym. Chem.,* **7**, 3674-3680 (2016).
40. Arsole-Containing π-Conjugated Polymer by the Post-Element-Transformation Technique (Y. Matsumura, M. Ishidoshiro, Y. Irie, H. Imoto, K. Naka, K. Tanaka, S. Inagi, and I. Tomita) *Angew. Chem. Int. Ed.,* **55**, 15040-15043 (2016).
41. Radical Cation of an Oligoarylamine Having a Nitroxide Radical Substituent: A Coexistent Molecular System of Localized and Delocalized Spins (A. Ito, R. Kurata, Y. Noma, Y. Hirao, and K. Tanaka) *J. Org. Chem.,* **81**, 11416-11420 (2016).
42. Borophosphonate Cages as Element-blocks: Ab Initio Calculation of the Electronic Structure of a Simple Borophosphonate, $[HPO_3BH]_4$, and Synthesis of Two Novel Borophosphonate Cages with Polymerizable Groups (J. Zapico, M. Shirai, R. Sugiura, N. Idota, H. Fueno, K. Tanaka, and Y. Sugahara) *Chem. Lett.,* **46**, 181-184 (2017).
43. Stereoisomerization of 1,4-Dihydroarsinetetracarboxylic Acid Diimides under Non-acidic Condition from cis- to trans-Forms (K. Naka, T. Kato, K. Abe, M. Ishidoshiro, S. Nishiyama, S. Tanaka, H. Imoto, S. Watase, K. Matsukawa, H. Fueno, and K. Tanaka) *Heterocycles*, **94**, 923-937 (2017).
44. Studies of Spherically Distributed LUMO and Electron-Accepting Properties of Caged Hexakis(germasesquioxanes) (J. Ohshita, T. Tsuchida, K. Komaguchi, K. Yamamoto, Y. Adachi, Y. Ooyama, Y. Harima, and K. Tanaka) *Organometallics*, **36**, 2536-2540 (2017).
45. Induced-Dipole-Directed, Cooperative Self-Assembly of a Benzotrithiophene (T. Ikeda, H. Adachi, H. Fueno, K. Tanaka, and T. Haino) *J. Org. Chem.,* **82**, 10062-10069 (2017).
46. A Stable Free Tetragermacyclobutadiene Incorporating Fused-ring Bulky EMind Groups (K. Suzuki, Y. Numata, N. Fujita, N. Hayakawa, T. Tanikawa, D. Hashizume, K. Tamao, H. Fueno, K. Tanaka, and T. Matsuo) *Chem. Commun.,* **54**, 2200-2203 (2018).

（以上学術論文）

【学術関係の受賞など】

2002-2007年　科学技術振興機構（JST）の戦略的創造研究推進事業（CREST）「精密分子設計に基づくナノ電子デバイス構築」研究代表者

2004-2005年　文部科学省知的クラスター創成事業「京都ナノテククラスター」のナノテク共同研究テーマ「mRNAの数理学的特異性抽出ソフトの開発と解析サービスの事業化展開」研究代表者

⑺ リサーチリーダー

【氏名】	高塚　和夫　（たかつか　かずお）
【職名】	リサーチリーダー
【所属】	福井謙一記念研究センター
【研究室】	209
【直通電話】	075-711-7902
【FAX】	075-711-7902
【電子メールアドレス】	kaztak@fukui.kyoto-u.ac.jp
【ホームページ】	http://mns2.fukui.kyoto-u.ac.jp
【研究分野】	理論化学，分子科学基礎論
【現在の研究課題】	非断熱電子動力学による化学反応論，超高速励起状態化学，化学動力学理論，多体量子動力学理論
【研究内容キーワード】	化学動力学・電子波束動力学・非断熱現象の科学・レーザー化学
【学歴】	1978年3月　大阪大学大学院基礎工学研究科化学系専攻学位取得卒業
【学位】	工学博士
【略歴】	1978年8月　ノースダコタ州立大学　博士研究員 1979年9月　カルフォルニア工科大学博士研究員 1982年1月　岡崎国立共同研究機構分子科学研究所理論研究系助手 1987年4月　名古屋大学教養部助教授（名古屋大学大学院工学研究科および理学研究科を担当） 1992年4月　名古屋大学大学院人間情報学研究科教授 1997年10月－2016年3月　東京大学大学院総合文化研究科教授 1998年4月－2016年3月　東京大学教授　理学系研究科化学専攻（兼担） 2001年4月－2016年3月　自然科学研究機構分子科学研究所教授（兼任）
【所属学会】	日本化学会，日本物理学会，アメリカ化学会，分子科学会，理論化学会
【学会活動】	計算分子科学研究拠点長（2016年3月まで）．各種評価委員会委員（非公開），Chem. Phys. 誌等編集委員
【主な著書、学術論文】 （過去5年以内）	論文 1. T. Yonehara, K. Hanasaki, K. Takatsuka.“Fundamental approaches to nonadiabaticity: Towards a chemical theory beyond the Born-Oppenheimer paradigm” *Chemical Reviews,* **112**, 499-542 (2012) 2. K. Takatsuka, S. Takahashi “Towards many-dimensional real-time quantum theory for heavy particle dynamics. II. Beyond semiclassics by quantum smoothing of singularity in quantum-classical correspondence” *Phys. Rev. A* **89**, 012109 (12 pages) (2014). 3. Kentaro Yamamoto and Kazuo Takatsuka “On photocatalytic cycle of water splitting with small manganese oxides and the roles of water cluster as a direct resource of oxygen molecules.” *PCCP,* **20**, 6708-6725 (2018) 4. Kazuo Takatsuka “Lorentz-like force emerging from kinematic interactions between electrons and nuclei in molecules. A quantum mechanical origin of symmetry breaking that can trigger molecular chirality.” *J. Chem. Phys.* **146**, 084312 (10 pages) (2017). 5. Kazuo Takatsuka “Theory of molecular nonadiabatic electron dynamics in condensed phases.” *J. Chem. Phys.* **147**, 174102 (13 pages) (2017). 単行本 1. Kazuo Takatsuka, Takehiro Yonehara, Kota Hanasaki, and Yasuki Arasaki “Chemical Theory beyond the Born-Oppenheimer Paradigm: Nonadiabatic Electronic and Nuclear Dynamics in Chemical Reactions”, (World Scientific, Singapore, 2014) 2. 高塚和夫，田中秀樹「分子熱統計力学」（東京大学出版会，2014）
【学術関係の受賞など】	分子科学会賞（2013年），日本化学会賞（2014年），Mizushima-Raman Lectureship Award（2016年）

⑻ 研究員

【氏名】	北浦　和夫（きたうら　かずお）
【職名】	研究員
【所属】	福井謙一記念研究センター　榊グループ
【電子メールアドレス】	kazuo.kitaura@riken.jp
【研究分野】	計算化学
【現在の研究課題】	巨大分子系の電子状態計算法
【研究内容キーワード】	巨大分子・タンパク質・電子状態
【学歴】	1976年3月 大阪市立大学理学研究科化学専攻博士課程修了
【学位】	1976年3月 理学博士（大阪市立大学）
【略歴】	1979年8月 分子科学研究所理論研究系助手、1981年9月 大阪市立大学理学部助手、1989年7月 岡崎国立共同研究機構分子科学研究所助教授（電子計算機センター）、1993年4月 大阪府立大学総合科学部教授、2001年7月 産業技術総合研究所計算科学研究部門グループ長、2007年4月 京都大学薬学研究科教授、2011年12月 神戸大学システム情報学研究科特命教授、2016年4月 京都大学福井謙一記念研究センター研究員
【所属学会】	日本化学会、日本薬学会
【主な著書、学術論文】（過去5年以内）	1. Hiroya Nakata, Takeshi Nagata, Dmitri G. Fedorov, Satoshi Yokojima, Kazuo Kitaura, Shinichiro Nakamura, "Analytic second derivatives of the energy in the fragment molecular orbital method", *J. Chem. Phys.* **138**, 164103 (2013). 2. Nakanishi, Isao; Murata, Katsumi; Nagata, Naoya; Masakuni Kurono, Takayoshi Kinoshita, Misato Yasue, Takako Miyazaki, Yoshinori Takei, Shinya Nakamura, Atsushi Sakurai, Nobuko Iwamoto, Keiji Nishiwaki, Tetsuko Nakaniwa,Y usuke Sekiguchi, Akira Hirasawa, Gozoh Tsujimoto Kazuo Kitaura, "Identification of protein kinase CK2 inhibitors using solvent dipole ordering virtual screening", *Eur. J. Med. Chem.* 96, 396-404 (2015). 3. Fedorov, Dmitri G.; Kitaura Kazuo, "ubsystem Analysis for the Fragment Molecular Orbital Method and Its Application to Protein-Ligand Binding in Solution", *J. Phys. Chem. A,* **120**, 2218-2231 (2016).

Ⅱ　博士研究員等

１．博士研究員組織

平成２９年度

職　名		氏　名
福井センターフェロー		多羅間 充輔
		伊丹 將人
		藪中 俊介
		Schnyder, Simon Kaspar
諸熊グループ	福井センターフェロー	伊勢川 美穂
		鈴木 聡
	研究フェロー	Sharma, Akhilesh Kumar
		Puripat, Maneeporn
榊グループ	福井センターフェロー	青野 信治
	研究フェロー	中垣 雅之
		Zheng, Hong
		Lu, Jing
		Zhong, Ronglin
		Julong. Jiang
高塚グループ	研究フェロー	松岡 貴英
		山本 憲太郎
		長谷川 太祐
		新崎 康樹

２．日本学術振興会外国人特別研究員

職　名		氏　名
榊グループ	外国人特別研究員	Ren, Xuefeng

３．日本学術振興会特別研究員

職　名		氏　名
高塚グループ	特別研究員	松崎 黎

４．博士研究員プロフィール

【氏名】	多羅間　充輔　（たらま　みつすけ）
【職名】	特定研究員
【所属】	福井謙一記念研究センター
【研究室】	208
【直通電話】	711-7863
【電子メールアドレス】	tarama@fukui.kyoto-u.ac.jp
【ホームページ】	http://www.fukui.kyoto-u.ac.jp/users/tarama/index.html
【研究分野】	非線形ダイナミクス、アクティブマター、ソフトマター
【現在の研究課題】	アクティブソフトマターのダイナミクス
【研究内容キーワード】	アクティブマター、ダイナミクス、変形、非線形ダイナミクス、細胞運動
【学歴】	修士（理学）2012/3/26　京都大学理学研究科 博士（理学）2015/3/23　京都大学理学研究科
【学位】	博士（理学）
【略歴】	福井センターフェロー（2015/4/1 より）
【所属学会】	日本物理学会
【学会活動】	アクティブマター研究会 2016（2016 年 1 月 22-23 日）の世話人をしました。 アクティブマター研究会 2017（2017 年 1 月 20-21 日）の世話人をしました。 アクティブマター研究会 2018（2018 年 1 月 19-20 日）の世話人をしました。
【主な著書、学術論文】（過去 5 年以内）	1. M. Tarama, Y. Itino, A.M. Menzel, and T. Ohta, "Individual and collective dynamics of self-propelled soft particles”, *Eur. Phys. J. Special Topics* **223**, 121–139 (2014). 2. M. Tarama, A.M. Menzel, and H. Löwen, "Deformable microswimmer in a swirl: Capturing and scattering dynamics”, *Phys. Rev. E* **90**, 032907 (2014). 3. M. Tarama, P. Cremer, D.Y. Borin, S. Odenbach H. Löwen, and A.M. Menzel, "Tunable dynamic response of magnetic gels: Impact of structural properties and magnetic fields”, *Phys. Rev. E* **90**, 042311 (2014). 4. T. Ohta, M. Tarama and M. Sano, "Simple model of cell crawling”, *Physica D* 318-319, 3-11 (2016). 5. M. Tarama and T. Ohta, "Reciprocating motion of active deformable particles”, *Europhys. Lett.* **114**, 30002 (2016). 6. M. Tarama, “Swinging motion of active deformable particles in Poiseuille flow”, *Phys. Rev. E* **96**, 022602 (2017). 7. M. Tarama, “Dynamics of Deformable Active Particles under External Flow Field”, *J. Phys. Soc. Jpn.* **86**, 101011 (2017). 8. M. Tarama and R. Yamamoto, “Mechanics of cell crawling by means of force-free cyclic motion”, *J. Phys. Soc. Jpn.* **87**, 044803 (2018).
【学術関係の受賞など】	Research Fellow of Japan Society for the Promotion of Science (DC1) (Apr. 2012 - Mar. 2015) ポスター発表 優秀賞（平成24年度未踏科学サマー道場、Aug. 2014） the Richard M. Noyes Fund Fellowship (Jul. 2014)

【氏名】	伊丹　將人　（いたみ　まさと）
【職名】	福井センターフェロー
【所属】	福井謙一記念研究センター
【研究室】	212 号室
【直通電話】	075-711-7894
【電子メールアドレス】	itami@fukui.kyoto-u.ac.jp
【研究分野】	統計物理学
【現在の研究課題】	表面での時空間平均応力ゆらぎの特異性・熱流に誘起された非平衡力
【研究内容キーワード】	ゆらぐ流体力学・大偏差理論・線形応答理論
【学歴】	2016 年 3 月　京都大学大学院理学研究科物理学宇宙物理学専攻博士課程修了
【学位】	2016 年 3 月　博士（理学）（京都大学）
【略歴】	2016 年 4 月　京都大学福井謙一記念研究センター・福井センターフェロー
【所属学会】	日本物理学会
【主な著書、学術論文】（過去 5 年以内）	1. Masato Itami and Shin-ichi Sasa, "Universal Form of Stochastic Evolution for Slow Variables in Equilibrium Systems" *J. Stat. Phys.* **167**, 46-63 (2017). 2. Masato Itami and Shin-ichi Sasa, "Derivation of Stokes' Law from Kirkwood's Formula and the Green-Kubo Formula via Large Deviation Theory" *J. Stat. Phys.* **161**, 532-552 (2015). 3. Masato Itami and Shin-ichi Sasa, "Nonequilibrium Statistical Mechanics for Adiabatic Piston Problem" *J. Stat. Phys.* **158**, 37-56 (2015). 4. Masato Itami and Shin-ichi Sasa, "Macroscopically measurable force induced by temperature discontinuities at solid-gas interfaces" *Phys. Rev. E* **89**, 052106 (2014).

【氏名】	藪中　俊介（やぶなか　しゅんすけ）
【職名】	福井センターフェロー
【所属】	京都大学福井謙一記念研究センター
【直通電話】	075-711-
【FAX】	075-781-4757
【電子メールアドレス】	yabunaka@fukui.kyoto-u.ac.jp
【ホームページ】	http://statphys.scphys.kyoto-u.ac.jp/~yabunaka/yabunaka/Welcome.html
【研究分野】	ソフトマター物理
【現在の研究課題】	選択的溶媒和効果を取り入れた電気二重層のダイナミクスの研究、アクティブ流体力学
【研究内容キーワード】	選択的溶媒和効果、電気二重層、アクティブマター
【学歴】	2014 年 3 月　京都大学大学院理学研究科物理学宇宙物理学専攻博士後期課程修了
【学位】	2014 年 3 月　理学博士（京都大学）
【略歴】	2012 年 4 月　JSPS Research Fellow (DC) 2014 年 4 月　JSPS Research Fellow (PD) 2016 年 12 月　京都大学福井謙一記念研究センターフェロー
【所属学会】	日本物理学会
【主な著書、学術論文】（過去 5 年以内）	1. “Collision between chemically-driven self-propelled drops”, Shunsuke Yabunaka and Natsuhiko Yoshinaga, *Journal of Fluid Mechanics,* November 2016, Pages 205-233 2. “Structure formation due to antagonistic salts”, Akira Onuki, Shunsuke Yabunaka, Takeaki Araki and Ryuichi Okamoto *Current Opinion in Colloid & Interface Science* Volume **22**, April 2016, Pages 59–64 3. “Functional renormalization group approach to noncollinear magnets”, B. Delamotte, M. Dudka, D. Mouhanna, and S. Yabunaka, *Phys. Rev. B* **93**, 064405 4. “Electric double layer composed of an antagonistic salt in an aqueous mixture: Local charge separation and surface phase transition”, Shunsuke Yabunaka,and Akira Onuki, *Physical review letters* **119**, 118001, (2017) 5. “Surprises in O (N) Models: Nonperturbative Fixed Points, Large N Limits, and Multicriticality”, Shunsuke Yabunaka and Bertrand Delamotte, *Physical review letters* **119**, 191602 (2017)
【学術関係の受賞など】	JSPS Research Fellowships for Young Scientists(DC) 2012-2014 JSPS Research Fellowships for Young Scientists(PD) 2014-2017 Journal of Chemical Physics Editors’choice 2015

【氏名】	Simon Kaspar Schnyder
【職名】	FIFC Fellow
【所属】	Fukui Institute for Fundamental Chemistry
【研究室】	Room 208
【直通電話】	075-711-7863
【電子メールアドレス】	schnyder@fukui.kyoto-u.ac.jp
【研究分野】	Soft matter physics, Biophysics, Computational physics
【現在の研究課題】	Structure and dynamics of cellular tissues, anomalous transport in heterogeneous media
【研究内容キーワード】	Cell migration, Epithelial tissues, Lorentz model, Porous media, Percolation, Anomalous diffusion
【学歴】	January 2010, Diploma in Physics, University of Konstanz, Konstanz, Germany May 2014, Doctor of Science , University of Düsseldorf, Düsseldorf, Germany
【学位】	Doctor of Science from University of Düsseldorf
【略歴】	June 2014 - November 2014, Postdoctoral Fellow, University of Düsseldorf December 2014 - December 2016, Postdoctoral Fellow, Department of Chemical Engineering, Kyoto University January 2017 - now, FIFC Fellow, Fukui Institute for Fundamental Chemistry, Kyoto University
【所属学会】	German Physical Society (DPG)
【主な著書、学術論文】 （過去 5 年以内）	1. S. K. Schnyder, & J. Horbach, “Crowding of interacting fluid particles in porous media through molecular dynamics: breakdown of universality for soft interactions”, *Physical Review Letters,* **120**(7), 78001 (2018). 2. J. Horbach, N. H. Siboni, & S. K. Schnyder, “Anomalous transport in heterogeneous media“, *The European Physical Journal Special Topics,* **226**(14), 3113–3128 (2017). 3. S. K. Schnyder, J. J. Molina, Y. Tanaka, R. Yamamoto, “Collective motion of cells crawling on a substrate: roles of cell shape and contact inhibition“, *Scientific Reports* **7**, 5163 (2017). 4. S. K. Schnyder, T. O. E. Skinner, A. Thorneywork, D. G. A. L. Aarts, J. Horbach, R. P. A. Dullens, “Dynamic heterogeneities and non-Gaussian behaviour in 2D randomly confined colloidal fluids”, *Physical Review E* (2017). 5. M. Heinen, S. K. Schnyder, J. F. Brady, H. Löwen, “Classical liquids in fractal dimension”, *Physical Review Letters* **115**, 097801 (2015). 6. S. K. Schnyder, M. Spanner, F. Höfling, T. Franosch, J. Horbach, “Rounding of the localization transition in model porous media”, *Soft Matter* **11**, 701 (2015).

【氏名】	伊勢川　美穂　（いせがわ　みほ）
【職名】	助教
【所属】	カーボンニュートラル・エネルギー国際研究所（I^2CNER），九州大学
【研究室】	I^2CNER, NEXT-FC
【直通電話】	092-802-6741
【電子メールアドレス】	isegawa.miho.169@m.kyushu-u.ac.jp
【研究分野】	計算化学
【現在の研究課題】	Reaction process for electrochemical and photochemical conversion of carbon dioxide
【研究内容キーワード】	触媒、分子変換機構、スペクトロスコピー、化学エネルギー変換
【学歴】	2009年9月 京都大学大学院理学研究科化学専攻博士課程修了
【学位】	2009年9月 京都大学理学博士
【略歴】	2010年1月　米国ミネソタ大学博士研究員 2013年3月　京都大学福井謙一記念研究センター研究員 2014年6月　ドイツ マックスプランク研究所化学エネルギー変換博士研究員 2016年1月　京都大学福井謙一記念研究センター研究員 2018年2月　九州大学、I^2CNER 助教
【主な著書、学術論文】 （過去5年以内）	1. DFT Study on Fe(IV)-Peroxo Formation and H Atom Triggered O_2 activation by NiFe Hydrogenase, M. Isegawa, A. K. Sharma, S. Ogo, K. Morokuma., *Organomettalics,* **37**, 1534 (2018). 2. Copper-catalyzed Enantioselective Boron Conjugate Addition: DFT and AFIR Study on Different Selectivities of Cu(I) and Cu(II) Catalysts, M. Isegawa, W. M. C. Sameera, A. K. Sharma, T. Kitanosono, Masako Kato, S. Kobayashi, K. Morokuma., *ACS Catalysis,* **7**, 5370 (2017). 3. Ionization Energies and Aqueous Redox Potentials of Organic Molecules: Comparison of DFT, Correlated ab Initio Theory and Pair Natural Orbital Approaches, M. Isegawa, F. Neese, D. A. Pantazis, *J.Chem. Theory Comput.* **12**, 2272 (2016). 4. Photochemical Ring Opening and Closing of Three Isomers of Diarylethene: Spin-Flip Time Dependent Density Functional Study, M. Isegawa and K. Morokuma, *J. Phys. Chem. A.* **119**, 4191 (2015). 5. Ab initio reaction pathways for photodissociation and isomerization of nitromethane on four singlet potential energy surfaces with three roaming paths, M. Isegawa, F. Liu, S. Maeda, K. Morokuma, *J. Chem. Phys.* **140**, 244310 (2014). 6. Predicting pathways for terpene from first principles-routes to known and new sesquiterpenes, M. Isegawa, S. Maeda, D. J. Tantillo, and K. Morokuma *Chemical Science,* **5**, 1555 (2014).

【氏名】	鈴木　聡　（すずき　さとし）
【職名】	研究員
【所属】	福井謙一記念研究センター
【研究室】	福井謙一記念研究センター　212 号室
【直通電話】	075-711-7647
【電子メールアドレス】	suzuki@fukui.kyoto-u.ac.jp
【研究分野】	理論化学　計算化学
【現在の研究課題】	蛍光分子の円錐交差探索
【研究内容キーワード】	励起状態、項間交差
【学歴】	2014 年 3 月　九州大学理学府　化学専攻修了
【学位】	2014 年 3 月　博士（理学）　九州大学
【略歴】	2014 年 4 月　福井謙一記念研究センター
【所属学会】	分子科学会、理論化学研究会
【主な著書、学術論文】 （過去 5 年以内）	1. S.Suzuki, S. Maeda, K. Morokuma, Exploration of Quenching Pathways of Multiluminescent Acenes Using the GRRM Method with the SF-TDDFT Method, *J. Phys. Chem. A,* **119** pp 11479-11487 (2015) 2. S.Sasaki, S.Suzuki, W.M.C. Sameera, K. Igawa, K. Morokuma, G. Konishi, Highly twisted N,N-dialkylamines as a design strategy to tune simple aromatic hydrocarbons as steric environment-sensitive fluorophores, *J. Am. Chem. Phys.*, **138**, 8194-8206 (2016) 3. S.Sasaki, S.Suzuki, K. Igawa, K. Morokuma, G. Konishi, The K-Region in Pyrenes as a Key Position to Activate Aggregation-Induced Emission: Effects of Introducing Highly Twisted N,N-Dimethylamines, *J. Org. Chem.,* **82**, 6865-6873 (2017)
【学術関係の受賞など】	2012 年 9 月　Best Poster Awardsat the Annual Meeting of the Japan Society for Molecular Science

【氏名】	Akhilesh Kumar Sharma
【職名】	Postdoctoral Fellow
【所属】	Fukui Institute for Fundamental Chemistry
【研究室】	Room No. 207
【直通電話】	075-711-7893
【FAX】	075-781-4757
【電子メールアドレス】	sharma@fukui.kyoto-u.ac.jp
【研究分野】	Computational Chemistry
【現在の研究課題】	Mechanistic study of organic and organometalic reactions
【研究内容キーワード】	DFT, AFIR, Reaction Mechanism, Stereoselectivity
【学歴】	Master of Science, Himachal Pradesh University, Shimla, India (2006)
【学位】	Ph.D., Indian Institute of Technology (IIT), Bombay, Mumbai, India (2014)
【略歴】	Research Associate, Indian Institute of Technology (IIT), Bombay, Mumbai, India (2014-2015)
【主な著書、学術論文】 （過去 5 年以内）	1. W. M. C. Sameera, Akhilesh K. Sharma, Satoshi Maeda, Keiji Morokuma, “Artificial Force Induced Reaction Method for Systematic Determination of Complex Reaction Mechanisms” *Chemical Record,* **16** (5), 2349-2363 (2016). 2. Ming-Chung Yang, Akhilesh K. Sharma, W. M. C. Sameera, Keiji Morokuma, and Ming-Der Su, “Theoretical Study of Addition Reactions of L4M(M = Rh, Ir) and L2M(M = Pd, Pt) to Li+@C60” *J. Phys. Chem. A,* **121** (13), 2665-2673 (2017). 3. Miho Isegawa, W. M. C. Sameera, Akhilesh K. Sharma, Taku Kitanosono, Masako Kato, Shu Kobayashi, and Keiji Morokuma, "Copper-catalyzed Enantioselective Boron Conjugate Addition: DFT and AFIR Study on Different Selectivities of Cu(I) and Cu(II) Catalysts" *ACS Catal.,* **7** (8), 5370–5380 (2017). 4. Akhilesh K. Sharma, W. M. C. Sameera, Masayoshi Jin, Laksmikanta Adak, Chiemi Okuzono, Takahiro Iwamoto, Masako Kato, Masaharu Nakamura, and Keiji Morokuma “DFT and AFIR Study on the Mechanism and the Origin of Enantioselectivity in Iron-Catalyzed Cross-Coupling Reactions” *J. Am. Chem. Soc.,* **139** (45), 16117-16125 (2017). 5. Miho Isegawa, Akhilesh K. Sharma, Seiji Ogo, and Keiji Morokuma, “DFT Study on Fe(IV)-Peroxo Formation and H Atom Transfer Triggered O_2 Activation by NiFe Complex” *Organometallics,* **37**(10), 1534-1545 (2018).
【学術関係の受賞など】	“2014 Eli Lilly and Company Asia Outstanding Thesis Award” for Best Thesis Fellowship from council for Scientific and Industrial Research (CSIR), India to Pursue PhD.

【氏名】	Maneeporn Puripat
【職名】	Research Fellow
【所属】	Nara Institute of Science and Technology Institute for Research Initiatives Graduate School of Materials Science
【研究室】	8916-5 Takayama-cho, Ikoma, Nara 630-0192, JAPAN
【直通電話】	0743-72-6026
【電子メールアドレス】	puripat@ms.naist.jp
【ホームページ】	http://www.naist.jp/en/
【研究分野】	Theoretical Chemistry
【現在の研究課題】	Theoretical/Computational Chemistry for Complex Molecular Systems
【研究内容キーワード】	Transition state, Catalysis, Catalytic reaction, Reaction mechanism
【学歴】	Ph.D. (Nanoscience Technology), Chulalongkorn University, Thailand (2016) B.Sc. (Physics, 2nd class Hon.), Chulalongkorn University, Thailand (2011)
【学位】	Doctor of Philosophy from Chulalongkorn University, Thailand
【略歴】	1. Special Lecturer, Rajamangala University of Technology Phra Nakhon (RMUTP), Bangkok, Thailand (2012-2016) 2. Research Fellow, Fukui Institute for Fundamental Chemistry (FIFC), Kyoto University, Kyoto, Japan (2016-2017) 3. Lecturer, Rajamangala University of Technology Thanyaburi (RMUTT), Pathum Thani, Thailand (2017-2018) 4. Research Fellow, Nara Institute of Science and Technology, Nara (NAIST), Japan (2018-present)
【主な著書、学術論文】（過去 5 年以内）	1. Maneeporn Puripat, Romain Ramozzi, Miho Hatanaka, Waraporn Parasuk, Vudhichai Parasuk, and Keiji Morokuma, “The Biginelli reaction is a ureacatalyzed organocatalytic multicomponent reaction” *J. Org. Chem.* **80** (14), 6959-6967 (2015). 2. Arifin, Maneeporn Puripat, Daisuke Yokogawa, Vudhichai Parasuk, and Stephan Irle, “Glucose transformation to 5-hydroxymethylfurfural in acidic ionic liquid: A quantum mechanical study” *J. Comput. Chem.* **37** (3), 327-335 (2016). 3. Tomoharu Oku, Masaki Okada, Maneeporn Puripat, Miho Hatanaka, Keiji Morokuma, and Jun-Chul Choi “Promotional effect of CH3I on hydroxycarbonylation of cycloalkene using homogeneous rhodium catalysts with PPh3 ligand” *J. Co2. Util.* **25**, 1-5(2018).
【学術関係の受賞など】	1. The Development and Promotion of Science and Technology Talents Project (DPST) (Royal Government of Thailand scholarship) of Thailand (2004-2016) 2. The New Energy and Industrial Technology Development Organization (NEDO). (2016-present)

【氏名】	青野　信治　（あおの　しんじ）
【職名】	特定研究員
【所属】	京都大学 福井謙一記念研究センター
【研究室】	福井記念研究センター 303 号室
【直通電話】	075-711-7907
【電子メールアドレス】	saono@fukui.kyoto-u.ac.jp
【研究分野】	溶液化学・計算化学・理論化学
【現在の研究課題】	溶液中の遷移金属錯体の化学反応の理論的解析
【研究内容キーワード】	3D-RISM-SCF 法、平均場 QM/MM 法、自由エネルギー解析、溶媒和構造解析、周期的分子結晶解析
【学歴】	2010 年 3 月　京都大学大学院理学研究科化学専攻博士後期課程研究指導認定退学
【学位】	2010 年 9 月　理学博士（京都大学）
【略歴】	2010 年 4 月　京都大学大学院理学研究科化学専攻 研修員 2010 年 5 月　京都大学 物質－細胞統合システム拠点 教務補佐員 2010 年 10 月　京都大学 物質－細胞統合システム拠点 特定研究員 2011 年 4 月　京都大学 福井謙一記念研究センター 特定研究員 2015 年 4 月　京都大学 福井謙一記念研究センター フェロー（榊研）
【所属学会】	分子科学会、理論化学会、錯体化学会
【主な著書、学術論文】 （過去 5 年以内）	1. Aono S., Hosoya T., and Sakaki S., “A 3D-RISM-SCF method with dual solvent boxes for a highly polarized system: application to 1,6-anhydrosugar formation reaction of phenyl alpha- and beta-D-glucosides under basic conditions” *Phys. Chem. Chem. Phys.* **17**, 6368, (2013) 2. Aono S., Nakagaki M., Kurahashi T., Fujii H., and Sakaki S., “Theoretical Study of One-Electron Oxidized Mn(III)− and Ni(II)−Salen Complexes: Localized vs Delocalized Ground and Excited States in Solution” *J. Chem. Theory Comput.* **10**, 1062, (2014). 3. Aono S., Mori T., and Sakaki S., “3D-RISM-MP2 Approach to Hydration Structure of Pt(II) and Pd(II) Complexes: Unusual H-Ahead Mode vs Usual O-Ahead One” *J. Chem. Theory Comput.* **12**, 1189-1206, (2016). 4. Aono S, Nakagaki M., and Sakaki S. “Theoretical Study of One-Electron Oxidized Salen Complexes of Group 7 (Mn(III), Tc(III), and Re(III)) and Group 10 Metals (Ni(II), Pd(II), and Pt(II)) with 3D-RISM-GMC-QDPT Method: Localized vs. Delocalized Ground and Excited States in Solution” *Phys. Chem. Chem. Phys.* **19**, 16831-16849, (2017).

【氏名】	Masayuki Nakagaki
【職名】	FIFC Fellow
【所属】	Fukui Institute for Fundamental Chemistry
【研究室】	Room 303
【直通電話】	075-711-7907
【電子メールアドレス】	nakagaki@fukui.kyoto-u.ac.jp
【ホームページ】	http://www.fukui.kyoto-u.ac.jp/
【研究分野】	Computational Chemistry
【現在の研究課題】	Electronic Structure of Inverted Sandwich Type Complexes
【研究内容キーワード】	Electronic Structure of Metal Complex, Multireference Theory
【学歴】	March 2005, Master of Sci., Graduate School of Science, Kyushu University March 2009, Doctor of Sci., Graduate School of Science, Kyushu University
【学位】	Doctor of Science from Kyushu University
【略歴】	Apr. 2009, Postdoctoral Fellow, Kyushu University
【所属学会】	Japan Society for Molecular Science The Chemical Society of Japan
【主な著書、学術論文】（過去５年以内）	1. Masayuki Nakagaki and Shigeyoshi Sakaki ““Hetero-dinuclear complexes of 3d metals with a bridging dinitrogen ligand: theoretical prediction of the characteristic features of geometry and spin multiplicity” *Phys. Chem. Chem. Phys.,* **18**, 26365-26375 (2016). 2. Takako Muraoka, Haruhiko Kimura, Gama Trigagema, Masayuki Nakagaki, Shigeyoshi Sakaki, and Keiji Ueno “Reactions of Silanone(silyl)tungsten and -molybdenum Complexes with MesCNO, (Me$_2$SiO)$_3$, MeOH, and H2O: Experimental and Theoretical Studies” *Organometallics,* **36**, 1009-1018(2017). 3. Masayuki Nakagaki and Shigeyoshi Sakaki “CASPT2 study of inverse sandwich-type dinuclear 3d transition metal complexes of ethylene and dinitrogen molecules: similarities and differences in geometry, electronic structure, and spin multiplicity” *Phys. Chem. Chem. Phys.* **17**, 16294-16305(2015) 4. Masayuki Nakagaki and Shigeyoshi Sakaki “CASPT2 Study of Inverse Sandwich-Type Dinuclear Cr(I) and Fe(I) Complexes of the Dinitrogen Molecule: Significant Differences in Spin Multiplicity and Coordination Structure between These Two Complexes” *J. Phys. Chem. A,* **118**, 1247-1257 (2014) 5. Shinji Aono, Masayuki Nakagaki, Takuya Kurahashi, Hiroshi Fujii, and Shigeyoshi Sakaki “Theoretical Study of One-Electron Oxidized Mn(III)– and Ni(II)–Salen Complexes: Localized vs Delocalized Ground and Excited States in Solution” *J. Chem. Theory Comput.,* **10** 1062-1073 (2014)

【氏名】	Jing Lu
【職名】	Research Fellow
【所属】	Fukui Institute for Fundamental Chemistry
【研究室】	Room 303
【直通電話】	075-711-7907
【電子メールアドレス】	jing@fukui.kyoto-u.ac.jp
【研究分野】	Computational Chemistry
【現在の研究課題】	Theoretical study of bimetallic alloyed nanoclusters/particles
【研究内容キーワード】	Bimetallic alloyed nanoclusters/particles, core-shell structure, oxygen reduction reaction
【学歴】	June 2016, Doctor of Sci., Faculty of Chemistry, Northeast Normal University, P.R. China
【学位】	Doctor of Science from Northeast Normal University
【略歴】	Aug. 2016, Postdoctoral Fellow, FIFC, Kyoto University
【主な著書、学術論文】（過去5年以内）	1. Lu, J.; Ishimura, K.; Sakaki, S., Theoretical Insight into Core–Shell Preference for Bimetallic Pt-M (M = Ru, Rh, Os, and Ir) Cluster and Its Electronic Structure. *J. Phys. Chem. C* **122**, 9081-9090 (2018). 2. Lu, J.; Zheng, Y.; Zhang, J., Computational design of benzo [1,2-b:4,5-b'] dithiophene based thermally activated delayed fluorescent materials. *Dyes and Pigments* **127**, 189-196 (2016). 3. Lu, J.; Zheng, Y.; Zhang, J., Rational design of phenoxazine-based donor-acceptor-donor thermally activated delayed fluorescent molecules with high performance. *Phys. Chem. Chem. Phys.* **17**, 20014-20020 (2015). 4. Lu, J.; Yao, Y.; Shenai, P. M.; Chen, L.; Zhao, Y., Elucidating the enhancement in optical properties of low band gap polymers by tuning the structure of alkyl side chains. *Phys. Chem. Chem. Phys.* **17**, 9541-9551 (2015). 5. Lu, J.; Zheng, Y.; Zhang, J., Tuning the color of thermally activated delayed fluorescent properties for spiro-acridine derivatives by structural modification of the acceptor fragment: a DFT study. *RSC Adv.* **5**, 18588-18592 (2015).

【氏名】	Rong-Lin Zhong
【職名】	Research Fellow
【所属】	Fukui Institute for Fundamental Chemistry
【研究室】	Room 303
【直通電話】	075-711-7907
【FAX】	075-711-7907
【電子メールアドレス】	zhongrl@fukui.kyoto-u.ac.jp
【ホームページ】	http://tcclab.jlu.edu.cn/info/1045/1082.htm
【研究分野】	Computational Chemistry
【現在の研究課題】	Theoretical Study of Complex Systems Including d-electrons
【研究内容キーワード】	Palladium catalysis, oxidative addition, reaction mechanism
【学歴】	June 2010, bachelor of Chemistry Education, Faculty of Chemistry, Northeast Normal University June 2015, Doctor of Physical Chemistry, Institute of Functional Material Chemistry, Faculty of Chemistry, Northeast Normal University
【学位】	Doctor of Physical Chemistry from Northeast Normal University
【略歴】	Otc. 2016, Lecturer, Jilin University
【主な著書、学術論文】 （過去5年以内）	1. Yadav, R. M.; Nagaoka, M.; Kashihara, M.; Zhong, R.-L.; Miyazaki, T.; Sakaki, S.; Nakao, Y. *J. Am. Chem. Soc.,* 2017, **139**, 9423-9426. 2. R.-L. Zhong, H.-L. Xu,* Z.-R. Li* and Z.-M. Su*. Role of Excess Electrons in Nonlinear Optical Response. *J. Phys. Chem. Lett.* 2015, **6**, 612-619 3. R.-L. Zhong, H.-L. Xu,* S.-L. Sun, Y.-Q. Qiu, and Z.-M. Su*. The Excess Electron in a Boron Nitride Nanotube: Pyramidal NBO Charge Distribution and Remarkable First Hyperpolarizability. *Chem. Eur. J.* 2012, **18**, 11350 – 11355. 4. R.-L. Zhong, H.-L. Xu,* S. Muhammad, J. Zhang and Z.-M. Su*. The stability and nonlinear optical properties: Encapsulation of an excess electron compound LiCN/Li within boron nitride nanotubes. *J. Mater. Chem.,* 2012, **22**, 2196–2202. 5. R.-L. Zhong, S.-L. Sun, H.-L. Xu,* Y.-Q. Qiu, and Z.-M. Su*. BN Segment Doped Effect on the First Hyperpolarizibility of Heteronanotubes: Focused on an Effective Connecting Pattern. *J. Phys. Chem. C* 2013, **117**, 10039-10044.
【学術関係の受賞など】	1. 2012, National scholarship for PhD candidate. 2. 2013, Excellent graduate student of Northeast Normal University.

【氏名】	松岡　貴英　（まつおか　たかひで）
【職名】	特別研究員
【所属】	理化学研究所　計算科学センター
【研究室】	501
【直通電話】	078-940-5678
【FAX】	078-304-4975
【電子メールアドレス】	matsuoka@fukui.kyoto-u.ac.jp
【研究分野】	計算分子科学
【学歴】	2011年3月　慶應義塾大学大学院理工学研究科前期博士課程修了 2014年3月　慶應義塾大学大学院理工学研究科後期博士課程修了
【学位】	2014年3月　博士（理学）（慶應義塾大学）
【略歴】	2014年4月　慶應義塾大学准訪問研究員、2015年7月　東京大学特定研究員、 2016年4月　京大福井センター研究フェロー
【所属学会】	日本化学会，分子科学会
【主な著書、学術論文】 （過去5年以内）	1. Takahide Matsuoka, Sayo Oonishi, Satoshi Yabushita, “Theoretical study on angular momentum polarization parameters, branching ratios, and anisotropy parameters of chlorine atoms from Photodissociation of Iodine Monochloride”, *Int. J. Quantum Chem.* **113**(3), 375—381 (2013). 2. Takahide Matsuoka, Satoshi Yabushita, “Theoretical study on the photofragment branching ratios and anisotropy parameters of ICl in the second absorption band”, *Chem. Phys. Lett.* **592**, 75—79 (2014). 3. Takahide Matsuoka, Satoshi Yabushita, “Quantum Interference Effects Theoretically Found in the Photodissociation Processes of the Second Absorption Bands of ICl and IBr Molecules”, *J. Phys. Chem. A* **119**(37), 9609—9620 (2015). 4. Takahide Matsuoka, Kazuo Takatsuka, “Dynamics of photoionization from molecular electronic wavepacket states in intense pulse laser fields: A nonadiabatic electron wavepacket study”, *J. Chem. Phys.* **146**(13), 134114 (2017). 5. Takahide Matsuoka, Kazuo Takatsuka, “Nonadiabatic electron wavepacket dynamics behind molecular autoionization”, *J. Chem. Phys.* **148**(1), 014106 (2018).

【氏名】	山本　憲太郎　（やまもと　けんたろう）
【職名】	研究フェロー
【所属】	福井謙一記念研究センター　高塚グループ
【研究室】	福井謙一記念研究センター　305
【電子メールアドレス】	kyamamoto@fukui.kyoto-u.ac.jp
【研究分野】	理論化学
【現在の研究課題】	非断熱電子動力学理論による化学反応の研究
【研究内容キーワード】	非断熱遷移，電荷分離
【学歴】	2015年3月　東京大学大学院理学系研究科化学専攻博士過程修了
【学位】	2015年3月　理学博士（東京大学）
【略歴】	2014年　東京大学技術補佐員，2015年　東京大学特任研究員
【所属学会】	分子科学会，理論化学研究会
【主な著書、学術論文】 （過去5年以内）	1. K. Yamamoto and K. Takatsuka, "Electronic quantum effects mapped onto non-Born-Oppenheimer nuclear paths: Nonclassical surmounting over potential barriers and trapping above the transition states due to nonadiabatic path-branching", *J. Chem. Phys.* **140**, 124111 (2014). 2. K. Yamamoto and K. Takatsuka, "An Electron Dynamics Mechanism of Charge Separation in the Initial-Stage Dynamics of Photoinduced Water Splitting in X–Mn–Water (X=OH, OCaH) and Electron–Proton Acceptors", *ChemPhysChem* **16**, 2534 (2015). 3. K. Yamamoto and K. Takatsuka, "Dynamical mechanism of charge separation by photoexcited generation of proton–electron pairs in organic molecular systems. A nonadiabatic electron wavepacket dynamics study", *Chem. Phys.* **475**, 39 (2016). 4. K. Yamamoto and K. Takatsuka, "Photoinduced Charge Separation Catalyzed by Manganese Oxides onto a Y-Shaped Branching Acceptor Efficiently Preventing Charge Recombination", *ChemPhysChem* **18**, 537 (2017). 5. K. Yamamoto and K. Takatsuka, "On the photocatalytic cycle of water splitting with small manganese oxides and the roles of water clusters as direct sources of oxygen molecules", *Phys. Chem. Chem. Phys.* **20**, 6708 (2018).

【氏名】	新崎　康樹　（あらさき　やすき）
【職名】	研究フェロー
【所属】	福井謙一記念研究センター　高塚グループ
【研究室】	東京大学駒場キャンパス 16 号館 408
【研究分野】	理論化学
【現在の研究課題】	非断熱動力学理論による化学反応
【研究内容キーワード】	非断熱相互作用、クラスター、励起状態動力学
【学歴】	2000 年 9 月　東京大学大学院総合文化研究科博士課程修了
【学位】	2000 年 9 月　博士（学術）（東京大学）
【略歴】	2000 年 10 月　東京大学インテリジェント・モデリング・ラボラトリー研究員 2002 年 10 月　東京大学大学院総合文化研究科　研究員
【所属学会】	分子科学会
【主な著書、学術論文】（過去 5 年以内）	1. Y. Arasaki and K. Takatsuka, Pulse-train photoelectron spectroscopy of electronic and nuclear dynamics in molecules, *ChemPhysChem* **14**, 1387-1396 (2013). 2. Y. Arasaki, Y. Mizuno, S. Scheit, and K. Takatsuka, Induced photoemission from driven nonadiabatic dynamics in an avoided crossing system, *J. Chem. Phys.* **141**, 234301 (2014, 14 pages). 3. Y. Arasaki, Y. Mizuno, S. Scheit, and K. Takatsuka, Stark-assisted quantum confinement of wavepackets. A coupling of nonadiabatic interaction and CW-laser, *J. Chem. Phys.* **144**, 044107 (2016, 10 pages). 4. Y. Arasaki and K. Takatsuka, Time-resolved photoelectron signals from bifurcating electron wavepackets propagated across conical intersection in path-branching dynamics, *Chem. Phys.* **493**, 42-48 (2017). 5. K. Takatsuka, T. Yonehara, K. Hanasaki, and Y. Arasaki, Chemical Theory Beyond the Born-Oppenheimer Paradigm: Nonadiabatic Electronic and Nuclear Dynamics in Chemical Reactions (*World Scientific,* Singapore, 2014).

５．日本学術振興会外国人特別研究員プロフィール

【氏名】	Xue-Feng Ren
【職名】	Postdoctoral Fellow
【所属】	Morokuma Group, Fukui Institute of Fundamental Chemistry
【研究室】	Room No.212
【直通電話】	075-711-7647
【FAX】	075-781-4757
【電子メールアドレス】	renxf@cumt.edu.cn
【研究分野】	Computational Chemistry
【現在の研究課題】	excited state emission decay
【研究内容キーワード】	DFT, AFIR, PES
【学歴】	Ph.D. Physical Chemistry, Jilin University, Changchun
【学位】	Ph.D. Physical Chemistry, Jilin University, Changchun
【略歴】	Nanjing University, 2010-2012, Ph.D fellow China University of Mining and Technology, Xuzhou, associate professor
【主な著書、学術論文】 （過去5年以内）	1. Xue-Feng Ren, Guo-Jun Kang, Qiong-Qiong He, and et. al, *Theor Chem Acc* 2016, **135**, 24 2. Xue Feng Ren, Guo Jun Kang, Shou Feng Zhang, and et. Al, *J. Photochem. Photobio. A: Chemistry,* 2015, **311**, 85 3. Guo Jun Kang, Xue Feng Ren,* Si Yu Bai, *J Organomet. Chem.* 2015, **785**, 44
【学術関係の受賞など】	JSPS Research Fellowships

６．日本学術振興会特別研究員プロフィール

【氏名】	松崎　黎　（まつざき　れい）
【職名】	FIFC フェロー
【所属】	高塚グループ
【研究室】	福井記念研究センター 303
【直通電話】	711-7907
【FAX】	711-7907
【電子メールアドレス】	matsuzaki@fukui.kyoto-u.ac.jp
【ホームページ】	http://mns2.fukui.kyoto-u.ac.jp/
【研究分野】	計算化学
【現在の研究課題】	非断熱電子動力学における核の量子性
【研究内容キーワード】	非断熱系、核の量子性
【学歴】	2017年3月　慶應義塾大学大学院基礎理工学専攻博士課程修了
【学位】	2017年3月　博士（理学）
【略歴】	2015年4月　慶應義塾大学助教（有期・研究奨励）、2016年4月　日本学術振興会特別研究員DC2、2017年4月　日本学術振興会特別研究員PD、2018年4月　福井謙一記念研究センター フェロー
【所属学会】	日本化学会、分子科学会
【主な著書、学術論文】（過去 5 年以内）	1. R.Matsuzaki, S.Asai, C.W.McCurdy, S.Yabushita, “Construction of complex STO-NG basis sets by the method of least squares and their applications”, *Theoretical Chemistry Accounts,* **133**, 1521 (2014) 2. R.Matsuzaki, S.Yabushita, “Optimization of complex slater-type functions with analytic derivative methods for describing photoionization differential cross sections”, *J.Comput.Chem*. **38**, 910 (2017) 3. R. Matsuzaki, S.Yabushita, “Calculation of photoionization differential cross sections using the complex Gauss-type orbitals”, *J.Comput.Chem*. **38**, 2030 (2017)
【学術関係の受賞など】	Journal of Physics B Atomic, Molecular and Optical Physics Best Poster Award 2013

Ⅲ　研究広報活動

１．福井謙一記念研究センターシンポジウム

第15回 京都大学 福井謙一記念研究センターシンポジウム

日　　時　2018年2月2日（金）　10:00 – 19:00

場　　所　京都大学 福井謙一記念研究センター（3F 大会議室）

講　　演　10:15 – 11:15
佐々　真一　（京都大学 大学院理学研究科）
「気液転移と熱伝導が出会うとき：19世紀科学から21世紀科学への展開」

11:30 – 12:30
北浦　和夫　（京都大学 福井謙一記念研究センター）
「The Group Molecular Orbital Method For Large Molecular Systems」

―　休　憩　―

13:50 – 14:50
幾原　雄一　（東京大学 大学院工学研究科）
「原子直視STEM法の新展開と材料科学への応用」

15:00 – 15:30　福井謙一奨励賞表彰式

15:30 – 17:20　ポスターセッション

17:30 – 19:00　懇親会（１F 多目的ルーム）

２．セミナー

(1) 第 15 回 福井センターセミナー

日　　時　2017 年（平成 29 年）5 月 25 日（木）　15:00 – 17:20

場　　所　京都大学 福井謙一記念研究センター（１階 106 室）

15:00 – 15:40
Yoshio Nishimoto (Kyoto Univ.)
“Analytic Derivatives with Fractional Occupation Number”

15:40 – 16:20
Mitsusuke Tarama (Kyoto Univ.)
“Nonlinear Dynamics of Active Deformable Particles : From Liquid Droplets to Biological Cells”

― Break ―

16:30 – 17:20
Dmitri G.Fedorov (Advanced Industrial Science and Technology)
“Large Scale Quantum-Mechanical Calculations with the Fragment Molecular Orbital Method”

(2) その他のセミナー

Contact	Speaker	Title	Affiliation	Date
Kazuo Takatsuka	Mikiya Fujii	Change separation pathways in P3HT/PCBM photovoltaic blends, and their crystalline dependencies.	The University of Tokyo	June 9 (Fri), 2017

Contact	Speaker	Title	Affiliation	Date
Shigeyoshi Sakaki	Alena Kremleva	Quantum chemical modeling of electrochemistry of Mn substituted Keggin polyoxoanions. Effects of electrolyte environment	Technische Universität München	November 1 (Wed), 2017
Shigeyoshi Sakaki	Vladimir G. Malkin	Relativistic calculations of EPR parameters And their interpretation	Slovak Academy Of Sciences	December 11 (Mon), 2017
	Olga L. Malkina	Contact betweek hydrogen atoms observed by through--space indirect NMR coupling	Slovak Academy Of Sciences	
Shigeyoshi Sakaki	Marek J. Wójcik	Theoretical Modeling of Vibrational Spectra of Hydrogen-Bonded Systems, Ice and Aqueous Ionic Solutions	Jagiellonian University	January 24 (Wed), 2018
Shigeyoshi Sakaki	Hirotaka Ihara	Self-organization-based Supramolecular Gel: Molecular Design and Applications	Kumamoto University	February 5 (Mon), 2018
Shigeyoshi Sakaki	Weston T. Borden	Why Are N_2 and O_2 Unreactive?	University of North Taxas	March 27 (Tue), 2018

3. 国際交流

当センター教員が海外の研究機関を訪問し、研究所の運営に関して意見交換を行った。（資料編を参照）

4. 社会へのアウトリーチ活動

＜研究紹介＞

（１）京都大学アカデミックデイへ参加　2017年（平成29年）9月30日

高塚 和夫 リサーチリーダー他が「ポスターを使っての対話」コーナーへ参加

ポスタータイトル：分子科学の超高速実験と動的電子描像

榊 茂好 リサーチリーダー他が「ちゃぶ台で対話」コーナーへ参加

話　題：フロンテイア軌道理論；役に立つの？

場　所：京都大学百周年時計台記念館

＜学術講演＞

（２）田中 一義 シニアリサーチフェロー　2017年（平成29年）11月2日

演　題：計算化学はどのように役立つか

行事名：京都グリーンケミカル・ネットワーク人材育成事業

場　所：京都市成長産業創造センター

5. 福井謙一奨励賞の創設及び奨励賞の授与

福井謙一博士の生誕百年を控え、日頃から、化学の将来の発展のためには若手研究者の育成の大切さを説いておられた福井博士の意志を汲み、基礎化学、理論化学の分野で顕著な研究業績を挙げた若手研究者を顕彰する福井謙一奨励賞を創設した。

平成29年秋に公募し、応募のあった中から委員会で選考の結果、次のとおり選考された。表彰式は、平成30年2月2日（金）に開催の福井謙一記念研究センターシンポジウムの中で行い受賞者に表彰状と記念楯が授与され、続いて受賞題目に関した講演が行われた。

受賞者：越知 正之（大阪大学　大学院理学研究科　助教）

受賞題目：第一原理波動関数理論の固体への展開：量子化学と固体電子論の融合

Ⅳ　研究業績

１．専任教員

Yoshio Nishimoto

Program-Specific Assistant Professor

1. Summary of the research of the year

Development of FMO-DFTB/AFO

Recent progress in linear-scaling quantum mechanical methods enables large-scale calculations for more than one million atoms. The fragment molecular orbital (FMO) method is one of the linear-scaling methods, and a combination with the density-functional tight-binding (DFTB) method is potentially applicable to even larger systems. I have been developing the combination, FMO-DFTB method [1], in these years.

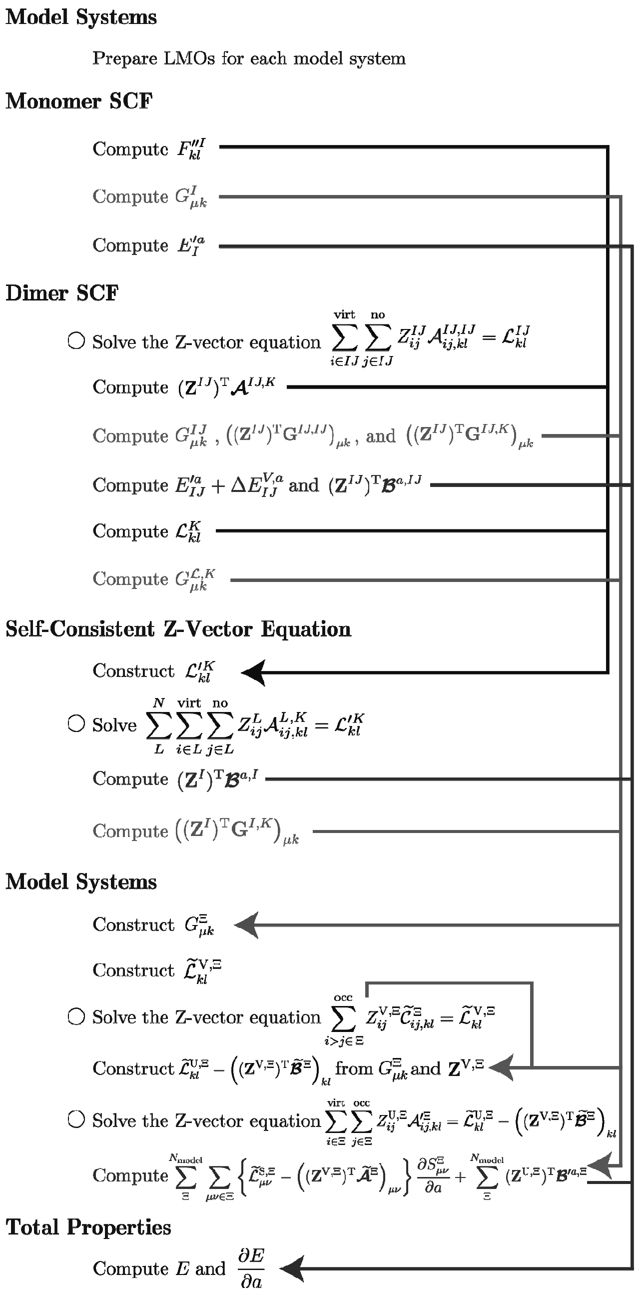

Fig. 1 Algorithm for computing FMO/AFO gradients. Each circle represents solving Z-vector equations. Arrows represent the flow of Lagrangian, localization, auxiliary density, and derivative contributions

In this fiscal year, I combined FMO-DFTB with the adaptive frozen orbital (AFO) treatment [2]. The whole algorithm is shown in Fig. 1. In FMO, one has to divide a large system into fragments. Although this sounds straightforward when the system consists of isolated molecules or cluster, such as water, a special care has to be paid when we try to divide it across covalent bonds. The conventional procedure is referred to as the hybrid orbital projection (HOP) approach. Users usually have to prepare sp3 hybrid orbitals in prior to calculations, and orbitals in fragments are projected out from the variational space to avoid duplication in the actual calculation. The AFO approach is conceptually similar, but it employs localized orbitals generated in model systems on the fly. Model systems are constructed from a subspace of the whole system. In spite of the similarity, derivations and implementations of the analytic derivative of the total energy with the AFO approach is not straightforward, and they have not been realized.

Eventually, first-order derivatives can be analytically computed as in Fig. 1. The algorithm implies that four types of response (Z-vector) equations have to be solved in FMO-DFTB/AFO, while the conventional FMO-DFTB/HOP required only the second Z-vector equation, called the self-consistent Z-vector equation. The first type of the Z-vector equations arises from freezing occupied and projecting out virtual orbitals in fragments. The third and fourth do from response contributions in model systems, because the geometry of the model system is dependent on coordinates of the real system. It is apparent that the latter contributions do not exist in the conventional FMO/HOP method, since hybrid orbitals to be projected out are generated for fixed structures. Because of the complexity, FMO/AFO is 1.6–2.3 times expensive than FMO/HOP. The extra cost is mostly relevant to matrix algebra, in particular matrix multiplications. The deviations of the implemented gradient from numerical gradients is on the order of 10^{-5} hartree/bohr, and the residual error should be attributed to the limited accuracy of numerical gradients. As a demonstrative example, FMO2-DFTB2/HOP had a large error for a zeolite system (+32.84 kcal/mol), but it decreased to only -0.60 kcal/mol with FMO2-DFTB2/AFO.

It is now possible to apply FMO-DFTB/AFO to molecular dynamics (MD) simulations. As a demonstration, we prepared a large boron-nitride nano-ring consisting of 1,180,800 atoms with 65,550 fragments and 131,100 detached bonds. It took 181 hours for 500 MD steps on a computer node with 24 CPU cores, so a single step took only 22 minutes on average. It thus shows that calculations for one million atom systems on a laboratory-scale computer resource are not challenging any more. Developers of FMO are planning that recent developments, including some improvements for previous implementations, are released in 2018, as a part of GAMESS-US.

Mechanism of a Pd-Catalyzed Aromatic C−H Coupling Reaction

C–H functionalization is a rapidly growing field in organic chemistry because of its potential applications in the synthesis of pharmaceuticals, natural products, agrochemicals, and organic materials. The utility of C–H functionalization is particularly pronounced when structural isomers and/or stereoisomers can be distinguished. As one of the most fundamental reactions, the C–H coupling of heteroarenes with arylboron compounds has been extensively studied both experimentally and theoretically. However, this type of reaction usually requires a stoichiometric amount of co-oxidants such as 1,4-benzoquinone, Cu(II) halides, and Ag(I) salts, which results in chemical waste except in some rare cases. Moreover, these catalysts generally exhibit low reactivity when sterically demanding substrates are employed.

Recently, Itami, Yamaguchi, and co-workers discovered an aromatic C–H coupling reaction of heteroarenes and sterically hindered arylboronic acids utilizing a Pd/Fe dual catalyst that could overcome the above-mentioned drawbacks [3]. The dual catalyst consists of Pd(II)-sulfoxide-oxazoline (sox) and iron-phthalocyanine (FePc), where FePc is considered to oxidize Pd(0) to Pd(II) with oxygen in the air as the terminal oxidant. Despite the aforementioned attractive features, the highest enantiomeric excess (ee) value was 61%, and understanding of the reaction mechanism, which would aid in developing a catalyst which delivers a higher ee, has been limited. We reported an experimental substituent effect study of a model reaction as well as a theoretical investigation to clarify the reaction mechanism of the representative reaction shown in Fig. 2 [4].

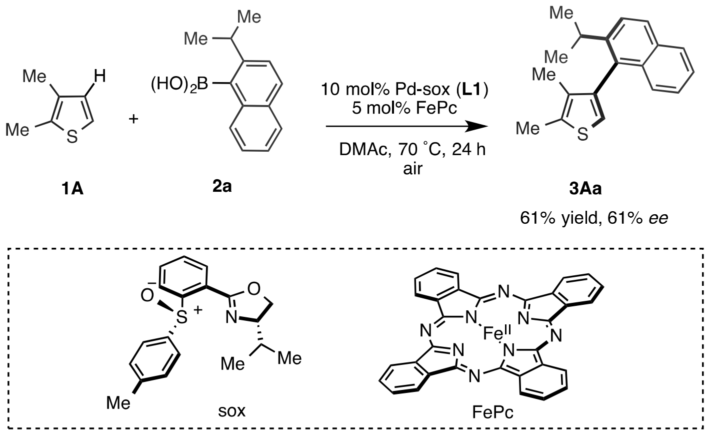

Fig. 2 Aromatic C–H coupling reaction of a thiophene derivative and a hindered arylboronic acid, assisted by a Pd/Fe dual catalyst.

All the structures were optimized using density functional theory (DFT) as implemented in Gaussian 09. We selected B3PW91 exchange–correlation functional with 6-31G(d) and LANL2DZ basis set for typical and Pd atoms, respectively (abbreviated as BSI). Energy refinement for optimized structures was performed as DF-SCS-MP2/(aug-)cc-pVTZ as implemented in MOLPRO 2012. We added augmented functions for N, O, and S atoms and pseudopotential (ECP28MDF) for Pd (BSII). Solvent effect was implicitly added by performing reference Hartree–Fock calculation with COSMO solvation model with nonelectrostatic energies of the SMD solvation model.

The reaction profile (Fig. 3) showed that the (*S*)-product should be dominant because the highest activation energy of the transition state (TS) leading to the (*S*)-product (**TS**$_{\mathbf{4\text{-}5}}^{\mathbf{S}}$) is 3.0 kcal/mol lower than the TS leading to the (*R*)-product (**TS**$_{\mathbf{4\text{-}5}}^{\mathbf{R}}$). This finding is consistent with the experimental conditions at 70°C. Other important TSs are the C–C bond formation step (**TS**$_{\mathbf{8\text{-}9}}^{\mathbf{S}}$ and **TS**$_{\mathbf{8\text{-}9}}^{\mathbf{R}}$) and the abstraction of a proton to

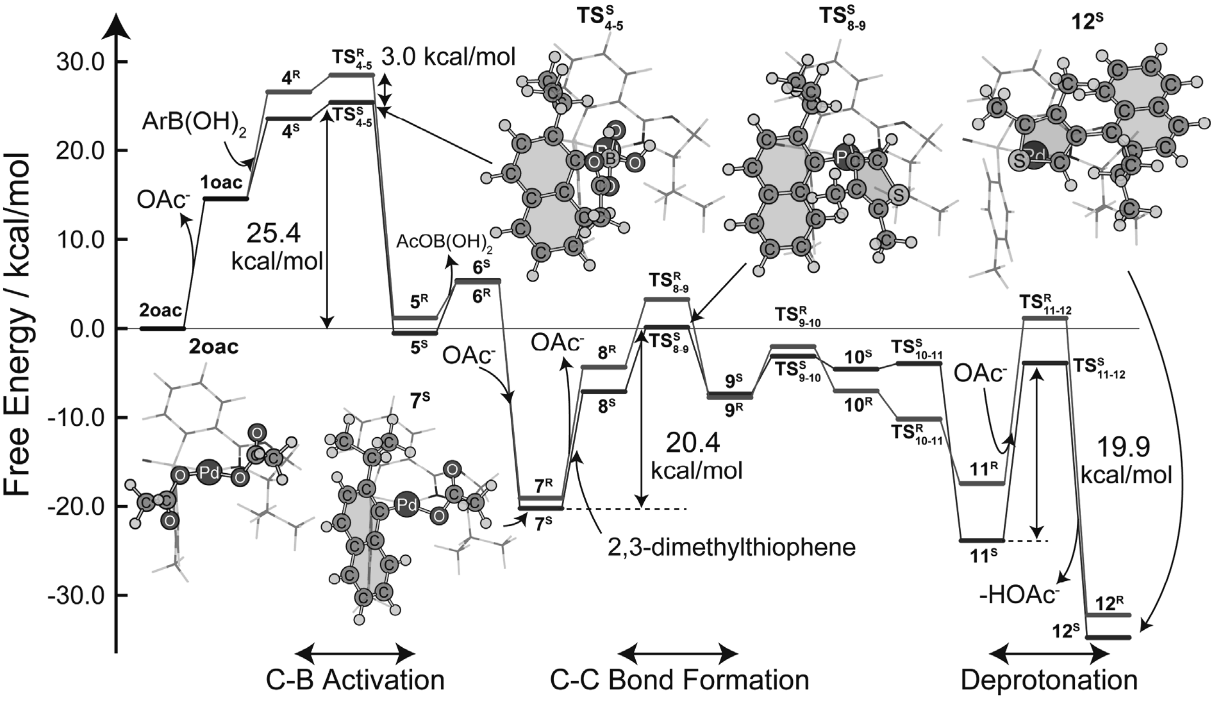

Fig. 3 Proposed reaction profile as the COSMO-DF-SCS-MP2/BSII//B3PW91/BSI level of theory. Blue and red lines (blue lines come lower except at **10** and **TS**$_{\mathbf{10\text{-}11}}$) represent free energies of reaction coordinates leading to (*S*)- and (*R*)-stereoisomers, respectively.

form a double bond on the thiophene ring (**TS$_{11\text{-}12}$^{S}** and **TS$_{11\text{-}12}$^{R}**). Activation energies of these steps are lower than that of the C–B bond transmetalation. The HOAc species generated in the catalytic cycle may be converted to OAc^{-} and water in the oxidation step. The water may then hydrolyze AcO–B(OH)$_2$ resulting in regeneration of **2oac**.

The main question is why the energy difference of 3.0 kcal/mol emerges at this enantioselective step. To address this, we calculated the interaction energy between the aryl group on the Pd center and the tolyl group of the sox ligand. The interaction energies at the DF-SCS-MP2/BSII level of theory was 1.9 and 1.8 kcal/mol for **TS$_{4\text{-}5}$^{S}** and **TS$_{4\text{-}5}$^{R}**, respectively, so the difference of 0.2 kcal/mol only represents ~5% of the total energy difference of 3.0 kcal/mol, implying that steric repulsion alone cannot reasonably explain the enantioselectivity of the catalytic reaction.

We next focused on the electronic structure effect of the rotation of the tolyl group. We adopted the natural bond orbital (NBO) analysis at the B3PW91/BSI level of theory. Our analysis revealed that **TS$_{4\text{-}5}$^{S}** and hypothetical **TS$_{4\text{-}5}$^{S}** with the dihedral angle between O–S–C–C atoms equivalent to that of **TS$_{4\text{-}5}$^{R}** are stabilized by 5.9 and 3.3 kcal/mol, respectively, by the interaction between the donor (occupied C–C π-orbital on the tolyl group) and the acceptor (unoccupied S–O σ*-orbital on the sox ligand) NBOs. The interaction corresponds to the hyperconjugation between these orbitals. The difference of the interaction energies is 2.6 kcal/mol, which is close to the difference of the activation energies at **TS$_{4\text{-}5}$^{S}** and **TS$_{4\text{-}5}$^{R}**, namely 3.0 kcal/mol. Although we suggested some substitutions which are expected to yield a better ee based on the analysis of stabilization energies of different substitutions of the sox ligand, these are difficult to realize experimentally.

In summary, our study indicates that the rate-determining and stereoselective step of the reaction is the C–B translmetalation of the arylboronic acid. NBO analysis reveals that the difference between the activation energy of two TSs leading to (*S*)- and (*R*)-products (**TS$_{4\text{-}5}$^{S}** and **TS$_{4\text{-}5}$^{R}**) is attributed to the hyperconjugation between π-orbitals on the tolyl and the S–O σ*-bonding orbitals on the sox ligand. Our investigations of the substituent effect of the sox ligand imply that the design of a highly selective catalyst is challenging.

References

[1] Nishimoto, Y.; Fedorov, D. G.; Irle, S. *J. Chem. Theory Comput.* **2014**, *10*, 4801–4812.
[2] Nishimoto, Y.; Fedorov, D. G. *J. Chem. Phys.* **2018**, *148*, 064115.
[3] Yamaguchi, K.; Kondo, H.; Yamaguchi, J.; Itami, K. *Chem. Sci.* **2013**, *4*, 3753–3757.
[4] Nishimoto, Y.; Kondo, H.; Yamaguchi, K.; Yokogawa, D.; Yamaguchi, J.; Itami, K.; Irle, S. *J. Org. Chem.* **2017**, *82*, 4900–4906.

2. Original papers

(1) Nishimoto, Y.; Kondo, H.; Yamaguchi, K.; Yokogawa, D.; Yamaguchi, J.; Itami, K.; Irle, S.
“Theoretical Elucidation of Potential Enantioselectivity in a Pd-Catalyzed Aromatic C–H Coupling Reaction”

J. Org. Chem. 82(9), 4900–4906 (2017).

(2) Kitoh-Nishioka, H.; Welke, K.; Nishimoto, Y.; Fedorov, D. G.; Irle, S.
“Multi-Scale Simulations on Charge Transport in Covalent Organic Frameworks: Including Dynamics of Transfer Integrals from FMO-DFTB/LCMO”
J. Phys. Chem. C 121(33), 17712–17726 (2017).

(3) Nishimoto, Y.; Fedorov, D. G.
“Adaptive frozen orbital treatment for the fragment molecular orbital method combined with density-functional tight-binding”
J. Chem. Phys. 148(6), 064115 (2018).

3. Presentation at academic conferences

(1) 西本　佳央
「巨大拡張系への応用に向けた少数軌道占有数を用いた解析的三次微分」
第20回理論化学討論会（1L07）、京都府、2017年5月16日

(2) Yoshio Nishimoto
“Analytic Hyperpolarizability and Polarizability Derivative with Fractional Occupation Numbers for Large Extended Systems”
11th Triennial Congress of the World Association of Theoretical and Computational Chemists (PO1-26), Munich, August 28th, 2017

(3) 西本　佳央
「少数軌道占有数を用いた二次の coupled-perturbed 方程式」
第11回分子科学討論会（1P083）、宮城県、2017年9月15日

4. Others

(1) Yoshio Nishimoto
“Analytic Derivatives with Fractional Occupation Number”
15th Fukui Center Seminar, Kyoto, May 25, 2017

(2) 西本　佳央
「フロンティア軌道理論について」
京都大学サマーデザインスクール2017、京都府、2017年9月13日

(3) 西本　佳央
「福井謙一生誕百年記念事業のご紹介とフロンティア軌道に関連した展示物の準備」
第15回福井謙一記念研究センターシンポジウム、京都府、2018年2月2日

２．FIFC リサーチフェロー

Shigeru Nagase

FIFC Research Fellow

1. Summary of the Research of the Year

(a) Van Der Waals Heterogeneous Layer-Layer Carbon Nonostructures Including π•••H-C-C-H•••π•••H-C-C-H Stacking Based on Graphene and Graphene Sheets

Noncovalent interactions such as π•••π stacking and CH•••π interaction are essential for supramolecular carbon nanostructures. Graphite is the typical homogenous carbon matter based on the π•••π stacking of graphene sheets. Even in the systems that do not contain aromatic groups, the stability of diamondoid dimer and layer-layer graphane dimer originates from the C-H•••H-C noncovalent interactions. Therefore, the structures and properties of novel heterogeneous layer-layer carbon-nanostructures containing the π•••H-C-C-H•••π stacking based on [n]-graphan, [n]-graphene and their derivatives are theoretically investigated for n = 16–54 using the dispersion-corrected density functional theory at the B3LYP-D3 level. The Energy decomposition analyses show that the dispersion interaction is the most important for the stabilization of both double- and multi-layer-layer [n]-graphane@graphene. Binding energies between graphane and graphene sheets show distinct additive CH•••π interactions. For comparison and simplicity, the H-H bond energy equivalent number of carbon atoms (NHEQ) is employed to describe the strength of these noncovalent interactions. The NHEQ of graphene dimers, graphane dimers, and double-layered graphane@graphene are 103, 143, and 110, respectively, which indicates that the strength of the CH•••π interaction is close to that of the π•••π interaction and is much stronger than that of the C-H•••H-C interaction in large size systems. Additionally, frontier molecular orbitals, electron density differences, and visualized noncovalent interaction regions are discussed to understand deeply the nature of the CH•••π stacking interaction in construction of heterogeneous layer-layer graphane@graphene structures. It is expected that the present study will be helpful in creating new functional supramolecular materials based on graphane and graphene carbon nanostructures.

(b) The Electron Transfer of Monotitanium-Encapsulated Fullerenes, Which Depends on Fused Pentagon Distributions

The novel properties of monotitanium-encapsulated fullerenes are investigated using density functional theory calculations. For encapsulation of a titanium atom inside a fullerene, it is the most interesting finding that the properties of the fullerene are very sensitive to the distributions of fused pentagonal carbon rings in the fullerene cage. When the titanium atom is bound on a doubly or triply fused pentagon part, the formed endohedral fullerenes exhibit entirely different electron-transfer character, unlike the current knowledge on mono-metallofullerenes. The titanium atom prefers to reside on the triply fused pentagon part because of stronger interactions between titanium and cage carbons in the highly strained fused part. This finding is remarkable because the important stabilization of triply fused pentagons upon endohedral doping has been underestimated up to now in the chemistry of endohedral metallofullerenes. It should be emphasized that endohedral titatium doping is a feasible approach to the stabilization of highly strained triply fused-pentagon part in the search for unconventional fullerenes for practical applications. The selective electron-transfer character is extended to the study of the encapsulation of other neighboring metal atoms such as calcium and scandium. Because of their different capability to accept d electrons, fullerene cages with fused pentagon parts show selective metal encapsulation character.

(c) Epoxy and Oxidoannulene Oxidation Mechanisms of Chlorofullerenes Containing Fused Pentagonal Carbon Rings

Recently, the oxidative functionalization of chlorofullerenes ($^{\#271}C_{50}Cl^{10}$ and $^{\#913}C_{56}Cl_{10}$) containing doubly fused pentagons in the fullerene cage was carried out, which leads to two monoepoxides with the oxygen atom added at the ortho site of pentalene in the doubly fused pentagon. It is of great interest to uncover how the reactivity of the chlorofullerenes violating the isolated pentagon rule upon is changed upon oxidation. Therefore, two possible formation processes (ozone molecule and oxygen radical served as oxidation reagents) of the two oxides were systematically investigated by density functional theory calculations. For the ozone oxidation, two possible pathways were explored, and the results indicate that the biradical mechanism $\mathrm{Path_{os}}$-RACDP is kinetically more favorable than $\mathrm{Path_{os}}$-RABP, where R, A, and P represent reactants, ozonide intermediates, and oxidation products, respectively, and B, C, and D represent another three oxygen-containing intermediates. The products obtained by ozone oxidation ([6,6]-55-closed epoxides $P-C_3-C_{29}$ for $^{\#271}C_{50}Cl_{10}$ and $P-C_{42}-C_{43}$ for $^{\#913}C_{56}Cl_{10}$ with oxygen atom added at the shortest and highest HOMO-contribution bonds) are consistent with experimental observations. However, the oxygen radical additions on these two chlorofullerenes favor the generation of two [5,6]-66-open oxidoannulene adducts ($P-C_3-C_2$ and $P-C_{42}-C_{54}$). Subsequent analyses of their geometrical features and structural stabilities suggest that these two open-ring oxidoannulene adducts are energetically unfavorable, which are converted to more stable closed ring epoxides via a pirouette-type transition state. In these two diverse oxidation procedures, the favorable C−C bonds for ozone attacking and C atoms for oxygen-adsorption are rationalized in terms of their bond lengths and HOMO contributions as well as pyramidalization angles

(d) Deciphering the Role of Long-Range Interactions in the Ambiguous Structures of Endohedral Metallofullerenes

Structure elucidation is a vital step to study endohedral metallofullerene (EMF). In this context, the theoretical investigation is very powerful in determining the structures of EMFs. Therefore, the ambiguous structures of Sc_2C_{70} of current interest were first investigated using four different density functional theory (DFT) methods at the wB97XD, M06-2X, B3LYP, and PBE0 levels, combined with statistical mechanics. The calculated results show that $Sc_2C_2@C_{2v}(6073)\text{-}C_{68}$ is the most stable and abundant for Sc_2C_{70} within the temperature of EMF formation. The DFT methods without long-range corrections, such as B3LYP and PBE0, tend to underestimate the stabilities of the $Sc_2C_2@C_{68}$ structures, as in the $Sc_2C_2@C_{72}$ cases. However, the B3LYP and PBE0 methods give the relative energies of the $La_2C_2@C_{94}$ isomers which are almost identical to the energies obtained by the M06-2X method. It was found that long-range interactions play an important role in the interaction energies between encapsulated species clusters and carbon cages for $Sc_2C_2@C_{68}$, $Sc_2C_2@C_{72}$, $La_2C_2@C_{94}$, and $La_2@C_{96}$, while they play a minor role for $Sc_2@C_{70}$ and $Sc_2@C_{74}$. This can be attributed to the structure differences. For $Sc_2C_2@C_{68}$, $Sc_2C_2@C_{72}$, $La_2C_2@C_{94}$, and $La_2@C_{96}$, the encapsulated species is not effectively coordinated by cage carbons because of the constraint of the shapes of encapsulated species ($Sc_2C_2@C_{68}$, $Sc_2C_2@C_{72}$, and $La_2C_2@C_{94}$) or the absence of pentalene fragments in carbon cages ($La_2C_2@C_{94}$ and $La_2@C_{96}$). This can be generalized to other EMFs. That is, long-range interactions play an important role for both clusterfullerenes and conventional fullerenes satisfying the well-known isolated pentagon rule. The DFT methods without long-range corrections give seemingly correct relative energies for some EMFs, because all the isomers are systemically overestimated to the same degree. However, it should be emphasized that the use of the DFT methods without long-range corrections are dangerous for the investigation of the reactivity and regioselectivity. The comparison of $Sc_2@C_{2v}(7854)$-C_{70} and $Sc_2C_2@C_{2v}(6073)$-C_{68} in the simulated UV−vis-NIR spectra also confirms that the experimentally isolated Sc_2C_{70} isomer is $Sc_2C_2@C_{2v}(6073)$-C_{68} (not $Sc_2@C_{2v}(7854)$-C_{70}).

(e) Effects of Substituents and Initial Degree of Functionalization of Alkylated Single-Walled Carbon Nanotubes on Their Thermal Stability and Photoluminescence Properties

Alkylated single-walled carbon nanotubes (SWNTs) have been thermally treated to determine the influence of substituents and the degree of functionalization on their thermal stability and photoluminescence (PL) properties. Alkylated SWNTs were prepared by treating SWNTs with sodium naphthalenide and alkyl bromide. The defunctionalization of the alkylated SWNTs was monitored by absorption and Raman spectra. Selective recovery of the characteristic absorption and radial breathing mode peaks was observed during the thermal treatment, which indicates that the thermal stability of the alkylated SWNTs decreases with increases in SWNT diameter and degree of functionalization. n-Butylated and phenethylated SWNTs showed higher thermal stability than sec-butylated and benzylated SWNTs for a similar degree of functionalization, respectively. The diameter selectivity and effect of substituents on the thermal elimination reaction were well confirmed by density functional theory calculations at reasonable levels. In addition, it was shown that the initial degree of functionalization of the alkylated SWNTs, with the alkyl group and degree of functionalization being kept constant after thermal treatment, strongly affects their PL properties such as Stokes shift and PL peak intensity.

(f) Formation of Stone-Wales Edge: Multistep Reconstruction and Growth Mechanisms of Zigzag Nanographene

The existence of Stone–Wales (5-7) defects at the graphene edge has been clarified experimentally. In contrast, the theoretical study on the formation mechanism is still imperfect. In particular, the regioselectivity of multistep reactions at the edge (self-reconstruction and growth with foreign carbon feedstock) is essential to understand the kinetic behavior of reactive boundaries, though the investigations are still lacking. Herein, by using finite sized models, multistep reconstructions and carbon dimer additions of a bared zigzag edge are introduced using density functional theory calculations. The zigzag to 5-7 transformation is proved as a site-selective process to generate alternating 5-7 pairs sequentially and the first step with the largest barrier is suggested as the rate-determining step. Conversely, successive C_2 insertions on the active edge are calculated to elucidate the formation of the 5-7 edge during graphene growth. A metastable intermediate with a triple sequentially fused pentagon fragment is proved as the key structure for the 5-7 edge formation. These findings are expected to be valuable to uncover the reactivity of unsaturated graphene edge and helpful to achieve controlled synthesis of graphene with desired edge structures for various device applications.

(g) Adamantylidene Addition to $M_3N@I_h$-C_{80} (M = Sc, Lu) and $Sc_3N@D_{5h}$-C_{80}: Experimental and Theoretical Characterization of the [5,6]-Open and [6,6]-Open Adducts

Additions of adamantylidene (Ad) to $M_3N@I_h$-C_{80} (M=Sc, Lu) and $Sc_3N@D_{5h}$-C_{80} have been accomplished by photochemical reactions with 2-adamantyl-2,3'-[3H]-diazirine. For $M_3N@I_h$-C_{80}, the addition led to rupture of the [6,6]- or [5,6]-bonds of the I_h-C_{80} cage, forming the [6,6]-open fulleroid as the major isomer and the [5,6]-open fulleroid as the minor isomer. For $Sc_3N@D_{5h}$-C_{80}, the addition also proceeded regioselectively to yield three major isomeric Ad mono-adducts, despite the fact that there are nine types of C-C bonds in the D_{5h}-C_{80} cage. The molecular structures of the seven Ad mono-adducts, including the positions of the encaged trimetallic nitride clusters, have been unambiguously determined through single-crystal XRD analyses. Furthermore, results have shown that stepwise addition of Ad to $Lu_3N@I_h$-C_{80} affords several Ad bis-adducts, two of which have been isolated and characterized. The X-ray structure of one bis-adduct clearly revealed that the second Ad addition took place at a [6,6]-bond close to an endohedral metal atom. The regioselectivity has been rationalized by performing density functional theory calculations.

(h) Other Research Subjects

(1) "Photoreactions of Endohedral Metallofullerene with Siliranes: Electronic Properties of Carbosilylated $Lu_3N@I_h$-C_{80}", (2) "Fullerene C_{70} as a Nanoflask that Reveals the Chemical Reactivity of Atomic Nitrogen", (3) "Temperature Dependence of Anisotropic Transient Conductivity of a $La@C_{2v}$-C_{82}(Ad) Crystal", (4) "Preparation, Structural Determination, and Characterization of Electronic Properties of [5,6]- and [6,6]-Carbosilylated $Sc_3N@I_h$-C_{80}", (5) "Synthesis, Electronic Structure, and Reactivities of Two-Sulfur Stabilized Carbones Exhibiting Four-Electron Donor Ability", (6) "$Eu@C_{72}$: Computed Comparable Populations of Two Non-IPR Isomers", (7) "Functionalization of Endohedral Metallofullerenes with Reactive Silicon and Germanium Compounds", (8) "Synthesis and Photoinduced Electron-Transfer Reactions in a $La_2@I_h$-C_{80}-Phenoxazine Conjugate", (9) "Concave Binding of Cationic Li to Quadrannulene", (10) "A Mechanistic Study on Cationic Li Prompted Diels-Alder Cycloaddition of Cycloparaphenylene", (11) "Stability Issues in Computational Screening of Carbon Nanostructures: Illustrations on La Endohedrals", (12) "Revisit of the Saito-Dresselhause-Dresselhaus C_2 Ingestion Model: On the Mechanism of Atomic-Carbon-Participated Fullerene Growth", (13) "Computational Comparison of

the Water-Dimer Encapsulation into D_2(22)-C_{84} and D_{2d}(23)-C_{84}", (14) "A Computational Characterization of CO@C_{60}"

2. Original Papers

(1) Y. Maeda, Y. Takehana, J. –S. Dang, M. Suzuki, M. Yamada, and S. Nagase,
"Effect of Substituents and Initial Degree of Functionalization of Alkylated Single-Walled Carbon Nanotubes on Their Thermal Stability and Photoluminescence Properties"
Chem. Eur. J., **23**, 1789-1794 (2017).

(2) K. Yuan, R. –S. Zhao, J. –J. Zheng, H. Zheng, S. Nagase, S. –D. Zhao, Y. –Z. Liu, and X. Zhao,
"Van der Waals Heterogeneous Layer-Layer Carbon Nanostructures Involving π•••H-C-C-H•••π•••H-C-C-H Stacking Based on Graphene and Graphane Sheets"
J. Comput. Chem., **38**, 730-739 (2017).

(3) M. Yamada, T. Abe, C. Saito, T. Yamazaki, S. Sato, N. Mizorogi, Z. Slanina, F. Uhlík, M. Suzuki, Y. Maeda, Y. Lian, X. Lu, M. M. Olmstead, A. L. Balch, S. Nagase, and T. Akasaka,
"Adamantylidene Addition to M_3N@I_h-C_{80} (M = Sc, Lu) and Sc_3N@D_{5h}-C_{80}: Synthesis and Crystallographic Characterization of the [5,6]-Open and [6,6]-Open Adducts"
Chem. Eur. J., **23**, 6552-6561 (2017).

(4) M. Kako, K. Minami, T. Kuroiwa, S. Fukazawa, Y. Arikawa, M. Yamada, Y. Maeda, Q. –Z. Li, S. Nagase, and T. Akasaka,
"Photoreactions of Endohedral Metallofullerene with Siliranes: Electronic Properties of Carbosilylated Lu_3N@I_h-C_{80}"
Molecules, **22**, 850 (10 pages) (2017).

(5) Y. Morinaka, R. Zhang, S. Sato, H. Nikawa, T. Kato, K. Furukawa, M. Yamada, Y. Maeda, M. Murata, A. Wakamiya, S. Nagase, T. Akasaka and Y. Murata,
"Fullerene C_{70} as a Nanoflask that Reveals the Chemical Reactivity of Atomic Nitrogen"
Angew. Chem. Int. Ed., **56**, 6488-6491 (2017).

(6) M. Yamada, S. Sato, W. Choi, S. Seki, T. Abe, M. Suzuki, Y. Maeda, S. Nagase, and T. Akasaka,
"Temperature Dependence of Anisotropic Transient Conductivity of a La@C_{2v}-C_{82}(Ad) Crystal"
Chem. Lett., **46**, 973-975 (2017).

(7) M. Kako, T. Sugiura, K. Miyabe, M. Yasui, M. Yamada, Y. Maeda, J. –D. Guo, S, Nagase, and T. Akasaka,
"Preparation, Structural Determination, and Characterization of Electronic Properties of [5,6]- and [6,6]-Carbosilylated Sc_3N@I_h-C_{80}"
Chem. Asian. J., **12**, 1391-1399 (2017).

(8) J. –S. Dang, W. –W. Wang, J. –J. Zheng, X. Zhao, and S. Nagase,
"Fused-Pentagon-Configuration-Dependent Electron Transfer of Monotitanium Encapsulated Fullerenes"
Inorg. Chem., **56**, 6890-6896 (2017).

(9) T. Morosaki, R. Iijima, T. Suzuki, W. –W. Wang, S. Nagase, and T. Fujii,

"Synthesis, Electronic Structure, and Reactivities of Two-Sulfur Stabilized Carbones Exhibiting Four-Electron Donor Ability"
Chem. Eur. J., **23**, 8694-8702 (2017).

(10) Z. Slanina, F. Uhlík, S. Nagase, T. Akasaka, L. Adamowicz, and X. Lu,
"Eu@C_{72}: Computed Comparable Populations of Two Non-IPR Isomers"
Molecules, **22**, 1053 (8 pages) (2017).

(11) Q. –Z. Li, J. –J. Zheng, X. Zhao, and S. Nagase,
"Epoxy and Oxidoannulene Oxidation Mechanisms of Fused-Pentagon Chlorofullerenes: Oxides Linked by a Pirouette-Type Transition State"
J. Org. Chem., **82**, 6541-6549 (2017).

(12) M. Kako, S. Nagase, and T. Akasaka,
"Functionalization of Endohedral Metallofullerenes with Reactive Silicon and Germanium Compounds"
Molecules, **22**, 1179 (17 pages) (2017).

(13) T. Akasaka, A. Nakata, M. Rudolf, W. –W. Wang, M. Yamada, M. Suzuki, Y. Maeda, R. Aoyama, T. Tsuchiya, S. Nagase, and D. M. Guldi,
"Synthesis and Photoinduced Electron-Transfer Reactions in a $La_2@I_h$-C_{80}-Phenoxazine Conjugate"
ChemPlusChem, **82**, 1067-1072 (2017).

(14) J. –S. Dang, W. –W. Wang, X. Zhao, and S. Nagase,
"Concave Binding of Cationic Li to Quadrannulene"
Phys. Chem. Chem. Phys., 19, 20773-20777 (2017).

(15) J. –S. Dang, W. –W. Wang, J. –J. Zheng, S. Nagase, and X. Zhao,
"Formation of Stone-Wales Edge: Multistep Reconstruction and Growth Mechanisms of Zigzag Nanographene"
J. Comput. Chem., **38**, 2241-2247 (2017).

(16) J. –S. Dang, W. –W. Wang, X. Zhao, and S. Nagase,
"A Mechanistic Study on Cationic Li Prompted Diels-Alder Cycloaddition of Cycloparaphenylene"
Org. Chem. Front., **4**, 1757-1761 (2017).

(17) R. Zhao, K.Yuan, S. Zhao, M. Ehara, S. Nagase, J. M. Poblet, and X. Zhao,
"Deciphering the Role of Long-Range Interaction in Endohedral Metallofullenes: A Revisit to Sc_2C_{70}"
J. Phys. Chem. C, **121**, 20481-20488 (2017).

(18) Z. Slanina, F. Uhlík, L. Adamowicz, T. Akasaka, S. Nagase, and X. Lu,
"Stability Issues in Computational Screening of Carbon Nanostructures: Illustrations on La Endohedrals"
Mol. Simul., **43**, 1472-1479 (2017).

(19) W. –W. Wang, J. –S. Dang, X. Zhao, and S. Nagase,
"Revisit of the Saito-Dresselhause-Dresselhaus C_2 Ingestion Model: On the Mechanism of Atomic-Carbon-Participated Fullerene Growth"

Nanoscale, **9**, 16742-16748 (2017).

(20) Z. Slanina, F. Uhlík, S. Nagase, T. Akasaka, L. Adamowicz, and X. Lu,
"Computational Comparison of the Water-Dimer Encapsulation into D_2(22)-C_{84} and D_{2d}(23)-C_{84}"
ECS, J. Solid State Sci. and Tech., **6**, M3113-M3115 (2017).

(21) Z. Slanina, F. Uhlík, S. Nagase, T. Akasaka, L. Adamowicz, and X. Lu,
"A Computational Characterization of CO@C_{60}"
Fullerenes, Nanotubes, Carbon Nanostruct., **25**, 624-629 (2017).

3. Review

M. Kako, S. Nagase, and T. Akasaka,
"Functionalization of Endohedral Metallofullerenes with Reactive Silicon and Germanium Compounds"
Molecules (Review), **22**, 1179 (17 pages) (2017).

３．シニアリサーチフェロー

Shigeyoshi Sakaki

Senior Research Fellow, Kenichi Fukui Memorial Research Groups II

1. Summary of the research of 2017

The complex systems consisting of transition metal element(s), heavy main-group element(s), organic group(s) play important roles as metal enzymes, industrial catalysts, catalysts for fine organic synthesis, photo-sensitizer, molecular switch, luminescence material and so on. Also, they are important research target in the physical chemistry and molecular science, because they exhibit a variety of new geometry, new chemical bond, rich molecular property, rich reactivity, and useful catalysis. All these features deeply relate to their electronic structures. In this regard, the theoretical and computational studies of the electronic structures of the complex systems are indispensable in further development of chemistry.

These complex systems are challenging research targets from the point of view of theoretical/computational chemistry, because their electronic structures are not simple but complicated in many cases. One good example is multi-nuclear transition metal complexes which need the application of multi-reference wave-function theory in theoretical calculation. Another example is significantly large coupling of electronic structure with surrounding atmosphere such as solvation effects, molecular crystal effects and so on.

Our group is theoretically investigating the complex systems bearing complicated electronic structure with electronic structure theory. In 2017, we performed various theoretical studies, as follows: (i) Reactivity of Mo−Mo Quintuple Bond for H−H, C−H, and O−H σ‑Bond Cleavages, (ii) Theoretical Study of [2 + 2]-type Reaction of Metal−Metal σ‑Bond with Fullerene Forming an η1‑C60 Metal Complex: Mechanistic Details of Formation Reaction and Prediction of a New η^1‑C$_{60}$ Metal Complex, (iii) Characteristic Features of CO$_2$ and CO Adsorptions to Paddle-Wheel-type Porous Coordination Polymer, (iv) Core−Shell versus Other Structures in Binary Cu38−nMn Nanoclusters (M = Ru, Rh, Pd, Ag, Os, Ir, Pt, and Au; n = 1, 2, and 6): Theoretical Insight into Determining Factors, (v) How to Control Inversion vs Retention Transmetalation between PdII−Phenyl and CuI−Alkyl Complexes, (vi) Theoretical Study of Nickel-Catalyzed Selective Alkenylation of Pyridine: Reaction Mechanism and Crucial Roles of Lewis Acid and Ligands in Determining the Selectivity, (vii) A coordination strategy to realize a sextuply-bonded complex, (viii) Theoretical study of one-electron-oxidized salen complexes of group 7 (Mn(III), Tc(III), and Re(III)) and group 10 metals (Ni(II), Pd(II), and Pt(II)) with the 3D-RISM-GMC-QDPT method: localized vs. delocalized ground and excited states in solution, (ix) Embedded Cluster Model for Al$_2$O$_3$ and AlPO$_4$ Surfaces Using Point Charges and Periodic Electrostatic Potential, and so on. We wish to report some of them, below.

(i) Reactivity of Mo−Mo Quintuple Bond for H−H, C−H, and O−H σ‑Bond Cleavages

Metal-metal multiple bond has been reported very old day by Professor Cotton. Since then, its interesting bonding nature attracted a lot of interests in molecular science and coordination chemistry. Roos/Gagliardi group and Out group have investigated the metal-metal multiple bond using multi-reference method and elucidated the interesting bonding nature of metal-metal multiple bond. However, the reactivity and catalysis of metal-metal multiple bond have not been reported for long time. Recently, several groups reported pioneering works on organometallic reaction and catalysis. But, the details of such reactivity and catalysis

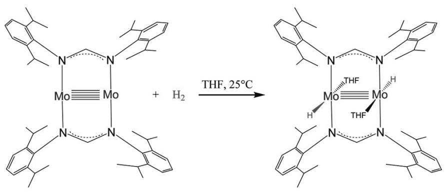

1   P$_{H\text{-}H}$

Scheme 1. Dinuclear Mo complex with Mo-Mo quintuple bond.

have not been investigate well.

We investigated the recently reported high reactivity of the Mo−Mo quintuple bond of $Mo_2(N\text{^}N)_2$ (**1**) {N^ N = μ-κ2-CH[N(2,6-*i*$Pr_2C_6H_3$)]$_2$} in the H−H σ-bond cleavage. DFT calculations disclosed that the H−H σ-bond cleavage by **1** occurs with nearly no barrier to afford the cis-dihydride species followed by cis−trans isomerization to form the trans-dihydride product, which is consistent with the experimental result. The O−H and C−H bond cleavages by **1** were computationally predicted to occur with moderate ($\Delta G^{\circ\ddagger}$ = 9.0 kcal/mol) and acceptable activation energies ($\Delta G^{\circ\ddagger}$ = 22.5 kcal/mol), respectively, suggesting that the Mo−Mo quintuple bond can be applied to various σ-bond cleavages. In these σ-bond cleavage reactions, the charge-transfer, CT(Mo→XH), from the Mo−Mo quintuple bond to the X−H (X = H, C, or O) bond and the CT(XH→Mo) from the X−H bond to the Mo−Mo bond play crucial roles. Though the HOMO (d_δ-MO) of **1** is at lower energy and the LUMO + 2 (d_δ*-MO) of 1 is at higher energy than those of $RhCl(PMe_3)_2$ (LUMO and LUMO + 1 of 1 are not frontier MO), the H−H σ-bond cleavage by **1** more easily occurs than that by the Rh complex. Hence, the frontier MO energies are not the reason for the high reactivity of **1**. The high reactivity of **1** arises from the polarization of d_δ-type MOs of the Mo−Mo quintuple bond in the transition state. Such a polarized electronic structure enhances the bonding overlap between the d_δ-MO of the Mo−Mo bond and the σ*-antibonding MO of the X−H bond to facilitate the CT(Mo→XH) and reduce the exchange repulsion between the Mo−Mo bond and the X−H bond. This polarized electronic structure of the transition state is similar to that of a frustrated Lewis pair. The easy polarization of the d_δ-type MOs is one of the advantages of the metal−metal multiple bond, because such polarization is impossible in the mononuclear metal complex.

(ii) Theoretical Study of [2 + 2]-type Reaction of Metal−Metal σ-Bond with Fullerene Forming an η1-C_{60} Metal Complex: Mechanistic Details of Formation Reaction and Prediction of a New η1-C_{60} Metal Complex

Reaction of fulerene with transition metal complex has been rare. However, $C_{60}[CpRu(CO)_2]_2$, only one transition-metal fullerene complex with pure η^1-coordinated bonds, was recently synthesized through the reaction between dinuclear Ru complex $[CpRu(CO)_2]_2$ and C_{60}. Though new properties can be expected in the η1-coordinated metal-fullerene complex, its characteristic features are unclear, and the [2 + 2]-type formation reaction is very slow with a very small yield. A density functional theory study discloses that the η1-coordinated bond is formed by a large overlap between the Ru dσ orbital and C pσ one involved in the lowest unoccupied molecular orbital (LUMO) (π*) of C_{60} unlike the well-known η2- coordinated metal-fullerene complex which has a π-type coordinate bond with metal dπ orbital. The binding energy per one Ru−C bond is much smaller than those of η^2-coordinated $Pt(PMe_3)_2(C_{60})$ and $IrH(CO)(PH_3)_2(C_{60})$ because the Ru d orbital exists at low energy. The formation reaction

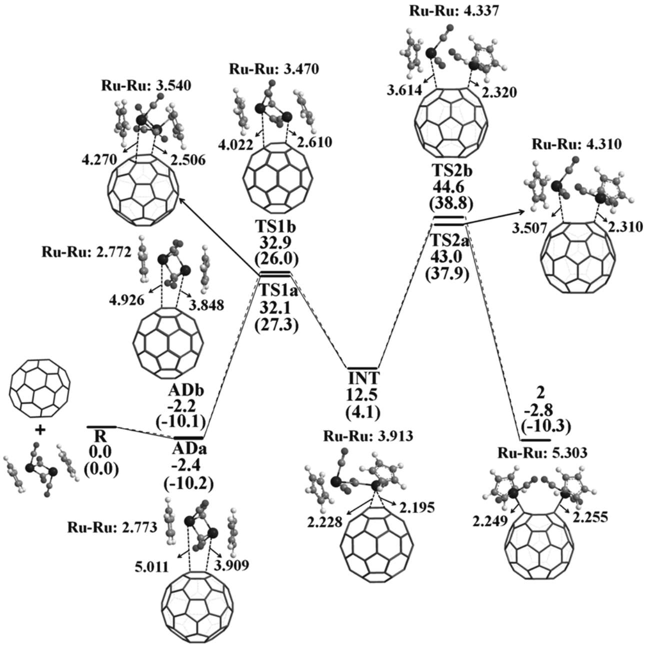

Figure 1. Gibbs energy profile of the reaction between C_{60} and $[CpRu(CO)_2]_2$

occurs via Ru−Ru bond cleavage on the C_{60} surface followed by a direction change of $CpRu(CO)_2$ to afford $C_{6}0[CpRu(CO)_2]_2$ in a stepwise manner via two asymmetrical transition states to avoid a symmetry-forbidden character. The calculated Gibbs activation energy ($\Delta G^{\circ\ddagger}$) is very large and the Gibbs reaction energy (ΔG°) is moderately negative, which are consistent with a very slow reaction rate and very small yield. The charge transfer from $CpRu(CO)_2$ to fullerene CT(Ru → C_{60}) is important in the reaction, but it is small due to the presence of the Ru d orbital at low energy, which is the reason for the large $\Delta G^{\circ\ddagger}$ and moderately negative ΔG°. The use of $Li^{+}@C_{60}$ is theoretically predicted to accelerate the reaction and increase the yield of $Li^{+}@C_{60}[CpRu(CO)_2]_2$, because the CT(Ru → C_{60}) is enhanced by the low energy LUMO of $Li^{+}@C_{60}$. It is also predicted that Li+@C60[Re(CO)4(PMe3)]2 is a next promising target for the synthesis of the η^1-coordinated metal-fullerene complex, but syntheses of $C_{60}[Co(CO)_4]_2$, $C_{60}[Re(CO)_5]_2$, $Li^{+}@C_{60}[Co(CO)_4]_2$, and $Li^{+}@C_{60}[Re(CO)_5]_2$ are difficult.

(iii) Characteristic Features of CO_2 and CO Adsorptions to Paddle-Wheel-type Porous Coordination Polymer

Porous coordination polymers (PCPs) or metal organic frameworks (MOFs) have attracted recent attention as potential materials for gas storage, gas separation, and catalysis. Because a variety of metal ions and organic linkers are available for synthesis, geometry and property of PCP can be well-tuned for achieving the purpose. Actually, many PCPs with excellent adsorption ability for target gas molecule have been designed and synthesized by tuning geometries and properties of PCPs. However, we do not have correct knowledge about the position and binding energy of gas molecule in PCPs.

In this work, we theoretically investigated adsorptions of CO, N_2, NO, and CO_2 in a paddle-wheel type porous coordination polymer (PCP) $[Cu(aip)]_n$ (aip = 5-azidoisophthalate) with ONIOM[MP4(SDQ):ωB97XD] method using a model system consisting of two $[Cu_2(O_2CC_6H_4\text{-}R)_4]$ units (R = H and Me) and one $[Cu_2(O_2CC_6H_4{-}R)_4]$ unit, namely, dimer and monomer models. The experimental CO adsorption position was reproduced well by the present calculation with the dimer model. For adsorptions of CO, N2, NO, and CO2 in the dimer model, the position of gas molecule deviates from the normal one that is found in the monomer model and becomes more distant from the surrounding phenyl group(s) of the neighbor [Cu(aip)] unit. For all of these gas molecules, the calculated binding energy (BE) at the deviating adsorption position is larger than that at the normal one against our expectation that the normal position is the best for the gas adsorption. The deviation of gas adsorption position arises from the interaction between the organic linker ($O_2CC_6H_4{-}R$ moiety) and gas molecule. For all cases, the exchange repulsion with the organic linker decreases to a larger extent than the attractive electrostatic and dispersion interactions decrease when going from the normal position to the deviating one. To enhance the binding energy of gas molecule, the introduction of electron-donating substituent on phenyl moiety is computationally recommended for this PCP.

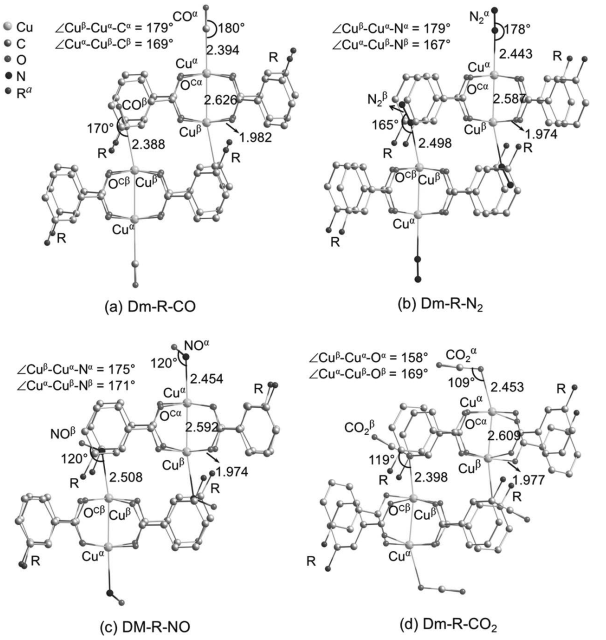

Figure 2. Optimized geometry of CO, N_2, NO, and CO_2 interacting with paddle-wheel Cu(II) PCPs.

(iv) Core−Shell versus Other Structures in Binary $Cu3_{8-n}M_n$ Nanoclusters (M = Ru, Rh, Pd, Ag, Os, Ir, Pt, and Au; n = 1, 2, and 6): Theoretical Insight into Determining Factors

Binary transition-metal (TM) nanoparticles consisting of two types of metal elements have attracted a great deal of interest recently because they are good candidates for such functional materials as heterogeneous catalysts, gas absorption materials, and magnetic storage materials. One good example is Pd−Pt binary nanodendrites, which exhibit a high activity for oxygen reduction. Other good examples include Pd−M (M = Pt or Au) and Ag−Cu binary nanoparticles, which are useful as dihydrogen gas absorption materials3,5,6 and catalysts for alkaline fuel cells, respectively. To understa effectively use such binary TM nanoparticles, on knowledge about their fundamental properties s geometry, electronic structure, and electron and sp about such properties is indispensable for mak nanoparticles. DFT calculations of binary transitio Pt, and Au; n = 1, 2, and 6) clearly show that a cor for M = Ru, Rh, Os, and Ir but unstable for M = segregation energies evaluated for $Cu_{37}M$. Electro Cu38−nMn(core) (M = Ru, Rh, Os, and Ir) than c substantially occurs for M = Ru, Rh, Os, and Ir be occupied. A linear relationship was first found d-orbital population of the core atom, indicating that the electron accumulation at the Mn core is one of the important factors for the segregation energy and the stabilization of the core−shell structure; in other words, a core−shell structure with M atom(s) in the core is stable when the d orbitals of M are not fully occupied. For M = Pd, Pt, and Au, the fused-alloy structure is more stable than the core−shell and phase-separated structures. For M = Ag, the fused-alloy structure is as stable as the phase-separated one but the core−shell structure is less stable. In these metals, the d orbitals are either nearly or fully occupied, and as a result, electron accumulation at the Mn core does not occur as much. For $Cu_{32}M_6$(core), the deformation energy of the Cu32 shell increases in the order Ru < Rh ≪ Pd < Ag and Os < Ir ≪ Pt < Au, because the size of the M6 core is substantially large for M = Pd, Ag, Pt, and Au. These results suggest that a large atom tends not to take the core position. The cohesive energies of Ru, Rh, Os, and Ir are larger than those of Pd, Ag, Pt, and Au, indicating that the cohesive energy is also an important property for understanding and discussing the structures of binary metal clusters/particles.

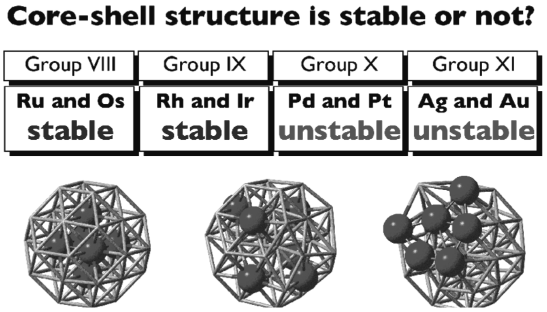

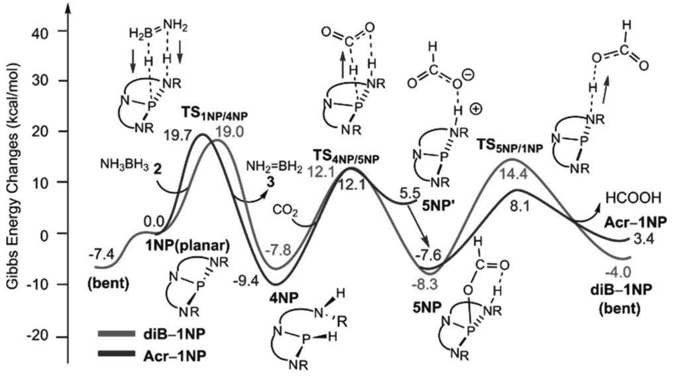

Figure 3. Energy and geometry changes in the CO_2 hydrogenation by three-coordinated P compounds

(v) How to Control Inversion vs Retention Transmetalation between Pd^{II}−Phenyl and Cu^{I}−Alkyl Complexes

Transition-metal-catalyzed cross-coupling reaction is an important reaction for C−C bond formation. Catalytic cycle of conventional cross-coupling reaction is well-known to consist of oxidative addition of aryl halide (ArX) to palladium(0) complex, transmetalation between palladium(II) aryl complex and organometallic reagent (R−M), and reductive elimination of product (Ar−R) from palladium(II) complex. For better understanding of the cross-coupling reaction, a theoretical study of each elementary step is necessary. Nakao and co-workers and Buchwald and co-workers have independently reported the reductive crosscoupling reaction between 1-arylalkenes and aryl bromides using Pd/Cu cooperative catalyst.

Transmetalation between $Pd(Br)(Ph^A)(PCyp_3)_2$ (Ph = phenyl, Cyp = cyclopentyl) and $Cu(C^aHMePh^B)(NHC)$ (NHC = 1,3-bis(2,6-diisopropylphenyl)-imidazolidin-2-ylidene) is an important elementary step in recently reported catalytic cross-coupling reaction by Pd/Cu cooperative system. DFT study discloses that the transmetalation occurs with inversion of the stereochemistry of the C^aHMePh^B group. In its transition state, the C^aHMePh^B group has almost planar structure around the C^a atom. That planar geometry is stabilized by conjugation between the π* orbital of the Ph^B and the 2p orbital of the C^a. Another important factor is activation entropy ($\Delta S^{\circ\ddagger}$); retention transmetalation occurs through Br-bridging transition state, which is less flexible than that of the inversion transmetalation because of the Br-bridging structure, leading to a smaller activation entropy in the retention transition state than in the inversion transition state. For C^aHMeEt group, transmetalation occurs in a retention manner. In the planar C^aHMeEt group of the inversion transition state, the C^a 2p orbital cannot find a conjugation partner because of the absence of π-electron system in the C^aHMeEt. Transmetalation of $C^aHMe(CH{=}CH_2)$ occurs in a retention manner because the vinyl π* is less effective for the conjugation with the C^a 2p because of its higher orbital energy than the Ph π*. The introduction of electronwithdrawing substituent on the Ph^B is favorable for inversion transmetalation. These results suggest that the stereochemistry of the C^a atom in transmetalation can be controlled by electronic effect of the C^aHMeR (R = phenyl, vinyl, or alkyl) and sizes of the substituent and ligand.

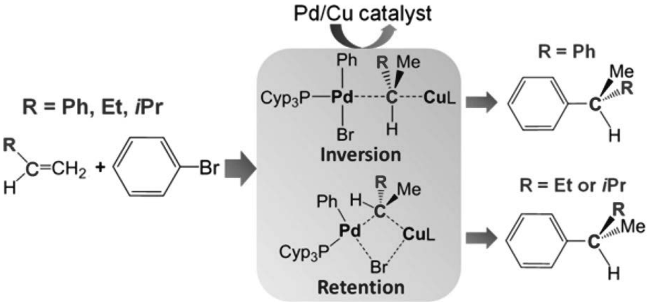

Scheme 2. Inversion vs. retention transmetallation between $Pd^{II}(Ph)$ and $Cu^I(alkyl)$ complexes.

2. Original Papers

(1) Ryoichi Fukuda, Nozomi Takagi, Shigeyoshi Sakaki, and Masahiro Ehara,
"On the Structures of Bimetallic Copper-Ruthenium Nanoparticles: Incoherent Interface and Surface Active Sites for Catalytic Nitric Oxide Dissociation"
J. Phys. Chem. C, 121, 300-307 (2017)..

(2) Vijay Singh, Yoshiaki Nakao, Shigeyoshi Sakaki, and Milind M. Deshmukh,
" Theoretical Study of Nickel-Catalyzed Selective Alkenylation of Pyridine: Reaction Mecha- nism and Crucial Roles of Lewis Acid and Ligands in Determining the Selectivity"
J. Org. Chem. 82, 289−301 (2017).

(3) Tao Yang, Ryoichi Fukuda, Saburo Hosokawa, Tsunehiro Tanaka, Shigeyoshi Sakaki, and Masahiro Ehara
"A Theoretical Investigation on CO Oxidation by Single-Atom Catalysts $M_1/\gamma\text{-}Al_2O_3$ (M = Pd, Fe, Co, and Ni)"
ChemCatChem, 9, 1222 – 1229 (2017).

(4) Takako Muraoka, Haruhiko Kimura, Gama Trigagema, Masayuki Nakagaki, Shigeyoshi Sakaki, and Keiji Ueno,
"Reactions of Silanone(silyl)tungsten and -molybdenum Complexes with MesCNO, $(Me_2SiO)_3$, MeOH, and H_2O: Experimental and Theoretical Studies"
Organometallics, 36, 1009−1018 (2017)..

(5) Yue Chen and Shigeyoshi Sakaki,
"Mo−Mo Quintuple Bond is Highly Reactive in H−H, C−H, and O−H □-Bond Cleavages Be-cause of the Polarized Electronic Structure in Transition State"
Inorg. Chem., 56, 4011−4020 (2017).

(6) Hong Zheng, Xiang Zhao, Shigeyoshi Sakaki, "[2+2]-type Reaction of Metal-Metal sigma-Bond

with Fullerene Forming an η^1-C_{60} Metal Complex: Mechanistic Details of Formation Reaction and Prediction of a New η^1-C_{60} Metal Complex"
Inorg. Chem., 56, 6746-6754 (2017)..

(7) Hajime Kameo, Yuki Baba, Shigeyoshi Sakaki, Didier Bourissou, Hiroshi Nakazawa, Hiroyuki Matsuzaka
"Iridium Hydride Mediated Stannane-Fluorine and -Chlorine sigma-Bond Activation: Re-versible Switching between X-Type Stannyl and Z-Type Stannane Ligands"
Organometallics, 36, 2096-2106 (2017).

(8) Yue Chen, Jyun-ya Hasegawa, Kazuya Yamaguchi, Shigeyoshi Sakaki,
"A coordination strategy to realize a sextuply-bonded complex"
Phys. Chem. Chem. Phys., 19, 14947-14954 (2017).

(9) Kenji Hirano, Hiroshi Nakano, Yoshihide Nakao, Hirofumi Sato, Shigeyoshi Sakai,
"Photo Absorption of p-Coumaric Acid in Aqueous Solution: RISM-SCF-SEDD Theory Approach"
J. Comp. Chem., 38, 1567-1573 (2017).

(10) Shinji Aono, Masayuki Nakagaki, Shigeyoshi Sakaki,
"Theoretical study of one-electron-oxidized salen complexes of group 7 (Mn(III), Tc(III), and Re(III)) and group 10 metals (Ni(II), Pd(II), and Pt(II)) with the 3D-RISM-GMC-QDPT method: localized vs. delocalized ground and excited states in solution"
Phys. Chem. Chem. Phys., 19, 16831-16849 (2017).

(11) M. Ramu Yadav, Masahiro Nagaoka, Myuto Kashihara, Rong-Lin Zhong, Takanori Miyazaki, Shigeyoshi Sakaki, Yoshiaki Nakao,
"The Suzuki–Miyaura Coupling of Nitroarenes"
J. Am. Chem. Soc., 139, 9423-9426 (2017).

(12) Shuwei Tang, Odile Eisenstein, Yoshiaki Nakao, and Shigeyoshi Sakaki,
"Aromatic C-H σ-Bond Activation by Ni0, Pd0, and Pt0 Alkene Complexes: Concerted Oxida-tive Addition to Metal vs Ligand-to-Ligand H Transfer Mechanism"
Organonetallics, 36, 2761-2771 (2017).

(13) Nozomi Takagi, Kazuya Ishimura, Masafuyu Matsui, Ryoichi Fukuda, Masahiro Ehara, and Shigeyoshi Sakaki,
"Core−Shell versus Other Structures in Binary Cu38−nMn Nanoclusters (M = Ru, Rh, Pd, Ag, Os, Ir, Pt, and Au; n = 1, 2, and 6): Theoretical Insight into Determining Factors"
J. Phys. Chem. C, 121, 10514−10528 (2017).

(14) Jingui Duan, Masakazu Higuchi, Jiajia Zheng, Shin-ichiro Noro, I-Ya Chang, Hyeon-Deuk Kim, Simon Mathew, Shinpei Kusaka, Easan Sivaniah, Ryotaro Matsuda, Shigeyoshi Sakaki, Susumu Kitagawa,
"Density Gradation of Open Metal Sites in the Mesospace of Porous Coordination Polymers"
J. Am. Chem. Soc., 139, 11576-11583 (2017).

(15) Jiajia Zheng, Shinpei Kusaka, Ryotaro Matsuda, Susumu Kitagawa, and Shigeyoshi Sakaki,
"Characteristic Features of CO_2 and CO Adsorptions to Paddle-Wheel-Type Porous Coordination Polymer"
J. Phys. Chem. C, 121, 19129-19139 (2017).

(16) Masafuyu Matsui and Shigeyoshi Sakaki,
"Embedded Cluster Model for Al_2O_3 and $AlPO_4$ Surfaces Using Point Charges and Periodic Electrostatic Potential"
J. Phys. Chem. C, 121, 20242-20253 (2017).

(17) Longfei Li, Ming Lei, and Shigeyoshi Sakaki,
"DFT Mechanistic Study on Alkene Hydrogenation Catalysis of Iron Metallaboratorene: Characteristic Features of Iron Species"
Organometallics, 36, 3530-3538 (2017).

(18) Hong Zheng, Kazuhiko Semba, Yoshiaki Nakao, and Shigeyoshi Sakaki,
"How to Control Inversion vs. Retention Transmetallation between Pd^{II}-Phenyl and Cu^{I}-Alkyl Complexes: Theoretical Insight"
J. Am. Chem. Soc., 139, 14065-14076 (2017).

3. Presentation at academic conferences

(1) S. Sakaki,
Catalysis by Combined System of Transition Metal Complex with Lewis Acid: Theoretical Insight into Crucial Role of Lewis Acid,
SouthEast Asia Catalysis Conference, May 22-23, 2017, Nanyang Technological University, Singapore (Kyenote)

(2) S. Sakaki
Theoretical Approach to CO_2 Adsorption to Flexible PCP
JST ACCEL R&D Project International Symposium, November 27-28, 2017; Kyoto (Invited).

(3) S. Sakai,
Theoretical Chemistry of Complex System of d Element: From Molecule to Functional Materials
2nd International Caparica Christmas Congress on Translational Chemistry, Dec. 5-7, 2017, Lisbon, Portogalu (Keynote)

(4) S. Sakaki
Theoretical Approach to Solid Systems such as MOFs and Metal Oxide Surface
The 8-th Asia-Pacific Confernece on Theoretical and Computational Chemistry, Indian Institute of Technology Bombay, Mumbai, India, Dec. 15-17, 2017.　(Invited)）

田中　一義

シニアリサーチフェロー

1．今年度の研究の要約

有機金属錯体における水素貯蔵の可能性探索は燃料電池の水素源確保の探索に向けて重要である。今年度は PH_3 を配位子とするメタロセン錯体（$M = Ti^{III}, Cr^{III}, Sc^{III}$ および V^{III}）における水素分子との反応と吸着について、遠距離および分散力補正を含めた DFT 計算(wB97XD/aug-cc-pVDZ)解析に基づく理論的検討を行った。特に Kubas 錯体の形成と余剰の水素分子の吸着に着目して反応および吸着エンタルピーの算出を行い、それぞれの金属錯体における水素吸蔵能の評価を行った。$[Cp_2Ti^{III}(PH_3)]^+$, $[Cp_2Sc^{III}(PH_3)]^+$ および $[Cp_2V^{III}(PH_3)]^+$ の場合には良好な水素分子吸着能が発現することが明らかになった。さらに V^{III} 錯体の場合には３重項状態が優勢となるという知見も得られた。一方、$[Cp_2Cr^{III}(PH_3)]^+$ では PH_3 が解離する傾向にあり、錯体そのものが形成されにくい。なおこの研究はトヨタ自動車と豊田中研との共同研究であり、平成 30 年 3 月の日化春季年会で発表済みの部分である。

【始めに】 燃料電池を搭載した自動車(FCV)における水素ガス供給法としては、通常の航続距離等を考慮した場合 700 気圧程度に加圧充填した水素タンクを積載する必要がある。これは必ずしも安全とは言えず、また高圧に耐える容器の重量および体積軽減など改善すべき問題点をいくつか含んでおり、その改善に向けた可能性を探ることが重要な課題となっている。その方策の一つとして、有機金属錯体における水素分子貯蔵の可能性を明らかにすることは意味があると考えられる。

有機金属錯体への水素分子付加反応について、従来は図 1 に示すような付加体（Kubas 錯体）の生成が知られている [1)]。この錯体では付加した水素分子が解離して金属 M との間に結合生成が起こるとされている。Kubas の原論文では明瞭にはふれられていないが、以下に述べるように、この Kubas 錯体には横(horizontal)Kubas 錯体と縦(vertical)Kubas 錯体がある。

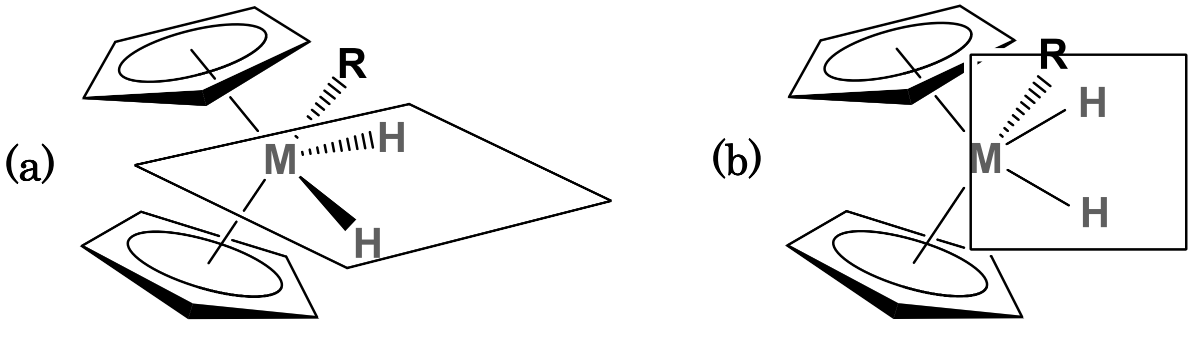

Fig. 1　Two kinds of Kubas complexes: (a) horizontal Kubas complex, and (b) vertical Kubas complex, where M stands for a transition metal of valence III state and R for an appropriate ligand.

本研究ではRをホスフィン($\mathrm{PH_3}$)とし、Mを$\mathrm{Ti^{III}}$, $\mathrm{Sc^{III}}$, $\mathrm{Cr^{III}}$および$\mathrm{V^{III}}$とするメタロセン錯体について水素分子付加に関する計算を行い、付加しうる水素分子数やその電子状態に関する解析を行った。

【計算方法】 計算は密度汎関数理論(DFT)に基づく wB97XD 法によって行い、基底としては aug-cc-pVDZ を用いて開殻系に対しては非制限法を適用した。計算には Gaussian09 ソフトを使用した 2)。具体的には$\mathrm{[Cp_2Ti^{III}(PH_3)]^+}$, $\mathrm{[Cp_2Sc^{III}(PH_3)]^+}$, $\mathrm{[Cp_2Cr^{III}(PH_3)]^+}$ および$\mathrm{[Cp_2V^{III}(PH_3)]^+}$について構造最適化を行い、これらの金属錯体に対する水素分子付加の可能性、最大付加数、付加錯体の構造最適化、さらに水素分子の電子状態等に関する知見を得るための解析を行った。

【$\mathrm{[Cp_2Ti^{III}(PH_3)]^+}$の解析結果

水素分子が付加する前のこの錯体は図 2(a)の形状であり、この錯体には最高で水素３分子が付加することが明らかとなった（図 2(b), (c)）。

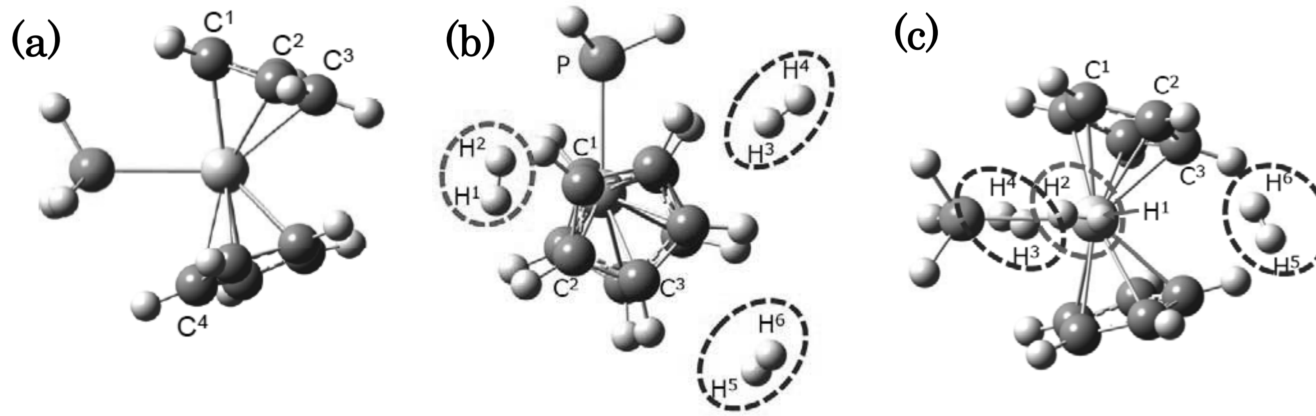

Fig. 2 Optimized structures of (a) $\mathrm{[Cp_2Ti^{III}(PH_3)]^+}$ complex and (b) that with three additional H_2 molecules. An H_2 molecule with red-broken oval makes a horizontal Kubas complex and those with blue-broken ovals are adsorbed ones. In (c) is indicated the same with (b) from a different angle.

$\mathrm{Ti^{III}}$は $3d^14s^0$の電子状態を持つとされるが、この錯体の多重度は１重項であった。横 Kubas 錯体形成によるエンタルピー安定化は 23.61 kJ/mol（298.15 K, 1 atm; 以下同じ)、第 2 および第 3 の水素分子付加によるエンタルピー安定化はそれぞれ 2.58, 1.65 kJ/mol であり、Kubas 錯体形成による値の１割程度である。H^1-H^2距離は 0.777 Å（WBI = 0.804）で、単一水素分子の結合距離 0.758 Å (WBI = 1.000)に比較してかなり緩んでいて、図 1(a)のような横 Kubas 錯体を作っていることが分かる。また Ti からのH^1とH^2への距離は 2.039 Å と 2.051 Å である。

一方、H^3-H^4およびH^5-H^6の結合距離は 0.758 Å (WBI = 0.987)および 0.757 Å (WBI = 0.997)で単一水素分子からの変化がほとんどなく、また Ti からの距離も遠い（3.496～4.581 Å 程度）など、この錯体に吸着されていると見てよいことが分かる。したがって、これら第 2 および第 3 の水素分子は燃料電池の水素源として使用できる可能性があることになる。

【$\mathrm{[Cp_2Sc^{III}(PH_3)]^+}$の解析結果】

水素分子が付加する前のこの錯体は図 3(a)の形状であり、この錯体にも最高で水素３分子が付加することが明らかとなった（図 3(b), (c)）。

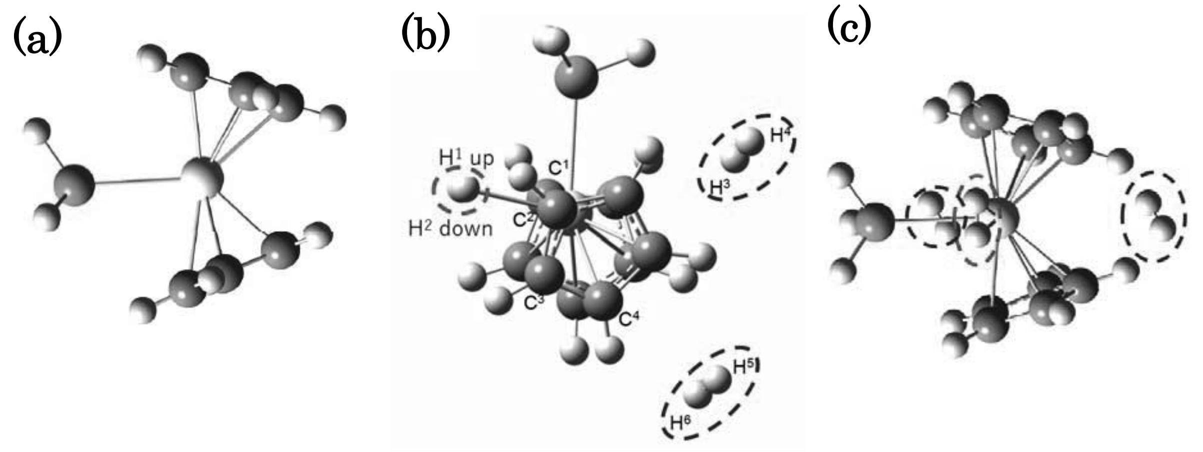

Fig. 3 Optimized structures of (a) $[Cp_2Sc^{III}(PH_3)]^+$ complex and (b) that with three additional H_2 molecules. An H_2 molecule with red-broken oval makes a horizontal Kubas complex and those with blue-broken ovals are adsorbed ones. In (c) is indicated the same with (b) from a different angle.

Sc^{III} は $3d^04s^0$ の電子状態を持つとされ、この錯体の多重度は１重項であった。Sc 錯体の場合は縦 Kubas 錯体が形成されており、これによるエンタルピー安定化は 16.97 kJ/mol、第 2 および第 3 の水素分子付加によるエンタルピー安定化はそれぞれ 1.87, 1.38 kJ/mol である。H^1-H^2 距離は 0.769 Å（WBI = 0.875）で、単一水素分子に比較してやはり緩んでいて、図 1(b)のような縦 Kubas 錯体を作っている。また Sc からの H^1 と H^2 への距離は 2.280 Å と 2.281Å である。

一方、H^3-H^4 および H^5-H^6 の結合距離はともに 0.757 Å (WBI = 0.988 および 0.996)で単一水素分子からほとんど変化がなく、また Sc からの距離も遠い（3.602～4.597 Å 程度）などから、この錯体でも第２および第３の水素分子は吸着されていると見てよいことが分かる。

【$[Cp_2Cr^{III}(PH_3)]^+$の解析結果】

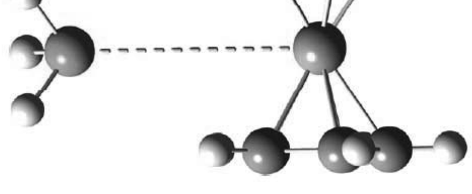

Fig. 4 Optimized structure of $[Cp_2Cr^{III}(PH_3)]^+$.

この錯体は図 4 の形状をしており、P-Cr 間の距離は 4.467 Å と遠くて PH_3 リガンドが脱離傾向にあり、この錯体自体の形状保持が困難である。ちなみに Cr^{III} は $3d^34s^0$ の電子状態を持つとされ、実際に２重項と４重項状態があるが、この錯体の多重度としては４重項状態が安定であった。さらに水素分子の付加を調べても構造は安定化せず、Cr が中心金属である場合には水素分子付加が困難であったので、これ以上の解析は中止した。

【$[Cp_2V^{III}(PH_3)]^+$の解析結果】

水素分子が付加する前のこの錯体は図 5(a)の形状であり、この錯体には最高で水素２分子が付加

することが明らかとなった（図 5(b), (c)）。ただし V の場合には Kubas 錯体は形成せずに、第 1 水素分子から吸着されることも分かった。

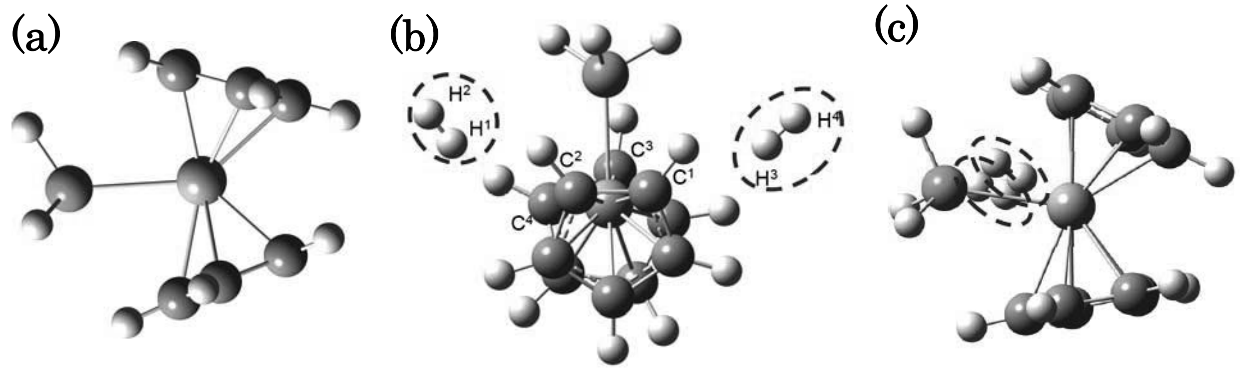

Fig. 5　Optimized structures of (a) $[Cp_2V^{III}(PH_3)]^+$ complex and (b) that with two additional H_2 molecules.　Both the two H_2 molecules with blue-broken ovals are adsorbed.　In (c) is indicated the same with (b) from a different angle.

V^{III} は $3d^24s^0$ の電子状態を持つとされ、実際に 1 重項と 3 重項状態があるが、この錯体の多重度としては 3 重項状態が安定であった。V 錯体の場合には上記のように、そもそも Kubas 錯体が形成されず、第 1 および第 2 の水素分子付加によるエンタルピー安定化はそれぞれ 3.14, 3.02 kJ/mol であった。H^1-H^2 および H^3-H^4 の結合距離はともに 0.758 Å (WBI = 0.979 および 0.980)で単一水素分子からほとんど変化がなく、また V からの距離も遠い（3.253～3.960 Å 程度）ことなど、この錯体でも第 1 および第 2 の水素分子が吸着されていると見てよい。

【まとめ】

以上のように PH_3 を配位子とするメタロセン錯体 (M = Ti^{III}, Cr^{III}, Sc^{III} および V^{III}) における水素分子との反応と吸着については、中心金属によってそれぞれの電子状態挙動には違いがあり、Ti^{III}, Sc^{III} および V^{III} 錯体には 2 個の水素分子が吸着しうることが明らかとなった。この吸着には分散力などが効いていることが考えられ、それ自体興味深い問題を提供している。また Kubas 錯体の形成状況にもそれぞれ差異があることが分かった。これは d 電子状態の特性の違いによるものと考えられる。これらの知見は燃料電池における水素源の開発にとって有用なものと期待できる。ここで解析した金属錯体の実際の使用法としては粉体状態での利用などを含めて今後考慮すべき点が多くあり、それらに関する検討も必要である。また同時に金属種や分子骨格の軽量化に向けても検討を広げる予定である。

【文献】 1) G. J. Kubas, *Acc. Chem. Res.*, **21**, 120-128 (1988). 2) Gaussian 09, Revision D.01, M. J. Frisch et al., Gaussian Inc., Wallingford, CT (2009).
2) Gaussian 09, Revision D.01, M. J. Frisch et al., Gaussian Inc., Wallingford, CT (2009).

2. 論文

(1) Kensuke NAKA, Takuji KATO, Koushi ABE, Makoto ISHIDOSHIRO, Shintaro NISHIYAMA, Susumu TANAKA, Hiroaki IMOTO, Seiji WATASE, Kimihiro MATSUKAWA, Hiroyuki FUENO, and Kazuyoshi TANAKA,
"Stereoisomerization of 1,4-dihydroarsinetetracarboxylic acid diimides under non-acidic condition from cis- to trans-forms"
Heterocycles 94(5), 923-937 (2017).

(2) Joji OHSHITA, Toshiyuki TSUCHIDA, Kenji KOMAGUCHI, Kazuki YAMAMOTO, Yohei ADACHI, Yousuke OOYAMA, Yutaka HARIMA, and Kazuyoshi TANAKA,
"Studies of spherically distributed LUMO and electron-accepting properties of caged hexakis(germasesquioxanes)"
Organometallics 36(14), 2536-2540 (2017).

(3) Toshiaki IKEDA, Hiroaki ADACHI, Hiroyuki FUENO, Kazuyoshi TANAKA, and Takeharu HAINO,
"Induced-dipole-directed, cooperative self-assembly of a benzotrithiophene"
J. Org. Chem. 82(19), 10062-10069 (2017).

(4) Katsunori SUZUKI, Yasuyuki NUMATA, Naoko FUJITA, Naoki HAYAKAWA, Tomoharu TANIKAWA, Daisuke HASHIZUME, Kohei TAMAO, Hiroyuki FUENO, Kazuyoshi TANAKA, and Tsukasa MATSUO,
A stable free tetragermacyclobutadiene incorporating fused-ring bulky EMind groups
Chem. Commun. 54(18), 2200-2203 (2018).

3. 総説

(1) 田中一義
「化学つれづれ草　第一回　理屈っぽい化学？」
化学 72, No. 5, 55 (2017).

(2) 田中一義
「化学つれづれ草　第二回　福井研究室の日常」
化学 72, No. 6, 31 (2017).

(3) 田中一義
「化学つれづれ草　第三回　博士課程 考」
化学 72, No. 7, 29 (2017).

(4) 田中一義
「化学つれづれ草　第四回　米国のベンチャー企業」
化学 72, No. 8, 27 (2017).

(5) 田中一義
「化学つれづれ草　第五回　米国の研究資金事情」

化学 72, No. 9, 18 (2017).

(6) 田中一義
「化学つれづれ草　第六回　日本の大学と研究資金」
化学 72, No. 10, 29 (2017).

(7) 田中一義
「化学つれづれ草　第七回　妄想と基礎研究資金」
化学 72, No. 11, 46 (2017).

(8) 田中一義
「化学つれづれ草　第八回　企業と大学の研究」
化学 72, No. 12, 28 (2017).

(9) 田中一義
「化学つれづれ草　第九回　オリジナルな研究」
化学 73, No. 1, 59 (2018).

(10) 田中一義
「化学つれづれ草　第十回　理論化学と計算化学」
化学 73, No. 2, 29 (2018).

(11) 田中一義
「化学つれづれ草　第十一回　分割統治と化学」
化学 73, No. 3, 24 (2018).

4. 学会発表

(1) Kazuyoshi Tanaka, Hiroyuki Fueno, Hiroyuki Suto, Takuji Kita, Mitsuru Matsumoto, and Takashi Kuzuya,
“Theoretical Examination on Absorption of Hydrogen Molecules to Metallocene Complex”
日本化学会第 98 春季年会(2018) 船橋 2018/3/21　2PA-132

5. その他

(1) 田中一義
「計算化学はどのように役立つか」京都グリーンケミカル・ネットワーク若手人材交流事業、京都（京都市成長産業創造センター）2017/11/2　（講演番号なし）

４．リサーチリーダー

Kazuo Takatsuka

Research Leader

Summary of the research of the year

We have been developing a basic framework of theoretical chemistry, which we call the theory of nonadiabatic electron wavepacket dynamics with an aim to cultivate new fields of theoretical chemistry. One outcome of such theoretical developments in this year is a novel formalism of molecular nonadiabatic electron dynamics in condensed phases such as in solvents. Also, we have discussed the notion of nonadiabatic dynamics beyond the frame work of quantum theory. Indeed a series of hierarchical subsystems of different time-scales in classical mechanics have been formulated, which are shown to have much similarity to quantum nonadiabatic dynamics.

In the aspect of applications of the theory of nonadiabatic dynamics, one of the major progresses made in this year of period is the analysis and proposal of photocatalytic cycle of water splitting with small manganese oxides and the roles of water cluster as a direct resource of oxygen molecules. We have also shown a mechanism of collision induced charge separation in ground-state water splitting dynamics. These findings are really epoch making in the field of charge separation dynamics in biological and/or organic systems. Another important branch of the applications is the nonadiabatic electron dynamics in molecular ionization such as multiphoton photoionization, auto ionization, and so on. The theoretical challenge made in our group has demonstrated that electron detachment dynamics can be treated in terms of ab initio scheme of nonadiabatic electron wavepacket dynamics just as in the standard quantum chemistry.

We are further developing a new concept of chemical bonding, which we call “dynamical chemical bond” or “hyper-resonance”, which will be published soon. Development of the theory of relativistic electron dynamics is also in progress. Besides, we have been constructing a methodology and algorithm for describing nuclear wavepackets besides the electron wavepakets simultaneously.

(i) Theory of molecular nonadiabatic electron dynamics in condensed phases. [1]

In light of the rapid progress of ultrafast chemical dynamics driven by the pulse lasers having width as short as several tens of attoseconds, we have developed a theory of nonadiabatic electron wavepacket dynamics in condensed phases, with which to directly track the dynamics of electronic-state mixing such as electron transfer in liquid solvents. Towards this goal, we combined a theory of path-branching representation for nonadiabatic electron wavepacket dynamics in vacuum [a mixed quantum-classical representation, Yonehara and Takatsuka, J. Chem. Phys.,**129**, 134109 (2008)] and a theory of entropy functional to treat chemical dynamics in condensed phases [a mixed dynamical-statistical representation, Takatsuka and Matsumoto, PCCP, **18**, 1771 (2016)]. Difficulty and complexity in the present theoretical procedure arise in embedding the Schrödinger equation into classically treated statistical environment. Nevertheless, it has been shown that the resultant equations of motion for electronic-state mixing due to the intrinsic nonadiabatic interactions and solute-solvent interactions, along with the force matrix that drives nuclear branching paths, both turn out to be clear enough to make it possible to comprehend the physical meanings behind. We also discussed briefly nonvalidness of naive application of the notion of nonadiabatic transition dynamics among free energy surfaces.

ii) On photocatalytic cycle of water splitting with small manganese oxides and the roles of water cluster as a direct resource of oxygen molecules. [2]

We theoretically have studied chemical principles behind photodynamics of water splitting; $2H_2O + 4h\nu + M \rightarrow 4H^+ + 4e^- + O_2 + M$. To comprehend this simple looking but very complicated reaction, the mechanisms of at least three crucial phenomena, among others, need to be clarified, each of which is supposed to constitute the foundation of chemistry: (i) Charge separation $4H^+ + 4e^-$, (ii) catalytic cycle for essentially same reactions to be repeated by each of four photon absorptions with a catalyst M, and (iii) generation of oxygen molecule of spin triplet. We clarified before the photodynamical mechanism of charge separation, which we refer to as coupled proton electron-wavepacket transfer (CPEWT), based on the theory of nonadiabatic electron wavepacket dynamics [K. Yamamoto and K. Takatsuka, 2017, ChemPhysChem, **18**, 537]. CPEWT gives an idea on how charge separation can be materialized at each single photon absorption. Yet, this mechanism alone cannot address the above crucial items (ii) catalytic cycle and (iii) O_2 formation. In the studies on these fundamental processes, we constructed a minimal possible chemical system and perform semi-quantitative quantum chemical analyses, with which to attain the insights about possible mechanisms of photochemical water splitting. The present study has been inspired by the idea underlying the so-called Kok cycle, although we do not aim at simulation of photosystem II in biological systems in nature. For instance, we here assumed that a catalyst M, actually simple manganese oxides in this particular study, is pumped up to its excited states leading to charge separation by four-time photon absorption, each excitation at which triggers individual series of chemical reactions including the reorganization of hydrogen-bonding network (cluster) of water molecules surrounding the photocatalytic center. It was shown that in the successive processes of restructuring of the relevant water cluster, O=O bond is formed and consequently oxygen molecule of spin triplet can be isolated within a range of given photon energy of about 3.0 eV.

iii) Collision induced charge separation in ground-state water splitting dynamics. [3]

In one type of photocatalytic dynamics of water splitting formally summarized as

$$2H_2O + 4h\nu + MH \rightarrow 2H_2O + M^*H \rightarrow 4H^+ + 4e^- + O_2 + MH$$

the catalytic center M mainly composed of Mn oxides (clusters) along with supporting molecules like proteins is directly photoexcited and discharges electrons and protons from it. The mechanism can be comprehended in terms of the coupled proton electron-wavepacket transfer (CPEWT). In another type proposed in the literature, M is not directly photoexcited, and instead, the lights are absorbed somewhere other than M, thereby creating complicated sequential steps (a ladder) of oxidation-reduction potential, thus sucking electrons successively from one molecular site to the next, and the final place providing electrons and protons is the catalytic center M. During the charge separation dynamics, M is assumed to remain in the electronic ground state, and this type can be schematically summarized as

$$MH + \Omega^+ \rightarrow M^+ + H\Omega,$$

where Ω indicates a cation species (a hole carrier) the site of photon absorption. It is widely believed that the latter mechanism is responsible for water splitting in plants and cynobacteria, and M in photosystem II (PSII) is known to include Mn_4CaO_5. However, heavy questions about this mechanism of ground-state charge separation in the latter reaction arise as to whether it is quantum mechanically possible and what is it, if indeed possible. Besides, the time-constant for this reaction reported in the literature is so long, actually far longer than the time-scale for energy dissipation for inter- and intra-molecular vibrational energy redistribution, that the quantum mechanical coherence of the reaction should not be able to be maintained. More seriously, we wonder how the protons and electrons can be isolated in the ground state, if any, and how they can be transferred unidirectionally (with no return)? We have addressed these fundamental questions and clarified them affirmatively by proposing a general chemical principle; collision induced charge separation dynamics in ground state.

iv) Time-resolved photoelectron signals from bifurcating electron wavepackets propagated across conical intersection in path-branching dynamics. [4]

A computational scheme of energy- and geometry-dependent photoelectron signals from the dynamics near a conical intersection based on a simplified path-branching representation of nonadiabatic electron wavepacket dynamics has been proposed. Taking the NO_2 X/A conical intersection as an example, the results of the present scheme compared to those from previous study based on the method of full quantum vibrational wavepacket shows qualitative agreement suggesting promising application to computation in larger systems intractable to full quantum exact methods.

v) Nonadiabatic electron wavepacket dynamics behind molecular autoionization. [5]

A theoretical method for real-time dynamics of nonadiabatic reorganization of electronic configurations in molecules has been developed, with dual aim that the intramolecular electron dynamics can be probed by means of direct and/or indirect photoionizations and that the physical origins behind photoionization signals attained in the time domain can be identified in terms of the language of time-dependent quantum chemistry. In doing so, we first formulated and implemented a new computational scheme for nonadiabatic electron dynamics associated with molecular ionization, which well fits in the general theory of nonadiabatic electron dynamics. In this method, the total nonadiabatic electron wavepackets are propagated in time directly with complex natural orbitals without referring to Hartree-Fock molecular orbitals, and the amount of electron flux from a molecular region leading to ionization is evaluated in terms of the relevant complex natural orbitals.

We have applied the method to electron dynamics in the elementary processes consisting of the Auger decay to demonstrate the methodological significance. An illustrative example was taken from an Auger decay starting from the 2a□ orbital hole-state of H_2O^+. The roles of nuclear momentum (kinematic) couplings in electronic-state mixing during the decay process were analyzed in terms of complex natural orbitals, which are schematically represented in the conventional language of molecular symmetry of the Hartree-Fock orbitals.

vi) Adiabatic and nonadiabatic dynamics in classical mechanics for coupled fast and slow modes: sudden transition caused by the fast mode against the slaving principle. [6]

Adiabatic and nonadiabatic dynamics in classical systems composed of fast and slow modes have been formulated. Theoretical consequences from both adiabatic and nonadiabatic dynamics have also been discussed. In particular, we aimed to identify a possible physical origin for drastic change of the slow dynamics to be induced by instability that happens to emerge in the fast mode. The Haken slaving principle and other theories like the adiabatic elimination method focus on the order formation led by the growth of the slow modes, with slaving the fast modes so as to faithfully follow the system dynamics. In this context, the fast modes are quite often regarded as "noise" or a factor of small fluctuation. However, in molecular nonadiabatic dynamics due to the breakdown of the Born-Oppenheimer approximation, the roles of the fast mode (due to electron dynamics) is far from that of "noise", and sometimes bring about a qualitative bifurcation of the dynamics of the slow subsystem, which we usually refer to as nonadiabatic transition. We have shown the similar sudden change can be caused by the fast mode in classical mechanics too. The similarity and difference between quantum and classical nonadiabatic dynamics were discussed. Recursive equations of motion for general hierarchical dynamics composed of three and more modes have been also given.

2. Original papers

[1] Theory of molecular nonadiabatic electron dynamics in condensed phases.
Kazuo Takatsuka, J. Chem. Phys. **147**, 174102 (13 pages) (2017).
https://doi.org/10.1063/1.4993240

[2] On photocatalytic cycle of water splitting with small manganese oxides and the roles of water cluster as a direct resource of oxygen molecules.
Kentaro Yamamoto and Kazuo Takatsuka, PCCP, **20**, 6708-6725 (2018)
DOI:10.1039/c7cP0717j

[3] Collision induced charge separation in ground-state water splitting dynamics
Kentaro Yamamoto and Kazuo Takatsuka, PCCP, **20**, 12229-12240 (2018).

[4] Time-resolved photoelectron signals from bifurcating electron wavepackets propagated across conical intersection in path-branching dynamics.
Yasuki Arasaki and Kazuo Takatsuka, Chem. Phys. **493**, 42-48 (2017)
DOI: 10.1016/j.chemphys.2017.06.008

[5] Nonadiabatic electron wavepacket dynamics behind molecular autoionization.
Takahide Matsuoka and Kazuo Takatsuka, J. Chem. Phys. **148**, 014106 (15 pages) (2018).
https://doi.org/10.1063/1.5000293

[6] Adiabatic and nonadiabatic dynamics in classical mechanics for coupled fast and slow modes: sudden transition caused by the fast mode against the slaving principle.
Kazuo Takatsuka, Mol. Phys. (Michael Baer Festschrift issue), accepted on line (2018.2.13).

3. Presentation at academic conferences

［国際研究集会］

1. “Time-Domain Quantum Chemistry”
Kazuo Takatsuka, Nonadiabatica2018, Jerusalem, Israel, 2018. 3. 15 (Invited)

2. “Electron Dynamics in Chemical Reactions: Time-Domain Quantum Chemistry.”
(Mizushima-Raman Lecture), Kazuo Takatsuka, CRSI, Raipur, India 2018. 2. 3 (Invited)

3. “Molecular Science beyond the Born-Oppenheimer Paradigm.” (Sadhan Basu Memorial Lecture) Kazuo Takatsuka, IACS, Kolkata India 2018.3.5 (Invited)

4. “Nonadiabatic electron dynamics in chemical reactions: Basic theory for chemical reactions in the age of real-time observation.”
Kazuo Takatsuka, APCTCC8. Mumbai, 1. 15-17. 2018 (Invited)

5. “Photocatalytic cycle of water splitting with small manganese oxides and the roles of water cluster as a direct resource of oxygen molecules.”
Kentaro Yamamoto and Kazuo Takatsuka, Sanibel Symposium, 2018. 2.14

6. “Auger Decay Process in Water Molecule: A Nonadiabatic Electron Dynamics Treatment.”
Takahide Matsuoka and Kazuo Takatsuka,2nd_International_Symposium_on_Attosecond_Science, 2017.8, 24 Riken

7. “Molecular Science of Nonadiabatic Electron Wavepackets: Trying to bridge between ultrafast nonadiabatic dynamics and chemistry”
Kazuo Takatsuka , Okazaki Conference, Okazaki, 2017.3.6. (Invited)

8. “Photodynamical electron-wavepacket mechanism of water-splitting catalyzed by manganese oxides involving hydrogen-bond network”
Kentaro Yamamoto and Kazuo Takatsuka, Okazaki Conference, Okazaki, 2017. 3.6.

［国内研究集会］

1）“古典動力学における時間階層性と非断熱過程－隷従原理と隷従者の反乱－”
高塚和夫，分子科学討論会2017. 15-18 東北大学

2）“高強度レーザー中の非断熱電子波束の対称性の破れについて”
松岡貴英，高塚和夫，分子科学討論会 2017. 15-18 東北大学

3）“生物系から着想を得た単純な系における衝突誘起の逐次的な電子移動；非断熱の電子波束による研究”
山本 憲太郎，高塚 和夫，第 11 回分子科学討論会，2017/09/15 – 18，東北大 川内北キャンパス

4）“配位空間の幾何学と量子波束ダイナミクス”

高橋 聡，高塚 和夫，第 11 回分子科学討論会，2017/09/15 – 18，東北大 川内北キャンパス

5）“Time-Domain Quantum Chemistry　－電子の運動が観える時代の化学理論－”
高塚和夫　近畿化学協会コンピュータ化学部会公開講演会　大阪科学技術センター
10.27.2017

6）“水分子のイオン化の背景にある非断熱電子動力学：Auger 電子と高強度レーザーによる光電子について”
松岡貴英，高塚和夫，第 20 回理論化学討論会，2017/05/16 – 18，京大時計台国際交流ホール

7）“電子波束動力学的な電荷分離の機構によって駆動される Mn 酸化物中の水の光分解サイクル”
山本 憲太郎，高塚 和夫， 第 20 回理論化学討論会，2017/05/16 – 18，京大時計台国際交流ホール

５．博士研究員

Mitsusuke Tarama

FIFC Fellow

1. Summary of the research of the year

Mechanics of cell crawling by means of force-free cyclic motion

Dynamics of active particles have attracted much attention from physicists over the past decade. In contrast to passive particles, active particles exhibit spontaneous motion such as directional translation without external forcing. This property of a vanishing force monopole is known as the force-free condition. Therefore, it is not trivial how active particles can achieve a net translational motion from an internal cyclic motion.

In his pioneering lecture, Purcell shed light on the importance of breaking the time-reversal symmetry [1]. His idea was theoretically investigated later by using a simple model swimmer composed of three linked spheres at low Reynolds number. The time-reversal symmetry can be broken by a phase shift between the periodic oscillations of at least two active linkers. This study was extended to include autonomous oscillation of the bond length and swimming in a viscoelastic suspension. All these studies are concerning microswimmers, i.e., microscopic objects that are moving in a fluid environment.

In contrast to microswimmers that swim through a fluid environment, there also exist microorganisms that migrate on a substrate. Such crawling motion is often observed for eukaryotic cells, such as Dictyostelium cells and keratocyte. Typically, the mechanism of crawling motion is widely believed to consist of the following four steps [2]:

1. Protrusion of the leading edge due to actin polymerization
2. Adhesion of the leading edge to the substrate underneath
3. Deadhesion of the trailing edge from the substrate
4. Contraction of the cell body due to actomyosin contraction

Despite a number of studies on each of these steps, the cycle of crawling mechanism itself has not been verified systematically. Therefore, we investigated the basic mechanism of cell crawling with a focus on the cycle of protrusion and contraction, as well as adhesion to the substrate underneath.

To this end, we proposed a mechanical model, where a cell is described by a set of subcellular elements connected by a viscoelastic bond [3]. The bond consists of a damper and an elastic spring, as well as an actuator that elongates cyclicly, as depicted in Fig. 1(a). The cyclic elongation of the actuator $\ell(t)$ represents the protrusion and contraction, which we modelled by a simple sinusoidal function with the frequency ω, $\ell(t) = -\ell_1 cos(\omega t)$. In addition, the adhesion to the substrate underneath and the deadhesion from it are included as a cyclic change in the strength of the substrate friction $\zeta_i(t)$, where the subscript i indicates the one of the two elements i=1,2. We assumed that the substrate friction takes the adhered stick state ζ_a and the deadhered slip state ζ_f for the same intervals, which represents the adhesion-deadhesion transition. We keep the frequency of the friction change same as the actuator elongation but with phase shift ψ_i. The phase shifts ψ_1 and ψ_2 are the two key parameters in this study, which may differ from each other. See Fig. 1(b). Then, the equations of motion are given by

$$\zeta_1(t)v_i + \xi(v_1 - v_2) = -k\{x_{12} - (\ell_0 + \ell(t))\}$$

$$\zeta_2(t)v_i + \xi(v_2 - v_1) = k\{x_{12} - (\ell_0 + \ell(t))\}$$

where v_1 and v_2 are the velocity of the element 1 and 2, respectively, and their distance is

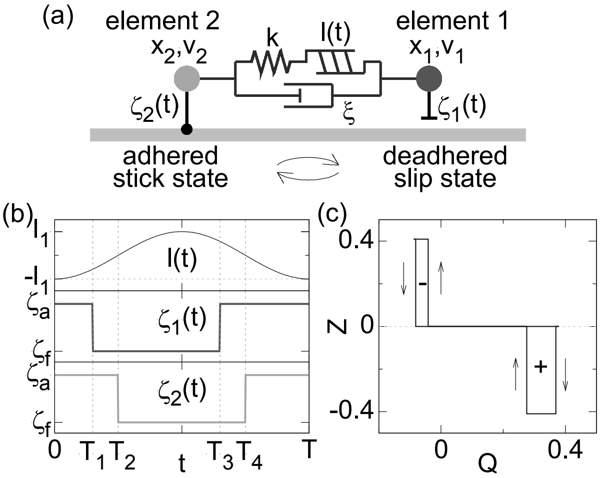

Fig. 1: (a) Schematics of the two-element model of a cell crawling on a substrate (grey). The red and cyan elements are connected by a viscoelastic bond (blue), which consists of a spring of elasticity k, a dashpot with dissipation rate ξ, and a linear actuator with time-dependent length l(t). The substrate friction $\zeta_i(t)$ of each element switches between the stick and slip states. (b) An example of the time series for l(t), $\zeta_1(t)$, and $\zeta_2(t)$, and (c) the corresponding trajectory in the Q–Z space, where the signed area enclosed by the curve denotes the distance over which the cell travels during the corresponding time interval. In panel (c), the black arrows show the time evolution direction and the plus and minus signs indicate the temporal forward and backward migration, respectively. This figure is reproduced from Ref. [3].

given by $x_{12} = |x_2 - x_1|$. k and ℓ_0 are the elastic constant and free length of the spring and ξ is the dissipation rate of the damper. Here, since the typical size of a cell is of order of tens of micrometers, the inertia term was neglected.

We measured the migration distance in one cycle ΔR, which is calculated as

$$\Delta R = \sum_{n=1}^{4} Z_n (Q_n - Q_{n-1})$$

where $Q_n = x_{12}(T_n) - \ell_0$ and $Z_n = (\zeta_2(T_n) - \zeta_1(T_n))/2(\zeta_1(T_n) + \zeta_2(T_n))$ represent the actual elongation of the cell and the symmetry breaking of the substrate friction at time T_n, respectively. Here, the time T_n (n=1,2,3,4) is the boundary of the time sections, within each of which both substrate frictions ζ_1 and ζ_2 are constant. See Fig. 1(b). Here, we assumed a steady state. This formula of ΔR indicates that the migration distance is given by the signed area enclosed by the trajectory in Q-Z space. The analytical formula of the solution ΔR is provided in Ref. [3].

In addition, we measured the efficiency of the crawling motion, which is defined by $\eta = (\Delta R / W_{in}) / max(\Delta R / W_{in})$. W_{in} is the input energy, which comes from the work done by the actuator. Since the cell moving horizontally on a flat substrate does not do any work, the output work is evaluated under an additional infinitesimal external force f_ϵ as $f_\epsilon \Delta R$. Note that the efficiency is normalized by the maximum value to eliminate f_ϵ. The exact formula of η was also obtained in Ref. [3].

The resulting ΔR and η are plotted against the phase shifts ψ_1 and ψ_2 in Fig. 2. The difference of the substrate friction at the adhered and deadhered states are set as $\zeta_a = 10\zeta_f$ and $\zeta_f \omega / k = 0.2\pi$. The other parameters are fixed as $T = 2\pi/\omega = 1$, $k = 1$, $\ell_0 = 1.5$, and $\ell_1 = 0.5$.

If the two elements are in phase indicated by the thick black line in Fig. 2, then the cell only oscillates its length around the stationary centre of mass as in Fig. 3 (b). Apart form the in-phase line, the cell starts to migrate. If the two elements are in anti-phase, there are optimum set of phase shifts (ψ_1, ψ_2) indicated by the plus and cross symbols in Fig. 2,

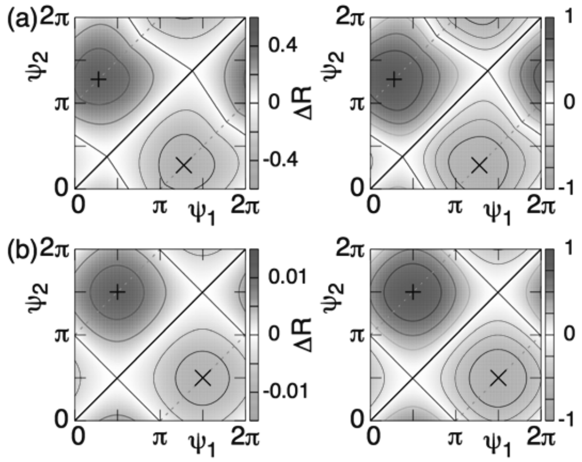

Fig. 2: The net crawling displacement of the two-element cell over one period ΔR and the efficiency η as functions of the phase shift ψ_1 and ψ_2 for different values of the intracellular dissipation rate: (a) $\xi\omega/k = 0.2\pi$ and (b) 20π. The red (cyan) colour corresponds to the forward (backward) motion, i.e., the motion towards element i = 1(2). The phase shifts that give the maximum and the minimum of ΔR and η are indicated by the plus and the cross signs, respectively. The diagonal thick black lines and the thin black lines represent the in-phase oscillatory motion and the reciprocating motion, neither of which show a net locomotion. This figure is reproduced from Ref. [3].

corresponding to the optimum forward and backward motions, respectively. The forward optimum crawling motion is depicted in Fig. 3(a). However, even if the anti-phase case, the cell cannot achieve a net migration if it undergoes reciprocating motion, i.e. back-and-forth motion, as displayed in Fig. 3(c).

In summary, we investigated the mechanism of cell crawling by focusing on how to obtain a net migration from the internal cyclic motion under the force-free condition. We introduced a mechanical model where a cell is described by two subcellular elements connected by a viscoelastic bond. The activity of the cell is included in the actuator elongation of the bond and the switch of the substrate friction, which represent the protrusion and contraction and the adhesion to the substrate underneath and deadhesion from it, respectively. We highlighted the importance of the phase shift of the substrate friction of each subcellular element with respect to the bond elongation to achieve a net migration.

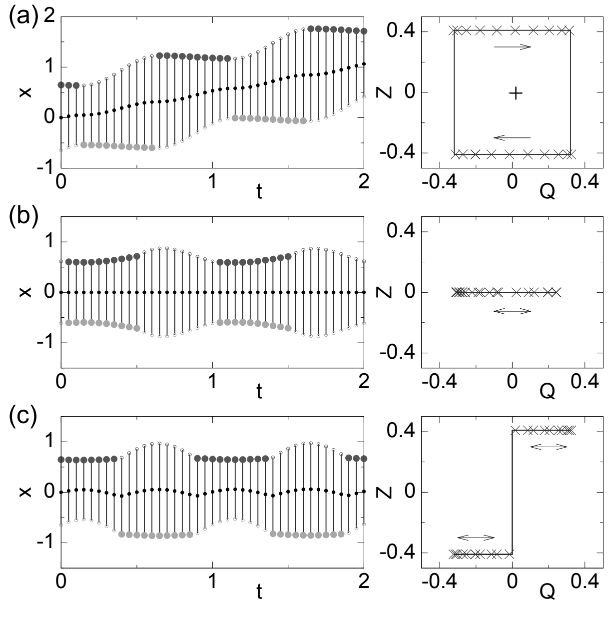

Fig. 3: Two-element cell for $\xi\omega/k = 0.2\pi$ and (a) $\psi_1 = 0.27\pi$ and $\psi_2 = 1.27\pi$, (b) $\psi_1 = \psi_2 = \pi$, and (c) $\psi_1 = 0.778794\pi$ and $\psi_2 = 1.778794\pi$. In each panel, the left subfigure shows the spatiotemporal plot for two periods. The right subfigure displays the corresponding trajectory in the Q–Z space. This figure is reproduced from Ref. [3].

References:

[1] E. M. Purcell, *Am. J. Phys.*, **45**, 3 (1977).
[2] R. Ananthakrishnan and A. Ehrlicher, Int. J. Biol. Sci. **3**, 303 (2007).
[3] M. Tarama and R. Yamamoto, J. Phys. Soc. Jpn. **87**, 044803 (2018).

2. Original papers

(1) Mitsusuke Tarama
“Swinging motion of active deformable particles in Poiseuille flow”
Phys. Rev. E **96**, 022602 (2017).

(2) Mitsusuke Tarama
“Dynamics of Deformable Active Particles under External Flow Field”
J. Phys. Soc. Jpn. **86**, 101011 (2017).

(3) Mitsusuke Tarama and Ryoichi Yamamoto
“Mechanics of cell crawling by means of force-free cyclic motion”
J. Phys. Soc. Jpn. **87**, 044803 (2018).

3. Presentation at academic conferences

(1) Mitsusuke Tarama,
“Swinging motion of active deformable particles in Poiseuille flow”
9th International Conference Engineering of Chemical Complexity, Neàpolis Auditorium, Vilanova i la Geltrú, Barcelona, Spain, 19 Jun, 2017 (oral).

(2) Mitsusuke Tarama,
“Dynamics of active deformable particles in Poiseuille flow”
10TH LIQUID MATTER CONFERENCE, Cankarjev dom Cultural and Congress Centre, Ljubljana, Slovenia, 17-18 Jul, 2017 (poster).

(3) Mitsusuke Tarama,
“Active Deformable Particles in Poiseuille Flow”
International Symposium on Fluctuation and Structure out of Equilibrium 2017, Sendai International Center, Sendai, Japan, 21 Nov, 2017 (poster).

(4) 多羅間充輔,
“生物細胞のメカノケミカル・モデル”
札幌非線形現象研究会 2017, 北海道大学 電子科学研究所, 30 Aug, 2017 (oral).

(5) Mitsusuke Tarama, Kenji Mori, and Ryoichi Yamamoto,
“Mechano-chemical modelling of biological cells”
A02 班 A03 班合同研究会「アクティブマターの概念で繋ぐ生命機能の階層性」
“Hierarchy of biological functions connected by concept of active matter”, 函館　グリーンピア大沼, 11 Sep, 2017 (oral).

(6) 多羅間充輔,
“ポワズイユ流れ中のアクティブソフトマターのダイナミクス”
第 7 回ソフトマター研究会, 京都大学・北部研究総合棟・益川ホール＆理学研究科セミナーハウス, 25 Oct, 2017 (oral: invited).

(7) 多羅間充輔,
“変形する自己推進粒子のポワズイユ流れの中での運動”
生物流体力学における基礎問題と応用問題, 京都大学 数理解析研究所, 31 Oct, 2017 (oral).

(8) 多羅間充輔,
“ポワズイユ流れ中のアクティブソフトマターの運動”
第 27 回　非線形反応と協同現象研究会, 福岡工業大学 FIT ホール, 9 Dec, 2017 (poster).

(9) Mitsusuke Tarama、Ryoichi Yamamoto,
“A minimal model of crawling cells under force-free condition”
Active Matter Workshop 2018, FIFC, Kyoto University, 19 Jan., 2018 (oral).

(10) 多羅間充輔,
“Deformable swimmers in Poiseuille flow”
15th FIFC Symposium, FIFC, Kyoto University, 2 Feb., 2018 (poster).

(11) 多羅間充輔,
“基盤上の細胞の這走運動”
京都若手ソフトマター研究会, 京都大学 セミナーハウス, 7 Mar., 2018 (oral).

(12) 多羅間充輔,
“基盤上を運動する細胞の力学モデル”
研究会 凝縮系の理論化学, 琉球大学 沖縄青年会館, 13 Mar., 2018 (oral: invited).

(13) 多羅間充輔,
“基盤上を這行する細胞運動の力学メカニズム”
日本物理学会　第 73 回年次大会, 東京理科大学 野田キャンパス, 23 Mar., 2018 (oral).

4. Others

(1) 多羅間充輔
“Nonlinear Dynamics of Active Deformable Particles: From Liquid Droplets to Biological Cells”
第１５回 福井センターセミナー, 京都大学福井謙一記念研究センター, 2017/5/25.

(2) 多羅間充輔
“微生物の力学：水中での遊泳から基盤上への這行へ”
山口大学　理学部　学術講演会、2018/3/5。

(3) 多羅間充輔
“Mechano-chemical modelling of crawling cells based on sub cellular element model”
山口大学　岩楯研究室セミナー、2018/3/6。

Masato Itami

FIFC Fellow

1. Summary of the research of the year

Singular Behavior of Time-Averaged Stress Fluctuations on Surfaces

In equilibrium statistical mechanics, fluctuations of thermodynamic quantities and their spatial correlations near a critical point universally characterize a continuous phase transition. In non-equilibrium statistical mechanics, fluctuations of time-averaged quantities and time correlations in equilibrium systems are related to responses to small perturbations or transport coefficients, following the linear response theory.

Fluctuations and correlations in fluids have been investigated in the framework of fluctuating hydrodynamics with Faxen's law or Green's function method. However, it remains difficult to calculate time-averaged surface stress fluctuations in a finite space. The main purpose of the present work is to propose a new approach to calculating the time-averaged stress fluctuations on surfaces by using the contraction principle, which is consistent with the linear response theory.

We consider a viscous incompressible fluid between two parallel plates, and study fluctuations of time-averaged shear stress per unit area on the top plate at equilibrium. We assume that (i) the fluctuating time-averaged stress is balanced in equilibrium at each position and that (ii) the fluctuating time-averaged stress obeys a Gaussian distribution on the restricted configuration space given by (i). Using these assumptions with the Green–Kubo formula for the viscosity, we can derive the large deviation function of the time-averaged stress fields. Then, using the saddle-point method for the large deviation function, or the contraction principle, we obtain the surface shear stress fluctuations. We show that the surface shear stress fluctuations are inversely proportional to the system size. Thus, we may evaluate the distance between the plates by only measuring the time- and surface-averaged stress fluctuation on the top plate at equilibrium.

Setup

We consider a viscous incompressible fluid between two parallel plates of length L_x and width L_y. The plates are oriented horizontally in the xy-plane and separated by a distance L_z. We impose periodic boundary conditions in the x- and y-directions. Let $\sigma_{ab}(\boldsymbol{r},t)$ denote the ab-component of the fluctuating viscous stress tensor $\overleftrightarrow{\boldsymbol{\sigma}}$ of the fluid at position $\boldsymbol{r}=(x,y,z)$ and time t in Cartesian coordinates. According to the conservation of angular momentum, the stress tensor is symmetric. Thus, we identify σ_{ab} with σ_{ba}. Let τ_{micro} denote the correlation time of the force acting on the top plate at $z=L_z$. Throughout this report, for any physical quantity $\mathrm{A}(\boldsymbol{r},t)$, we define the finite time-averaged quantity as

$$\overline{\mathrm{A}}(\boldsymbol{r}) \equiv \frac{1}{\tau}\int_0^{\tau} \mathrm{d}t\, \mathrm{A}(\boldsymbol{r},t),$$

where τ is taken to satisfy $\tau \gg \tau_{\mathrm{micro}}$. We define the zx-component of the time-averaged stress tensor per unit area on the top plate as

$$\bar{\sigma}_* \equiv \frac{1}{L_x L_y}\int_0^{L_x} \mathrm{d}x \int_0^{L_y} \mathrm{d}y \ \bar{\sigma}_{zx}(x,y,L_z). \tag{1}$$

In accordance with the method of our previous paper, we study fluctuations of σ_* in the equilibrium system at temperature T, whose intensity is denoted by $\langle \bar{\sigma}_*^2 \rangle_{\mathrm{eq}}$.

For later convenience, we decompose $\bar{\sigma}_{ab}$ into traceless and trace parts:

$$\bar{\sigma}_{ab}(\boldsymbol{r}) = -\bar{p}(\boldsymbol{r})\delta_{ab} + \bar{s}_{ab}(\boldsymbol{r})$$

with

$$\bar{p}(\boldsymbol{r}) = -\frac{\bar{\sigma}_{xx}(\boldsymbol{r}) + \bar{\sigma}_{yy}(\boldsymbol{r}) + \bar{\sigma}_{zz}(\boldsymbol{r})}{3},$$

where p and $\overleftrightarrow{\bar{\boldsymbol{s}}}$ are called the mean pressure and the stress deviator tensor, respectively. Because the stress deviator tensor is traceless, we have

$$\bar{s}_{xx}(\boldsymbol{r}) + \bar{s}_{yy}(\boldsymbol{r}) + \bar{s}_{zz}(\boldsymbol{r}) = 0.$$

Assumptions

We assume that (i) the fluctuating time-averaged stress is balanced in equilibrium at each position, which is expressed as

$$\nabla \cdot \overleftrightarrow{\bar{\boldsymbol{\sigma}}}(\boldsymbol{r}) = \boldsymbol{0}. \tag{2}$$

We also assume that (ii) $\overleftrightarrow{\bar{\boldsymbol{s}}}$ obeys a Gaussian distribution on the restricted configuration space given by the traceless condition and the assumption (i). Because $\overleftrightarrow{\bar{\boldsymbol{s}}}$ is obtained by integrating a microscopic stress over a suitable region, it is reasonable, by considering the central limit theorem, to assume (ii). In this subsection, we derive the probability density of the time-averaged stress fields in the equilibrium viscous fluids.

According to the Green--Kubo formula, the shear viscosity of the fluid η is related to the stress fluctuation in the bulk of the fluid as

$$\langle \bar{\sigma}_{xy}(\boldsymbol{r})\bar{\sigma}_{xy}(\boldsymbol{r}')\rangle_{\mathrm{eq}} = \frac{2k_{\mathrm{B}}T\eta}{\tau}\delta(\boldsymbol{r}-\boldsymbol{r}'),$$

where k_{B} is the Boltzmann constant and τ is assumed to be much larger than the correlation time of σ_{xy}. Using the traceless condition, the Green--Kubo formula, the symmetric property of the stress tensor, and the isotropic property, we obtain the statistical property of $\overleftrightarrow{\bar{\boldsymbol{s}}}$:

$$\langle \bar{s}_{ab}(\boldsymbol{r})\bar{s}_{a'b'}(\boldsymbol{r}')\rangle_{\mathrm{eq}} = \frac{2k_{\mathrm{B}}T\eta}{\tau}\varDelta_{aba'b'}\delta(\boldsymbol{r}-\boldsymbol{r}')$$

with

$$\varDelta_{aba'b'} = \delta_{aa'}\delta_{bb'} + \delta_{ab'}\delta_{ba'} - \frac{2}{3}\delta_{ab}\delta_{a'b'}.$$

For later convenience, we express $\varDelta_{aba'b'} = \varDelta_{ij}$ with $g(ab) = i$ and $g(a'b') = j$, where $g(xx) = 1$, $g(yy) = 2$, $g(zz) = 3$, $g(xy) = g(yx) = 4$, $g(yz) = g(zy) = 5$, and $g(zx) = g(xz) = 6$. That is, $\varDelta$ is interpreted as a 6×6 matrix. From the assumptions (i) and (ii), the probability density of the time-averaged stress tensor in equilibrium is given by

$$\mathcal{P}(\{\bar{\sigma}_{ab}(\boldsymbol{r})\}) = C\exp[-\tau\mathcal{I}(\{\bar{\sigma}_{ab}(\boldsymbol{r})\})]\prod_{\boldsymbol{r}}\delta\left(\nabla \cdot \overleftrightarrow{\bar{\boldsymbol{\sigma}}}(\boldsymbol{r})\right)$$

with

$$\mathcal{J}(\{\bar{\sigma}_{ab}(\boldsymbol{r})\}) = \frac{1}{4k_{\mathrm{B}}T\eta}\int_0^{L_x}\mathrm{d}x\int_0^{L_y}\mathrm{d}y\int_0^{L_z}\mathrm{d}z\sum_{i,j}\bar{s}_{ab}(\boldsymbol{r})\Delta^{-1}_{aba'b'}\bar{s}_{a'b'}(\boldsymbol{r}),$$

where C is a normalization constant and Δ^{-1} is the pseudo-inverse of Δ.

Results

From $\mathcal{P}(\{\bar{\sigma}_{ab}(\boldsymbol{r})\})$, we formally obtain the probability density of $\bar{\sigma}_*$:

$$P(\bar{\sigma}_*) = \int\prod_i \mathcal{D}\bar{\sigma}_{ab}\ \mathcal{P}(\{\bar{\sigma}_{ab}(\boldsymbol{r})\})\delta\left(\bar{\sigma}_* - \frac{1}{L_xL_y}\int_0^{L_x}\mathrm{d}x\int_0^{L_y}\mathrm{d}y\ \bar{\sigma}_{zx}(x,y,L_z)\right).$$

In the asymptotic regime $\tau \gg \tau_{\mathrm{micro}}$, the functional integral may be accurately evaluated by the saddle-point method. By introducing the Lagrange multiplier field $\boldsymbol{u}(\boldsymbol{r}) = (u_x(\boldsymbol{r}), u_y(\boldsymbol{r}), u_z(\boldsymbol{r}))$ to take the constraint (i) into account, we obtain

$$P(\bar{\sigma}_*) = C_*\exp[-\tau I(\bar{\sigma}_*)]$$

with

$$I(\bar{\sigma}_*) = \min_{\{\bar{\sigma}_{ab}(\boldsymbol{r})\},(1)}\frac{1}{4k_{\mathrm{B}}T\eta}\int_0^{L_x}\mathrm{d}x\int_0^{L_y}\mathrm{d}y\int_0^{L_z}\mathrm{d}z\ \mathcal{L}(\{\bar{\sigma}_{ab}(\boldsymbol{r})\}),$$

and

$$\mathcal{L}(\{\bar{\sigma}_{ab}(\boldsymbol{r})\}) = \sum_{i,j}\bar{s}_{ab}(\boldsymbol{r})\Delta^{-1}_{aba'b'}\bar{s}_{a'b'}(\boldsymbol{r}) + \sum_{a,b}2\eta u_a(\boldsymbol{r})\partial_b\,\bar{\sigma}_{ab}(\boldsymbol{r}),$$

where C_* is a normalization constant. Note that the saddle-point method for the large deviation function has been rigorously verified under certain conditions. This is called the contraction principle in probability theory.

As boundary conditions of the variational problem, the natural boundary conditions are given by

$$\int_0^{L_x}\mathrm{d}x\int_0^{L_y}\mathrm{d}y\int_0^{L_z}\mathrm{d}z\sum_a\partial_z\left[u_a(r)\delta\bar{\sigma}_{az}(\boldsymbol{r})\right] = 0,$$

where $\delta\bar{\sigma}_{az}(\boldsymbol{r})$ is a variation of $\bar{\sigma}_{az}(\boldsymbol{r})$. Recalling (1), we impose the following boundary conditions:

$$\boldsymbol{u}(x,y,0) = \boldsymbol{0}, u_x(x,y,L_z) = V_0, u_y(x,y,L_z) = u_z(x,y,L_z) = 0,$$

where V_0 is a constant.

With this setup, the surface contribution of the variation vanishes, and we obtain the Euler–Lagrange equations

$$\frac{\partial\mathcal{L}}{\partial\bar{\sigma}_{ab}} - \sum_c\partial_c\left(\frac{\partial\mathcal{L}}{\partial(\partial_c\bar{\sigma}_{ab})}\right) = 0,$$

which are equivalent to

$$\bar{\sigma}_{ab} = -\bar{p}\delta_{ab} + \eta(\partial_a u_b + \partial_b u_a). \tag{3}$$

Note that the definition of $\bar{p}$ is equivalent to $\nabla\cdot\boldsymbol{u} = 0$ in the expression of the above equation. The set of equations (2), (3), and $\nabla\cdot\boldsymbol{u} = 0$ coincide with the Stokes equations $\eta\nabla^2\boldsymbol{u} = \nabla\bar{p}$ and $\nabla\cdot\boldsymbol{u} = 0$ with (3). Thus, we may interpret $\boldsymbol{u}(\boldsymbol{r})$ as the virtual velocity fields of the fluid generated by the most probable stress fields for given $\bar{\sigma}_*$. Note that the natural boundary conditions are not related to boundary conditions for the real velocity fields of the fluid. (If the boundary conditions for the virtual velocity fields are related to those for the real velocity fields, the fluctuations of $\bar{\sigma}_*$ depend crucially on whether the top plate is fixed or movable in equilibrium.)

By referring to the solution of the Stokes equations with the natural boundary conditions and (1), we obtain

$$u_x(\boldsymbol{r}) = \frac{\bar{\sigma}_* z}{\eta}, \qquad u_y(\boldsymbol{r}) = u_z(\boldsymbol{r}) = 0, \qquad \bar{p}(\boldsymbol{r}) = p_0,$$

where p_0 is a constant. These results with (3) lead to

$$\bar{\sigma}_{xx}(\boldsymbol{r}) = \bar{\sigma}_{yy}(\boldsymbol{r}) = \bar{\sigma}_{zz}(\boldsymbol{r}) = -p_0, \qquad \bar{\sigma}_{xy}(\boldsymbol{r}) = \bar{\sigma}_{yz}(\boldsymbol{r}) = 0, \qquad \bar{\sigma}_{zx}(\boldsymbol{r}) = \bar{\sigma}_*.$$

Thus, we obtain

$$I(\bar{\sigma}_*) = \frac{L_x L_y L_z}{4 k_{\mathrm{B}} T \eta} \bar{\sigma}_*^2,$$

which leads to

$$\langle \bar{\sigma}_*^2 \rangle_{\mathrm{eq}} = \frac{2 k_{\mathrm{B}} T \eta}{L_x L_y L_z \tau}. \tag{4}$$

Because $\bar{\sigma}_*$ is the time- and surface-averaged quantity, we naively expect the central limit theorem:

$$\langle \bar{\sigma}_*^2 \rangle_{\mathrm{eq}} \propto \frac{1}{L_x L_y \tau},$$

where $\propto$ implies that we only focus on the $L_x L_y$ and τ dependencies of a function. With regard to these dependencies, the result (4) is consistent with the above expectation. In addition to this standard behavior, (4) implies that the fluctuations of $\bar{\sigma}_*$ are inversely proportional to L_z, which may originate from the long-range stress correlations via the virtual Couette flow generated by the most probable stress fields for given $\bar{\sigma}_*$. Such L_z dependence is singular because the fluctuations vanish in the limit $L_z \to \infty$. Furthermore, we may evaluate the vertical system size L_z by only measuring the time- and surface-averaged stress fluctuation on the top plate in equilibrium. We stress that the assumption (i) expressed as (2) is essential to the long-range stress correlations.

We can check the validity of (4) or the assumptions (i) and (ii) in terms of the linear response theory. When the top plate moves at constant velocity V which is assumed to be much slower than the sound velocity of the fluid (and the bottom plate is attached to a heat bath of temperature T), the surface average of $\sigma_{zx}(x, y, L_z)$ in the steady state is given by

$$\frac{1}{L_x L_y} \int_0^{L_x} \mathrm{d}x \int_0^{L_y} \mathrm{d}y \ \langle \bar{\sigma}_{zx}(x, y, L_z) \rangle_{\mathrm{st}} = \frac{L_x L_y \tau}{2 k_{\mathrm{B}} T} \langle \bar{\sigma}_*^2 \rangle_{\mathrm{eq}} V.$$

This equation and (4) lead to

$$\frac{1}{L_x L_y} \int_0^{L_x} \mathrm{d}x \int_0^{L_y} \mathrm{d}y \ \langle \bar{\sigma}_{zx}(x, y, L_z) \rangle_{\mathrm{st}} = \frac{\eta V}{L_z},$$

which is consistent with the standard hydrodynamics, namely the shear stress in Couette flow at low Reynolds numbers with stick boundary conditions.

2. Presentation at academic conferences

(1) Masato Itami and Shin-ichi Sasa
“Universal form of stochastic evolution for slow variables in equilibrium systems”
30th Marian Smoluchowski Symposium on Statistical Physics, Kraków, Poland, Sep. 4-8, 2017 (poster).

(2) 伊丹將人、佐々真一
「ソレー効果と断熱ピストン問題における熱誘起力の差異」
日本物理学会2017年秋季大会、岩手大学、2017年9月21-24日（口頭）

(3) 伊丹將人、佐々真一
「平衡流体における時間平均応力ゆらぎの超均一性II」
日本物理学会第73回年次大会、東京理科大学、2018年3月22-25日（口頭）

3. Others

(1) Masato Itami and Shin-ichi Sasa
“The difference between the heat-induced forces of the Soret effect and the adiabatic piston”
The 15th symposium of Fukui Institute for Fundamental Chemistry, Kyoto, Feb. 2, 2018 (poster).

Shunsuke Yabunaka

FIFC Fellow

1. Summary of the research of the year

Emergence of epithelial cell density waves

Pattern-forming instabilities play a pivotal role in the morphogenesis and spatio-temporal organization of living organisms. Paradigmatic examples include the morphogen patterns of developing embryos and the cooperative behavior of large assemblies of microorganisms, for instance in bacterial colonies. At the scale of the tissue, Serra-Picamal et al. discovered that the expansion into free space of Madin-Darby canine kidney (MDCK) epithelial cell monolayers is accompanied by traveling mechanical waves of the velocity, strain rate, traction force and stress fields (X. Serra Picamal et. al., Nature Physics 8 628, 2012).

By employing our hydrodynamics model of cellular tissues including (1) active contractile force (2) cell motility (3) cell polarity, we investigated pattern formation in epithelia. Previously, we have found that mechanical wave appears via Hopf bifurcation above threshold of active parameters when there is uniform polarity initially[4]. As shown in Fig. 1, in this study, we found that mechanical wave appears as a result of the secondary bifurcation after the first bifurcation where standing wave appears, for cases where there is no uniform polarity initially. We also found that a chaotic pattern can appear with even stronger activity[5].

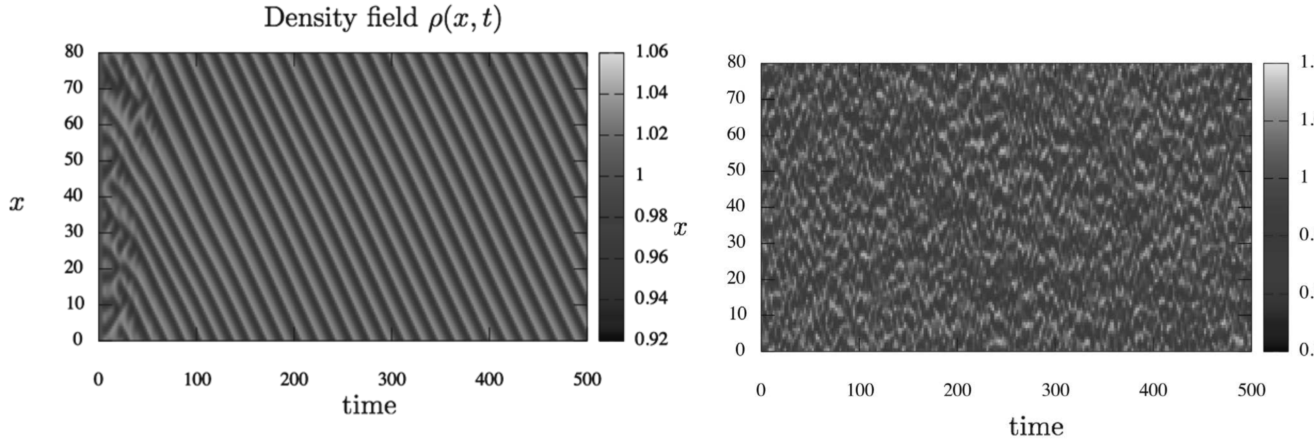

Fig. 1 Mechanical wave as a result of the secondary bifurcation(left) and chaotic pattern (right).

Critical adsorption profiles around a sphere and a cylinder in at criticality

We study universal critical adsorption on a solid sphere and a solid cylinder in a fluid at bulk criticality, where preferential adsorption occurs. We use a local functional theory proposed by Fisher et al. [M. E. Fisher and P. G. de Gennes, C. R. Acad. Sci. Paris Ser. B 287, 207 (1978); M. E. Fisher and H. Au-Yang, Physica A 101, 255 (1980)]. We calculate the mean order parameter profile $\psi(r)$, where r is the distance from the sphere center and the cylinder axis, respectively [2]. The resultant differential equation for $\psi(r)$ is solved exactly around a sphere and numerically around a cylinder. A strong adsorption regime is realized except for very small surface field h1, where the surface order parameter $\psi(a)$ is determined by h1 and is independent of the radius a. If r considerably exceeds a, $\psi(r)$ decays as $r^{-(1+\eta)}$ for a sphere and $r^{-(1+\eta)/2}$ for a cylinder in three dimensions, where η is the critical exponent in the order parameter correlation at bulk criticality.

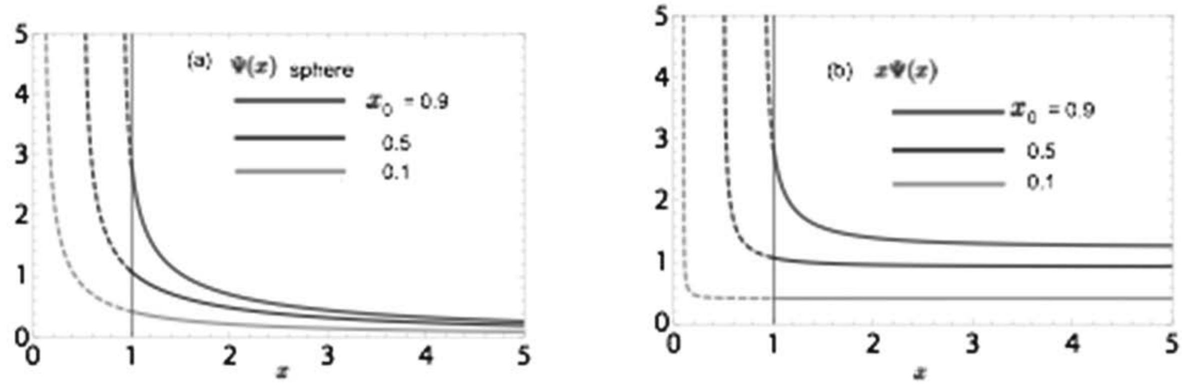

Fig. 2 Normalized order parameter as a function of x=r/a as a function of the distance from the sphere center r around a solid sphere with radius a at criticality. Here η is set to 0.

Nonperturbative fixed points in O(N) and tensor models

It is by now widely believed that everything is known about the criticality of the O(N) models either exactly or with an accuracy that is limited only by our finite computational ability. For the Wilson-Fisher fixed point, almost all the theoretical formalisms have been tested and they all yield consistent result.

However, for the multicritical fixed points, the situation is less clear. For example, a nontrivial multicritical fixed point with two unstable directions, which we call T_2, branches from the Gaussian fixed point at d=3 dimension, below which the six-order term becomes relevant. The same scenario also repeats in each critical dimension d_n=2+2/n: a nontrivial multicritical fixed point with n unstable directions branches from the Gaussian fixed point. However, in the large N limit, only the gaussian and WF fixed points have been found in generic dimension 2<d<4 so far.

In this study, we investigate the multicritical fixed point structure of the O(N) models by means of nonperturbative (also called functional) renormalization group (NPRG) and find some surprising features. In particular, we find new nonperturbative fixed points in three dimensions (d=3) as well as at N=\infty, as shown in Fig. 3 [1]. These fixed points come together with an intricate double-valued structure when they are considered as functions of d and N, as shown in Fig. 4. Many features found for the O(N) models are shared by the O(N)□O(2) models relevant to frustrated magnetic systems.

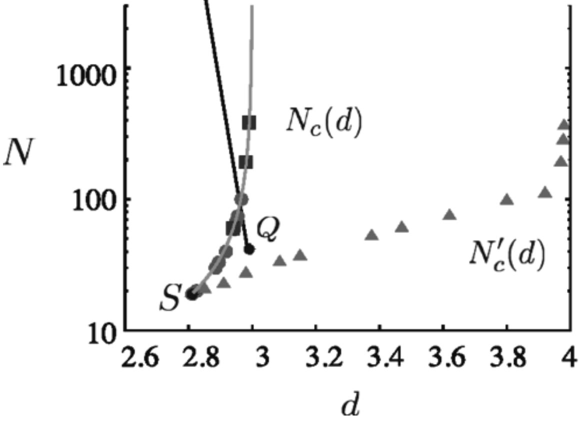

Fig. 3. Two curves $d_c(N)$ and $d'_c(N)$. We found that T_2 vanishes at d= $d_c(N)$ by colliding with another nonperturbative fixed point, which we call C_3, when decreasing d starting from d=3 for N>18. We followed C_3 increasing d and found that it disappears at d=$d'_c(N)$ by colliding with yet another nonperturbative fixed point, which we call C_2, with two unstable directions.

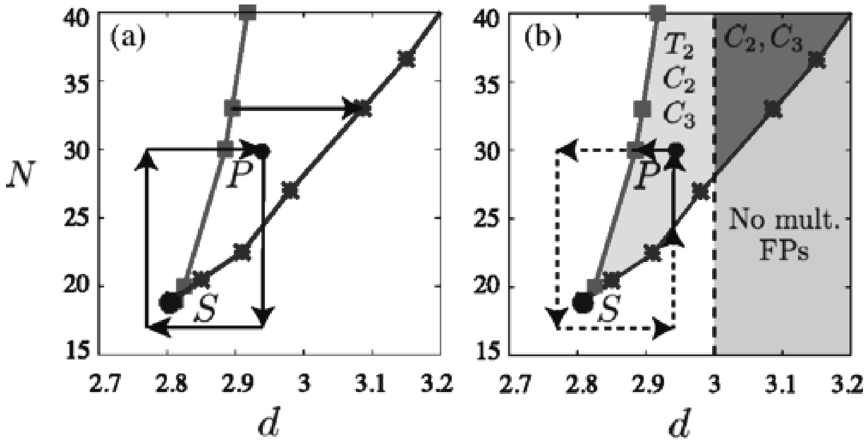

Fig. 4. Singular point S and the two lines $N_c(d)$ (red squares) and $N'_c(d)$ (blue stars). Starting from P, the FP T_2 is followed along a clockwise (left) or anticlockwise (right) closed path surrounding S. On the clockwise path, T_2 becomes C_2 after a full rotation. On the anticlockwise path, T_2 collides with C_3 on $N_c(d)$ and disappears. It actually becomes complex-valued and remains so all along the dashed path. On $N'_c(d)$ it becomes real again but is now C_2. The path joining $N_c(d)$ and $N'_c(d)$ at fixed N=33 is also shown in panel (a). In panel (b), we indicate which (real) multicritical FPs exist in each region. In the white region, there is only one multicritical FP with two directions of instability that can be continuously followed from both T_2 and C_2 depending on the path followed.

2. Original papers

(1) Shunsuke Yabunaka and Bertrand Delamotte, “Surprises in O (N) Models: Nonperturbative Fixed Points, Large N Limits, and Multicriticality” Physical review letters 22, 19, 191602 1-5

(2) Shunsuke Yabunaka and Akira Onuki, "Critical adsorption profiles around a sphere and a cylinder in a fluid at criticality: Local functional theory” Physical review E, 96, 3 032127 1-7 (2017)

(3) Shunsuke Yabunaka and Akira Onuki, “Electric double layer composed of an antagonistic salt in an aqueous mixture: Local charge separation and surface phase transition” Physical review letters 19, 118001 1-5 (2017)

(4) Shunsuke Yabunaka and Marcq Philippe, “Cell growth, division, and death in cohesive tissues: A thermodynamic approach”, Physical review E, 96, 2, 022406 1-9, 2017

(5) Shunsuke Yabunaka and Marcq Philippe, “Emergence of epithelial cell density waves”, Softmatter, 13, 39, 7046-7052 (2017)

3. Presentation at academic conferences

(1) 藪中俊介、“増殖するアクティブマターの連続体理論”、 生物流体力学における基礎問題と応用問題, Kyoto, Oct. 31, 2017.

(2) 藪中俊介、小貫明、”二元混合系中の選択的溶媒和効果を持つ塩で構成された電気二重層：局所電荷分離と表面相転移”、ソフトマター研究会、Kyoto, Oct. 23, 2017

(3) 藪中俊介、小貫明、”二元混合系中の選択的溶媒和効果を持つ塩で構成された電

気二重層:局所電荷分離と表面相転移”、日本物理学会 2017 年秋季大会 24pN23-3, Morioka, Sep.24, 2017

(4) 藪中俊介、Bertrand Delamotte,
“非摂動くりこみ群による Large N での多重臨界現象の研究”
日本物理学会 2017 年秋季大会 24aJ25-4, Morioka, Sep.24, 2017

(5) 藪中俊介、Philippe Marcq, ”増殖するアクティブマターの連続体理論”, 日本物理学会 2017 年秋季大会 22pJ16-1 Morioka, Sep.22, 2017

4. Others

(1) Shunsuke Yabunaka
“Surprises in O (N) Models: Nonperturbative Fixed Points, Large N Limits, and Multicriticality” Theory Group seminar at Institut Curie, March 1, 2018

(2) Shunsuke Yabunaka
“Surprises in O (N) Models: Nonperturbative Fixed Points, Large N Limits, and Multicriticality” 京大佐々研セミナー, November 13, 2018

Simon K. Schnyder

FIFC Fellow

1. Summary of the research of the year

Collective motion of cells

Contact inhibition plays a crucial role in cell motility, wound healing, and tumour formation. By mimicking the mechanical motion of cells crawling on a substrate, we constructed a minimal model of migrating cells that naturally gives rise to contact inhibition of locomotion (CIL). Despite the simplicity of the model, the collective behaviour of the cells is highly non-trivial and depends on both the shape of the cells and whether CIL is enabled.

The model cell consists of two disks, a front disk (a pseudopod) and a back disk (cell body), which are connected by a finite extensible spring, see Fig. 1. CIL is achieved my coupling the migration force F_{mig} linearly to the cell extension r_{bf}. For comparison, we also worked with no-CIL cells by making the migration force constant. CIL cells with a small front disk (i.e., a narrow pseudopod) form immobile colonies, see Fig. 2a. In contrast, cells with a large front disk (e.g., a lamellipodium) exhibit coherent migration without any explicit alignment mechanism in the model, see Fig. 2b. This result suggests that crawling cells often exhibit broad fronts because this helps facilitate alignment.

When investigating the collective dynamics in more detail, we find that the CIL model naturally reproduces the strong linear decrease of the cell speed when the cells are packed at high densities, in contrast to the no-CIL cells which barely adjust their speed, see Fig. 3a. The CIL cells' response closely matches that of real cells, as can be inferred from experimental data, see Fig. 3b. In addition, the typical log-normal distribution of cell speeds which can be observed in experiments, only arises in the CIL version of the model, i.e. when contact inhibition is enabled.

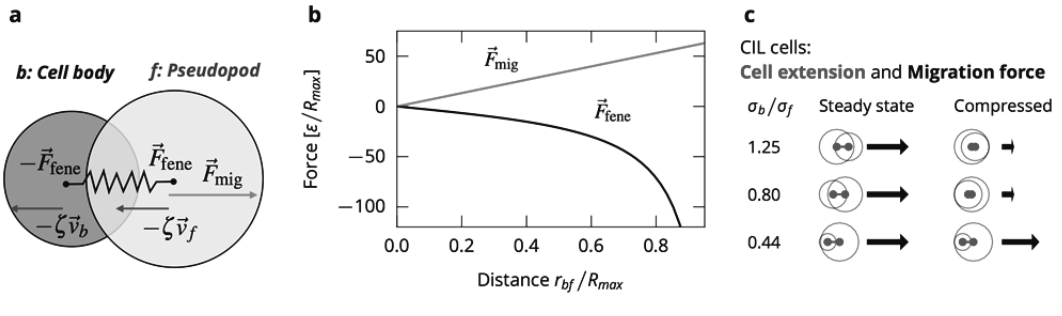

Fig. 1: Illustration of the cell model. (a) Schematic of a cell with a finite extensible non-linear elastic spring connecting the disks and exerting the force F_{fene}, the migration force F_{mig} acting on the front disk (Eq. 2), and the friction forces $-\zeta v_b$ and $-\zeta v_f$. (b) The forces acting on the two disks composing a cell separated by a distance r_{bf}. (c) Cell extension r_{bf} (red line segment) and migration force (black arrow) for the CIL cells in the steady state and a compressed state in which the disks are fully overlapping.

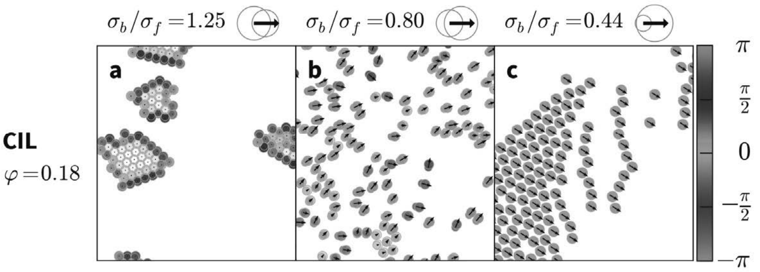

Fig. 2: Dynamic states. Snapshots of CIL cells for a range of cell shapes. Cell velocities are given as arrows and color. Hue indicates deviation from average direction, and slower cells are lighter in color. The cells undergo a transition from a clustering/disordered state to an ordered state upon change of the cell shape.

Collective alignment is typically measured with the polar order, the average orientation of the cells. The alignment transition visible in the snapshots of Fig. 2 persists over nearly the full density range, see Fig. 4a. This is unrealistic, since, typically, cells only start coherently migrating at higher densities, while they show random behavior at low densities. We find the correct behavior by adding noise to the motion of the cells, which models the erratic motion of cells more accurately. In this way, at low densities, the collective cell dynamics become dominated by the random motions of single cells, while at high densities frequent cell collisions lead to collective alignment, see black line in Fig. 4a. This is precisely what is observed in experiments. We also find that the alignment transition is qualitatively the same for CIL and no CIL cells, only that it occurs earlier for CIL cells. Therefore we conclude that contact inhibition enhances alignment.

In the transition toward the arrest of cells with σ_b / σ_f = 0.80, areas of dynamic arrest begin to continuously form and dissolve. The arrested areas grow in size with density until they form system-spanning waves (Fig. 5a), which suggests that there is a growing length scale. The waves travel against the direction of motion of the cells (Fig. 5d), akin to traffic jams in models of car traffic. In this state, the cell speed distribution shows a peak at or near 0 and a long tail (see data for ϕ = 1.0 in Fig. 3c). The onset of system-spanning arrest waves roughly coincides with the decrease in the order parameter at $\phi \approx 0.85$. We do not observe such waves in the non-CIL systems (Fig. 5b). Thus, the waves are directly associated with the CIL. Furthermore, the waves only occur when contact inhibition is strong; the cells withσ_b / σ_f = 0.44, which have a weaker slowdown at high densities (Fig. 1c), always travel coherently (Fig. 5c). Because they

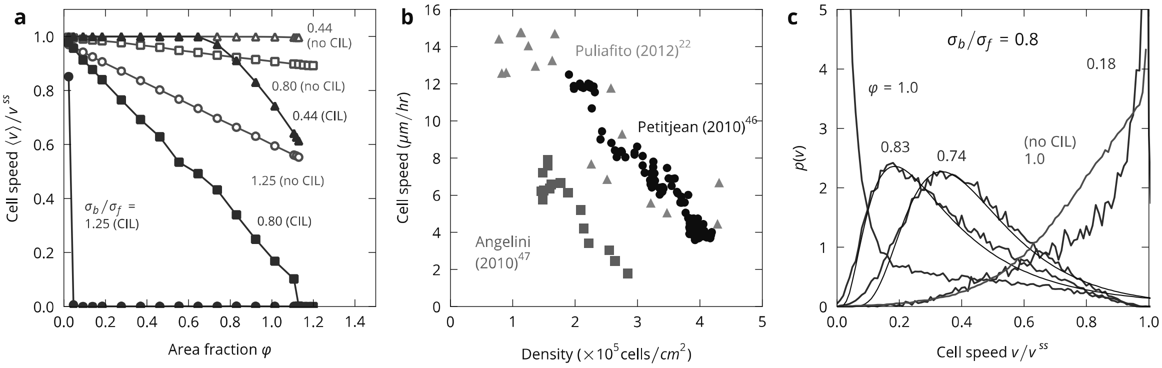

Figure 3. Cell speeds. (a) Average cell speed, normalized by the steady-state speed of a solitary cell v^{ss}, with (closed symbols) and without (open symbols) contact inhibition for a range of cell shapes. (b) Speed of MDCK cells in a growing cell colony and in confluent monolayers. (c) Speed histograms at σ_b / σ_f = 0.80. Black lines are fit to the data with a log-normal distribution.

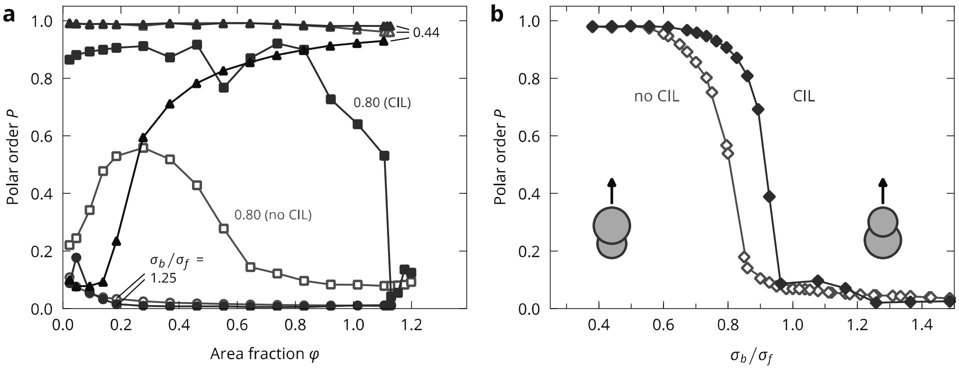

Figure 4. Collective alignment. (a) Polar order p as a function of area fraction for a range of cell shapes. Simulations with cell noise at σ_b / σ_f = 0.44 are shown in black. (b) Polar order p as a function of cell shape at area fraction $\varphi \approx$ 0.18.

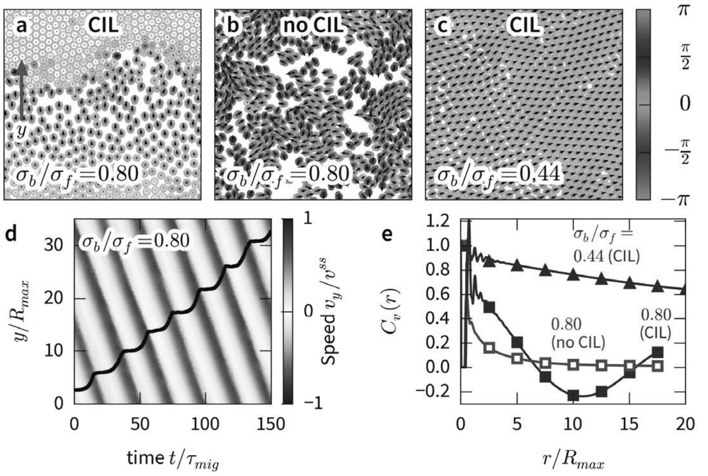

Fig. 5: Velocity waves. (a–c) Simulation snapshots of CIL and no-CIL cells at area fraction $\varphi = 0.92$ with cell velocities shown as arrows. Hue indicates the deviation from the average direction, and slower cells are lighter in colour. (d) Kymograph of simulation shown in (a). Average of cell velocities in the y-direction, see arrow in (a), as a function of time. Trajectory of one cell superimposed in black. (e) Velocity correlation functions for simulations shown in (a–c).

slow down less abruptly, they never fully jam. The correlation function of cell speed fluctuations of the CIL cells becomes negative on the length scale of the extent of the traffic jam with a minimum at approximately 10 R_{max}, see Fig 5e. The VACF of corresponding no-CIL cells decays on the length scale of a few R_{max} and never becomes negative. This result reveals that cells move in small correlated clusters.

Anomalous transport in heterogeneous media

Transport of mesoscopic particles in simple solvents is often dominated by thermal motion. First observed by Robert Brown in 1827 in the motion of organelles and later theoretically described by Albert Einstein, this Brownian motion is found practically everywhere in soft matter and biological physics. The key insight in understanding this motion was that the particles perform many frequent and uncorrelated collisions with the fluid molecules. This leads to trajectories which can be seen as composed of independent increments. As a generic result, we find that such trajectories become diffusive, in which the mean-squared displacement (MSD) grows linearly in time, $\delta r^2(t) \sim t$.

Since the assumptions for this theory are seemingly so simple and general, it may come as a surprise that so many systems exhibit *anomalous* diffusion, i.e. the MSD grows with a (often time-dependent) power $\gamma(t)$ that is not 1, i.e. $\delta r^2(t) \sim t^{\gamma(t)}$. Many experiments show that transport is subdiffusive, $\gamma(t) < 1$, such as crowding phenomena in biology, ion conduction in silicate glasses and other situations. These systems have in common that they consist of at least two components, characterized by a strong separation of time scales. The more mobile component often exhibits anomalous diffusion over long periods of time.

The question driving my research has been whether the observed exponents merely represent transient behavior, or whether they can be connected to a universal behavior with a well-defined exponent.

A paradigm for the modeling of transport in heterogeneous media is the Lorentz model (LM), where the anomalous diffusion arises as a universal long-time limit: In its simplest version, a single mobile particle moves in the static void space formed by overlapping hard disk obstacles. At low obstacle density, the mobile particle freely explores the system and exhibits regular diffusion. At high densities, it becomes trapped in finite pockets of obstacles. In between, there is a localization transition, where the void space of the system stops to percolate, the system becomes self-similar, and anomalous diffusion occurs. This transition is a dynamic critical phenomenon and the exponent of the anomalous diffusion is universal.

The LM can be generalized by introducing interacting mobile particles and soft instead of hard interactions, making it more comparable to realistic porous materials. But how such generalizations change the dynamics is not well understood. One the one hand, an extension of the mode coupling theory (MCT) of the glass transition predicted the LM localization transition to persist for interacting fluids in porous media, i.e., that the nature of the transition is unchanged by the interactions, and that the critical behavior is

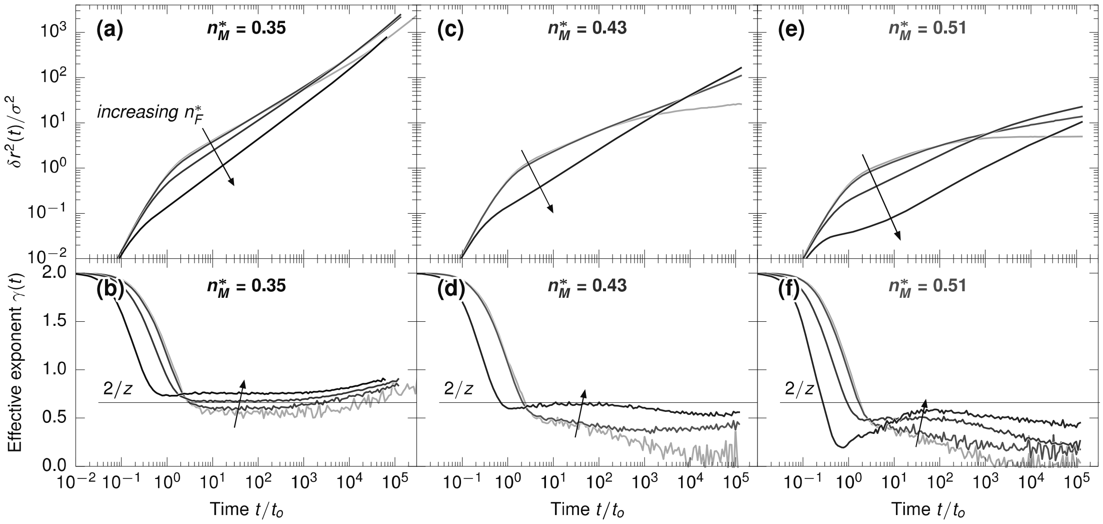

Fig. 6: Anomalous transport. Mean-squared displacements $\delta r^2(t)$ and effective exponents $\gamma(t)$ for a range of matrix densities n_M^* and fluid densities n_F^*. Fluid densities are n_F^* = 0, 0.016, 0.094, 0.313 for (a), (b) (n_F^* = 0.016 in purple for clarity); n_F^* = 0, 0.013, 0.264 for (c), (d); and n_F^* = 0, 0.020, 0.160, 0.400 for (e), (f). In (b), (d), (f), the critical exponent of the two-dimensional LM 2/z = 2/3.036 is shown as a black line as a guide to the eye.

qualitatively the same. On the other hand, evidence from simulations of model porous media with interacting particles, both with hard and soft interactions, has been inconclusive. While a localization transition and extended anomalous diffusion are observed, the exponents seldom match the predictions. Still, so far, it seemed to be evident that porous media with soft or hard potentials are qualitatively equivalent, even though energy barriers in systems with soft potentials are finite and, therefore, are crossable by soft particles.

We performed molecular dynamics simulations of interacting soft disks confined in a soft heterogeneous matrix of obstacles. By systematically moving away from the single-particle case, we investigated how interactions between the mobile particles influence the dynamics. With increasing obstacle density, the system exhibited a gradual transition from delocalized to localized dynamics, see Fig. 6. Subdiffusion with constant exponents could be identified for up to three decades in time.

However, our results showed that the system exhibits fundamentally different dynamics from the LM. Whereas, for the single-particle case, a mapping onto the LM transition was still possible, we found, here, that the universality of the dynamics breaks down. The interaction of particles with each other makes each particle's energy time-dependent; the free area available to it changes with each collision with other mobile particles. In that sense, the free volume in soft systems is dynamic—not static as in the LM—with drastic consequences. Mobile particles help each other over potential barriers, speeding up the dynamics when the mobile particle density is increased. This is impossible for interacting hard disks, thus, giving a rare example where soft and hard interactions are qualitatively different.

The soft interactions are therefore responsible for a breakdown of the universality of the dynamics. Even though exponents similar to the LM exponent may occur, we show that they merely represent effective, non-universal exponents which are highly tunable via the particle interactions. Thus, they should not be linked to the anomalous exponent of the LM. In experiments, where interactions are typically quite complex, the LM can, therefore, at best, serve as a tool for qualitative interpretation. Our work demonstrates that the wide range of exponents seen, e.g., in crowding experiments of cellular fluids is likely a result of the soft interactions between the components of those systems. Therefore, we expect that such crowding phenomena cannot be associated with universal anomalous diffusion.

2. Original papers

(1) S. K. Schnyder, & J. Horbach, “Crowding of interacting fluid particles in porous media through molecular dynamics: breakdown of universality for soft interactions”, Physical Review Letters, 120(7), 78001 (2018).

(2) J. Horbach, N. H. Siboni, & S. K. Schnyder, “Anomalous transport in heterogeneous media“, The European Physical Journal Special Topics, 226(14), 3113–3128 (2017).

(3) S. K. Schnyder, J. J. Molina, Y. Tanaka, R. Yamamoto, “Collective motion of cells crawling on a substrate: roles of cell shape and contact inhibition“, Scientific Reports 7, 5163 (2017).

3. Presentations at academic conferences

(2) S. K. Schnyder, J. J. Molina, and R. Yamamoto,
“Colony growth of cells on a substrate”,
Active Matter Workshop,
Fukui Institute for Fundamental Chemistry, Kyoto (19/01/2018).

(3) S. K. Schnyder, J. J. Molina, and R. Yamamoto,
“Colony growth of cells on a substrate”,
International Symposium on Fluctuation and Structure out of Equilibrium,
Sendai (21/11/2017).

(4) S. K. Schnyder, J. J. Molina, and R. Yamamoto,
“Collective motion of cells crawling on a substrate: roles of cell shape and contact inhibition”,
10th Liquid Matter Conference, Ljubljana, Slovenia (17-21/7/2017).

(5) S. K. Schnyder, J. J. Molina, and R. Yamamoto,
“Colony growth of cells on a substrate”,
4th Research Area Meeting, Tokyo (6/2017).

4. Others

(6) S. K. Schnyder, J. J. Molina, and R. Yamamoto,
“Colony growth of cells on a substrate”,
The 15th Symposium of Fukui Institute for Fundamental Chemistry, Kyoto (02/02/2018).

(7) Seminar: S. K. Schnyder
“Collective motion of cells: roles of cell shape and contact inhibition”,
Groups of Prof. Joachim Rädler and Prof Erwin Frey, LMU Munich, Germany (7/2017).

Miho Isegawa

FIFC Fellow (To 31 Jan. 2018)

1. Summary of the research of the year

DFT Study on Fe(IV)-Peroxo Formation and H-Atom Transfer Triggered O_2 Activation by NiFe Complex

Hydrogenases are some of the most extensively studied metalloenzymes because of its catalytic ability to convert the hydrogen molecule into protons and electrons, or hydrogen evolution from protons and electrons in the reverse reaction. This diverse group of metalloenzymes can be classified into three groups, NiFe, FeFe and Fe-only hydrogenase, based on the composition of catalytic center. Among them, NiFe hydrogenase is known to be the most robust for the oxygen, and it shows reversible inactivation under oxygen exposure. Further, two distinctive inactive oxidized states, Ni-A (Fe^{II}(O–OH)Ni^{III}) and Ni-B (Fe^{II}(OH)Ni^{III}), has been trapped in experiment.

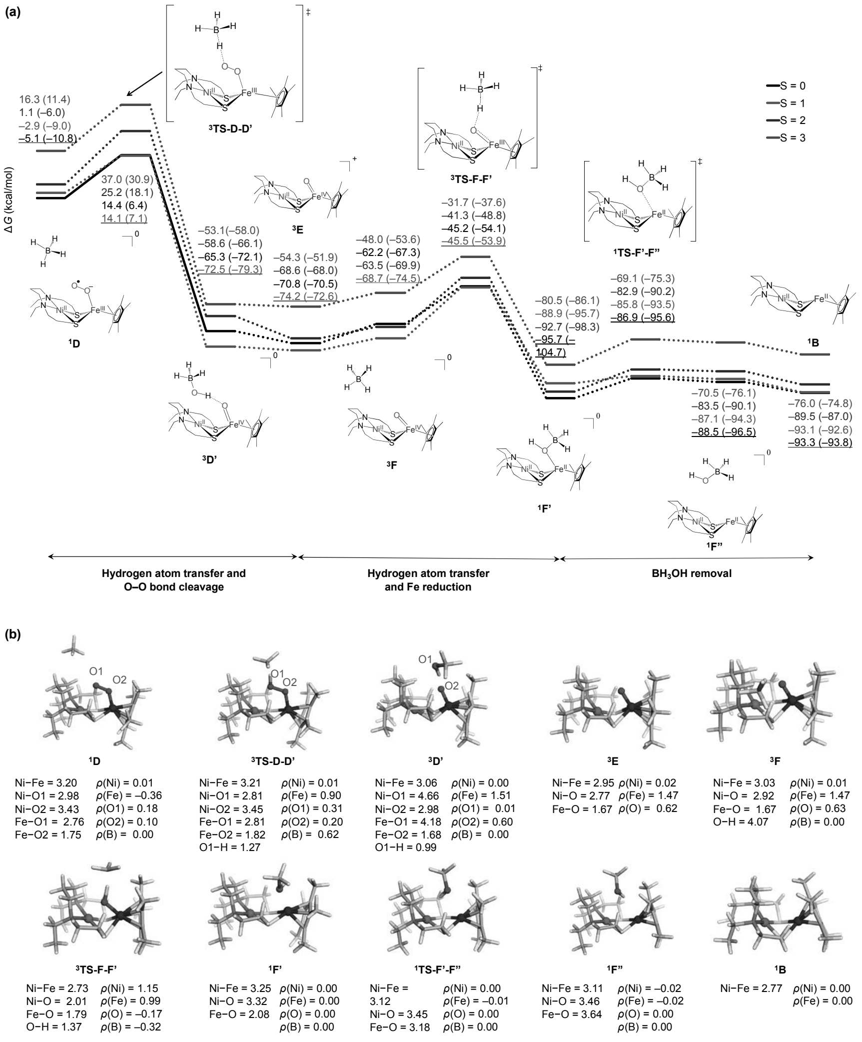

Figure 1. (a) Free energy profiles of (i) the first hydrogen atom transfer and O–O bond cleavage, (ii) the second hydrogen atom transfer and Fe center reduction, and (iii) BH_3OH^- removal in four spin states (S = 0, 1, 2, and 3). ΔG and ΔH (in parentheses) are given in kcal/mol. (b) Optimized stationary points with selected bond lengths (Å) and the Mulliken spin densities (ρ) for the lowest energy spin state.

Most of the experimental and theoretical studies have targeted the activation and formation of hydrogen in enzyme and biomimetic models. However, a reaction between NiFe catalytic center and dioxygen, which relates to the generation of inactive states and reactivation, has not been well studied. Therefore, elucidation of the mechanism for dioxygen activation is essential for the development of novel biomimetic catalysts, and understanding the reactivation process of NiFe hydrogenase. In this study, the mechanism for dioxygen activation using the biomimetic model complex of [NiFe]-hydrogenase, $[\mathrm{NiLFe}(\eta^5\text{-}\mathrm{C_5Me_5})]^+$ [L = *N,N*'-diethyl-3,7-diazanonane-1,9-dithiolato] was established using density functional theory (DFT) and artificial force-induced reaction (AFIR) methods. Our computational results suggest that O_2 binds to the FeII center in an end-on fashion and forms a high-valent iron complex, NiFe–peroxo ($\mathrm{Ni^{II}Fe^{IV}}(\eta^2\text{–}O_2)$), which has been experimentally observed. The O–O bond cleavage occurs in the presence of borohydride (BH_4^-) through hydrogen atom transfer (HAT). Once the HAT occurs, the generated BH_3 radical anion ($BH_3^{\cdot-}$) binds to the terminal oxygen of NiFe–OOH, giving rise to BH_3OH– and $\mathrm{Ni^{II}Fe^{IV}}$=O. The second HAT from BH_4^- to the oxygen of $\mathrm{Ni^{II}Fe^{IV}}$=O leads to BH_3OH^- and Fe reduced $\mathrm{Ni^{II}Fe^{II}}$ complex. Importantly, the dioxygen activation is triggered by HAT, not by proton transfer or hydride transfer. The O_2 is activated by the Fe center and the oxidation state of Fe varies during the process, while the oxidation state of Ni is conserved. These mechanistic insights into O_2 activation are essential in understanding the formation of the inactive state and reactivation process in hydrogenase.

DFT Investigation on Electron and Hydride Transfer in NiFe Hydride Complex

Molecular hydrogen is a promising candidate of the next generation of clean energy resource alternative to the fossil fuel which is finite and emits undesirable chemical compounds, CO_2, NO_x, and SO_x into the environment. The development of the catalyst which can efficiently and selectively splits or generates the hydrogen molecule, is highly demanded. It is known that the biological enzyme hydrogenase found in cyanobacteria can catalyze this process. For this enzyme, a number of experimental and theoretical investigations have been performed to reveal the function and the reaction mechanism.

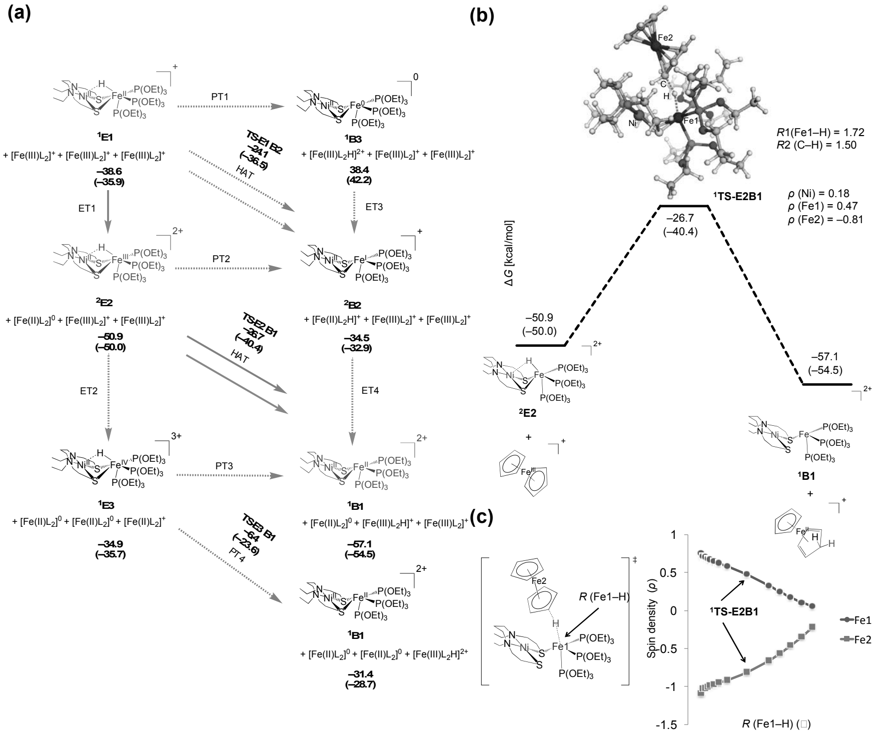

Figure 2. (a) Schematic depiction of the redox states and ET, HAT and PT reaction of interested. The most plausible pathway is represented by stick arrows. The free energy (kcal/mol) is calculated relative to complex **^{1}A1**, and enthalpy is given in parenthesis. (b) Free energy profile (kcal/mol) of HAT with optimized TS structure (**^{1}TS-E2B1**), where the selected bond lengths are given in angstrom. (c) Plots of spin densities of two irons, Fe1 and Fe2, along the reaction coordinate.

Despite of the remarkable catalytic ability of the hydrogenase, the molecular catalyst with higher catalytic efficiency is further demanded for the industrial application. For this purpose, it is sensible to create the catalyst using non-precious metals such as Ni, Fe, and Mn which are involved in metalloenzymes. For the creation of the ideal catalyst, many bio-inspired models to mimic the function of hydrogenase have been developed and analyzed.

We investigated mechanistic details in formation of NiFe hydride complex and electron and hydride transfer processes from the hydride complex using density functional theory and artificial force induced reaction methodology. The NiFe hydride complex derived from NiFe complex ($[Ni^{II}(L)Fe^{II}(MeCN)[P(OEt)_3]_3]$, L = *N,N'*-diethyl- 3,7-diazanonane-1,9-dithiolato) with reaction H_2 is the first reported hydride complex which conducts three reactions, electron, hydride, and proton transfers (Ogo et al. *Science,* **2013,** *339*, 682-684). In the generated hydride complex, the hydride binds to Fe, which is different from Ni-R state in hydrogenase in which hydride locates between Ni and Fe. In the reaction with ferrocenium ion, our calculation suggested that the first electron transfer occurs from NiFe hydride complex into ferrocenium ion, then the hydrogen atom transfer takes place subsequently. The oxidation state of Fe varies during the redox process, which differs from the NiFe hydrogenase where oxidation state of Ni varies. Singlet step hydride transfer occurs in the presence of 10-methylacridinium ion ($AcrH^+$) which is kinetically feasible compared with the HAT. While, the proton transfer occurs barrierlessly from protonated diethyl ether. The revealed reaction mechanism guides the interpretation of the catalytic cycle of NiFe hydrogenase and development of efficient biomimetic catalyst for H_2 generation and electron/hydride transfer.

2. Presentation at academic conferences

(1) 伊勢川 美穂, WMC Sameera, Akhilesh K. Sharma, 小江誠司, 諸熊奎治 “ヒドロゲナーゼモデル錯体による水素分子活性化の理論的研究”, 第 20 回理論化学討論会, 5 月 16-18, 2017, 京都.

(2) Miho Isegawa “DFT Study on Fe(IV)-Peroxo Formation and H-Atom Transfer Triggered O_2 Activation in a Bio-Inspired Model of [NiFe]-Hydrogenase”, I^2CNER International Workshop, Catalytic Materials transformation division, Feb 2, 2018, Fukuoka.

Satoshi Suzuki

FIFC Fellow

1. Summary of the research of the year

1.1 チオフラビンＴの発光特性について

チオフラビンＴ（図 1）は溶媒粘度に応答する発光分子で、低粘度の溶媒中ではほとんど蛍光を示さないのに対し、粘性の高い溶媒中では強く発光する。そのため、軸に沿った回転により非発光性の“ねじれた分子内電荷移動（TICT）状態”に到達する速度が溶媒に依存するのではないかと考えられている。

また、チオフラビンＴはアルツハイマー病患者によく見られるアミロイドβ、特にβシート構造に強く結合し、蛍光を示す。アミロイドβと結合した際に蛍光を示すメカニズムについても、溶媒粘度依存性と同じようなメカニズムではないかと考えられる。

そこで、タンパク質環境においてどのようにチオフラビン Ｔ が発光性を獲得するのかを調査した。まず、気相での TICT 状態の構造最適化を行い、その近傍の円錐交差構造を探した。

過去の報告では、ねじれ角に対しての TDDFT による一次元 scan が行われているが円錐交差近傍で TDDFT が正しくない振る舞いをすることがあるため、本当にそこに極小値があることは保障されない。本研究では MCSCF により円錐交差と TICT 状態の構造を最適化した。

次に、チオフラビン Ｔ とアミロイドβの結合状態での同様の計算を試みた。アミロイドβ（PDB ID：2BEG）とチオフラビン Ｔ に対し分子ドッキングシミュレーションを行い、アミロイドβへの結合サイトを推測した。最高ランクの構造から ONIOM(HF/6-31G(d):MM)レベルで構造最適化を行った。

気相中での計算の結果、TICT 状態の安定構造が得られた。また、この構造の近くに円錐交差（図 2）が存在することがわかった。この円錐交差は CASSCF レベルでは TICT 構造より 30kJ/mol 程度高いが、それでも垂直励起状態よりはエネルギーが低い。また TICT 状態から基底状態への遷移双極子モーメントは小さく、したがって、この構造からの発光は起こりにくく、円錐交差を経由した無輻射失活が起こりやすいことがわかる。

一方、たんぱく質中（図 3a）では TICT 状態、円錐交差共に大きく不安定化されることがわかった（表）。これは、ThT の近くにあるフェニルアラニンとの衝突を避けるためにチアゾール環が大きく変形することに由来する（図 3b）。また、TICT 状態での遷移双極子モーメントは１程度と大きい。結果として、円錐交差を経由した無輻射失活が起こりにくく、発光の方が起こりやすいことが説明される。

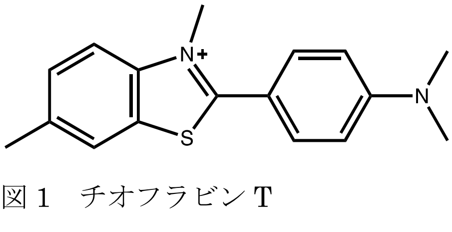

図１　チオフラビンＴ

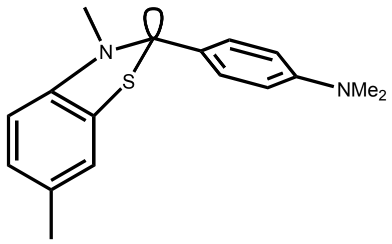

図２　チオフラビン T の円錐交差

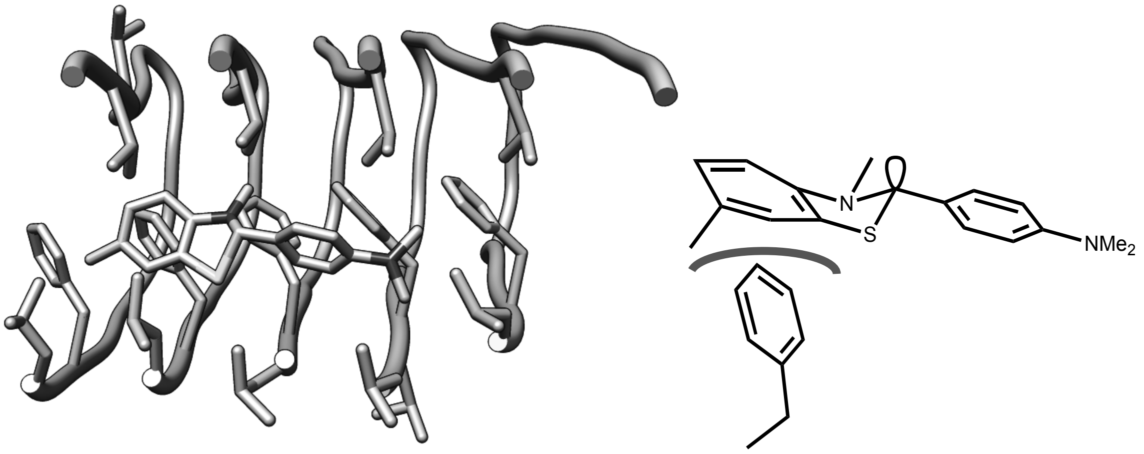

図３　a)アミロイドβ中におけるチオフラビンTの円錐交差 b)近接するフェニルアラニンから立体障害を受けて大きく歪んだ円錐交差

	isolated ThT			ThT+Amyloid		
	S_1 FC	S_1MIN	S_1/S_0 MECI	S_1 FC	S_1MIN	S_1/S_0 MECI
S_0	0.0	28.1	389.1	0.0	17.5	473.1
S_1	405.5	360.3	389.2	411.9	373.3	473.3

表　(4,4)CASSCF/6-31G(d)による各構造のエネルギー

2. Original papers

(1) S.Suzuki, S. Maeda, K. Morokuma
Exploration of Quenching Pathways of Multiluminescent Acenes Using the GRRM Method with the SF-TDDFT Method
J. Phys. Chem. A, **119**, 11479–11487 (2015)

(2) S.Sasaki, S.Suzuki, W.M.C. Sameera, K. Igawa, K. Morokuma, G. Konishi,
Highly twisted N,N-dialkylamines as a design strategy to tune simple aromatic hydrocarbons as steric environment-sensitive fluorophores
J. Am. Chem. Soc., **138**, 8194-8206

(3) S.Sasaki, S.Suzuki, K. Igawa, K. Morokuma, G. Konishi,
“The K-Region in Pyrenes as a Key Position to Activate Aggregation-Induced Emission: Effects of Introducing Highly Twisted N,N-Dimethylamines”
J. Org. Chem., 2017, 82 (13), pp 6865–6873

3. Presentation at academic conferences

(1) “凝集誘起発光を示すアルキルアミノアレーンにおける発光挙動の理論化学的解析”
◯鈴木聡　諸熊奎治　理論化学討論会 2017

(2) “凝集誘起発光を示すアルキルアミノアレーンの理論的解析と分子設計指針”
◯鈴木聡　諸熊奎治　分子科学討論会 2017

(3) “最小エネルギー円錐交差に着目した凝集誘起発光材料の開発：理論化学で内部転換を視る(1)” (特別企画講演・招待講演)
第 98 回日本化学会春季年会

4. Others

Akhilesh Kumar Sharma

Postdoctoral Fellow

1. Summary of the research of the year 2017

1.1 Mechanism and Selectivity in PdSIPr-Catalyzed Ring-Opening and Cross-Coupling of 2-Arylaziridines with Arylboronic Acids

The strained small ring compounds such as oxiranes, aziridine, are being utilized in organic synthesis for variety of transformations. The aziridines are important synthons for formation of variety of N-containing compounds of synthetic importance, such as β-amino-functionalized motifs. The organometalic catalysts are effective for regioselective and stereospecific ring-opening of aziridines. The formed adducts after ring-opening can be further functionalized or used to generate products with regio- or chemo- or stereo-selectively. Recently, Takeda et al. reported a Pd/NHC-catalyzed enantiospecific and regioselective ring-opening and cross-coupling of 2-arylaziridines with arylboronic acids to give β-aryl β-phenethylamine derivatives (Scheme 1).

In current study we have explored mechanism of this reaction. Besides studying mechanism of cross-coupling, we have also studied active species generation viz., Pd(II) to Pd(0) conversion. The aziridine ring-opening is studied by multicomponent artificial force induced reaction method (MC-AFIR) to explore possible reaction paths systematically and explain regioselectivity and stereospecificity.

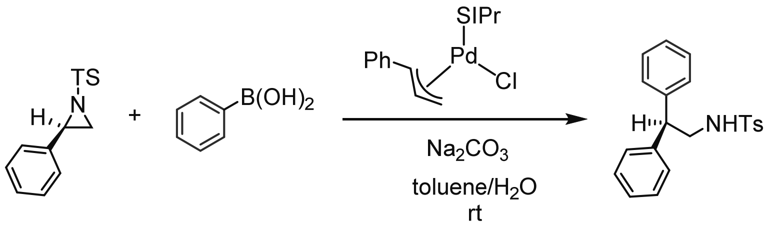

Scheme 1. Stereospecific and regioselective Suzuki-Miyaura coupling of 2-arylaziridines.

Active Catalytic Species Generation

The reaction involves first generation of active catalytic Pd(0) species. The mechanism of Pd(0) generation is not well studied in Pd-NHC catalyzed reactions. The reported computational studies propose direct reductive elimination from catalyst or after replacement of chloride with base ($O\text{-}tBu^-$). However, in current reaction we found that reductive elimination from catalyst have high activation barrier (32.3 kcal/mol). Reaction barrier for Pd(0) generation is lowered in presence of phenylboronic acid, base and water. The highest activation barrier is for reductive elimination (TS3) from intermediate I4 (~20 kcal/mol). Hence, the Pd(0) generation also involve mechanism similar to Suzuki-Miyaura couling reaction.

Cross-Coupling Reaction Mechanism

The different steps in the current cross-coupling reaction involve oxidative addition (aziridine ring opening), protonation, transmetalation and reductive elimination.

From the exhaustive sampling of TSs (transition states) for aziridine ring opening, we found that oxidative addition occurs by S_N2 attack of Pd(0) to benzylic-carbon (type B) of aziridine (Fig. 1). It is important to

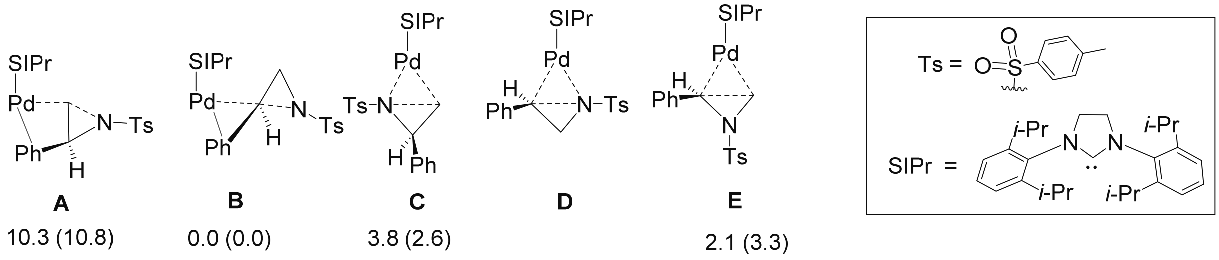

Fig 1. Type of Transition states for the aziridine ring opening with calculated free energy in kcal/mol (Enthalpy is given in parenthesis).

note that, in the lowest energy TS phenyl group of substrate is coordinated *anti* to the NHC ligand and benzylic carbon is in syn-orientation. The phenyl group of substrate helps the reaction to proceed regioselectively. Hence, the reaction occurs through type B TSs, which lead to desired product and explains the regioselectivity and enantiospecificity of reaction.

Regioselective aziridine ring-opening by TS type B leads to higher energy intermediate **I8** (-17.1 kcal/mol, Fig. 2). The intermediate is stabilized by water through H-bonding. Upto three water molecules were used to stabilize the intermediate, in accordance with previous study. The intermediate with two water, **I8.2H2O** (-25.3 kcal/mol) is more stable. The TSs for the proton transfer involve relatively low barrier. It leads to lower energy intermediate **I9**.

Next step is transmetalation, it involved coordination of $PhB(OH)_2$ to hydroxyl group leading to intermediate **I10**. From **I10** intermediate transmetalation occurs leading to lower energy intermediate **I11**. After decoordination of B(OH)3 intermediate **I12** undergo reductive elimination leading to cross-coupling product. The activation barrier for this process is ~15 kcal/mol. Hence, in this study we have revealed the full mechanism of the reaction, which will be further helpful in development of the reaction.

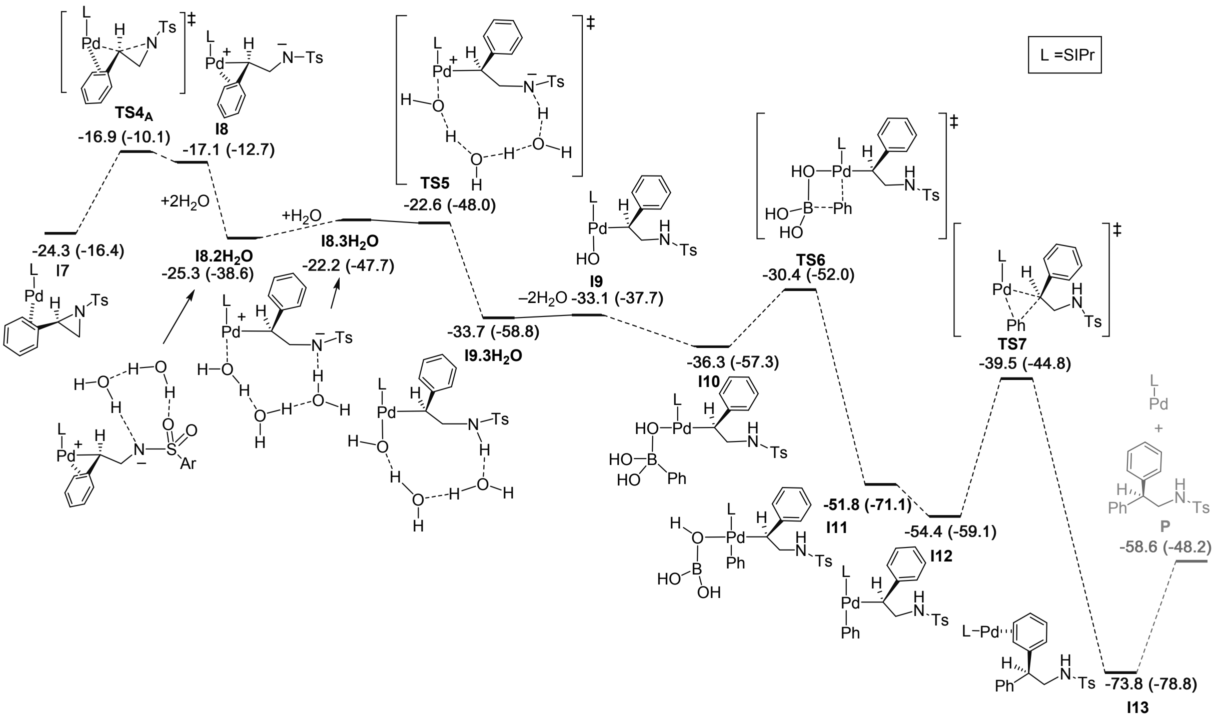

Fig 2. Free energy profile at $PCM_{Toluene}$/B3LYP-D3/SDD(Pd),cc-pVTZ//$PCM_{Toluene}$/B3LYP-D3 /SDD(Pd);6-31+G(d)(B,N,O,S;6-31G(d)(C,H) for cross coupling . Relative energies are in kcal/mol.

1.2 Theoretical Study on the Mechanism of Phoshoranide-Trihydroborate Reaction with Methyl Iodide

Phoshorous-Borane, Lewis acid-base complexes are isoelectronic to C-C bond. Phoshino-Boranes are now getting more attention as reagent, hydrogen storage material and polymer precursors, beside their importance in coordination chemistry. Formation of tetra- or penta-coordinated phosphorus complex with boron is difficult. The first compound (**1**) having trihydroborate coordinating to a pentacoordinated phosphorus was synthesized and crystallized recently by Kano *et al.*. In one of recent results of Kano *et al.*, the reaction of trihydroborate **1** with an excess of methyl iodide (MeI) in toluene at room temperature gives a 1:1 mixture of bicylic compound **2** and the P-methylated derivative **3** (Scheme 2). Interestingly, if the reaction occurs at 100°C the P-methylated bicyclic compound **3** has been obtained exclusively without compound **2**.

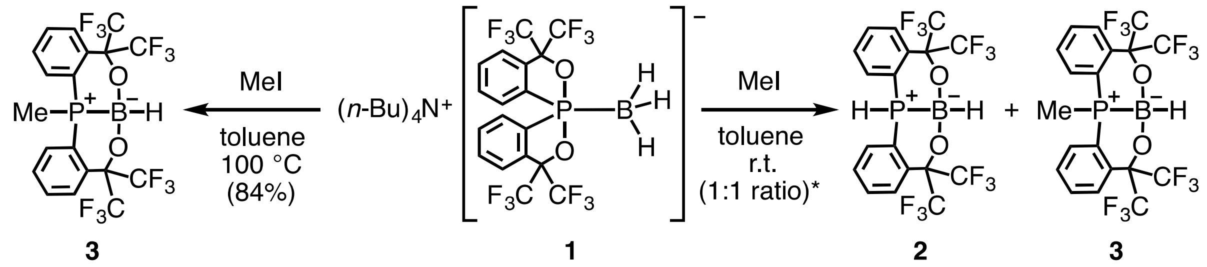

Scheme 2.

In this study the mechanism of this reaction is studied through computational methods. The reaction path was explored by AFIR (artificial force induced reaction) method available in GRRM program. The stationary points was further optimized using Gaussian 09 program and with SMD(Toluene)/B3LYP-D3BJ/6-311++G(2d,p), 6-311G**(for Iodine) method.

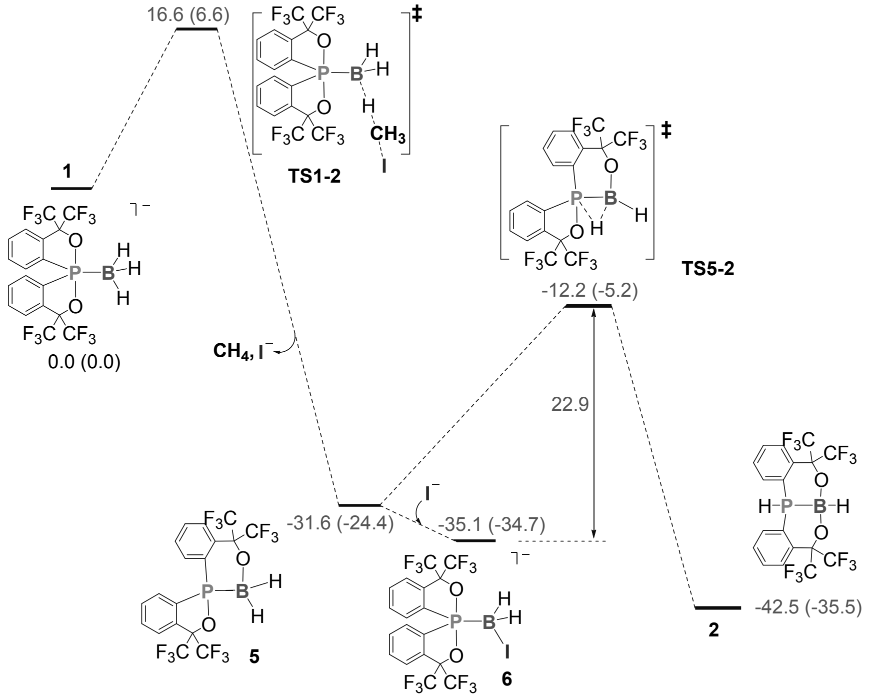

Fig 3. Free energy (kcal/mol) profile for intermediate **2** formation. Enthalpy is given in parenthesis.

Formation of intermediate 2

From AFIR search, five different paths were found for reaction of MeI with **1**. The lowest energy paths involve S_N2 attack of hydride on methyl group of MeI (**TS1**) leading to formation of methane (Fig. 3). The S_N2 attack of hydride on I-atom of MeI is kinetically (ΔG‡= 68.1 kcal/mol) and thermodynamically (ΔG = 60.0 kcal/mol) less likely as it involves formation of highly unstable methyl-anion.

The intermediate **5** and **I⁻**

can easily isomerize to intermediate **6**. **6** is 3.5 kcal/mol lower in energy than **5**. The intermediate **5** can also isomerize to **2** by hydride transfer from boron to phosphorus. The activation barrier for this process is 22.9 kcal/mol leading to formation of lower energy **2**. Hence, formation of **2** is thermodynamically more probable and explains the experimental detection of this intermediate (Scheme 1).

Reaction of 2 with MeI. We have further studied reaction of **2** with MeI. The process involves $\mathbf{S_N2}$ attack of P on methyl group of MeI with Iodide removal. The next step involves proton abstraction from phosphorus leading to formation of HI and product **3**. The highest barrier for **2** to **3** conversion is 31.3 kcal/mol. The attack of hydride from B-H of **2** to methyl group of MeI is 0.5 kcal/mol lower in energy. Hence, the S_N2 attack by P and hydride of B will be competitive. The S_N2 attack by hydrogen of phosphorus on MeI is both kinetically and thermodynamically unfavorable. As the activation barrier for all these processes are very high (>30 kcal/mol), these processes are less likely.

Reaction of 5 with MeI. For the S_N2 attack by P-atom of **5** to MeI, involve first isomerization of **5** to higher energy species **19** with B-atom decoordinated from P-atom. The B-atom further interact with iodide formed in first step leading to formation of **20**. The reaction of MeI with **20** has 27.6 kcal/mol activation barrier and lead to formation of intermediate **21**. **21** is almost of same energy as **5**. Since the barrier for **TS20-21** is higher than **TS 5-2** (Fig. 3), this process is less likely than formation of **2**.

Formation of H_2

The HI formed during the process for formation of **3**, can further react with the substrate (**1**) (Fig. 4). The HI can directly react with hydride and lead to formation of **11** or the proton from HI first transferred to oxygen leading to lower energy intermediate **12**. From **12** transfer of H from oxygen to boron lead to formation of **11** through 11.4 kcal/mol barrier. The **11** is a unique species with σ-bond of H2 interacting with empty p-orbital of B. The **11** is easily converted to **5** by removal of H_2 from B. This reaction have low barrier and lead to formation of H_2 and intermediate **5**. This result agrees with experimental detection of H_2 during the reaction.

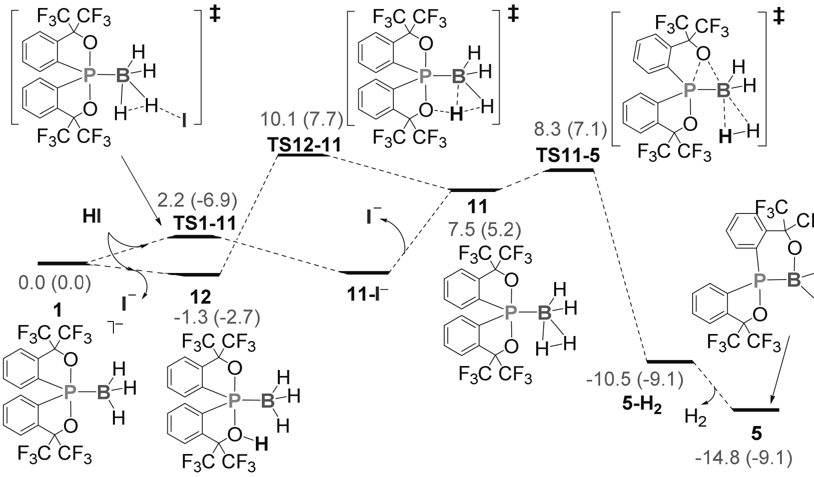

Fig. 4. Free energy (kcal/mol) profile for H_2 formation. Enthalpy is given in parenthesis.

In current computational study we have explained mechanism for formation of **2** and H_2. Exploration Mechanistic study for product **3** formation is currently in progress.

2. Original papers

(1) Akhilesh K. Sharma, W. M. C. Sameera, Masayoshi Jin, Laksmikanta Adak, Chiemi Okuzono, Takahiro Iwamoto, Masako Kato, Masaharu Nakamura, and Keiji Morokuma,
“DFT and AFIR Study on the Mechanism and the Origin of Enantioselectivity in Iron-Catalyzed Cross-Coupling Reactions”
J. Am. Chem. Soc. 139, 16117-16125 (2017).

(2) Miho Isegawa, Akhilesh K. Sharma, Seiji Ogo, and Keiji Morokuma,
"DFT Study on Fe(IV)-Peroxo Formation and H Atom Transfer Triggered O_2 Activation by NiFe Complex”
Organometallics 37, 1534-1545 (2018).

3. Presentation at academic conferences

(1) Akhilesh K. Sharma, W. M. C. Sameera, Masaharu Nakamura, Keiji Morokuma
“Computational Insights on Mechanism Iron-SciOPP-Catalyzed Alkyl-Aryl Coupling Reaction”
20th Annual Meeting of Theoretical Chemistry Society, Kyoto, May 16-18, 2017.

4. Others

(1) Akhilesh K. Sharma, W. M. C. Sameera, Masaharu Nakamura, Keiji Morokuma
“Theoretical Study on the Mechanism of Phoshoranide-Trihydroborate Reaction with Methyl Iodide”
The 15th symposium of Fukui Institute for Fundamental Chemistry, Kyoto, Feb. 2, 2018.

Maneeporn Puripat

Research Fellow (To 15 Sept. 2017)

1. Summary of the research of the year

Theoretical Investigation of Catalytic Hydrocarboxylation of Olefins with CO_2

[Abstract] Carboxylic acids can be directly formed from CO_2, H_2, and simple olefins by using rhodium(I) catalyst. In this reaction, the addition of iodide compounds, such as CH_3I, is indispensable to increase the yield of the product. To understand the role of the iodide additives, we studied the mechanism of the catalytic hydrocarboxylation of cyclohexene with CO_2 and H_2 by using an automated reaction search method, called multi-component artificial force induced reaction (MC-AFIR) method. The reaction can be divided into two parts. First, CO and H_2O is obtained from CO_2 and H_2 through the formation of formic acid. Then, the CO and olefin convert to the carboxylic acid. The iodide additive plays two important roles. One is the formation of cyclohexyl iodide to promote the oxidative addition to the rhodium(I) catalyst. Another is the stabilization of intermediates and transition states through the interaction with phosphine ligands.

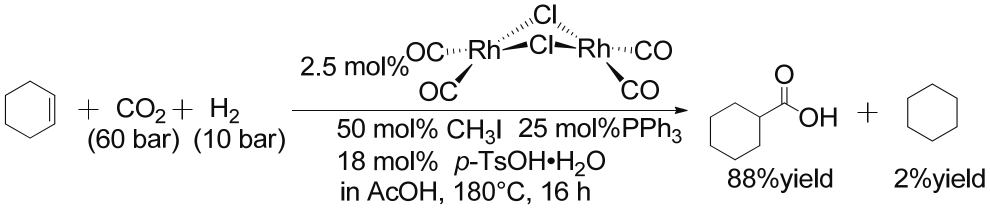

Fig. 1 Catalytic hydroxycarbonylation of olefins with CO_2 and H_2 catalyzed by the rhodium complex. [1]

[Introduction] The CO_2 is an attractive C1 building block which leads carboxylic acids and their derivatives. To establish the catalytic systems to form the carboxylic acids from CO_2, the mechanical understanding is indispensable. Leitner et al. reported an effective catalytic system for the hydroxycarbonylation of simple olefin with CO_2 and H_2 leading the carboxylic acid as shown in Fig. 1 [1] Several experimental measurements were performed to discuss the mechanism of this catalytic system. First, it was found that the carboxylic group was constructed not by CO_2 but by CO and H_2O according to the nuclear magnetic resonance spectroscopy. Second, the yield of the carboxylic acid increased dramatically by the addition of iodide compounds, such as CH_3I. Third, the formation and consumption of cyclohexyl iodide was observed by the mass spectrometry, which implied that the role of the CH_3I additive was the conversion of cyclohexene to cyclohexyl iodide and cyclohexyl iodide could be a reactant instead of cyclohexene. Forth, to discuss the effect of the intermediates, the same reaction starting from other reactants, such as cyclohexyl iodide, cyclohexanol, and cyclohexyl acetate, were performed. Contrary to the expectation, the product yield depended on the reactant. Cyclohexanol and cyclohexyl acetate provided high product yield as cyclohexene. Whereas, the product yield starting from cyclohexyl iodide was only 21 %, even though cyclohexyl iodide was assumed to be formed and consumed during the catalytic reaction. To get the more detailed insights of this catalytic system, we performed one of the methods in the Global Reaction Route Mapping (GRRM) strategy, called the artificial force induced reaction (AFIR) method,[2] to search systematically all possible reaction pathways. In this study, we also discuss about the role of iodide additives and the reason of the product yield dependency on the reactants based on the calculated Gibbs free energy profile.

[Methods] First, approximate reaction pathways were explored by the MC-AFIR method, in which the AFIR functions were minimized with γ = 300-400 kJ mol^{-1}. The initial AFIR search was carried out at M06-L/Def2SV level of theory. Then, all the obtained approximate local minima and transition states (TSs) were re-optimized without artificial force at the B3LYP-D3/SDD (for Rh and I) and 6-31g(d) (for other atoms) levels. Single point energies were calculated at B3LYP-D3/SDD (for Rh and I); 6-31+g(d,p) (for other atoms) levels of theory. The solvation free energy was included by the PCM model with a dielectric constant of 6.3 (acetic acid) for all the calculations. The intrinsic reaction coordinate (IRC) was calculated to confirm the reaction pathway. All these AFIR search, optimizations and IRC calculations were performed with the GRRM program[3] using energies, first, and second energy derivatives computed with the Gaussian09 program.

[Results and Discussion] The reaction system can be divided into two catalytic cycles. One is for the formation of CO and H_2O from CO_2 and H_2 (Cycle I) and the other cycle is for the producing the carboxylic acid from CO and olefin (Cycle II). The Cycle I starts from the oxidative addition of H_2 to the Rh(I) complex, followed by the CO_2 insertion. Thus, we firstly investigated about the stability and the catalytic ability of the mononuclear Rh(I) complexes with different number of PPh_3 ligands ($RhCl(CO)_n(PPh_3)_m$: n, m = 0, 1, 2). The reaction barrier of the oxidative addition of H_2 depended on the coordination number of phosphine ligands. The most stable complex was the Vaska-type $RhCl(CO)(PPh_3)_2$ complex, which was detected by the NMR spectroscopy. [4] The most favorable pathway started from the dissociation of the phosphine ligand from the Vaska-type Rh(I) complex $RhCl(CO)(PPh_3)_2$, followed by the oxidative addition of H_2. The activation barrier of the oxidative addition of H_2 to the Vaska-type complex and the following CO2 insertion, however, was too high. To reduce the activation barrier, the CH_3I additive played an important role. The CH_3I additive promoted the dissociation of one of the PPh_3 ligands from the Vaska-type complex by the formation of the phosphonium iodide $[Ph_3P(CH_3)]I$. The activation barrier of the oxidative addition of H_2 and insertion of CO_2 was lowered by the dissociation of PPh_3 ligand from the Vaska-type complex, which was consistent with the experimental result that the yield reduced dramatically without addition of CH_3I. [1,4] Then, the CO_2 and H_2 in the Rh(I) complex converted to formic acid, which can be decomposed into CO and H_2O. Although, the formation of CO and H_2O from CO_2 and H_2 (Cycle I) was the endothermic reaction, this catalytic reaction could take place because of the exothermicity of the following Cycle II.

The Cycle II started from the formation of the cyclohexyl iodide from cyclohexene and CH_3I to promote the following oxidative addition to the Rh(I) catalyst. Then, the insertion of the CO, which was obtained from the Cycle I, took place, followed by the transformation leading to the desired carboxylic acid. The rate-determining step (RDS) of the overall catalytic process was the carbonylation step in Cycle I, with an activation barrier of 33.7 kcal mol^{-1}.

It should be noted that the hydrido-Rh(III) intermediate, which was obtained by the oxidative addition of H_2, could give cyclohexane (the by-product shown in Fig. 1) with the activation barrier of 35.7 kcal mol^{-1}, which was only 2.0 kcal mol^{-1} higher than that of the CO_2 insertion. It means that the Cycle I causes the formation of the by-product, cyclohexane. Therefore, the yield of cyclohexane could decrease by changing the reactant from CO_2 and H_2 to HCOOH. It was confirmed by the experimental study. [4]

[Acknowledgements] This presentation is based on results obtained from a project (P16010) commissioned by the New Energy and Industrial Technology Development Organization (NEDO).

[References]

[1] T.G. Ostapowicz, W. Leitner et al. Angew. Chem. Int. Ed. 52, 12119-12123 (2013).

[2] S. Maeda, K. Ohno, K. Morokuma, Phys. Chem. Chem. Phys. 15, 3683-3701 (2013).

[3] GRRM14: S. Maeda, Y. Harabuchi, Y. Osada, T. Taketsugu, K. Morokuma, and K. Ohno, http://grrm.chem. tohoku.ac.jp/GRRM/index_e.html.

[4] T. Oku, M. Okada, M. Puripat, M. Hatanaka, K. Morokuma, J. Choi. J. CO2 Util. 25, 1-5 (2018).

2. Original papers

(1) Tomoharu Oku, Masaki Okada, Maneeporn Puripat, Miho Hatanaka, Keiji Morokuma, and Jun-ChulChoi
“Promotional effect of CH_3I on hydroxycarbonylation of cycloalkene using homogeneous rhodium catalysts with PPh_3 ligand”
J. Co2. Util. 25, 1-5(2018).

3. Presentation at academic conferences

(1) Maneeporn Puripat, Miho Hatanaka, and Keiji Morokuma
“Theoretical Investigation of Catalytic Hydrocarboxylation of Olefins with CO_2”
The 11th Annual Meeting of Japan Society for Molecular Science (1P095), Sendai, September 15-18, 2017

4. Others

(1) -

青野　信治

センターフェロー（榊研）

1. 今年度の研究の要約

今年度は電子移動錯体について研究を行った。

【序】金属サレン錯体の一電子酸化体は、金属、置換基、溶媒分子の種類によって、ラジカル中心がサレン配位子内で局在化もしくは非局在化した原子価異性状態を示し、電子状態の観点からも興味深い。Ni(II)や Mn(III)の四配位平面型錯体では、サレン内の２つの(OPh-CN)基が同じ置換基 *R* を持つ場合、Ni(II)では２つの(OPh-CN)間にラジカル中心が非局在化したクラス３（Robin-Day の分類）、Mn(III)では片方の(OPh-CN)に局在化したクラス２に分類される。[1] これらの電子状態の違いと溶媒依存性について、我々は溶媒分布を積分方程式で決定する 3D-RISM 法を多参照電子状態理論の GMC-QDPT 法を組み合わせた 3D-RISM-GMC-QDPT 法を用いて、第７族３価、第１０族２価の金属のを中心に持つ一電子酸化サレン錯体について系統的に調べてきた。[2]

一方、Co(II)の五配位四角錐型錯体（Fig. 1）の一電子酸化体は第７族、第１０族のものに比べて複雑な振る舞いを示し、DMSO のような強い配位性溶媒中では金属の酸化状態 $\mathrm{Co^{III}}$(salen)が観測されるが、$\mathrm{CH_2Cl_2}$のような無配位性溶媒中では、**L** = トリフラート(OTf)やトシル(OTs)の場合、$\mathrm{Co^{III}}$(salen)状態とサレン配位子が酸化した状態 $\mathrm{Co^{II}}(\mathrm{salen}\cdot)^+$の両方の性質を示す事が、近年、実験的に明らかになっている。[3]

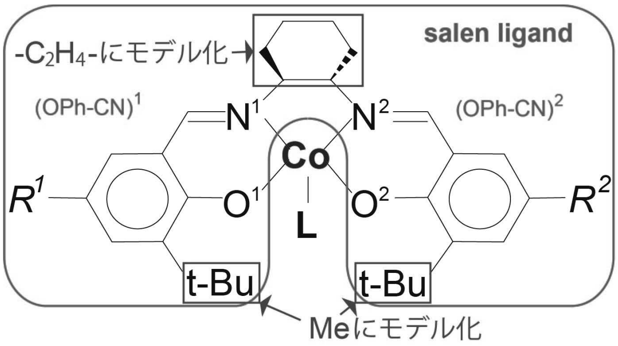

(R^1, R^2): **a** = (OMe, OMe) and **b** = (Cl, OMe)

Fig. 1: Co-salen complex

NMR 測定から三重項が基底状態である事は明らかであるが、その分解能では $\mathrm{Co^{III}}$(salen)と $\mathrm{Co^{II}}(\mathrm{salen}\cdot)^+$の共存が共鳴効果（Fig. 2）と熱平衡のどちらに由来するのか、結論付けられていない。この電子状態を精査するには、多参照電子状態理論が必要不可欠であり、本研究では GMC-QDPT 法を用いて検討を行った。また溶液中での配位子 **L** による電子状態の違いについても調べた。

【方法】CH_2Cl_2溶媒中の錯体構造と溶媒和構造は 3D-RISM- DFT/M06 法で求めた[2]。また結晶構造は対称性の観点からそれを構成する最小ユニットを QM（DFT/M06）に、それ以外の周期的な部分を MM に選び、MM 分子の点電荷は QM 分子のそれから自己無撞着的に決める QM/MM 法によって決定した。[4] なお、結晶の格子定数は実験値を使用した。励起エネルギーΔE と振動子強度 f は、構造最適化で定めた溶媒効果、結晶効果を考慮に入れ、４状態平均(4SA) GMC-QDPT 法で求めた（Fig.2）。計算コスト削減の為、-C_6H_{10}-を-C_2H_4-に、t-Bu を Me に置き換えてモデル化した。以下、(R^1, R^2) =(OMe, OMe)、(Cl, OMe)を持つ四配位 Co 錯体を **1a**、**1b**、配位分子 **L**（OH_2, OTf^-, OTs^-）を持つ場合、**1a-L**、**1b-L** と称す。

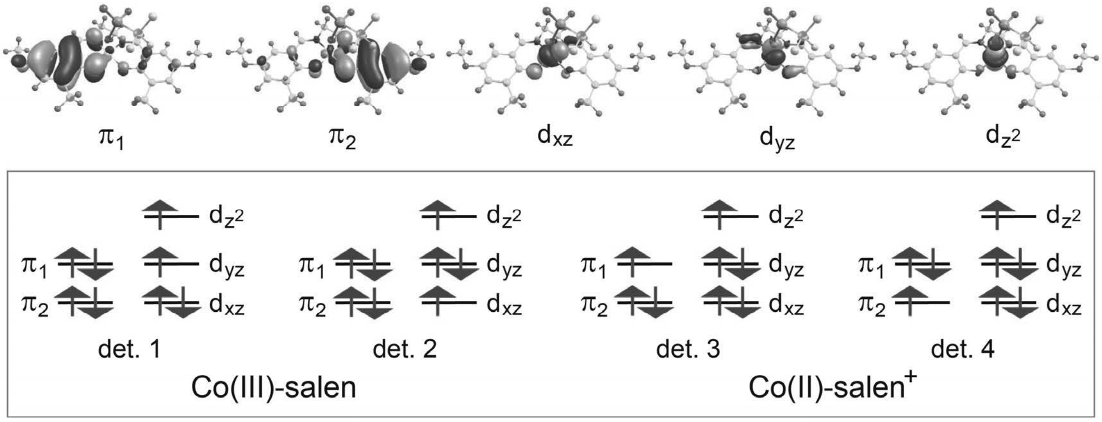

Fig. 2 : Important triplet configurations in resonance.

【結果・考察】Co-salcn 錯体 **1^{R}a-OTf** の分子性結晶は OTf$^-$の配向の異なる２つの構造 **1^{R}a-OTf-I** と **1^{R}a-OTf-II** から構成されており、salcn を salen と置き換えた両者 **1a-OTf-I** と **1a-OTf-I** の構造は、実験値に比べて誤差 0.05Å 程度で良く再現されている。更に３重項の他、これらの１重項、５重項の構造および結晶エネルギーを DFT レベルで調べた（Table 1）。

Table 1: Geometry and stability of spin states at DFT/M06. Units are in [Å] and [kcal/mol]

	Orient.		Co-O^1	Co-O^2	Co-N^1	Co-N^2	Co-**L**	Spin(Co)	$E_{QM/MM}$
Calc.	**1a-OTf-I**	1et	1.87	1.88	1.88	1.89	1.93		24.2
		3et	1.86	1.86	1.87	1.88	2.16	1.60	0.0
		5et	1.87	1.88	1.99	1.99	2.09	2.99	0.8
Expt.	**1^{R}a-OTf-I**	3et	1.86	1.83	1.87	1.88	2.12		
Calc.	**1a-OTf-II**	1et	1.88	1.88	1.88	1.89	1.92		22.8
		3et	1.85	1.87	1.87	1.87	2.17	1.63	0.0
		5et	1.86	1.89	2.01	2.00	2.09	2.99	-0.2
Expt.	**1^{R}a-OTf-II**	3et	1.84	1.86	1.87	1.87	2.13		

Table 1 が示す通り、計算によって得られた３重項構造は実験結果を良く再現しているが、１重項構造は Co-**L** 間の距離が観測値よりも 0.2 Å ほど短く、５重項構造は Co-N 間の距離が 0.1 Å ほど長い結果となっており、理論的にも実験で測定される構造は３重項構造である事を示唆している。また DFT/M06 の計算結果によると、３重項状態は Co(III)-salen 性が 60 %、Co(II)-salen•$^+$性が 40 %という結果を示しているのに対し、５重項状態は Co(II) -salen•$^+$性がほぼ 100 %の割合となっている事を Co 上のスピン数が示唆している。

M06 汎関数による DFT は３重項構造を良く再現しているが、３重項構造と５重項構造のエネルギーがほぼ等しい結果となっており、３重項構造のみが観測される実験結果とは一致していない。このスピン状態についての相対安定性を調べる為に、B3LYP*、B3LYP、B3LYP-D3、B3PW91、PBE0、M06、M06-L、M06-2X、M06-HF、GMC-QDPT による相対エネルギー計算した（Table 2)。Table 2 によると１重項が３重項よりも不安定である事はどの計算レベルでも変わらないが、ハートリーフォック交換項(HF ex)の割合が少ない DFT では３重項の方が５重項よりも安定であるのに対して、HF ex の割合が増加すると５重項の方が３重項よりも安定となっている。また GMC-QDPT では DFT 計算とは異なり、５重項構造が最も不安定であるという結果になっている。

GMC-QDPT 計算によると Fig. 2 に挙げた主配置の CI 係数から算出された Co^{III}(salen)と Co^{II}(salen$\cdot^{+}$)状態は、**1a-OTf-I**、**1a-OTf-II** の両者とも 30 %と 50 %であり、実験値の 60 %と 40 %[3]に近い結果が得られ、２つの構造 **1a-OTf-I**、**1a-OTf-II** の間に Co^{III}/Co^{II} 性の差はなく、Co^{III} と Co^{II} の共存は共鳴効果による事が示された。

Table 2: Dependence of $E_{QM/MM}$ on DFT and GMC-QDPT in **1a-OTf-I**. unit is in [kcal/mol].

	HF ex.	1et	3et	5et		HF ex.	1et	3et	5et
B3LYP*	15 %	0.0	-15.7	-2.8	PBE0	25 %	0.0	-20.4	-16.1
B3LYP-D3	20 %	0.0	-15.0	-7.2	M06	27 %	0.0	-24.2	-23.4
B3LYP	20 %	0.0	-16.8	-8.4	M06-L	0 %	0.0	-15.2	-5.4
B3PW91	20 %	0.0	-18.6	-10.9	M06-2X	54 %	0.0	-24.7	-35.5
GMC-QDPT		0.0	-16.8	20.3	M06-HF	100 %	0.0	-32.1	-49.7

次に **L** による電子状態の違いを調べる為、CH_2Cl_2 溶媒中の **1a-L**（L=none, OH_2, OTf^-, OTs^-, OAc^-）および、DMSO 溶媒中の 1a-DMSO について溶質、溶媒和構造を 3D-RISM-DFT/M06 法で求め、B3LYP-D3 汎関数で自由エネルギーを求めた。まず **1a** に対して１つの配位子 **L** を加えた５配位構造について調べた（Table 3)。ただし、**L** = OAc^- の場合のみ OAc^- の２つの O 原子が Co に配位した６配位構造 **1a-κ2-OAc** を取り得るため、これも比較した。

３重項状態における配位エネルギーによると配位力は $OH_2 < OTf^- < OTs^- < OAc^-$ である事が示唆されており、この順で Co-**L** 間の距離も短くなっている事、この順で Co 上のスピン数が増加して Co(III)性が増加している事が分かる。

Table 3: ΔG of 5-coordinated **1a-L** at B3LYP-D3

	ΔG			Spin (Co)		Co-**L**	G_{3et}(1**a**-**L**) − G_{3et}(**1a** + **L**)
L	1et	3et	5et	3et	5et	3et	[with BSSE corr.]
None	0.0	-6.2	-3.7	1.30	2.81		
OH_2	0.0	-24.1	-21.5	1.40	2.84	2.21	-1.7
OTf^-	0.0	-19.9	-10.5	1.53	2.88	2.18	-8.8
OTs^-	0.0	-11.3	-7.4	1.68	2.90	2.08	-13.7
OAc^-	0.0	-4.4	-1.2	1.76	2.95	1.94	-14.6
κ^2-OAc^-	-5.3	-2.7	-1.4	1.74	2.97	2.08, 2.26	-13.4
DMSO	0.0	-10.6	-5.5	1.65	2.90	2.10	-4.7

５配位構造では３重項状態が最も安定という結果になっているが、**L** ＝ OAc$^-$の場合に 1a-OAc の３重項よりも **1a-κ2-OAc** の１重項の方が安定な結果となっている。この事から他の **L** についても６配位構造と５配位構造での相対安定性の比較を行った（Table 4）。配位力が弱い OH$_2$、OTf$^-$、OTs$^-$、Cl$^-$では５配位３重項構造が安定であるが、配位力の強い OAc$^-$では６配位１重項κ^{2}構造が安定であり、DMSO では２つの DMSO による６配位１重項構造が安定である事が分かり、この結果は実験結果に良く合っている。

Table 4: ΔG of 6-coordinated **1a-2L** vs. 5-coordinated **1a-L** at B3LYP-D3

1a-2L and **1a-L** + **L**	1et	3et	5et	**1a-2L** and **1a-L** + **L**	1et	3et	5et
1a-2OH$_2$	0.0	-11.3	-9.1	**1a-2Cl**	0.0	-2.2	6.8
1-OH$_2$ + OH$_{2(1et)}$	11.0	-13.1	-10.5	**1a-Cl** + Cl$^-_{(1et)}$	5.1	-3.8	0.1
1a-2OTf	0.0	-14.4	-2.1	**1a-2OAc**	0.0	4.6	7.3
1-OTf + OTf$^-_{(1et)}$	10.4	-17.0	-4.9	**1a-κ^2-OAc** + OAc$^-_{(1et)}$	-0.6	2.3	3.4
				1a-OAc + OAc$^-_{(1et)}$	5.0	0.6	3.8
1a-2OTs	0.0	-1.4	4.9	**1a-2DMSO**	0.0	1.5	17.5
1a-OTs + OTs$^-_{(1et)}$	10.1	-1.7	2.8	**1a-DMSO** + DMSO$_{(1et)}$	13.2	2.7	7.6

CH_2Cl_2溶媒中の **1a-L**、**1b-L**（**L** = OH$_2$, OTf$^-$, OTs$^-$）について溶質および、溶媒和構造を 3D-RISM-DFT/M06 法で求め、4SA-GMC-QDPT 計算を行った（Table 5）。**1a-L**（**L** = OH$_2$, OTf$^-$, OTs$^-$）の場合、第一励起への *f* が第二、第三励起への *f* より非常に大きい。これは実験の吸収スペクトルが低エネルギー領域において１つのピークを示す特徴[3]と一致している。またΔE の実験値が OH$_2$ (0.93 eV) < OTf$^-$ (1.08 eV) < OTs$^-$ (1.23 eV)の順に大きくなる傾向[3]も再現された。基底状態は、**L** = OH$_2$, OTf$^-$, OTs$^-$の順に Co^{III} 性が増大している。しかし、**L** のない **1a** の基底状態では Co^{III}(salen)性が示されなかった。

一方、**1b-OTf** の場合、1.03、1.24 eV に２つのピークが実験的に観測されているが[3]、4SA-GMC-QDPT 計算でもΔE = 1.05、1.53 eV に２つの吸収が示され、それらの *f* は同程度の値となっており、実験結果を再現した。これは第一励起への *f* のみが大きい **1b** や **1b-OH$_2$** の場合とは異なる特徴であり、共鳴効果の程度の違いから生じている。ただし **1b-OTs** に関しては **1a-OTs** と異なり基底状態の Co(II)性の大きな減少が見られるが、これは４状態平均 MCSCF における問題であり、平均状態数を増やすと **1b-OTf** の結果に近付く事も分かった。

Table 5: Excitation energy ΔE, oscillator strength *f*, and weight of Co^{II}/Co^{III} character in CH_2Cl_2.

L		1a-L				1b-L			
		State0	State1	State2	State3	State0	State1	State2	State3
OH$_2$	ΔE [eV]	–	0.723	1.663	2.057	–	0.936	1.540	2.076
	f [au]	–	0.390	0.046	0.014	–	0.349	0.075	0.020
	III/II [%]	9/69	–/78	81/–	70/11	22/60	14/67	77/–	51/30
OTf$^-$	ΔE [eV]	–	1.027	1.668	2.198	–	1.046	1.531	2.179
	f [au]	–	0.423	0.107	0.015	–	0.243	0.188	0.038
	III/II [%]	33/47	11/68	69/13	31/51	37/42	32/47	59/24	33/47
OTs$^-$	ΔE [eV]	–	1.105	1.825	2.414	–	(0.889)	(1.210)	(1.638)
	f [au]	–	0.481	0.080	0.023	–	(0.209)	(0.178)	(0.011)
	III/II [%]	46/36	7/72	75/9	37/44	(8/73)	(31/51)	(56/25)	(74/10)

【引用文献】

[1] T. Kurahashi and H. Fujii, *J. Am. Chem. Soc.* **133**, 8307 (2011).
[2] S. Aono *et al.*, *J. Chem. Theory Comput.* **10**, 1062 (2014); *Phys. Chem. Chem. Phys.* **19**, 16831 (2017).
[3] T. Kurahashi and H. Fujii *Inorg. Chem.* **52**, 3908 (2013).
[4] S. Aono and S. Sakaki, *J. Phys. Chem. B* **116**, 13045 (2012).

2. 論文

(1) Shinji Aono, Nakagaki Masayuki, and Shigeyoshi Sakaki
″Theoretical Study of One-Electron-Oxidized Salen Complexes of Group 7 (Mn(III), Tc(III), and Re(III)) and Group 10 Metals (Ni(II), Pd(II), and Pt(II)) with 3D-RISM-GMC-QDPT Method: Localized vs. Delocalized Ground and Excited States in Solution”
Phys. Chem. Chem. Phys. 19, 16831-16849, (2017).

3. 学会発表

(1) 青野信治○　中垣雅之　榊茂好
７族、１０族金属サレン錯体の一電子酸化体の局在/非局在性電子状態：吸収スペクトルと溶媒効果
第２０回理論化学討論会　京都　2017/05/16　P29
(2) 青野信治○　中垣雅之　榊茂好
「五配位四角錐型コバルトサレン錯体の局在・非局在性電子状態と吸収スペクトルにおける結晶・溶媒効果」
第１１回分子科学討論会　仙台　2017/09/17　3D08

4. その他

(1) 青野信治○　中垣雅之　榊茂好
「結晶、溶媒中における五配位四角錐型コバルトサレン錯体の混合原子価電子状態と吸収スペクトル」
福井謙一京都大学第１５回京都大学福井謙一記念研究センターシンポジウム　京都　2018/2/2　P10

中垣　雅之

FIFC フェロー

1. 今年度の研究の要約

【緒言】ケイ素化合物は最近、遷移金属錯体類似の反応性を示すことが報告され注目されている。例えば、ルイス塩基によって安定化されたシリレン(スキーム 1)は、室温においてフェニルシランの可逆的なS-H 結合の切断・再生反応を行う[1]。これは遷移金属における酸化付加・還元脱離反応に類似しており触媒反応などへの応用も期待されている。ルイス塩基による始原系の安定化が可逆性に寄与していると定性的に説明されているが、どのような機構で進行するのか、何故、反応障壁が低く、又、可逆反応であるのかなど詳細な解明は行われていない。本研究では、理論計算により反応機構と電子的過程を明らかにし、電子構造の観点から反応の理解を深め、効率的な分子設計の提案を目的とした。

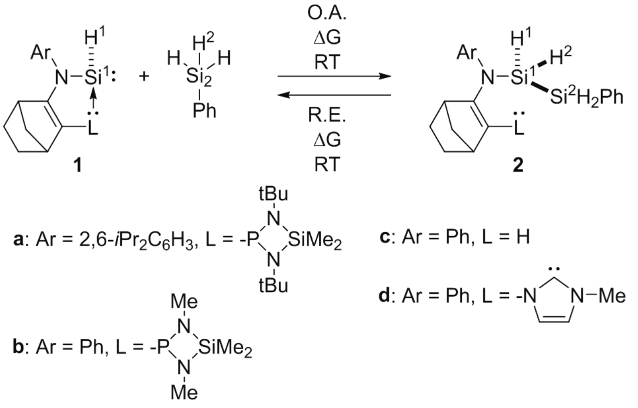

スキーム１

【モデル及び計算方法】実験で用いられたシリレン(a)は大きな置換基を持つことからスキーム１に示すようにモデル化(b)した。構造最適化には B3LYP-D3 法を、エネルギーの評価には SCS-MP2 法を用いた。基底関数は DFT には 6-31G*を用い、SCS-MP2 法には 6-311G**を用い、SiH_3Ph に diffuse 関数を加えた。また、溶媒効果（ベンゼン）は PCM 法で考慮した。

【結果及び考察】モデル分子(b)を用い、反応経路として直接生成物に至る経路及び中間体を経由する経路を検討した(スキーム２)。孤立系でのギブズエネルギー変化を図１に示す。最も安定な遷移状態($TS_{Si\text{-}Si}$)において、Si^1-Si^2 結合長は 2.348Å と生成物の結合長(2.359Å)に非常に近い。一方、解離する水素原子はシランケイ素(Si^2)からは 1.715 Å、シリレンケイ素(Si^1)からは 1.972 Å に位置しており、シリレンケイ素との結合は形成されていないことから Si^1-Si^2 結合生成は Si^1-H^2 結合生成に先行して起こる。また P 原子は生成物ではシリレンケイ素からは解離するが、遷移状態での Si^1-P 結合長(2.285 Å)は反応物(2.334 Å)よりも短い。エネルギーに SCS-MP2 法を用い、溶媒効果を加えた反応障壁は 25.6 kcal/mol であり、室温で起こるという実験結果と矛盾しない。以降、この遷移状態に関して考察を行う。

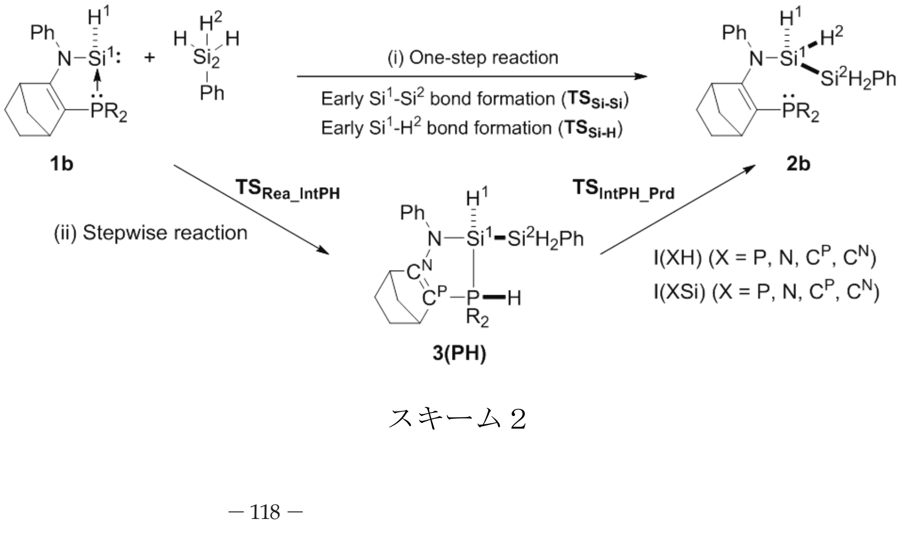

スキーム２

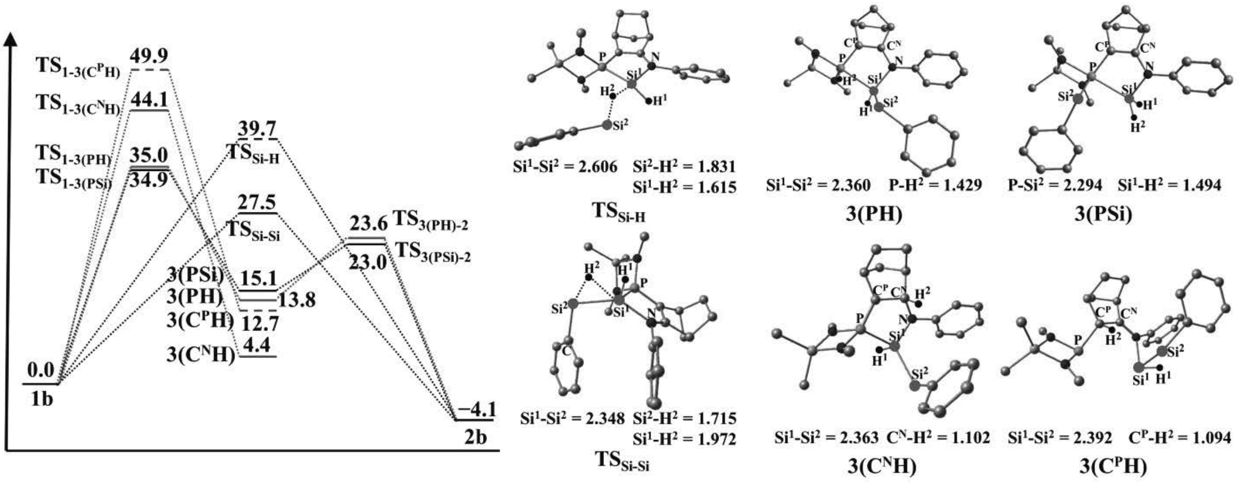

図１　**1b** の複数の反応経路の Gibbs エネルギー変化

ルイス塩基を持たないシリレン(**c**)の遷移構造及びエネルギー変化を図２に示す。**c** の遷移状態($TS_{1c\text{-}2c}$)では、Si^1-Si^2 結合長は $TS_{1b\text{-}2b}$ よりわずかに長い(2.383Å)。一方、Si^1-H^2 = 1684Å、Si^2-H^2 = 1760Å と Si^1-H^2 結合は Si^1-Si^2 結合と協奏的に生成される。この違いは H^2 原子が $TS_{1b\text{-}2b}$ では Si^1-N の σ*軌道に配位するのに対し、$TS_{1c\text{-}2c}$ では Si^1 の空の p 軌道に配位することに由来する。

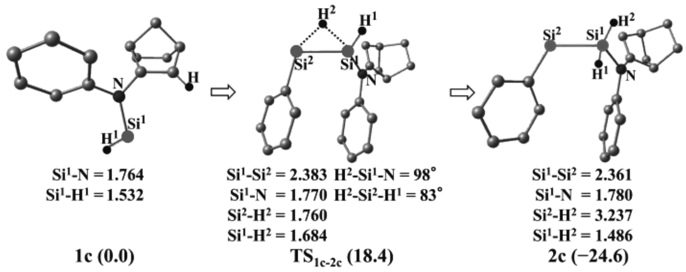

図２　**1c** の構造及び Gibbs エネルギー変化

遷移状態近傍の IRC に沿った結合変化及び電荷変化を図３に示す。1b から IRC ≈ 4.0 に進むに従って Si^1-P 結合長は僅かに減少するが Si^1-P 結合長距離は増加する。これは負電荷をもった H^2 原子が Si-N σ*軌道に作用するためである。また遷移状態近傍でシラン側に負電荷、シリレン側に正電荷の電荷移動が起こる。これらの結合・電荷の変化は次のように理解できる。初めに Si^1 の非共有電子対によって Si^1-Si^2 結合が生成され Si^2 が５配位構造をとる(スキーム 3a)。その後、Si^1-H^2 結合が生成され Si^1 が５配位構造をとり(スキーム 3b)、最後にルイス塩基(P)が解離する(スキーム 3c)。これらはルイス塩基が配位したシリレンに特徴的な反応機構であり、**1c** ではその特徴は見られない(図 3b)。

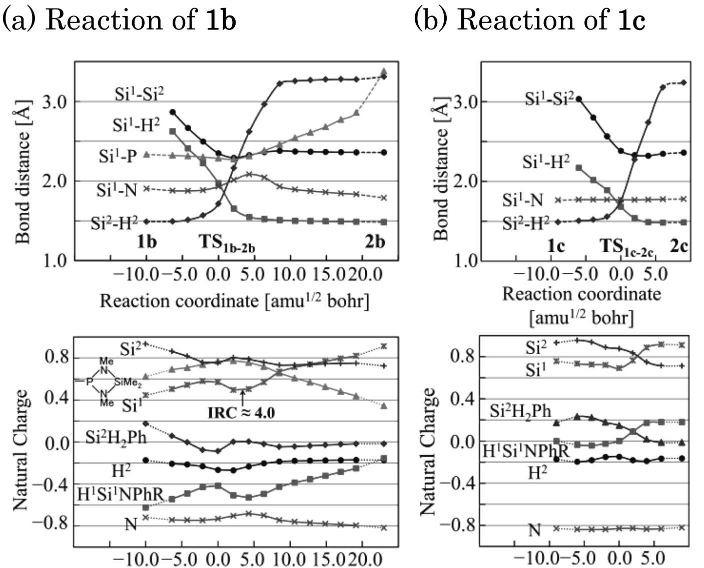
(a) Reaction of **1b**　(b) Reaction of **1c**

図３　IRC に沿った反応座標の結合及び電荷変化

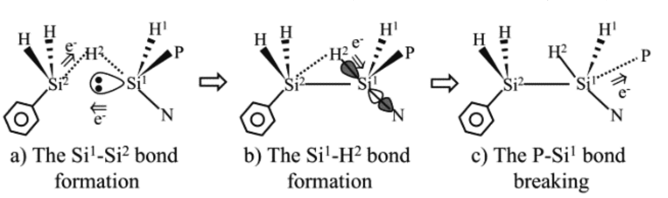

a) The Si^1-Si^2 bond formation　b) The Si^1-H^2 bond formation　c) The P-Si^1 bond breaking

スキーム３

ルイス塩基が活性化エネルギーに及ぼす影響を調べるため、強さの異なるルイス塩基をもつシリレン(**1b**, **1d**, **1e**$_x$, x = CF_3, CH_3, Pr, Et)と塩基を持たない**1c**の反応エネルギー及び活性化エネルギーを求めた(表１)。ルイス塩基とシリレンの結合エネルギー($\Delta E_{\mathrm{Si\text{-}L}}$)は **1e**$_{\mathrm{CF3}}$ < **1e**$_{\mathrm{CH3}}$ < **1e**$_{\mathrm{Pr}}$ < **1e**$_{\mathrm{Et}}$ < **1b** < **1d** の順序で強くなり、その結果始原系が安定化されるため同様の順序で反応エネルギーが正へシフトする。一方､活性化エネルギーはルイス塩基が配位することにより **1c**(18.4 kcal/mol)に比べ増加する。弱いルイス塩基が配位した **1e**$_{\mathrm{CF3}}$が最も高く(30.0 kcal/mol), **1e**$_{\mathbf{Pr}}$で最も低くなる(21.2 kcal/mol)が,より強い塩基である **1b**(25.6 kcal/mol)や **1d**(24.4 kcal/mol)では再び増加する。これは電子供与であるルイス塩基が配位することにより遷移状態におけるシリレン→シランの電荷移動が促進され，より安定化するためと考えられる。

表１．様々なルイス塩基を用いた反応エネエネルギー($\Delta G°$),[a] 活性化エネルギー ($\Delta G^{\circ\ddagger}$),[a] LP 軌道エネルギー($\varepsilon_{\mathrm{LP}}$),[b] 及び シリレンとルイス塩基の結合エネルギー($\Delta E_{\mathrm{Si\text{-}L}}$)(in kcal/mol)。

Compound 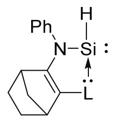	**1c**	**1e**$_{\mathrm{CF3}}$	**1e**$_{\mathrm{CH3}}$	**1e**$_{\mathrm{Pr}}$	**1e**$_{\mathrm{Et}}$	**1b**	**1d**
−L	-H	$-P(CF_3)_2$	$-P(CH_3)_2$	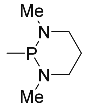	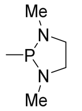	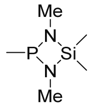	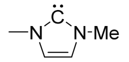
$\varepsilon_{\mathrm{LP}}$		−10.89	−8.80	−8.04	−7.99	−7.83	−9.85
$\Delta E_{\mathrm{Si\text{-}L}}$		5.3	14.2	17.5	18.2	18.9	38.8
$\Delta G^{\circ\ddagger}$	18.4	30.0	26.3	21.2	24.4	25.6[c]	24.4
ΔG°	−24.6	−25.1	−14.4	−11.6	−8.9	−9.8[c]	4.3

[a] SCS-MP2/6-311G** (in kcal mol^{-1}). [b] The $\varepsilon_{\mathrm{LP}}$ (in eV) was evaluated for free Lewis-base at the level of Hartree-Fock/6-311G**; see Scheme S2 in SI. [c] These values differ from those of Figure 1 because SCS-MP2-calculated values are presented here.

カルベン(*N*-heterocyclic carbine, NHC)は非常に強いルイス塩基であり、カルベンの配位したシリレン(**1d**)の反応は吸熱的($\Delta G°$ = 4.3 kcal mol^{-1})になる。生成物の構造を見ると、リン化合物のルイス塩基とは異なり Si^1 は N-Si1-H2 を C_3 軸とした C 両三角錐 5 配位構造をとっている(図 4)。**1b** と同様に活性化エネルギーが低く、また反応エネルギーが大きく異なることから **1d** に関しても **1b** 同様に詳細な検討を行う。

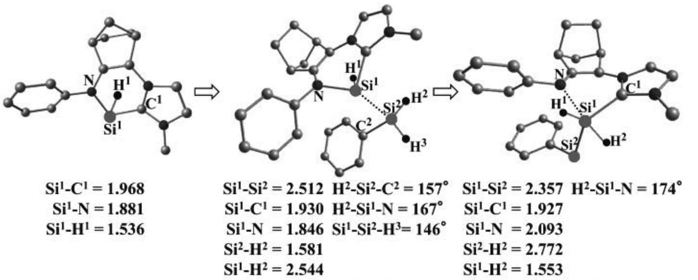

図４ **1d** の構造及び Gibbs エネルギー変化

より低い活性化エネルギーの達成のため、フェニルシランへの置換基導入の効果を検討した。フェニル基のパラ位により強い電子吸引基を導入することにより、反応エネルギーと活性化エネルギーはともに低下する(CH_3 > Ph ≳ PhF^p ≳ $PhCN^p$ > $PhNO_2{}^p$) (表 2)。従って **1b** と $H_3SiPhNO_2{}^p$を反応させた場合の活性化エネルギーは$\Delta G^{\circ\ddagger}$ = 19.1 kcal mol^{-1}まで低下し反応の進行が期待されるが、反応

エネルギーは$\Delta G^{\circ} = -13.4$ kcal mol^{-1}と大きく発熱的になることから逆反応は起こりにくくなる。一方、**1d**とH_3SiPhの反応は吸熱的であることから、$H_3SiPhNO_2{}^{p}$を用いた時には$\Delta G^{\circ\ddagger} = 19.2$ kcal mol^{-1}、$\Delta G^{\circ} = -0.8$ kcal mol^{-1}と可逆的な酸化還元反応が期待できる。

表 2. フェニルシランの置換基導入による反応エネルギー (ΔG°)及び活性化エネルギー ($\Delta G^{\circ\ddagger}$)変化 (in kcal/mol)。

−X	CH_3	Ph	PhF^{p}	$PhCN^{p}$	$PhNO_2{}^{p}$
A) silylene complex with a phosphine ligand (**1b**)					
$\Delta G^{\circ\ddagger}$	31.3	25.6	24.7	22.7	19.1
ΔG°	−6.6	−9.8	−10.3	−10.6	−13.4
B) silylene complex with a NHC ligand (**1d**)					
$\Delta G^{\circ\ddagger}$	32.3	24.4	24.2	21.5	19.2
ΔG°	8.9	4.3	4.3	3.0	−0.8
C) Bond energies of reactants					
Si^2-H^2	93.7	96.9	97.1	94.8	93.3
D) Bond energies of products					
Si^1-H^2	88.8	88.3	88.8	88.8	88.8
Si^1-Si^2	72.5	77.5	78.1	75.9	77.8

Si-C結合の活性化は一般的にSi-H結合の活性化よりも困難であるが重要な反応であることから、メチル基(−CH_3)、ビニル基(−CH=CH_2)、エチニル基(−C≡CH)をもつトリメトキシシラン(TMS)を用いて検討を行った。**1b**とTMSのSi-C結合の活性化エネルギー$G^{\circ\ddagger}$は $-CH_3 > -CH{=}CH_2 > -C{\equiv}CH$基の順に低下していき、HC≡C-Si$(OMe)_3$では$\Delta G^{\circ\ddagger} = 26.4$ kcal mol^{-1}とフェニルシランのSi-H結合の活性化エネルギー(25.6 kcal mol^{-1})と近い値が得られた(表 3)。従ってHC≡C-Si$(OMe)_3$のSi-C結合はルイス塩基安定化シリレンを用いることで温和な反応条件下での切断が期待できる。Si-C結合の活性化反応の遷移状態(**TS**$_{\mathbf{1b\text{-}4b}}$)においても Si-H 結合の遷移状態(**TS**$_{\mathbf{1b\text{-}2b}}$)と類似した構造の特徴が見られた(図 5)。Si^1-Si^2 結合は既に形成されており (2.300 Å)、Si^1-C 結合(2.487 Å)はSi^2-C 結合(2.283 Å)よりも長くエチニル基はシランケイ素(Si^1)に近い。生成物(**4b**)においてSi-P結合は2.318ÅとSi^1原子から解離しておらず、Si^1はN-Si-CをC_3軸とする両三角錐の５配位構造をとる(図 5)。

表３. **1b**及び**1d**とメチル-, ビニル-, エチニル-トリメトキシシランとのSi-C結合の反応エネルギー(ΔG°)及び活性化エネルギー ($\Delta G^{\circ\ddagger}$) 及び遷移状態における歪み(DE)・相互作用(INT)エネルギー(in kcal/mol)。

	A) phosphine ligand (**1b**)			B) NHC ligand (**1d**)		
−R	$-CH_3$	$-CH{=}CH_2$	$-C{\equiv}CH$	$-CH_3$	$-CH{=}CH_2$	$-C{\equiv}CH$
$\Delta G^{\circ\ddagger}$	45.4	34.9	26.4	45.1	37.1	24.3
ΔG°	9.6	4.1	3.4	15.7	8.8	4.2
DE(silane)	71.5	67.7	73.5	74.3	71.5	78.1
DE(silylene)	7.7	7.9	7.8	12.3	12.9	13.4
INT	52.4	56.0	72.5	58.3	63.1	82.8

遷移構造における歪みエネルギー及び相互作用エネルギーの解析から $HC\equiv C\text{-}Si(OMe)_3$ ではメチル基やビニル基に比べ、エチニル基とシランの間の相互作用エネルギーが大きい(72.5 kcal mol^{-1})ことが分かった。これはエチニル基によって求電子性が増したために、シリレン→シラン($Si^1 \rightarrow Si^2$)の電荷移動相互作用が増加したと考えられる。実際、エチニル基のもつ電荷は、反応物から遷移状態に向かうにつれて−0.55 *e* から−0.70 *e* へと増加し、これはメチル基(−0.52*e* から−0.60 *e*)やビニル基(−0.51 *e* から−0.60 *e*)の増加量と比べて大きい。遷移状態や生成物において、５配位構造である Si^1 は陰イオン的であることから、最も電子吸引的であるエチニル基が Si^1 の安定化に最も寄与すると考えられる。**1d** を用いた場合、$HC\equiv C\text{-}Si(OMe)_3$ の Si-C 結合の活性化エネルギーは 24.3 kcal/mol であり、**1b** の活性化エネルギー(26.4 kcal/mol)よりも低く Si-C 結合の活性化反応により有効であると考えられる。

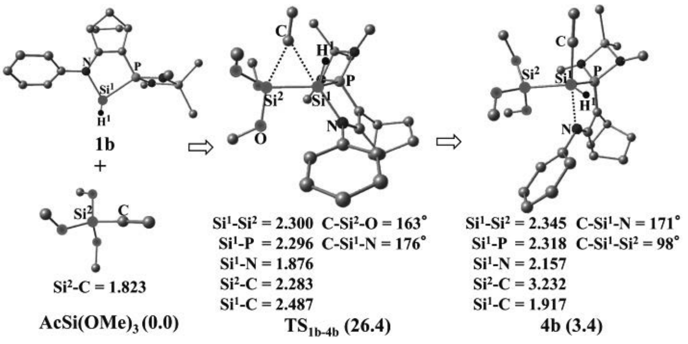

図 5　**1b** とエチニル-トリメトキシシランの反応の構造及び Gibbs エネルギー変化

本研究によりルイス塩基安定化シリレンの可逆的な Si-H 結合活性化反応の反応機構を明らかにした。本反応では、ルイス塩基をもたないシリレンでは見られない遷移状態におけるシリレン→シランの電荷移動相互作用が活性化エネルギーの減少に寄与している。このことから、ルイス塩基の選択やフェニルシランへの電子吸引性置換基の導入により活性化エネルギーを下げることができることを示した。また同様の反応機構により、ルイス塩基安定化シリレンを用いたエチニルトリメトキシシランの Si-C 結合の活性化反応の可能性を理論的に示唆した。

【文献】

[1] R. Rodriguez et al., *Angew. Chem. Int. Ed.,* **55**, 14355 (2016).

2. 論文

(1) Masayuki Nakagaki, Antoine Baceiredo, Tsuyoshi Kato, and Shigeyoshi Sakaki
“Reversible Oxidative Addition/Reductive Elimination of Si-H bondto Base-stabilized Silylenes: A Theoretical Insight”
Chem. Eur. J., accepted

3. 学会発表

(1) 中垣 雅之，Ricardo Rodriguez，加藤 剛，榊茂好
「ルイス塩基安定化シリレン分子を用いた可逆的 Si-Si(H)結合生成反応の機構解明と制御」
第 20 回理論化学討論会，京都, 2017/5/16-18, P28 ポスター

(2) 中垣雅之，中谷直輝，榊茂好
「金属多重結合錯体の分子内電荷移動励起状態の理論的研究」
第 11 回分子科学討論会 2017 仙台，仙台，2017/9/15-18 2P94　ポスター

(3) 青野信二，中垣雅之，榊茂好

「五配位四角錐型コバルトサレン錯体の局在・非局在性電子状態と吸収スペクトルにおける結晶・溶媒効果」
第 11 回分子科学討論会 2017 仙台，仙台，2017/9/15-18 3D08　口頭

4. その他

(1) 中垣 雅之， Antoine Baceiredo，加藤 剛，榊茂好
「ルイス塩基安定化シリレン分子を用いたSi-H結合の可逆的酸化的付加/還元的脱離反応の機構解明と制御」
第15回京都大学福井謙一記念研究センターシンポジウム，京都, 2018/2/2

Jing Lu

FIFC Fellow

1. Summary of the research of the year

Catalytic ability of $Ru_{13}@Pt_{42}$ and Pt_{55} toward oxygen reduction reaction: a DFT study

Proton exchange membrane fuel cells (PEMFCs) are regarded as a leading candidate of clean and sustainable energy source to cope with the growing energy need and environmental concern. Pt-based clusters/particles have attracted immense interest in catalysis for oxygen reduction reaction (ORR, $1/2O_2 + 2H^+ + 2e^- \rightarrow H_2O$) at the cathode in PEMFCs. Pt alloys with core-shell structure (M@Pt) is expected to be useful for the new generation ORR catalyst due to their higher activity and lower cost than pure Pt. In our previous work, 55-atom Pt-based particles were investigated. For bimetallic $Pt_{42}Ru_{13}$ cluster, the icosahedron-like core-shell structure ($Ru_{13}@Pt_{42}$) exhibited much higher stability than the non-core-shell structures ($Pt^{core\text{-}1}Ru_{12}@Pt_{41}Ru^{edge}$ and $Pt^{core\text{-}1}Ru_{12}@Pt_{41}Ru^{vertex}$). Furthermore, the potential of $Ru_{13}@Pt_{42}$ as less expensive catalyst for ORR was predicted. However, the current knowledge of catalytic performance of $Ru_{13}@Pt_{42}$ and Pt_{55} for ORR and corresponding reaction mechanism is rather limited. In this work, the preferential sites on the Pt_{42} surface for interaction with oxygen species (O_2, OH, O, and OOH), as well as possible mechanism of O-O bond activation catalyzed by $Ru_{13}@Pt_{42}$ and Pt_{55} were studied using first-principle calculations.

All spin-polarized calculations were performed with the Vienna Ab initio Simulation Package (VASP). The PBE-D3 method was employed for geometry optimizations with an energy cutoff of 400 eV. The clusters were placed in a sufficiently large supercell (25 Å × 25 Å × 25 Å) to ensure enough separation by vacuum. The thresholds for energy and force were set to 0.0001 eV and 0.01 eV/Å, respectively. Reaction barrier was calculated using Nudged Elastic Band (NEB) method.

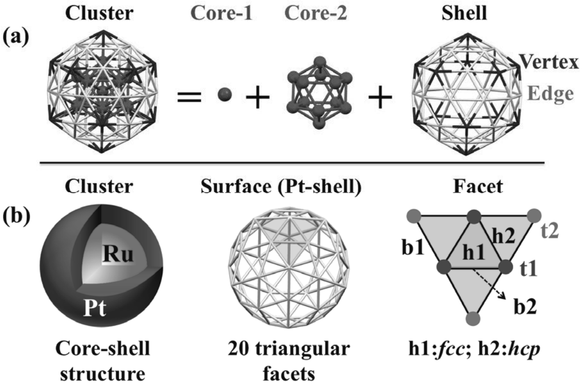

Scheme 1. (a) Models of 55-atom icosahedron-like cluster (green: core-1; red: core-2; blue: vertex; grey: edge). (b) Binding sites of icosahedron-like Pt_{42} shell.

Binding sites. As shown in Scheme 1, there are 20 triangular facets on the Pt_{42} surface of icosahedron-like 55-atom cluster. On each facet, there are three types of binding sites: top (t), bridge (b), and hollow (h) sites. The binding site notations are illustrated as follows:

- Top site: adsorbate binds with one Pt atom at the edge or vertex position, denoted as t1 or t2.
- Bridge site: adsorbate binds with two adjacent Pt atoms at the edge and vertex positions, or at both edge positions, denoted as b1 or b2.
- Hollow site: *fcc*-like position between three Pt atoms at the edge positions, denoted as h1; *hcp*-like position between both Pt atoms at the edge positions and one Pt atom at the vertex position, denoted as h2.

Binding energy (E_b) is defined as the energy difference between the species adsorbed on the catalyst and the sum of the catalyst and species. The more negative E_b value indicates the stronger binding ability.

O_2 binding. The binding energy (E_b) for O_2 adsorption at different sites is listed in Table 1. In the case of Pt_{55} and $Ru_{13}@Pt_{42}$, $E_b(O_2)$ value decreases in the order of h1–η^1 > t1-η^1 > t2-η^1 > b2-η^2 > b1-η^2 and h1-η^1 > b2-η^2 > t1-η^1 > t2-η^1 > b1-η^2, respectively. The O_2 species are found to migrate from h2-η^1 to t2-η^1. The expression of "A/x" (A = adsorbate, x = binding site) represents that the adsorbate is located at the x site hereafter. Obviously, O_2 is preferentially adsorbed at the b1 site with η^2-side-on orientation (O_2/b1-η^2). The $E_b(O_2/\text{b1-}\eta^2)$ values are -1.70 eV and -0.95 eV for Pt_{55} and $Ru_{13}@Pt_{42}$, respectively. The most stable O_2/b1-η^2-binding species will be further discussed as the initial structure for the process of O-O bond activation, $O_2 \rightarrow O$.

Notably, $E_b(O_2)$ for $Ru_{13}@Pt_{42}$ is less negative than that for Pt_{55} at the same site, indicating that the O_2-binding ability of $Ru_{13}@Pt_{42}$ catalyst is weaker than that of Pt_{55}. These results suggest that the O_2 adsorption on the Pt_{42} surface is significantly influenced by the presence of Ru_{13} core. The reason for the stronger O_2 adsorption on the surface of Pt_{55} than $Ru_{13}@Pt_{42}$ will be elucidated in the latter section.

Table 1 Binding energies (E_b, in eV) for O_2 and OOH/x-binding species.

Site x	**Pt_{55}**	**$Ru_{13}@Pt_{42}$**	**Pt_{55}**	**$Ru_{13}@Pt_{42}$**
	O_2		**OOH**	
t1-η^1	-1.05 (11et)[a]	-0.37 (9et)	-4.18 (10et)	-3.57 (6et)
t2-η^1	-1.13 (13et)	-0.72 (7et)	**-4.30 (14et)**	**-3.98 (6et)**
h1–η^1	-0.25 (13et)	0.42 (7et)	-3.75 (14et)	-3.15 (8et)
h2–η^1	t2-η^1	t2-η^1	t2-η^1	t2-η^1
b1-η^2	**-1.70 (11et)**	**-0.95 (7et)**	-[b]	-3.89 (6et)
b2-η^2	-1.41 (11et)	-0.19 (9et)	t1-η^1	t1-η^1

[a] The most stable spin state is given in parentheses.

[b] OOH decomposes into O and OH at the top sites, where O is connected at t2 site and OH is connected at t1 site.

OOH-binding. The OOH-binding species is one of the important intermediates for ORR process. As listed in Table 1, the stability of OOH/x-binding species increases in the order of OOH/h1-η^1 < OOH/t1-η^1 < OOH/t2-η^1 for Pt_{55} and OOH/h1-η^2 < OOH/t1-η^1 < OOH/b1-η^1 < OOH/t2-η^1 for $Ru_{13}@Pt_{42}$, respectively. The adsorbed OOH at the h2 (b2) site could be easily converted to t2 (t1) site. For Pt_{55}, OOH-binding at the b1 site with η^2-side-on orientation is unstable. Spontaneously, OOH decomposes into O and OH, where O and OH are located at the t2 and t1 sites, respectively. Also we found that the OOH-binding with $Ru_{13}@Pt_{42}$ is weaker than that with Pt_{55} at the same adsorption site.

O-binding. Single O atom is preferentially adsorbed at the *fcc*-like h1 site with E_b(O/h1) of -5.01 eV and -4.41 eV for Pt_{55} and $Ru_{13}@Pt_{42}$, respectively, as listed in Table 2. For Pt_{55}, the E_b(O) decreases in the order of O/t1 > O/t2 > O/b1 > O/h2 > O/h1. The adsorbed O atom at the b2 site could easily slide off to *hcp*-like h2 site due to the minuscule activation barrier of the reaction pathway between b2 and h2 sites. For $Ru_{13}@Pt_{42}$, the E_b decreases in the following order: O/t1 > O/b1 > O/t2 > O/h2 > O/h1. The O atom migrates from b2 to h2 site, similar to the Pt_{55} case discussed above. The binding ability of single O at the same site on the surface of $Ru_{13}@Pt_{42}$ is found to be weaker than that of Pt_{55}.

OH-binding. For OH-binding, the ability increases in the order of OH/h1 < OH/t1 < OH/t2 ≈ OH/b1 for Pt_{55} and OH/h1 < OH/t1 < OH/b1 < OH/t2 for $Ru_{13}@Pt_{42}$, respectively. Both t2 and b1 sites are proved to be the preferred sites for Pt_{55} with E_b of -3.35 eV and -3.38 eV, respectively, while only t2 is the most favorable site for $Ru_{13}@Pt_{42}$ with E_b(OH/t2) of -3.06 eV, as listed in Table 2. Similarly, the ability to bind with OH species in the case of $Ru_{13}@Pt_{42}$ is weaker than that of Pt_{55}. The weak OH and O-binding are desirable because it is advantageous for H_2O desorption.

H-binding. In order to discuss the whole ORR mechanism, it is likely that H_{ad} is available as a reactant on the surface as discussed in previous results. As shown in Table 2, b1 is the preferred site with E_b(H/b1) of -3.07 eV for Pt_{55} and -2.70 eV for $Ru_{13}@Pt_{42}$, respectively. The H-binding ability increases in the orders of h1 ≈ t2 < t1 < h2 < b1 for Pt_{55} and t1 < t2 < h1 < h2 < b1 for $Ru_{13}@Pt_{42}$, respectively.

Table 2 Binding energies (E_b, in eV) for O, OH, and H/x-binding species.

Site x	**Pt_{55}**	**$Ru_{13}@Pt_{42}$**	**Pt_{55}**	**$Ru_{13}@Pt_{42}$**	**Pt_{55}**	**$Ru_{13}@Pt_{42}$**
	O [a]		**OH** [b]		**H** [c]	
t1	-4.14 (15et)	-3.30 (9et)	-3.19 (12et)	-2.59 (6et)	-2.95 (12et)	-2.45 (8et)
t2	-4.46 (15et)	-4.25 (7et)	**-3.35 (12et)**	**-3.06 (6et)**	-2.77 (14et)	-2.55 (6et)
h1	**-5.01 (11et)**	**-4.41 (7et)**	-2.94 (14et)	-2.35 (8et)	-2.76 (14et)	-2.60 (8et)
h2	-4.91 (11et)	-4.33 (7et)	t2	t2	-3.00 (12et)	-2.63 (8et)
b1	-4.84 (13et)	-4.22 (9et)	**-3.38 (10et)**	-2.86 (8et)	**-3.07 (12et)**	**-2.70 (8et)**

[a] O migrates from b2 to *hcp*-like h2. [b] OH migrates from b2 to *fcc*-like h1. [c] H migrates from b2 to *hcp*-like h2.

O_2 adsorption The band structure is one of important factors to explain the ability of O_2 adsorption. The calculated *d*-band center for $Ru_{13}@Pt_{42}$ (-2.18 eV) is lower than that for Pt_{55} (-2.02 eV), indicating the weaker O_2 binding for $Ru_{13}@Pt_{42}$ compared with Pt_{55}, with reference to the prediction of Hammer-Nørskov model. The density of states (DOS) analysis for Pt_{55}, $Ru_{13}@Pt_{42}$ and corresponding O_2/(b1-η^2)-binding species was shown in Figure 1. *d*-DOS of Pt_{42} shell makes a large contribution to the total *d*-DOS for Pt_{55}, $Ru_{13}@Pt_{42}$, and their corresponding O_2/(b1-η^2)-binding species. O_2 binding decreases the DOS of band-top near the Fermi level, suggesting that the CT occurs from Pt_{55} ($Ru_{13}@Pt_{42}$) to O_2 fragments.

O-O bond activation. The O-O bond activation (cleavage) can occur via two mechanisms: one is direct O-O bond cleavage of O_2 ($O_2 \rightarrow 2O$), and the other is OOH formation followed by O-OH cleavage

(O_2+H→OOH→OH+O). Direct O-O bond cleavage of O_2 is difficult to occur with the activation barrier of 0.49 eV and 0.33 eV in gas phase for Ru_{13}@Pt_{42} and Pt_{55}, respectively. However, the O-OH bond cleavage of OOH occurs with lower activation barriers of 0.18 eV and 0.12 eV for Ru_{13}@Pt_{42} and Pt_{55}, respectively.

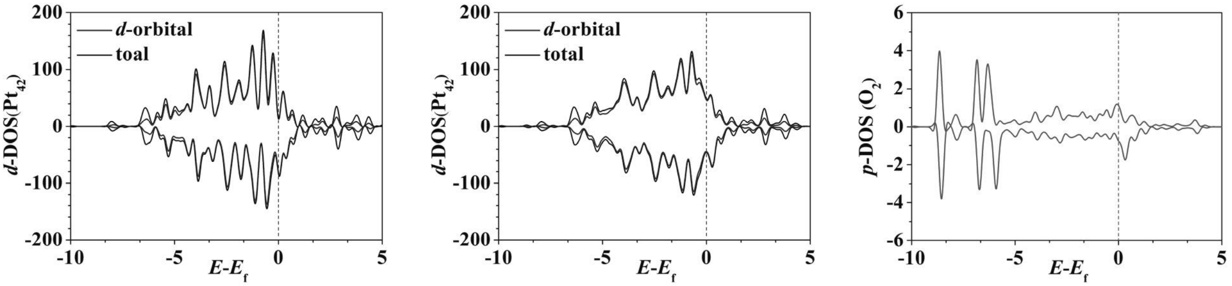

Pt_{55} **Pt_{55}-O_2/b1-η^2**

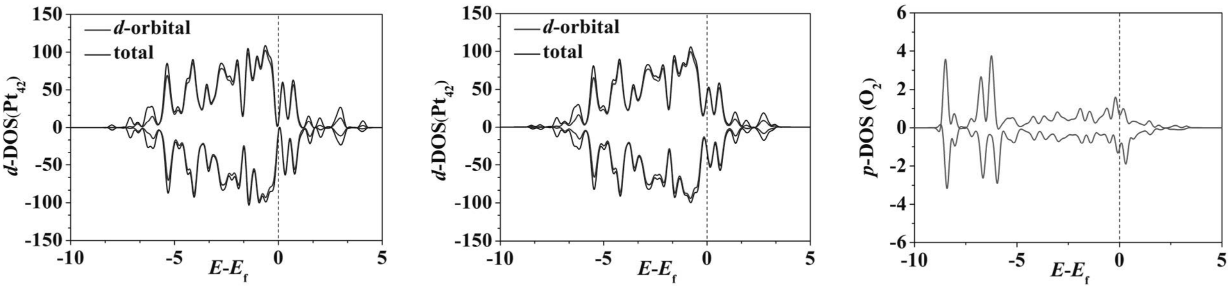

Ru_{13}@Pt_{42} **Ru_{13}@Pt_{42}-O_2/b1-η^2**

Figure 1 Density of states for Pt_{55}, Ru_{13}@Pt_{42}, and their corresponding O_2/(b1-η^2)-binding species.

These results reveal that Ru_{13}@Pt_{42} is capable of activating O_2 molecule but does not bind with oxygen species too strongly, which leads to facile and rapid H_2O desorption. In addition, the O-OH bond cleavage in the case of Ru_{13}@Pt_{42} occurs easier than that of Pt_{55}. Such characteristic behaviors of Ru_{13}@Pt_{42} could render it potentiality as a promising heterogeneous catalyst for ORR like Pt_{55}.

2. Original papers

(1) Jing LU, Kazuya ISHIMURA, and Shigeyoshi SAKAKI,
"Theoretical Insight into Core–Shell Preference for Bimetallic Pt-M (M = Ru, Rh, Os, and Ir) Cluster and Its Electronic Structure."
J. Phys. Chem. C 122 (16), 9081-9090 (2018).

3. Presentation at academic conferences

(1) Jing LU, Kazuya ISHIMURA, and Shigeyoshi SAKAKI,
"Understanding segregation behavior and electronic structures in 38, 55 and 147-atom bimetallic Pt-Tc and Pt-Re nanoclusters: a first-principles study"
The 11th Annual Meeting of the Japan Society for Molecular Science (2P107), Sendai, September 15–18, 2017

Rong-Lin Zhong

Research Fellow

1. Summary of the research of the year

How to Perform Suzuki-Miyaura Reaction of Nitroarene or Nitration of Bromoarene Using Pd^0(Phosphine) Complex: Theoretical Insight and Prediction

The Pd-catalyzed Suzuki-Miyaura reaction is one of the most efficient and versatile methods for constructing carbon-carbon bond. Aryl halides are employed as electrophilic coupling reagent in this reaction. To broaden its application scope, a lot of efforts have been made to use alternative compounds such as aryl ethers, aryl esters, and arenols. However, the use of nitroarenes has not been succeeded for a long time despite of weak Ar-NO_2 (Ar = aryl) bond. Notably, the Suzuki-Miyaura reaction of nitroarenes was very recently succeeded by us using Pd^0(BrettPhos) as a catalyst, as shown in Scheme 1. Usual monodentate phosphine could not be used in this reaction. On the other hand, Fors and Buchwald succeeded Pd-catalyzed nitration of aryl halides using a similar Pd^0(^{t}Bu-BrettPhos) as a catalyst. In this reaction, the last step should be reductive elimination of Ar-NO_2 bond from Pd^{II}(Ar)(NO_2)(^{t}Bu-BrettPhos). This is reverse to the oxidative addition of Ar-NO_2 which is the first step of the Suzuki-Miyaura reaction. Considering these two reports by Buchwald group and us, we address following points; (1) why the Ar-NO_2 bond cleavage is more difficult than the Ar-Br bond cleavage, (2) why usual monodentate phosphine could not be used for the Suzuki-Miyaura reaction of nitroarenes but BrettPhos could be, (3) why Brettphos was used for the Suzuki-Miyaura reaction of nitroarenes but the similar ^{t}Bu-BrettPhos was used for the nitration of aryl halides despite of tiny difference between these two phosphines. We theoretically investigated the oxidative addition of nitroarene to Pd^0(BrettPhos) to elucidate characteristic features of the oxidative addition of nitroarenes and to provide clear answers to the above-mentioned questions.

Scheme 1. The Suzuki-Miyaura reaction of nitroarenes and nitration of aryl halides.

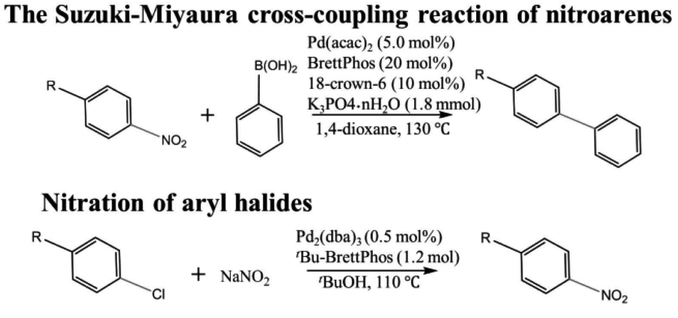

BrettPhos, PMe_3, R-BrettPhos (R = ^{t}Bu, Me, CF_3, C_6F_5, *o*-tol, and 2,6-dimethylphenyl), XPhos, and BrettPhos-NMe_2 were investigated as ligand. The molecular structures of these ligands are shown in Scheme 2. As nitroarene, 4-nitroanisole (Rea) was employed for calculations because this compound was used as a typical reagent in the experiment of the Suzuki-Miyaura reaction.

Scheme 2. Molecular structures of BrettPhos and R-BrettPhos (R = ^{t}Bu, Me, CF_3, C_6F_5, *o*-tol, and 2,6-dimethylphenyl), XPhos, and BrettPhos-NMe_2.

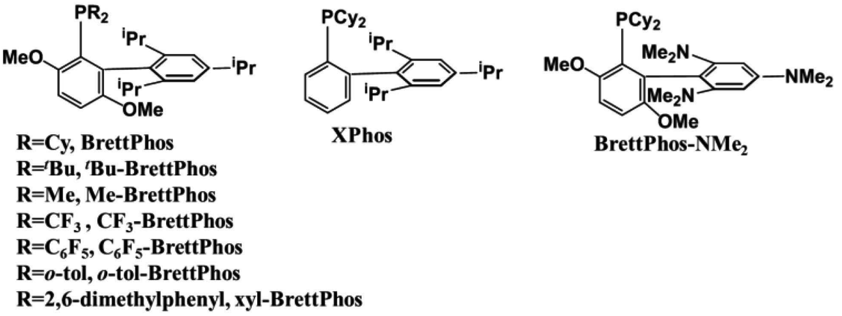

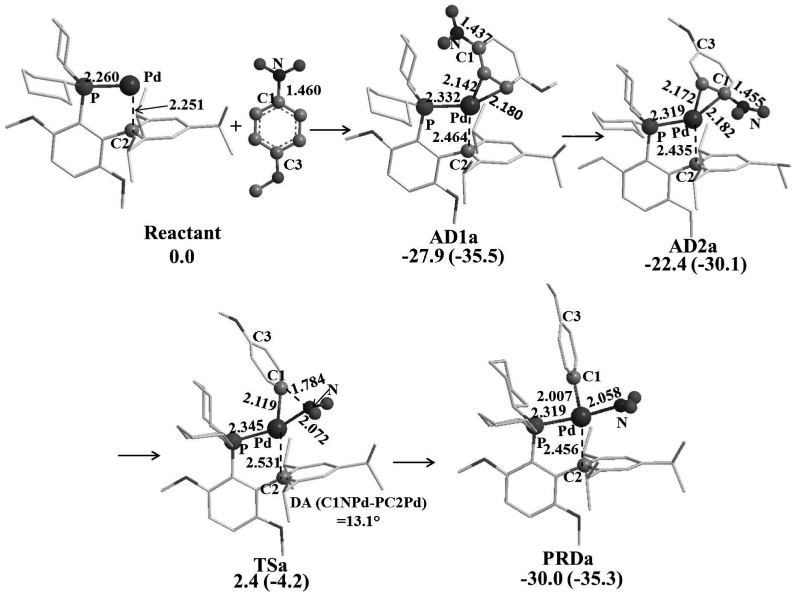

Figure 1. Optimized geometries in oxidative addition of 4-nitroanisole to Pd^0(BrettPhos) complex.

Results and Discussion

Oxidative Addition of 4-nitroanisole (Rea) and its Bromo derivative to Pd^0(BrettPhos) and $Pd^0(PMe_3)_2$.

The geometry and energy change of oxidative addition of **Rea** to Pd^0(BrettPhos) **1** is shown in Figure 1. **Rea** approaches **1** to form stable η^2-coordinated adducts, **AD1a#1** and **AD1a#2**, in which the C^2-C^3 and C^1-C^2 bonds coordinate with the Pd, respectively. The oxidative addition occurs through a three-membered transition state **TS1a** to afford a palladium(II) complex $Pd^{II}(NO_2)(C_6H_4\text{-}OMe^p)$(Brettphos) (**PRD1a**). The Gibbs activation energy ($\Delta G^{\circ\ddagger}$) is 30.3 kcal mol^{-1} and the Gibbs reaction energy ($\Delta G^{\circ}_{(R)}$) is -2.1 kcal mol^{-1} relative to the most stable reactant adduct **AD1a#1**. This oxidative addition needs rather large activation energy but it is exergonic.

Oxidative addition of 4-bromoanisole (**Reb**) to **1** occurs through similar η^2-coordinated adducts and transition state to afford a palladium(II) complex $Pd^{II}(Br)(C_6H_4OMe^p)$(Brettphos). The

$\Delta G^{o\ddagger}$ (16.3 kcal mol^{-1}) is much smaller and the $\Delta G^{o}{}_{(R)}$ (-15.0 kcal mol^{-1}) is much more negative than those of the oxidative addition of **Rea**. Therefore, the oxidative addition of nitroarene is much more difficult than that of bromoarene kinetically and thermodynamically. To investigate the difference in $\Delta G^{o\ddagger}$ between these two oxidative additions, we separated the reaction system into Pd^{0}(BrettPhos) and substrate moieties, as shown in Scheme 3, and made deformation/interaction energy analysis. As shown in Table 1, the potential energy barrier (E_a) is much larger for **TS1a** than for **TS1b**, indicating that the analysis of E_a provides the reason why the oxidative addition of **Rea** is more difficult than that of **Reb**. In **TS1a**, the deformation energy (E_{Def} = 33.2 kcal mol^{-1}) of **Rea** is much larger than that (6.2 kcal mol^{-1}) of **Reb** in **TS1b**. Interaction energy E_{Int} is defined as a stabilization energy provided by the interaction between reagent (**Rea** or **Reb**) and Pd^{0} complex, where both have deformed geometries like in TS. The E_{Int} (-42.1 kcal mol^{-1}) between **Rea** and Pd^{0}(BrettPhos) in **TS1a** is much larger than that (-24.6 kcal mol^{-1}) in **TS1b** by 17.5 kcal mol^{-1}, where a negative value means the stabilization energy. However, this large E_{Int} of **TS1a** cannot overcome the overly large E_{Def} of **Rea** at **TS1a**. As a result, **TS1a** becomes higher in energy than **TS1b**. These results lead to a conclusion that the large E_{Def} of **Rea** is the origin of larger E_a and larger $\Delta G^{o\ddagger}$ for Ar-NO_2 bond cleavage than those for Ar-Br bond cleavage. In **TS1a**, the NO_2 group changes its direction toward the Pd because the sp^{2} orbital of NO_2 must change its direction to form a bonding interaction with the Pd, which gives rise to the large E_{Def} value of **Rea**. On the other hand, Br has a spherical valence orbital which can start to form the bonding interaction with the Pd, keeping the Ar-Br bonding interaction. Therefore, **Reb** can reach **TS1b** without significant distortion. This is the reason why bromoarene is more reactive for the oxidative addition than nitroarene.

Scheme 3. Definition of fragments a and b in TS1a (R=NO_2), TS1b (R=Br), and TS3a.

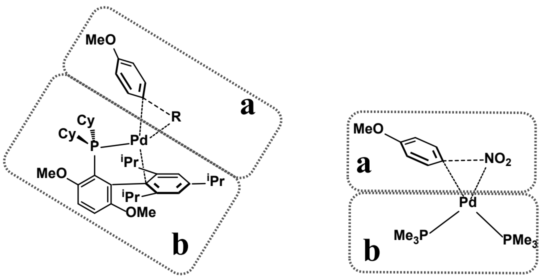

TS1a/TS1b **TS3a**

Table 1. Activation barrier (E_a), deformation energy (E_{Def}) of each moiety and interaction energy (E_{int}) between them in transition state (in kcal mol^{-1}).

	TS1a	TS1b	TS2a	TS3a
ΔE	-4.2	-14.1	-2.4	15.9
E_a	31.3	16.9	30.1	30.2
$E_{Def\text{-}a}$	33.2	6.2	33.0	35.5
$E_{Def\text{-}b}$	4.7	4.3	5.4	19.9

Oxidative addition of **Rea** to $Pd^0(PMe_3)_2$ **3** was investigated for making comparison between BrettPhos and usual monodentate phosphine PMe_3. This reaction occurs with $\Delta G^{\circ\ddagger}$ of 29.1 kcal mol^{-1}. Though this value does not differ very much from that of the reaction with **1**, its transition state **TS3a** is at much higher energy than the sum of reactants, **3** + **Rea**, indicating that **Rea** more easily dissociates from **3** than it completes the oxidative addition via **TS3a**. Thus, it is concluded that the oxidative addition of **Rea** to **3** does not occur.

The deformation/interaction energy analysis clearly shows that the higher energy transition state **TS3a** arises from the larger E_{Def} value (19.0 kcal mol^{-1}) of $Pd^0(PMe_3)_2$ in **TS3a** (Table 1). The large $E_{\text{Def-a}}$ value arises from significantly small P-Pd-P angle in **TS3a** (Figure 1). It is of importance to elucidate the reason why such large distortion is needed in **TS3a**. In the oxidative addition, CT from metal moiety to substrate is important. In **TS1a**, charge-transfer (CT) occurs from the HOMO of Pd ($\phi_{\text{Pd-HOMO}}$) to the LUMO and LUMO+1 of **Rea**, as shown in Figure 2. The $\phi_{\text{Pd-HOMO}}$ at high energy can form large CT. As shown in Figure 3(a), the $\phi_{\text{Pd-HOMO}}$ of $Pd^0(PMe_3)_2$ in equilibrium geometry is calculated at much lower energy (-7.81 eV) than that (-5.82 eV) of Pd^0(BrettPhos). To raise the $\phi_{\text{Pd-HOMO}}$ energy, $Pd^0(PMe_3)_2$ must be distorted by decreasing the P-Pd-P angle; as shown in Figure 3(a), the $\phi_{\text{Pd-HOMO}}$ energy certainly becomes higher (-5.73 eV) in the distorted geometry of **TS3a**.

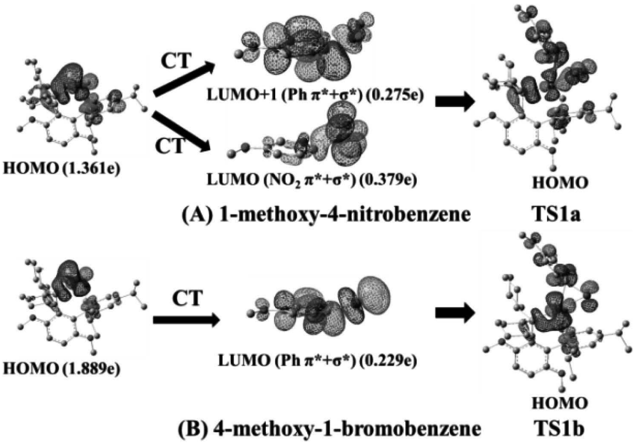

Figure 2. Orbital interactions in the transition state of the oxidative addition of 4-nitroanisole (a) and 4-bromoanisole (b) to Pd^0(BrettPhos).

On the other hand, Pd^0(BrettPhos) is distorted little at **TS1a**. The reason can be easily found by seeing Figure 3(b). In the case of BrettPhos, the lone pair orbital on the P atom and the π orbital on the phenyl group overlap with the Pd d_π orbital in an antibonding way to afford the $\phi_{\text{Pd-HOMO}}$ of **1**. As a result, the $\phi_{\text{Pd-HOMO}}$ orbital energy is -5.82 eV in Pd^0(BrettPhos) even with equilibrium geometry. It indicates that the 2,4,6-tris-isopropylphenyl group plays crucially important role to raise the d_π orbital energy like usual chelating diphosphine. It is concluded that the oxidative addition of $Ar\text{-}NO_2$ to $Pd^0(PR_3)_2$ is difficult because the transition state suffers from two large deformation energies of $Ar\text{-}NO_2$ and $Pd^0(PR_3)_2$ moieties. On the other hand, Pd^0(Brettphos) is reactive for the oxidative addition of $Ar\text{-}NO_2$ because the d_π orbital is at high energy even without distortion of

Pd^0(Brettphos) and the transition state suffers from only one deformation energy of the Ar-NO_2 moiety. This means that the presence of 2,4,6-tris-isopropylphenyl group is crucially important in BrettPhos because its π orbital interacts with the Pd d_π orbital to raise the $\phi_{\text{Pd-HOMO}}$ energy (Figure 3b). It is a strong point of BrettPhos-type ligand for the oxidative addition that both of phosphine lone pair and π orbital of 2,4,6-tris-isopropylpheny participate in raising the $\phi_{\text{Pd-HOMO}}$ energy.

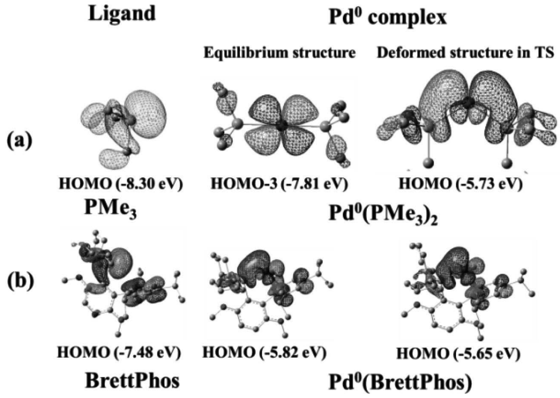

Figure 3. HOMOs of PPh_3, BrettPhos, and their Pd^0 complexes with deformed structure in TS.

Comparison between Pd^0(BrettPhos) and Pd^0(^{t}Bu-BrettPhos). Oxidative addition of **Rea** to Pd^0(^{t}Bu-BrettPhos) **2** occurs through similar geometry changes. The $\Delta G^{o\ddagger}$ value (28.3 kcal mol^{-1}) is moderately smaller than that to **1** but the $\Delta G^{o}_{(R)}$ is positive (5.8 kcal mol^{-1}), indicating that the oxidative addition of Ar-NO_2 bond to **2** is endergonic. This means that **2** can be applied to the reductive elimination of nitroarenes, which is consitent with the fact that the nitration of aryl halides was succeeded with **2**, as was reported by Fors and Buchwald. As shown in Table 2, the deformation energy in **TS2a** differs little from that in **TS1a** but the interaction energy is moderately less negative than in **TS1a**. As results, **TS2a** is moderately less stable than **TS1a**. These results suggest that not the electronic factor but the steric factor is responsible for the positive $\Delta G^{o}_{(R)}$ of the oxidative addition of **Rea** to Pd^0(^{t}Bu-BrettPhos). In **PRD2a**, the $P(^tBu)_2$ moiety of ^{t}Bu-BrettPhos takes the cis-position to the $C_6H_4OMe^p$ group to induce the steric repulsion, whereas such steric repulsion is small in **TS2a** because the $C_6H_4OMe^p$ group is distant from ^{t}Bu-BrettPhos. The larger steric repulsion of ^{t}Bu-BrettPhos is supported by the longer Pd-P bond length (2.393 Å) in **PRD2a** than in **PRD1a** (2.319 Å) and the larger P-Pd-($C_6H_4OMe^p$) angle (99°) in **PRD2a** than in **PRD1a** (90°). The larger cone angle of $P(^tBu_3)_3$ than that of PCy_3 is also one evidence that $P(^tBu)_2$ group of ^{t}Bu-BrettPhos is more bulky than PCy_2 group of BrettPhos. Because the steric effect of the ^{t}Bu group is larger than that of the Cy group, the ^{t}Bu-Brettphos gives rise to the larger steric repulsion with the $C_6H_4OMe^p$ group to destabilize **PRD2a** compared to **PRD1a**. It should be concluded that Pd^0(^{t}Bu-BrettPhos) is advantageous for the reductive elimination of Ar-NO_2 because of the large steric repulsion of ^{t}Bu-Brettphos with the $C_6H_4OMe^p$ group.

2. Original papers

(1) M. Ramu Yadav, Masahiro Nagaoka, Myuto Kashihara, **Rong-Lin Zhong**, Takanori Miyazaki

Shigeyoshi Sakaki, and Yoshiaki Nakao, “The Suzuki–Miyaura Coupling of Nitroarenes”，J. Am. Chem. Soc., 139 (28), 9423–9426 (2017).

(2) Feng-Wei Gao, **Rong-Lin Zhong**, Hong-Liang Xu, and Zhong-Min Su, “Intra- and Intermolecular Charge Transfer in a Novel Dimer: Cooperatively Enhancing Second-Order Optical Nonlinearity”，J. Phys. Chem. C, 121 (45), 25472–25478 (2017).

3. Presentation at academic conferences

(1) **Rong-Lin Zhong**, Masahiro Nagaoka, Yoshiaki Nakao, and Shigeyoshi Sakaki, “New Oxidative Addition of Nitrobenzene to Palladium(0) Complex: Characteristic Features in Electronic Process”, 20th Annual Meeting of Theoretical Chemistry Society, Kyoto, May 16-18, 2017.

(2) **Rong-Lin Zhong**, Masahiro Nagaoka, Yoshiaki Nakao, Shigeyoshi Sakaki “Oxidative Addition of Nitrobenzene to Palladium(0) Complex: Theoretical Analysis of Unexpected Ligand Effect”, 11th Annual Meeting of Japan Society for Molecular Science, Sendai, Sep.15-18, 2017.

松岡　貴英

研究フェロー

1. 今年度の研究の要約

水分子の自動イオン化の背景にある非断熱電子動力学

近年の高強度レーザーの発展により，アト秒スケールの電子ダイナミックスの観測が可能となり，汎用性のある理論計算手法の確立が求められている．強光子場中の分子系は Highorder Harmonic Generation 機構と Above Threshold Ionization を考慮するために外場と電子，電子と核，電子間の動的相互作用を同等に扱ってイオン化過程を記述する必要がある．我々は，非断熱電子動力学計算手法[1]にイオン化過程を記述する方法[2]を盛り込み，強光子場中の H_2 と H_2O 分子のイオン化過程における非断熱相互作用の影響を明らかにした[3]．強光子場中の高励起状態の光電子スペクトルは Auger 過程によって複雑化するが，2s を空孔とした H_2O^+を具体例に電子動力学を追跡し，その過程における Auger 効果を調べた．

非断熱電子動力学計算では電子基底Φ_Iで展開した電子波束$\Psi(t) = \sum_I C_I(t)\Phi_I$の係数についての coupled equation に従って時間発展する[1]．

$$\mathrm{i}\hbar\partial_t C_I = \sum_J \left[\mathcal{H}_{IJ}^{(\mathrm{el})} - \mathrm{i}\hbar\sum_k^{3N_\mathrm{n}}\left(\dot{R}_k - \frac{Z_k e}{c}A_k\right)X_{IJ}^k - \frac{\hbar^2}{4}\sum_k^{3N_\mathrm{n}}\left(Y_{IJ}^k + Y_{IJ}^{k*}\right)\right]C_J$$

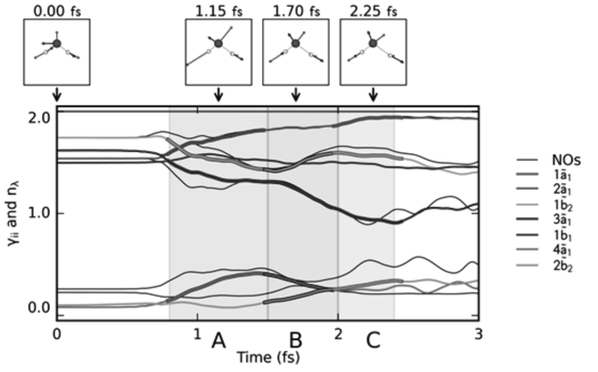

Figure 1. HF 基底密度行列の対角成分（色付き太線）と自然軌道の電子占有数（黒の実線）．

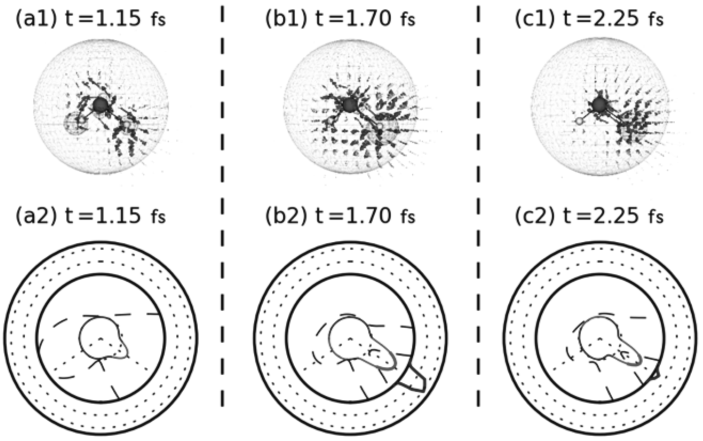

Figure 2. 各時刻における電子 flux．（a1-c1）境界面における flux.（a2-c2）境界面のノルム方向の flux．点線は OH 結合方向.

$\mathcal{H}^{(\mathrm{el})}$, X_k, Y_kはそれぞれ電子 Hamiltonian と１次と２次の kinetic coupling $X_{IJ} = \langle \Phi_I | \partial_k \Phi_J \rangle$, $Y_{IJ} = \langle \Phi_I | \partial_k^2 \Phi_J \rangle$である．本計算では complex natural orbitals (CNO)によるイオン化過程の記述の試み[2]のため，各時刻における CNO を一電子軌道とした配置関数を基底とし，電子占有数が大きい CNO を被占軌道とした参照配置空間を用いた．H_2O^+の $2a_1$軌道(O(2s))を空孔とした断熱電子状態を t = 0 における電子状態とし，核は反対称伸縮モードを初期運動とした．初期の電子状態が単一断熱電子状態であるから，核には全対称の力が働く．図 1 の各 CNO の電子占有数n_λは 0.8 fs から 1.5 fs に至るまでに，$2\tilde{a}_1$(O[2s])と$4\tilde{a}_1$が上昇し，$1\tilde{b}_2$(O[2p$_x$])と$3\tilde{a}_1$ (O[2p$_z$])が減少している．ここで，各時刻における HF 軌道は初期の HF 軌道との連続性を考慮した上でその既約表現にチルダを付している．反対称伸縮方向の核の運動によって$1\tilde{b}_2 \rightarrow 2\tilde{a}_1$への失活と$3\tilde{a}_1 \rightarrow 4\tilde{a}_1$への励起が誘起される(Process A)．1.5 fs から 2.0 fs においては， 全対称の核の運動によって$3\tilde{a}_1 \rightarrow 1\tilde{b}_2$への失活と$4\tilde{a}_1 \rightarrow 2\tilde{b}_2$への励起が誘起される(Process B)．2.0 fs から 2.4 fs では，$1\tilde{b}_2 \rightarrow 2\tilde{a}_1$の失活と$3\tilde{a}_1 \rightarrow 2\tilde{b}_2$の励起が全対称の核の運動によって誘起される(Process C)．初期の電子状態の主配置から Process B が起こり難いことから，Process A と B は連続して誘起され，Process A が生じなかった重ね合わせ状態に Process C が誘起されると言える．Process B と C は全対称の核の運動によって誘起され，この時刻において電子 flux は OH 結合方向へ強く見られることが分かった（図 2）．H_2O の 2 電子イオン化過程のうち直接イオン化と自動イオン化の 2 段階過程では自動イオン化電子は OH 結合方向に分布する[4]．本計算結果は，2 段階イオン化過程における自動イオン化電子の分布と一致し，その自動イオン化過程は反対称伸縮振動モードによって誘起されることを示す.

[1] K. Takatsuka, T. Yonehara, K. Hanasaki and Y. Arasaki, “Chemical Theory Beyond the Born-Oppenheimer Paradigm: Nonadiabatic Electronic and Nuclear Dynamics in Chemical Reactions.” (World Scientific, 2014).
[2] K. Takatsuka, J. Phys. B: At. Mol. Opt. Phys. 47, 124038 (2014).
[3] T. Matsuoka and K. Takatsuka, J. Chem. Phys. 146, 134114 (2017).
[4] H. Sann, et al., Phys. Rev. Lett. 106, 133001 (2011).

高強度レーザー中の非断熱電子波束の対称性の破れ

断熱状態が密集する高励起状態において核と外場の非断熱相互作用が電子波束の対称性

へ及ぼす影響に着目し，電子波束の対称性の破れがいかに観測されるかに着目した．

Semiclassical Ehrenfest theory では核は force matrix の期待値の，path-branching 法では force matrix の固有値の運動方程式に従う．

$$F_{IJ}^{k} = -\partial_k \mathcal{H}_{IJ}^{(\mathrm{el})} - \sum_{K}^{N_H} \left(X_{IK}^{k}\mathcal{H}_{KJ}^{(\mathrm{el})} - \mathcal{H}_{IK}^{(\mathrm{el})} X_{KJ}^{k} \right) + \mathrm{i}\hbar \sum_{l}^{3N_n} \dot{R}_l \left(\partial_k X_{IJ}^{l} - \partial_l X_{IJ}^{k} \right)$$
$$+ \left[-\frac{Z_k e}{c}\partial_t A_k + \frac{e}{c}\sum_{l}^{3N_n} \dot{R}_l \left(Z_l \partial_k A_l - Z_k \partial_l A_k\right) \right] \delta_{IJ}.$$

第 3 項の Lorentz-like force が核の速度と垂直に見かけ上の力として働き，対称性の破れを誘起する[2].特に path へ分岐する際には結合方程式と運動方向の force matrix$\sum_k F_{IJ}^{k} \dot{R}_k$ の交差項がゼロであることが要請され，結合方程式の固有状態個々の force 期待値から Lorentz-like force の働き方を調べることができる．特に縮重している状態は断熱状態の円錐交差と同様に$\boldsymbol{g}-\boldsymbol{h}$平面を定義できる．

$$g^{k} = \frac{1}{2}\left(\sum_{IJ}^{N_H} C_I^{(1)*} F_{IJ}^{k} C_J^{(1)} - \sum_{IJ}^{N_H} C_I^{(2)*} F_{IJ}^{k} C_J^{(2)} \right), \quad \forall k \in [1,3N_n],$$
$$h^{k} = \sum_{IJ}^{N_H} C_I^{(1)*} F_{IJ}^{k} C_J^{(2)}, \quad \forall k \in [1,3N_n].$$

核が seam に沿って運動している場合に$\boldsymbol{g}$と$\boldsymbol{h}$は任意に入れ替えることが可能で対称性が破れる方向を$\boldsymbol{g}$に選ぶことが可能である．

基底状態の H_2O に波長$\lambda = 800$ nm 強度$I = 225$ TW/cm^2 の 3-cycle パルスを照射した系を計算した．レーザーの分極方向は C_2 軸に，核の初期運動は対称伸縮振動モード方向に設定した．外場によって電子波束は多くの状態へ広く分布し，レーザーのピーク ($t = 5$ fs)において 550 eV 程度離れた状態へも分布を示す(図 3a). これは電子と親イオンの再衝突による内殻空孔状態への励起を示している.図 4 の HF 軌道基底の一電子密度行列の $1a_1$ 軌道対角成分はレーザーピークにおいて減少する.各状態に働く力は変角振動モード成分(図 3b)と対称伸縮振動(図 3c)モード成分が主であるが，レーザーピーク近傍以降は，反対称伸縮振動モード成分が非ゼロである状態が出現する(図 3d). Lorentz-like force によ

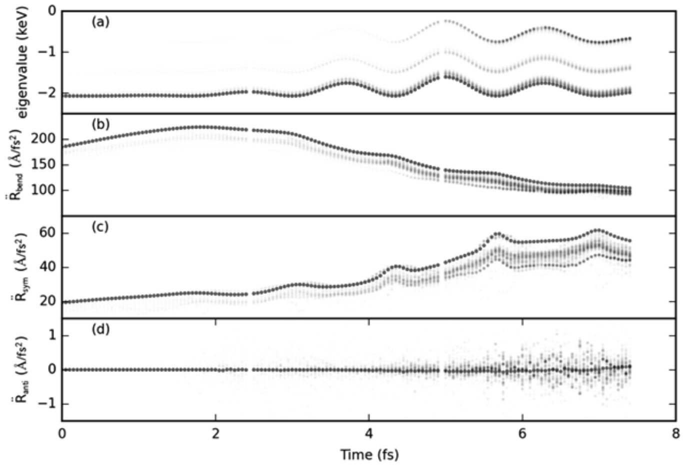

Figure 3. (a)結合方程式の固有値. 各固有状態の(b)変角振動モードと(c)対象伸縮振動モードと(d)反対称伸縮振動モード方向の加速度．濃淡は各固有状態と電子波束の重なりの大きさを表す．

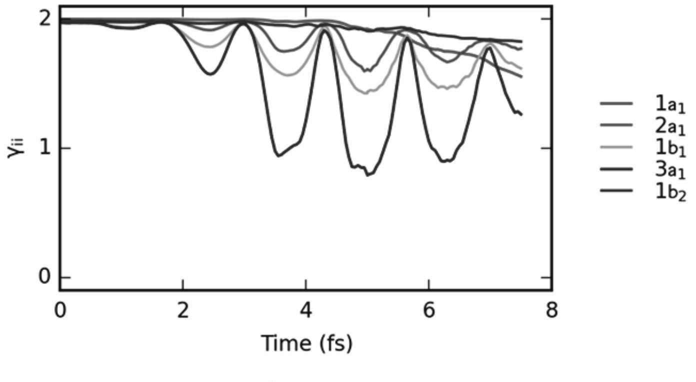

Figure 4. HF 軌道基底の密度行列成分.

る見かけ上の力は相殺するように対称性が破れる方向に働くことがわかる．これは密集する多くの状態に波束が分布し，それらの状態の Lorentz-like force が反対称伸縮振動モード方向の力としてあらわれていることによる．

[1] T. Matsuoka and K. Takatsuka, J. Chem. Phys. 146, 134114 (2017).

[2] K. Takatsuka, J. Chem. Phys. 146, 084312 (2017).

2. Original papers

(1) Takahide Matsuoka, and Kazuo Takatsuka,
“Nonadiabatic electron wavepacket dynamics behind molecular autoionization”
J. Chem. Phys. 148, 014106 (2018).

3. Presentation at academic conferences

(1) 松岡貴英・高塚和夫
「水分子のイオン化の背景にある非断熱電子動力学：Auger 電子と高強度レーザーによる光電子について」
第 20 回理論化学討論会 新宿 2017/5/17 2L14

(2) Takahide Matsuoka, and Kazuo Takatsuka,
“Auger Decay Process in Water Molecule: A Nonadiabatic Electron Dynamics Treatment”
2nd International Symposium on Attosecond Science (P4), Wako, Aug. 26, 2017

(3) 松岡貴英・高塚和夫
「高強度レーザー中の非断熱電子波束の対称性の破れについて」
第 11 回分子科学討論会 2017 仙台 2017/9/17 3A05

山本　憲太郎

研究フェロー（高塚グループ）

１．今年度の研究の要約

今年度は，Mn を含む触媒系における非断熱動力学的な電荷分離の基底状態の機構の理論的研究を行った．

【序】生化学的にはしばしば，生物系における電子伝達はいくつかの分子を基底状態で逐次的に経由すると理解されている．たとえば天然光合成系の photosystem II（PSII）における水分解では，P680 ←tyrosine Z←Mn cluster←水の順に電子が移動するとされている．しかしながら，量子力学的には，このような逐次的な電子移動の機構は自明ではない．そこで本研究では，生物系から着想を得た単純な系に対する非断熱の電子波束動力学の解析から，このような逐次的な電子移動の機構を提案した．

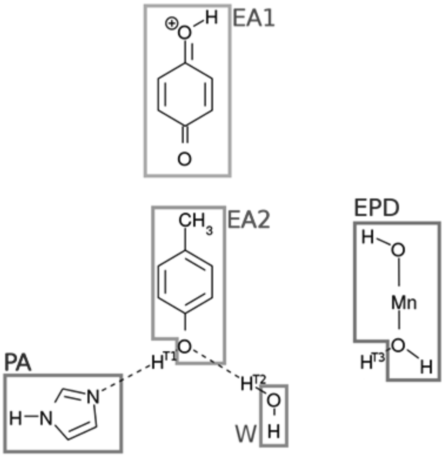

Fig. 1. Bio-inspired model system.

【方法】 Fig. 1 に示すような，PSII の tyrosine Z（Y_Z）から着想を得た単純な model system を考える．EA1 = electron acceptor 1（semiquinone cation），EA2 = electron acceptor 2（4-methylphenol），PA = proton acceptor（imidazole），W = water（OH），そして EPD = electron-proton donor（$Mn(OH)OH_2$）からなる．System 全体として cation であり，初期状態では，charge は EA1 上に局在する．PSII の Y_Z 周辺における逐次的な電子移動（P680 ← Y_Z ← Mn cluster）は，本研究の system では EA1 ← EA2 ← EPD のそれに相当する．動力学計算は，path-branching representation に基づく.[1] この理論では，量子的な電子波束が，原子核の経路に沿って時間発展する．この方法では，原子核と電子の動的なカップリングを，あらわに考慮する．事前の静的な解析に基づいて，EA1←EA2 の electron transfer が起こる直前を初期構造とする．

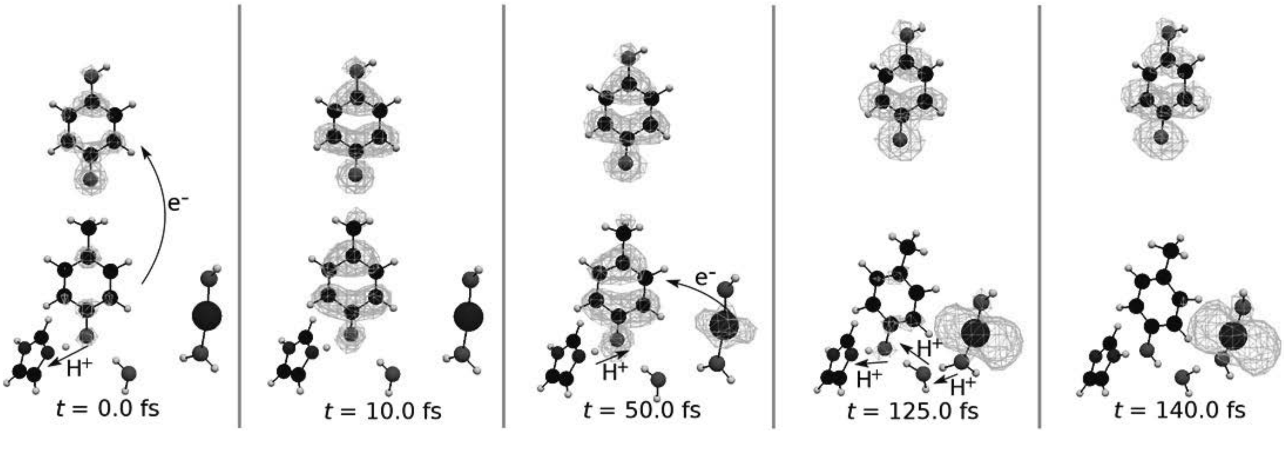

Fig. 2. Selected snapshots of the unpaired electron density along the path of electron-wavepacket dynamics.

その後，EA1 が離脱しつつ，EPD が EA2 および W に衝突するように初期運動量を与える．初期の電子波束は，断熱基底状態とする．

【結論】 Fig. 2 に示すある典型的な path に沿った unpaired electron density の空間分布の時間変化のスナップショットを用いて，proton と electron の dynamics を概観する．最初の約 10 fs の間に，PA ← EA2 の proton transfer に伴って，EA1 ← EA2 の electron transfer が起こる．これに伴って，EA1 と EA2 上に，biradical state が生じる．このとき，EA1 ← EPD の proton および electron transfer は，ほとんど見られない．これは単純に，EA1 と EPD の距離が離れているためだと考えられる．その後，EPD が W および EA2 に接近する．このとき，EA1 は徐々に離脱する．この間，電子状態に重要な変化はない．そして t = 50 fs 付近で，EA2←EPD の electron transfer だけが起こり，同じ donor-acceptor 間での proton transfer は起こらない．ただし，ほぼ同じタイミングで EA2←PA の proton transfer が起こっており，これが electron transfer と couple しているように見える．最後に，t = 125 fs 付近の H^{T1}-H^{T2}-H^{T3} が関与する PA←EA2←W←EPD の proton relay-transfer が起こる．以上の proton-electron coupled dynamics の結果として，実効的に，PA←EPD の proton transfer, EA1←EPD の electron transfer がなされる．Electron-wavepacket は全体を通して，ground state が支配的である．これは生化学的な描像と一致する．しかしながら，主に proton の運動と couple して，電子状態の性質が変化する．したがって，この場合の逐次的な電子移動は，proton transfer に伴って非断熱領域を断熱的に通過することに対応する．よって，分子構造の変化に伴う複数の電子状態の変化をあらわに考慮しなければ，この電子移動の機構は理解できない．

本研究は，生物学的な電子移動のさらなる理解のためには，静的な情報だけではなく，それぞれの donor-acceptor pair の運動と，それに伴う複数の電子状態の変化をあらわに追跡する必要があることを示唆する．今年度は，このような dynamics の詳細に加えて，複数の電子状態が反応経路に沿ってどのように絡み合うか，そして励起状態で見出されていた類似の電荷分離の機構[2, 3]との関係などについて議論した．

【参考文献】

[1] T. Yonehara, K. Hanaksaki, and K. Takatsuka, *Chem. Rev.* **112**, 499 (2012).
[2] K. Yamamoto and K. Takatsuka, *Chem. Phys*. **475**, 39 (2016) (perspective).
[3] K. Yamamoto and K. Takatsuka, *ChemPhysChem* **18**, 537 (2017).

2. 論文

(1) Kentaro YAMAMOTO and Kazuo TAKATSUKA,

“"On the photocatalytic cycle of water splitting with small manganese oxides and the roles of water clusters as direct sources of oxygen molecules”

Phys. Chem. Chem. Phys. 20, 12229-12240 (2018)

3. 学会発表

(1) 山本憲太郎，高塚和夫
「電子波束動力学的な電荷分離の機構によって駆動される Mn 酸化物中の水の光分解サイクル」第 20 回理論化学討論会, 京都 2017/5/16-18 2L16.

(2) 山本憲太郎，高塚和夫
「生物系から着想を得た単純な系における衝突誘起の逐次的な電子移動; 非断熱の電子波束による研究」第 11 回分子科学討論会, 仙台 2017/9/15-18 2D03.

(3) Kentaro Yamamoto and Kazuo Takatsuka“Photocatalytic cycle of water splitting with small manganese oxides and water clusters as source of oxygen molecules”, 第15回京都大学福井謙一記念研究センターシンポジウム, Kyoto, Japan 2018/2/2 P17.

(4) Kentaro Yamamoto and Kazuo Takatsuka“Photocatalytic cycle of water splitting with small manganese oxides and the roles of water cluster as a direct resource of oxygen molecules”, The 58th Sanibel Symposium, St. Simons Island, Georgia, 2018/2/18-23 5P13.

新崎　康樹

研究フェロー（高塚グループ）

1. 今年度の研究の要約

今年度はホウ素クラスター系における、個々の断熱状態が意味をなくすほど強く非断熱相互作用する電子状態およびそれを反応場ととらえた場合の動力学の理論研究を行った。

【序】 これまで電子状態の断熱描像、その描像における非断熱相互作用は化学反応の解釈に重要な役割を果たしてきた。一方で分子に内在する非断熱相互作用や外場によるその制御の研究が進むにつれて、従来の断熱電子状態という描像ではとらえきれないような状態を考える可能性が出てきた。そのような電子状態を反応場として利用する新規な化学反応の開発に繋げたい。

【方法論】 原子核の時間発展と同時に、多くの断熱電子状態が強く相互作用する電子状態が時間発展する系を理論計算により取り扱いたい。まずはそのような扱いを最も簡単に実現できる半古典エーレンフェスト理論による動力学計算を行う。ここでは断熱電子状態ではなく、電子の配置状態関数（CSF）を基底として電子状態を展開し、その展開係数 $\{C_I(t)\}$ を時間発展させることで非断熱相互作用の強い系を必ずしも断熱状態で記述することなく扱う。

$$i\hbar\frac{\partial}{\partial t}C_I(t)=\sum_{J=1}^{N_\mathrm{S}}\left[H_{IJ}^{(\mathrm{el})}(\boldsymbol{R}(t))-i\hbar\sum_{k=1}^{3N_\mathrm{N}}\dot{R}_k(t)X_{IJ}^{k}(\boldsymbol{R}(t))\right]C_J(t) \tag{1}$$

原子核座標 $\boldsymbol{R}(t)$ はその電子状態の平均場フォースに駆動されるとする。

$$m_k\ddot{R}_k(t)=-\sum_{I=1}^{N_\mathrm{S}}\sum_{J=1}^{N_\mathrm{S}}C_I^{*}(t)F_{IJ}^{k}(\boldsymbol{R}(t))C_J(t) \tag{2}$$

平均場フォースは

$$F_{IJ}^{k}(\boldsymbol{R}(t))=\sum_{K=1}^{N_\mathrm{S}}\left[X_{IK}^{k}(\boldsymbol{R}(t))H_{KJ}^{(\mathrm{el})}(\boldsymbol{R}(t))-H_{IK}^{(\mathrm{el})}(\boldsymbol{R}(t))X_{KJ}^{k}(\boldsymbol{R}(t))\right]+\bar{F}_{IJ}^{k}(\boldsymbol{R}(t)) \tag{3}$$

によって計算される（最後の項は CSF 基底ハミルトニアンの空間微分）。このとき電子、原子核の時間発展はともに CSF 間の相互作用行列要素

$$X_{IJ}^{k}(\boldsymbol{R}(t))=\left\langle \Phi_I(\boldsymbol{R}(t))\middle|\frac{\partial}{\partial R_k}\middle|\Phi_J(\boldsymbol{R}(t))\right\rangle_{\boldsymbol{r}} \tag{4}$$

の影響を受ける。電子状態、核座標の時間発展は $H_{IJ}^{(\mathrm{el})}$ 、 X_{IJ}^{k} 非対角項による CSF 間の混合の影響を強く受ける。

【ホウ素クラスターによる電子混合状態の検討】 ホウ素原子は電子が 5 つであり、2p 軌道に電子が 1 つの基底配置をとる。そのためホウ素クラスターでは多数の安定な励起状態が密に存在し、電子励起状態では原子核の運動にともない非断熱相互作用により電子状態が強く混合される。そのような励起状態での動力学は少数の断熱状態とその間の相互作用と解釈するよりは、個々の断熱状態が区別できない混合状態と解釈することが妥当であることが先行研究で示唆されている[1,2]。本研究ではまずこの新規な状態の特徴を動力学計算から探った。B_6、B_{12} クラスターで非断熱相互作用を含む時間発展と仮想的な断熱時間発展との比較により、非断熱相互作用がなければ解離する条件の軌跡であっても、頻繁に強く非断熱相互作用することによって解離が阻害される場合のあることが確認できた（図１）。これは実効的には強い非断熱相互作用が存在する場合にのみ、原子核運動によって維持される「結合状態」ととらえることができる。

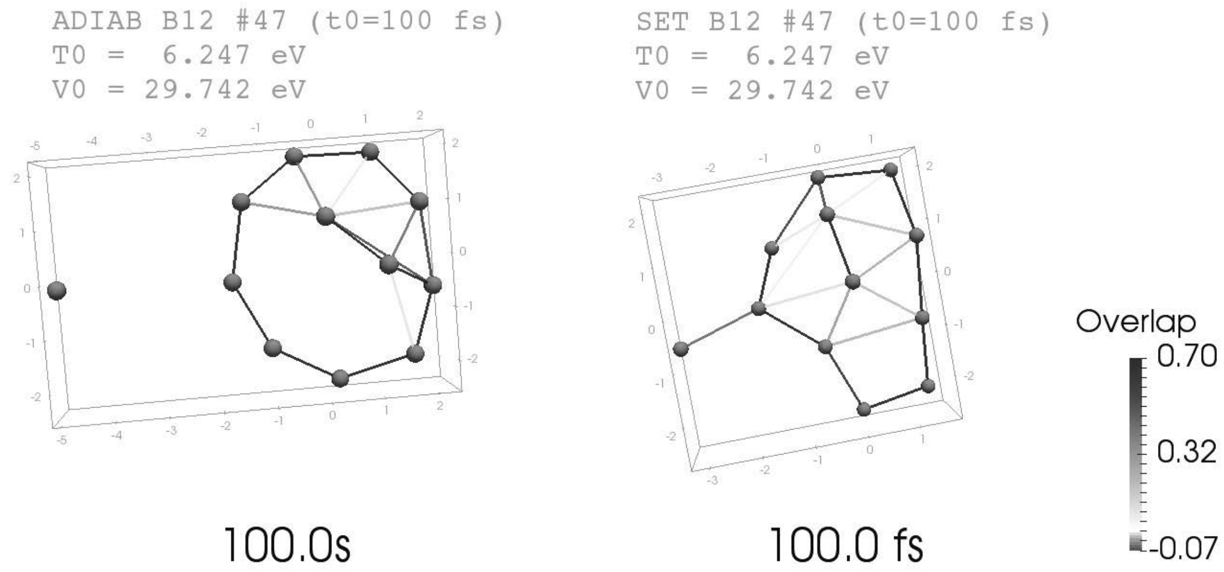

図１　B_{12} クラスターで断熱時間発展では解離する（左）が非断熱相互作用により束縛される（右）例。

【反応場としての電子混合状態】 さらに、上記のような非断熱相互作用によって維持される励起状態クラスターを反応場とした場合の特徴を検討するために、B_{12} クラスターに N_2、Be_2、Mg_2 を添加した場合の動力学を調べた。B_{12} クラスターの自由度の高い電子状態が N_2 の強い結合を弱め、あるいは Be_2、Mg_2 の弱い結合を強める場合があることが見られる。このような働きを含め、電子混合状態における反応を特徴づける指標やその法則性の検討を現在進めている（図２）。

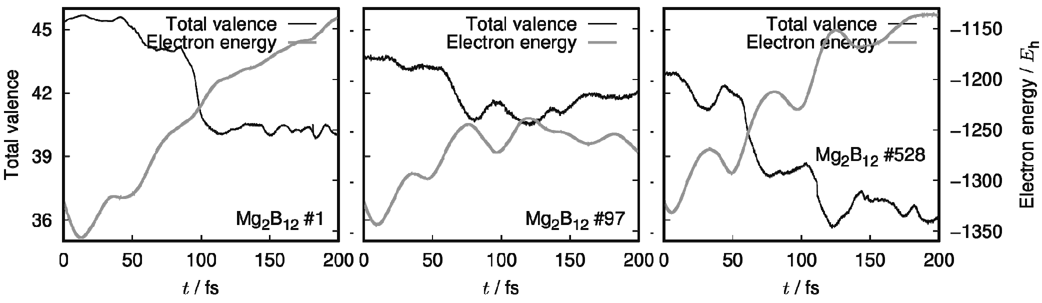

図２　Mg_2B_{12} クラスターの初期断熱状態（#1、#97、#528）別の電子エネルギーと総原子価の時間発展。

【参考文献】

[1] T. Yonehara and K. Takatsuka, J. Chem. Phys. **137**, 22A520 (2012).

[2] T. Yonehara and K. Takatsuka, J. Chem. Phys. **144**, 164304 (2016).

2. 論文

(1) Yasuki ARASAKI and Kazuo TAKATSUKA,
“Time-resolved photoelectron signals from bifurcating electron wavepackets propagated across conical intersection in path-branching dynamics”
Chem. Phys. 493, 42-48(2017).

６．日本学術振興会外国人特別研究員

Xue-Feng Ren

JSPS Fellow

1. Summary of the research of the year

Computational Insights into the Non-radiative Deactivation Pathways of phosphorescent Pt(□) Emitter

For emitters, a large radiative rate constant (k_{r}) and a small non-radiative rate constant (k_{nr}) are highly pursued to achieve high quantum yield. With the development of phosphorescent materials, great success has been achieved on revealing radiative process by the discussions of the absorption spectra, spin-orbit coupling (SOC) matrix elements in the $T_m \rightarrow S_n$ transition, and energy gaps between $E(T_m)$ and $E(S_n)$. However, revealing the non-radiative decay is intrinsically more difficult, since it involves possibilities of the internal conversion (IC) and intersystem crossing (ISC). The non-radiative decay efficiently takes place between two nearly degenerate electronic states. Regarding phosphorescence quantum yield, the intensive competition between the emission from the local minimum of T_1 state and non-radiative pathway to the singlet ground electronic state S_0 through MESX point. Therefore, the geometry and energy of MESX between the lowest triplet excited state (T_1) and the ground state (S_0) should play a key role in intersystem crossing.

Recently, a new type of Pt emitting materials with high color purity and improved quantum yields (Φ) by replacing the ppy ligand of complex 1 with tpy moiety (ppy=2-phenylpyridine, dmpt=4,5-dimethyl-3-phenylthiazol, as shown in Fig. 1). The Φ of complex 2 has been greatly improved by 0.57, while it is only 0.01 of complex 1. Though the analyses by Escudero and co-workers, the k_{r} $(T_{em} \rightarrow S_0)$ of complex 1 is $2.730 \times 10^3 (s^{-1})$, thus the non-radiative decay is crucially responsible for explaining the low Φ. Therefore, to effectively and accurately estimate the emission behavior, a deep understanding of the mechanism of non-radiative decay is a great demand. In this work, we will investigate the geometry and energy of MESX between the lowest lying triplet excited state (T_1) and the ground state (S_0). After that, the mechanism of non-radiative decay of complex 1 and complex 2 will be analyzed to reveal how the dmpt (dmpt=4,5-dimethyl-3-phenylthiazole) ligand influences the decay process. Based on the above analyzes, some valuable information for promising emitters with difficulty in non-radiative decay will be provided.

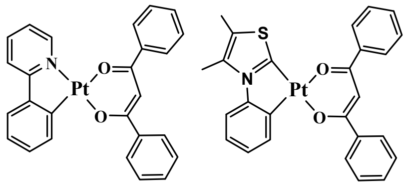

complex 1: (ppy)Pt(dbm) **Φ<0.01**

complex 2: (dmpt)Pt(dbm) **Φ=0.57**

Fig. 1. Structures of studied complexes: 1: (ppy)Pt(dbm) and complex 2: (dmpt)Pt(dbm), together with the quantum yield.

Computational details

The ground-state equilibrium geometries (S_0) of studied complexes were fully optimized utilizing by M06L functional. Unrestricted Kohn-Sham DFT (UKS) was applied to optimize the local minimum geometries of T_1 state. The minimum energy seams of crossings (MESXs) between T_1 and S_0 were explored by single-component artificial force induced reaction (SC-AFIR) method associated with the seam model function (SMF). After SC-AFIR search on SMF surfaces, MESXs were fully optimized by UM06L method without artificial force. To study the mechanism of thermal deactivations, the TS geometries between T_1-M_1 and MESX were optimized by UM06L functional. After verification of vibrational frequency, the connection between the T_1-M_1 and MESX through each TSs were confirmed by the intrinsic reaction coordinate (IRC) calculations. All the calculations were performed with the development version of the GRRM program combined with the Gaussian 09 electronic structure calculation program.

Results:

The non-radiative decay process of complex 1

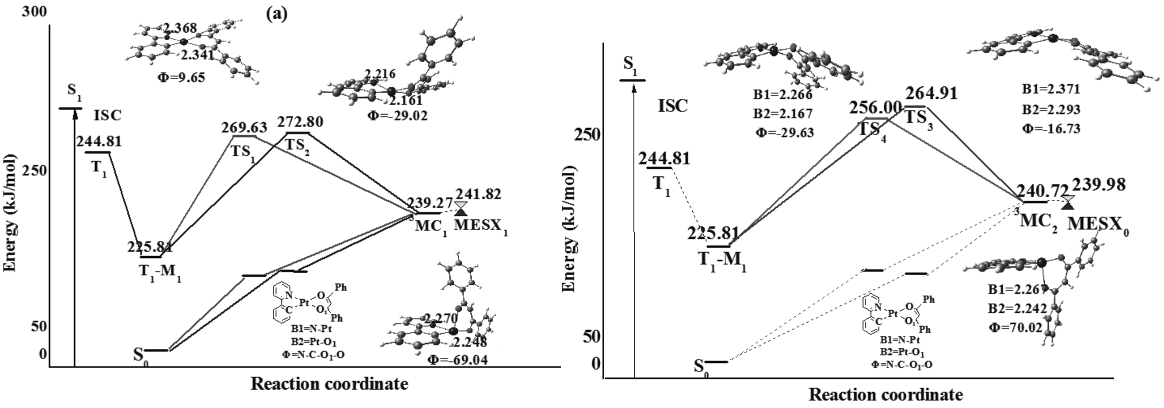

The non-radiative decay process of complex 2

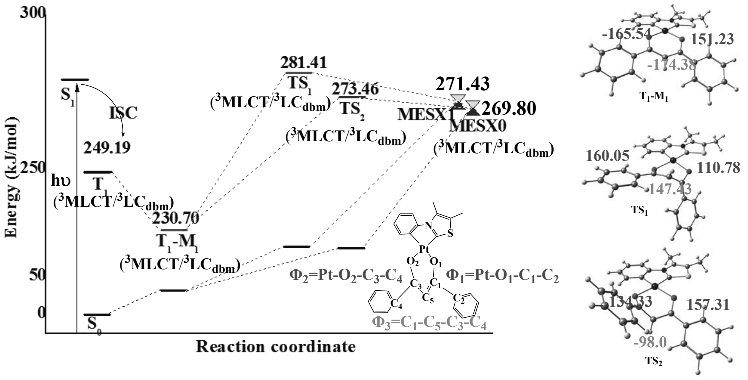

The results revealed that the MESX of complex 1 had out-of-plane bending of phenyl moiety, which low energy was compared with the T_1 state at Frank-Condon (FC). While for complex 2, the MESX had two phenyl rings bent out of plane, which was higher than T_1 at FC by 20.6kJ/mol. The energy barrier of most favorable deactivation process from ^{3}MLCT/^{3}LC$_{dbm}$ state to triplet metal-centered (^{3}MC) character of complex 1 was 29.46 kJ/mol, while the energy barrier of decay process of complex 2 was 42.76 kJ/mol. Clearly, the non-radiative decay process of complex 2 cannot easily take place, which can explain the great improvement of the observed quantum yields

(Φ=0.57) relative to complex 1 (Φ<0.01).

The ways to improve emission quantum yield

The kinetics of quenching is determined by the energies of MESXs and TSs connecting the FC and the MESXs. We tried to modify ligands to improve emission quantum yield. To improve the emissive behavior, one successful approach is to import the -CN at the dbm ligand. The MESX of designed complex (239.73 kJ/mol) is higher than the T_1 state at FC (224.3 kJ/mol). Furthermore, a large energy barrier is necessary (47.29 kJ/mol) from the T_1 state to go over the MESX. Therefore, the non-radiative decay is difficult for designed complex, which means that the phosphorescent process might be dominant.

Original papers

Xue Feng Ren, Satoshi Suzuki, Pedro J. Castro Pelaez, Satoshi Maeda, Keiji Morokuma, "Computational Insights into the Non-radiative Deactivation Pathways of phosphorescent Pt(□) Emitter", In preparation.

2. Presentation at academic conferences

(1) Xue Feng Ren and Keiji Morokumma
"The potential energy surface of non-radiative process: a type of Pt emitters", The 11th Annual Meeting of Japan Society for Molecular Science, 2017,9,15-18, Tohoku university, Poster

７．日本学術振興会特別研究員

Rei Matsuzaki

JSPS Fellow

1. Summary of the research of the year

Flux analysis of nonadiabatic electron transfer reaction in LiF

Nonadiabatic transition is one of the key notions with which to comprehend sudden transition of molecular states on the way of chemical reactions such as radiation less decay from an electronic excited state, and so on. Among many nonadiabatic dynamics, intra- and intermolecular electron transfers through the so-called avoided crossing are particularly interesting, in which potential surfaces of ionic and covalent character mutually avoid-cross at a relatively long interatomic distance such as $\mathrm{LiF} \leftrightarrow \mathrm{Li}^{+}\mathrm{F}^{-}$ or $\mathrm{NaI} \leftrightarrow \mathrm{Na}^{+}\mathrm{I}^{-}$. Since the nonadiabatic transitions are ultrafast process, direct experimental observation of the instance of the passing of quantum wavepackets across the crossing regions still face technical difficulties and limitations. Therefore, theoretical studies can play a vital role to explore the hidden features of nonadiabatic dynamics, which may in turn give a guiding principle of experimental studies. We have performed a flux analysis of full quantum mechanical dynamics of a nonadiabatic electron transfer process in the system of $\mathrm{LiF} \leftrightarrow \mathrm{Li}^{+}\mathrm{F}^{-}$ and interesting features of electron flow have observed. We also have surveyed a flux-flux correlation between nuclear and electronic motion, which clearly exposes the deviation from the Born-Oppenheimer dynamics in a quantitative manner.

Here, we calculated the electronic and nuclear wave function of LiF by using the Born-Huang expansion within the two states model. We set the initial state as well localized gauss type wave packet on the first excited state (the covalent state). Then, we evaluated the electronic flux $\boldsymbol{j}(\boldsymbol{r}, Q, t)$ and nuclear flux $J(\boldsymbol{r}, Q, t)$ from the wave function. $\boldsymbol{r}$ is electron coordinate in the molecular frame and Q is internuclear distance. In our coordinate F atom is located at $\boldsymbol{r} = (0,0,0)$ and Li atom is located at $\boldsymbol{r} = (0,0,Q)$. To extract sufficient characteristic features of the electron flux, we introduce the reduced quantity

$$f_Q(Q,t) = \int \mathbf{e}_z \cdot \boldsymbol{j}(\boldsymbol{r}, Q, t) d\boldsymbol{r}.$$

Figures 1 shows the reduced quantity $f_Q(Q,t)$. Starting at $t = 0$ fs and up to about $t = 50$ fs, the electron flux represented in f_Q have almost zero values, since the nonadiabatic interaction is very weak in this region. At $t = 90$ fs, the nuclear wavepacket enters the crossing region (the potential crossing at $Q = 6.1$ Å) and the electronic flux a large there. This nonadiabatic reaction can be expressed as $\mathrm{LiF} \rightarrow \mathrm{Li}^{+}\mathrm{F}^{-}$ thereby representing the electron transfer from Li to F. Passing across the nonadiabatic transition at $t = 90$ fs, f_Q oscillates as a function of Q. We will discuss these oscillations later. At $t = 250$ fs, the nuclear wave packet turns back because of attractive ionic potential and the electron flux occurs again with the inverse reaction ($\mathrm{Li}^{+}\mathrm{F}^{-} \rightarrow \mathrm{LiF}$).

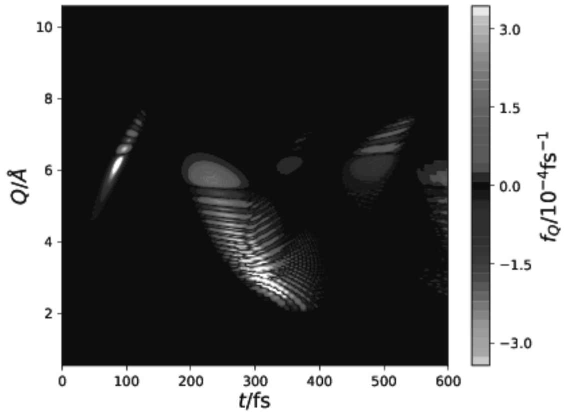

Figure 1. The reduced electron flux $f_Q(Q,t)$.

We analyze this spatiotemporal oscillation of Figure 1 and its physical implication. In terms of the Born-Huang expansion, the electron flux can be rewritten as

$$\boldsymbol{j}(\boldsymbol{r},Q,t)=\frac{\hbar}{m_{\mathrm{e}}}[\mathbf{e}_{12}(\boldsymbol{r};Q)-\mathbf{e}_{21}(\boldsymbol{r};Q]\mathrm{Im}\,[\chi_1^*(Q,t)\chi_2(Q,t)],$$

where $\mathbf{e}_{IJ}$ is matrix element of electron flux between two electronic states. In this expression, the diagonal term vanishes. Recall that the nuclear wave packets χ_1 and χ_2 run on the different potential curves (the ionic and covalent potential curves) and the product $\chi_1^*\chi_2$ may show a complicated phase and amplitude variations in space time as long as the interfere coherently. Figure 1 is seen to reflect such an interference pattern between the two wavefunctions with weighting factor of $\hbar\boldsymbol{v}/m_{\mathrm{e}}$. Here, we want to emphasize that the electron transfer dynamics is far from a simple and uniform flow.

Finally, we studied the correlation of the electronic and nuclear fluxes. The adiabatic approximation assumes that electrons in a molecule instantaneously follow and adjust the nuclear dynamics. It is widely known through that this is not actually the case, since electrons can only move with finite speed, which gives the physical foundation of nonadiabatic transition. Our task here is to quantify the deviation of the actual dynamics from the Born-Oppenheimer limit. To figure out the extent of this deviation from the view point of flux analysis, we consider the following flux-flux correlation function between electronic and nuclear dynamics

$$C(\mathrm{t})=\int dz_1'dQ'\langle\Psi|\hat{f}_z(z_1')\,\hat{F}_Q(Q')|\Psi\rangle_{z,Q},$$

where the operators $\hat{f}_z(z_1')$ and $\hat{F}_Q(Q')$ are defined as the operator form of the reduced flux $f_z(z,t)$ and $F_Q(Q,t)$, respectively. In Figure 2 (a) $C(t)$ are shown for the current LiF dynamics along with the time-variation of the state populations as plotted in panel (b). These two panels share the same time coordinate (horizontal one). Figure 2(a) shows that during the time-interval from $t=0$ fs and $t=70$ fs, $C(t)$ takes only values close to zero, because the dynamics is nearly adiabatic in this region. Then the first large negative peak is observed around $t=90$ fs. After all a total of four major groups of significant peaks are seen in the correlation function in Figure 2(a); (A) negative peak around $t=90$ fs, (B) negative one around $t=220$ fs

, (C) transition from negative to positive one around $t = 350$ fs, and (D) negative peak around $t = 480$ fs. The peaks (A), (B) and (D) are all associated with the nonadiabatic crossings, as identified in the panel (b). The origin of the peak (C) is obviously different from the others. In the current calculation, the nonadiabatic electron transfer has been induced in the vicinity of the inner turning point and this is origin of the peak (C). Aside from the precise interpretation as above for deeper understanding of the flux-flux correlation function, we have seen that the flux-flux correlation function can well quantify the extent of the breakdown of the Born-Oppenheimer approximation not only by the absolute magnitude but also in the local directions of moving electrons and nuclei.

The present flux analysis for both electronic and nuclear wave packets in LiF has revealed novel features in the electron transfer driven by nonadiabatic dynamics. In particular, the spatiotemporal oscillatory pattern observed in Figure 2 in terms of our defined reduced electronic flux is found not only interesting but instructive in the deeper understanding of electronic and nuclear coupled dynamics. We also have demonstrated that the flux-flux correlation between electrons and nuclei describe the deviation from the Born-Oppenheimer approximation.

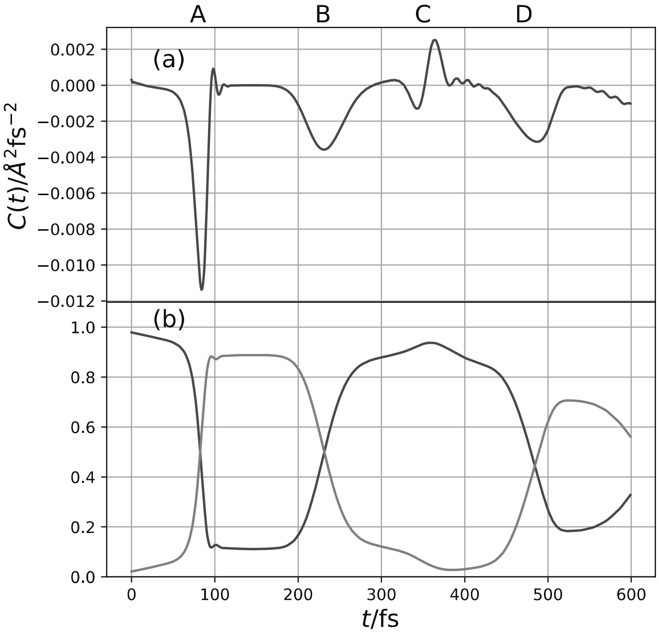

Figure 2. (a) Flux-Flux correlation function $C(t)$ between electrons and nuclei. (b) The time variation of the state populations. Blue and orange lines are for the covalent and ionic states in the diabatic representation.

2. Original papers

(1) Rei Matsuzaki, Satoshi Yabushita, “Calculation of Photoionization differential cross sections using complex Gauss-type orbitals”, J. Comput. Chem. **38**, 2030 (2017).

(2) Rei Matsuzaki, Kazuo Takatsuka, “Electronic and Nuclear Flux Analysis on Nonadiabatic Electron Transfer Reaction”, J. Comput. Chem. (投稿中)

3. Presentation at academic conferences

(1) 松崎黎、薮下聡,
“複素基底関数法による光イオン化微分断面積の計算”, 第２０回理論化学論会,京都,2017 年 5 月

(2) 松崎黎、高塚和夫,
“非断熱過程における電子と原子核フラックス” , 第２１回理論化学討論会,岡崎,2018 年５月

4. Others

(1) Rei Matsuzaki, Kazuo Takatsuka, “Flux analysis on nonadiabatic chemical dynamics”, 学
第６回京都大学福井謙一記念研究センターシンポジウム　京都　2018年2月

Ⅴ　資料

1．研究業績一覧（平成 29 年度）

№	Authors	Title	Journal	Volume (Number), first page to last page	year
西本　佳央					
1	Yoshio Nishimoto, Hiroki Kondo, Kazuya Yamaguchi, Daisuke Yokogawa, Junichiro Yamaguchi, Kenichiro Itami, and Stephan Irle	Theoretical Elucidation of Potential Enantioselectivity in a Pd-Catalyzed Aromatic C—H Coupling Reaction	*J. Org. Chem.*	82(9), 4900-4906	2017
2	Hirotaka Kitoh-Nishioka, Kai Welke, Yoshio Nishimoto, Dmitri G. Fedorov, and Stephan Irle	Multiscale Simulations on Charge Transport in Covalent Organic Frameworks Including Dynamics of Transfer Integrals from the FMO-DFTB/LCMO Approach	*J. Phys. Chem. C*	121(33), 17712-17726	2017
3	Yoshio Nishimoto and Dmitri G. Fedorov	Adaptive frozen orbital treatment for the fragment molecular orbital method combined with density-functional tight-binding	*J. Chem. Phys.*	148(6), 064115	2018
永瀬　茂					
4	Y. Maeda, Y. Takehana, J. –S. Dang, M. Suzuki, M. Yamada, and S. Nagase	Effect of Substituents and Initial Degree of Functionalization of Alkylated Single-Walled Carbon Nanotubes on Their Thermal Stability and Photoluminescence Properties	*Chem. Eur. J.*	23, 1789-1794	2017
5	K. Yuan, R. –S. Zhao, J. –J. Zheng, H. Zheng, S. Nagase, S. –D. Zhao, Y. –Z. Liu, and X. Zhao	Van der Waals Heterogeneous Layer-Layer Carbon Nanostructures Involving π H-C-C-H π H-C-C-H Stacking Based on Graphene and Graphane Sheets	*J. Comput. Chem.*	38, 730-739	2017
6	M. Yamada, T. Abe, C. Saito, T. Yamazaki, S. Sato, N. Mizorogi, Z. Slanina, F. Uhlík, M. Suzuki, Y. Maeda, Y. Lian, X. Lu, M. M. Olmstead, A. L. Balch, S. Nagase, and T. Akasaka	Adamantylidene Addition to $M_3N@I_h$-C_{80} (M = Sc, Lu) and $Sc_3N@D_{5h}$-C_{80}: Synthesis and Crystallographic Characterization of the [5,6]-Open and [6,6]-Open Adducts	*Chem. Eur. J.*	23, 6552-6561	2017
7	M. Kako, K. Minami, T. Kuroiwa, S. Fukazawa, Y. Arikawa, M. Yamada, Y. Maeda, Q. –Z. Li, S. Nagase, and T. Akasaka	Photoreactions of Endohedral Metallofullerene with Siliranes: Electronic Properties of Carbosilylated $Lu_3N@I_h$-C_{80}	*Molecules*	22, 850 (10 pages)	2017
8	Y. Morinaka, R. Zhang, S. Sato, H. Nikawa, T. Kato, K. Furukawa, M. Yamada, Y. Maeda, M. Murata, A. Wakamiya, S. Nagase, T. Akasaka and Y. Murata	Fullerene C_{70} as a Nanoflask that Reveals the Chemical Reactivity of Atomic Nitrogen	*Angew. Chem. Int. Ed.*	56, 6488-6491	2017
9	M. Yamada, S. Sato, W. Choi, S. Seki, T. Abe, M. Suzuki, Y. Maeda, S. Nagase, and T. Akasaka	Temperature Dependence of Anisotropic Transient Conductivity of a La@C_{2v}-C_{82}(Ad) Crystal	*Chem. Lett.*	46, 973-975	2017

№	Authors	Title	Journal	Volume (Number), first page to last page	year
10	M. Kako, T. Sugiura, K. Miyabe, M. Yasui, M. Yamada, Y. Maeda, J. –D. Guo, S, Nagase, and T. Akasaka	Preparation, Structural Determination, and Characterization of Electronic Properties of [5,6]- and [6,6]-Carbosilylated $Sc_3N@I_h$-C_{80}	*Chem. Asian. J.*	12, 1391-1399	2017
11	J. –S. Dang, W. –W. Wang, J. –J. Zheng, X. Zhao, and S. Nagase	Fused-Pentagon-Configuration-Dependent Electron Transfer of Monotitanium-Encapsulated Fullerenes	*Inorg. Chem.*	56, 6890-6896	2017
12	T. Morosaki, R. Iijima, T. Suzuki, W. –W. Wang, S. Nagase, and T. Fujii	Synthesis, Electronic Structure, and Reactivities of Two-Sulfur Stabilized Carbones Exhibiting Four-Electron Donor Ability	*Chem. Eur. J.*	23, 8694-8702	2017
13	Z. Slanina, F. Uhlík, S. Nagase, T. Akasaka, L. Adamowicz, and X. Lu	$Eu@C_{72}$: Computed Comparable Populations of Two Non-IPR Isomers	*Molecules*	22, 1053 (8 pages)	2017
14	Q. –Z. Li, J. –J. Zheng, X. Zhao, and S. Nagase	Epoxy and Oxidoannulene Oxidation Mechanisms of Fused-Pentagon Chlorofullerenes: Oxides Linked by a Pirouette-Type Transition State	*J. Org. Chem.*	82, 6541-6549	2017
15	M. Kako, S. Nagase, and T. Akasaka	Functionalization of Endohedral Metallofullerenes with Reactive Silicon and Germanium Compounds	*Molecules (Review)*	22, 1179 (17 pages)	2017
16	T. Akasaka, A. Nakata, M. Rudolf, W. –W. Wang, M. Yamada, M. Suzuki, Y. Maeda, R. Aoyama, T. Tsuchiya, S. Nagase, and D. M. Guldi	Synthesis and Photoinduced Electron-Transfer Reactions in a $La_2@I_h$-C_{80}-Phenoxazine Conjugate	*ChemPlusChem*	82, 1067-1072	2017
17	J. –S. Dang, W. –W. Wang, X. Zhao, and S. Nagase	Concave Binding of Cationic Li to Quadrannulene	*Phys. Chem. Chem. Phys.*	19, 20773-20777	2017
18	J. –S. Dang, W. –W. Wang, J. –J. Zheng, S. Nagase, and X. Zhao	Formation of Stone-Wales Edge: Multistep Reconstruction and Growth Mechanisms of Zigzag Nanographene	*J. Comput. Chem.*	38, 2241-2247	2017
19	J. –S. Dang, W. –W. Wang, X. Zhao, and S. Nagase	A Mechanistic Study on Cationic Li Prompted Diels-Alder Cycloaddition of Cycloparaphenylene	*Org. Chem. Front.*	4, 1757-1761	2017
20	R. Zhao, K.Yuan, S. Zhao, M. Ehara, S. Nagase, J. M. Poblet, and X. Zhao	Deciphering the Role of Long-Range Interaction in Endohedral Metallofullenes: A Revisit to Sc_2C_{70}	*J. Phys. Chem. C*	121, 20481-20488	2017
21	Z. Slanina, F. Uhlík, L. Adamowicz, T. Akasaka, S. Nagase, and X. Lu	Stability Issues in Computational Screening of Carbon Nanostructures: Illustrations on La Endohedrals	*Mol. Simul.*	43, 1472-1479	2017
22	W. –W. Wang, J. –S. Dang, X. Zhao, and S. Nagase	Revisit of the Saito-Dresselhause-Dresselhaus C_2 Ingestion Model: On the Mechanism of Atomic-Carbon-Participated Fullerene Growth	*Nanoscale*	9, 16742-16748	2017

№	Authors	Title	Journal	Volume (Number), first page to last page	year
23	Z. Slanina, F. Uhlík, S. Nagase, T. Akasaka, L. Adamowicz, and X. Lu	Computational Comparison of the Water-Dimer Encapsulation into D_2(22)-C_{84} and D_{2d}(23)-C_{84}	*ECS, J. Solid State Sci. and Tech.*	6, M3113-M3115	2017
24	Z. Slanina, F. Uhlík, S. Nagase, T. Akasaka, L. Adamowicz, and X. Lu	A Computational Characterization of CO@C_{60}	*tubes, Carbon Nanostruct.*	25, 624-629	2017
榊　茂好					
25	Ryoichi Fukuda, Nozomi Takagi, Shigeyoshi Sakaki, and Masahiro Ehara	On the Structures of Bimetallic Copper-Ruthenium Nanoparticles: Incoherent Interface and Surface Active Sites for Catalytic Nitric Oxide Dissociation	*J. Chem. Theory Comput.*	121, 300-307	2017
26	Vijay Singh, Yoshiaki Nakao, Shigeyoshi Sakaki, and Milind M. Deshmukh	Theoretical Study of Nickel-Catalyzed Selective Alkenylation of Pyridine: Reaction Mecha- nism and Crucial Roles of Lewis Acid and Ligands in Determining the Selectivity	*J. Org. Chem.*	82, 289-301	2017
27	Tao Yang, Ryoichi Fukuda, Saburo Hosokawa, Tsunehiro Tanaka, Shigeyoshi Sakaki, and Masahiro Ehara	A Theoretical Investigation on CO Oxidation by Single-Atom Catalysts M1/γ-Al_2O_3 (M = Pd, Fe, Co, and Ni)	*ChemCatChem,*	9, 1222-1229	2017
28	Takako Muraoka, Haruhiko Kimura, Gama Trigagema, Masayuki Nakagaki, Shigeyoshi Sakaki, and Keiji Ueno	Reactions of Silanone(silyl)tungsten and -molybdenum Complexes with MesCNO, $(Me_2SiO)_3$, MeOH, and H_2O: Experimental and Theoretical Studies	*Organometallics*	36, 1009-1018	2017
29	Yue Chen and Shigeyoshi Sakaki	Mo−Mo Quintuple Bond is Highly Reactive in H−H, C−H, and O−H σ-Bond Cleavages Be-cause of the Polarized Electronic Structure in Transition State	*Inorg. Chem.*	56, 4011-4020	2017
30	Hong Zheng, Xiang Zhao, Shigeyoshi Sakaki	[2+2]-type Reaction of Metal-Metal sigma-Bond with Fullerene Forming an η^1-C_{60} Metal Complex: Mechanistic Details of Formation Reaction and Prediction of a New η^1-C_{60} Metal Complex	*Inorg. Chem.*	56, 6746-6754	2017
31	Hajime Kameo, Yuki Baba, Shigeyoshi Sakaki, Didier Bourissou, Hiroshi Nakazawa, Hiroyuki Matsuzaka	Iridium Hydride Mediated Stannane-Fluorine and -Chlorine sigma-Bond Activation: Re-versible Switching between X-Type Stannyl and Z-Type Stannane Ligands	*Organometallics*	36, 2096-2106	2017
32	Yue Chen, Jyun-ya Hasegawa, Kazuya Yamaguchi, Shigeyoshi Sakaki	A coordination strategy to realize a sextuply-bonded complex	*Phys. Chem. Chem. Phys.*	19, 14947-14954	2017
33	Kenji Hirano, Hiroshi Nakano, Yoshihide Nakao, Hirofumi Sato, Shigeyoshi Sakai	Photo Absorption of p-Coumaric Acid in Aqueous Solution: RISM-SCF-SEDD Theory Approach	*J. Comp. Chem.*	38, 1567-1573	2017

№	Authors	Title	Journal	Volume (Number), first page to last page	year
34	Shinji Aono, Masayuki Nakagaki, Shigeyoshi Sakaki	Theoretical study of one-electron-oxidized salen complexes of group 7 (Mn(III), Tc(III), and Re(III)) and group 10 metals (Ni(II), Pd(II), and Pt(II)) with the 3D-RISM-GMC-QDPT method: localized vs. delocalized ground and excited states in solution	*Phys. Chem. Chem. Phys.*	19, 16831-16849	2017
35	M. Ramu Yadav, Masahiro Nagaoka, Myuto Kashihara, Rong-Lin Zhong, Takanori Miyazaki, Shigeyoshi Sakaki, Yoshiaki Nakao	The Suzuki–Miyaura Coupling of Nitroarenes	*J. Am. Chem. Soc.*	139, 9423-9426	2017
36	Shuwei Tang, Odile Eisenstein, Yoshiaki Nakao, and Shigeyoshi Sakaki	Aromatic C-H σ-Bond Activation by Ni^0, Pd^0, and Pt^0 Alkene Complexes: Concerted Oxida-tive Addition to Metal vs Ligand-to-Ligand H Transfer Mechanism	*Organonetallics*	36, 2761-2771	2017
37	Nozomi Takagi, Kazuya Ishimura, Masafuyu Matsui, Ryoichi Fukuda, Masahiro Ehara, and Shigeyoshi Sakaki	Core−Shell versus Other Structures in Binary Cu38−nMn Nanoclusters (M = Ru, Rh, Pd, Ag, Os, Ir, Pt, and Au; n = 1, 2, and 6): Theoretical Insight into Determining Factors	*J. Phys. Chem. C*	121, 10514-10528	2017
38	Jingui Duan, Masakazu Higuchi, Jiajia Zheng, Shin-ichiro Noro, I-Ya Chang, Hyeon-Deuk Kim, Simon Mathew, Shinpei Kusaka, Easan Sivaniah, Ryotaro Matsuda, Shigeyoshi Sakaki, SusumuKitagawa	Density Gradation of Open Metal Sites in the Mesospace of Porous Coordination Polymers	*J. Am. Chem. Soc.,*	139, 11576-11583	2017
39	Jiajia Zheng, Shinpei Kusaka, Ryotaro Matsuda, Susumu Kitagawa, and Shigeyoshi Sakaki	Characteristic Features of CO_2 and CO Adsorptions to Paddle-Wheel-Type Porous Coordination Polymer	*J. Phys. Chem. C*	121, 19129-19139	2017
40	Masafuyu Matsui and Shigeyoshi Sakaki	Embedded Cluster Model for Al_2O_3 and $AlPO_4$ Surfaces Using Point Charges and Periodic Electrostatic Potential	*J. Phys. Chem. C*	121, 20242-20253	2017
41	Longfei Li, Ming Lei, and Shigeyoshi Sakaki	DFT Mechanistic Study on Alkene Hydrogenation Catalysis of Iron Metallaboratorene: Characteristic Features of Iron Species	*Organometallics*	36, 3530-3538	2017
42	Hong Zheng, Kazuhiko Semba, Yoshiaki Nakao, and Shigeyoshi Sakaki	How to Control Inversion vs. Retention Transmetallation between Pd^{II}-Phenyl and Cu^{I}-Alkyl Complexes: Theoretical Insight	*J. Am. Chem. Soc.*	139, 14065-14076	2017

№	Authors	Title	Journal	Volume (Number), first page to last page	year
田中　一義					
43	Kensuke Naka, Takuji Kato, Koushi Abe, Makoto Ishidoshiro, Shintaro Nishiyama, Susumu Tanaka, Hiroaki Imoto, Seiji Watase, Kimihiro Matsukawa, Hiroyuki Fueno, and Kazuyoshi Tanaka	Stereoisomerization of 1,4-Dihydroarsinetetracarboxylic Acid Diimides under Non-acidic Condition from *cis*- to *trans*-Forms	*Heterocycles*	94(5), 923-937	2017
44	Joji Ohshita, Toshiyuki Tsuchida, Kenji Komaguchi, Kazuki Yamamoto, Yohei Adachi, Yousuke Ooyama, Yutaka Harima, and Kazuyoshi Tanaka	Studies of Spherically Distributed LUMO and Electron-Accepting Properties of Caged Hexakis(germasesquioxanes)	*Organometallics*	36(14), 2536-2540	2017
45	Toshiaki Ikeda, Hiroaki Adachi, Hiroyuki Fueno, Kazuyoshi Tanaka, and Takeharu Haino	Induced-Dipole-Directed, Cooperative Self-Assembly of a Benzotrithiophene	*J. Org. Chem.*	82(19), 10062-10069	2017
46	Katsunori Suzuki, Yasuyuki Numata, Naoko Fujita, Naoki Hayakawa, Tomoharu Tanikawa, Daisuke Hashizume, Kohei Tamao, Hiroyuki Fueno, Kazuyoshi Tanaka, and Tsukasa Matsuo	A Stable Free Tetragermacyclobutadiene Incorporating Fused-ring Bulky EMind Groups	*Chem. Commun.*	54(18), 2200-2203	2018
高塚　和夫					
47	Kazuo Takatsuka	Lorentz-like force emerging from kinematic interactions between electrons and nuclei in molecules. A quantum mechanical origin of symmetry breaking that can trigger molecular chirality	*J. Chem. Phys.*	146, 084312 (10 pages)	2017
48	Takahide Matsuoka, Kazuo Takatsuka,	Dynamics of photoionization from molecular electronic wavepacket states in intense pulse laser fields: A nonadiabatic electron wavepacket study	*J. Chem. Phys.*	146,134114 (14 pages)	2017
49	Yasuki Arasaki and Kazuo Takatsuka	Time-resolved photoelectron signals from bifurcating electron wavepackets propagated across conical intersection in path-branching dynamics	*Chem. Phys.*	493, 42-48 (2017)	2017
50	Kazuo Takatsuka	Theory of molecular nonadiabatic electron dynamics in condensed phases	*J. Chem. Phys.*	147, 174102 (13 pages)	2017
51	Takahide Matsuoka and Kazuo Takatsuka	Nonadiabatic electron wavepacket dynamics behind molecular autoionization	*J. Chem. Phys.*	148, 014106 (15 pages)	2018

№	Authors	Title	Journal	Volume (Number), first page to last page	year
52	Kazuo Takatsuka	Adiabatic and nonadiabatic dynamics in classical mechanics for coupled fast and slow modes: sudden transition caused by the fast mode against the slaving principle.	*Mol. Phys.*	DOI:10.1080/00268976.2018.1430389	2018
53	Kentaro Yamamoto and Kazuo Takatsuka,	On photocatalytic cycle of water splitting with small manganese oxides and the roles of water cluster as a direct resource of oxygen molecules	*PhysChemChem Phys*	20, 6708-6725	2018
54	Kentaro Yamamoto and Kazuo Takatsuka,	Collision induced charge separation in ground-state water splitting dynamics	*PhysChemChem Phys*	20, 12229-12240	2018
多羅間　充輔					
55	M. Tarama	Swinging motion of active deformable particles in Poiseuille flow	*Phys. Rev. E*	96, 022602	2017
56	M. Tarama	Dynamics of Deformable Active Particles under External Flow Field	*J. Phys. Soc. Jpn.*	86, 101011	2017
57	M. Tarama and R. Yamamoto	Mechanics of cell crawling by means of force-free cyclic motion	*J. Phys. Soc. Jpn.*	87, 044803	2018
藪中　俊介					
58	Shunsuke Yabunaka and Bertrand Delamotte	Surprises in O (N) Models: Nonperturbative Fixed Points, Large N Limits, and Multicriticality	*Physical review letters*	19, 191602 1-5	2017
59	Shunsuke Yabunaka and Akira Onuki	Critical adsorption profiles around a sphere and a cylinder in a fluid at criticality: Local functional theory	*Physical review E*	96, 3, 032127 1-7	2017
60	Shunsuke Yabunaka and Akira Onuki	Electric double layer composed of an antagonistic salt in an aqueous mixture: Local charge separation and surface phase transition	*Physical review letters*	19, 118001 1-5	2017
61	Shunsuke Yabunaka and Marcq Philippe	Cell growth, division, and death in cohesive tissues: A thermodynamic approach	*Physical review E*	96, 2, 022406 1-9	2017
62	Shunsuke Yabunaka and Marcq Philippe	Emergence of epithelial cell density waves	*Softmatter*	13, 39, 7046-7052	2017
Simon K. Schnyder					
63	S. K. Schnyder, J. J Molina, Y. Tanaka, R. Yamamoto	Collective motion of cells crawling on a substrate: roles of cell shape and contact inhibition	*Scientific Reports*	7, 5163	2017
64	J. Horbach, N. H. Siboni, & S. K. Schnyder	Anomalous transport in heterogeneous media	*The European Physical Journal Special Topics*	226(14), 3113-3128	2017

№	Authors	Title	Journal	Volume (Number), first page to last page	year
65	S. K. Schnyder, & J. Horbach	Crowding of interacting fluid particles in porous media through molecular dynamics: breakdown of universality for soft interactions	*Physical Review Letters*	120(7), 78001	2018
伊勢川　美穂					
66	Miho Isegawa, W. M. C. Sameera, Akhilesh K. Sharma, Taku Kitanosono, Masako Kato, Shū Kobayashi, Keiji Morokuma	Copper-catalyzed Enantioselective Boron Conjugate Addition: DFT and AFIR Study on Different Selectivities of Cu(I) and Cu(II) Catalysts	*ACS Catalysis*	7, 5370-5380	2017
67	Miho Isegawa,, Akhilesh K. Sharma, Seiji Ogo, Keiji Morokuma	DFT Study on Fe(IV)-Peroxo Formation and H Atom Transfer Triggered O2 Activation by NiFe Complex	*Organometallics*	37, 1534-1545	2018
鈴木　聡					
68	S.Sasaki, S.Suzuki, K. Igawa, K. Morokuma, G. Konishi,	The K-Region in Pyrenes as a Key Position to Activate Aggregation-Induced Emission: Effects of Introducing Highly Twisted N,N-Dimethylamines	*J. Org. Chem.*	82, 6865-6873	2017
Akhilesh Kumar Sharma					
69	Akhilesh K. Sharma, W. M. C. Sameera, Masayoshi Jin, Laksmikanta Adak, Chiemi Okuzono, Takahiro Iwamoto, Masako Kato, Masaharu Nakamura, and Keiji Morokuma	DFT and AFIR Study on the Mechanism and the Origin of Enantioselectivity in Iron-Catalyzed Cross-Coupling Reactions	*J. Am. Chem. Soc.*	139(45), 16117-16125	2017
70	Miho Isegawa, Akhilesh K. Sharma, Seiji Ogo, and Keiji Morokuma	DFT Study on Fe(IV)-Peroxo Formation and H Atom Transfer Triggered O2 Activation by NiFe Complex	*Organometallics*	37(10), 1534-1545	2018
Maneeporn Puripat					
71	Tomoharu Oku, Masaki Okada, Maneeporn Puripat, Miho Hatanaka, Keiji Morokuma, and Jun-ChulChoi	Promotional effect of CH_3I on hydroxycarbonylation of cycloalkene using homogeneous rhodium catalysts with PPh_3 ligand	*J. Co2. Util.*	25, 1-5	2018
青野　信治					
72	Shinji Aono, Nakagaki Masayuki, and Shigeyoshi Sakaki	Theoretical Study of One-Electron-Oxidized Salen Complexes of Group 7 (Mn(III), Tc(III), and Re(III)) and Group 10 Metals (Ni(II), Pd(II), and Pt(II)) with 3D-RISM-GMC-QDPT Method: Localized vs. Delocalized Ground and Excited States in Solution	*Phys. Chem. Chem. Phys.*	19, 16831-16849	2017

№	Authors	Title	Journal	Volume (Number), first page to last page	year
中垣　雅之					
74	Takako Muraoka, Haruhiko Kimura, Gama Trigagema, Masayuki Nakagaki, Shigeyoshi Sakaki, and Keiji Ueno	Reactions of Silanone(silyl)tungsten and -molybdenum Complexes with MesCNO, $(Me_2SiO)_3$, MeOH, and H_2O: Experimental and Theoretical Studies	*Organometallics*	36, 1009-1018	2017
Jing Lu					
73	Jing Lu, Kazuya Ishimura, and Shigeyoshi Sakaki	Theoretical Insight into Core–Shell Preference for Bimetallic Pt-M (M = Ru, Rh, Os, and Ir) Cluster and Its Electronic Structure	*J. Phys. Chem. C*	122 (16), 9081-9090	2018
Rong-Lin Zhong					
75	M. Ramu Yadav, Masahiro Nagaoka, Myuto Kashihara, Rong-Lin Zhong, Takanori Miyazaki Shigeyoshi Sakaki, and Yoshiaki Nakao	The Suzuki–Miyaura Coupling of Nitroarenes	*J. Am. Chem. Soc.*	139(28), 9423-9426	2017
76	Feng-Wei Gao, Rong-Lin Zhong , Hong-Liang Xu, and Zhong-Min Su	Intra- and Intermolecular Charge Transfer in a Novel Dimer: Cooperatively Enhancing Second-Order Optical Nonlinearity	*J. Phys. Chem. C*	121(45), 25472-25478	2017
松岡　貴英					
77	Takahide Matsuoka, and Kazuo Takatsuka	Nonadiabatic electron wavepacket dynamics behind molecular autoionization	*J. Chem. Phys.*	148(1), 014106	2018
山本　憲太郎					
78	Kentaro Yamamoto and Kazuo Takatsuka	On the photocatalytic cycle of water splitting with small manganese oxides and the roles of water clusters as direct sources of oxygen molecules	*Phys. Chem. Chem. Phys.*	20(9), 6708-6725	2017
新崎　康樹					
79	Yasuki Arasaki and Kazuo Takatsuka	Time-resolved photoelectron signals from bifurcating electron wavepackets propagated across conical intersection path-branching dynamics	*Chem. Phys.*	493, 42-48	2017
松崎　黎					
80	Rei Matsuzaki, and Satoshi Yabushita	Calculation of photoionization differential cross sections using complex Gauss-type Orbitals	*J. Comput. Chem.*	38(23), 2030-2040	2017

２．共同研究者受入れ状況（平成 29 年度）

受入れ教員	共同研究者名	受入れ身分	受入れ期間	所属機関・職	研究内容
諸熊奎治 榊　茂好	REN, Xuefeng	招へい外国人学者	平成 28 年 6 月 18 日～ 平成 30 年 6 月 17 日	中国鉱山技術大学（中国）・准教授	光機能性分子の発行阻害機構の理論化学的研究
諸熊奎治 榊　茂好	畑中　美穂	共同研究者	平成 28 年 8 月 1 日～ 平成 29 年 7 月 31 日	奈良先端科学技術大学院大学（日本）・特任准教授	反応経路自動探索法を基盤とする化学反応の理論設計技術
榊　茂好	BAO, Xiaoguang	招へい外国人学者	平成 30 年 1 月 13 日～ 平成 30 年 3 月 3 日	蘇州大学（中国）・教授	均一触媒反応の反応機構に関する理論化学・計算化学研究

３．海外渡航一覧（平成 29 年度）

職　　名	氏　　名	期間（自）	期間（至）	目　的　地
研　究　員	田中　一義	2017/6/3	2017/6/11	アメリカ合衆国
特定研究員	多羅間 充輔	2017/6/13	2017/6/28	ドイツ、スペイン
特定研究員	多羅間 充輔	2017/7/12	2017/7/27	ドイツ、スロベニア
特定研究員	SCHNYDER, Simon Kaspar	2017/7/16	2017/7/28	スロベニア、ドイツ
特定研究員	薮中　俊介	2017/8/1	2017/9/20	フランス
特定助教	西本　佳央	2017/8/27	2017/9/2	ドイツ
特定研究員	伊丹　將人	2017/9/3	2017/9/10	ポーランド
研　究　員	高塚　和夫	2017/12/13	2017/12/19	インド
特定研究員	薮中　俊介	2018/1/1	2018/3/15	フランス
研　究　員	高塚　和夫	2018/1/29	2018/2/9	インド
特定研究員	山本 憲太郎	2018/2/17	2018/2/25	アメリカ合衆国
研　究　員	高塚　和夫	2018/3/9	2018/3/17	イスラエル

4．福井謙一記念研究センターシンポジウム　ポスター・プログラム

第15回

京都大学 福井謙一記念研究センターシンポジウム

開会式（Opening）

［開会の辞］田中 勝久（センター長）　10:00–10:05
［ご挨拶］北村 隆行（工学研究科長）　10:05–10:15

講演会（Lecture Session）

佐々 真一（京都大学 大学院理学研究科）　10:15–11:15
「気液転移と熱伝導が出会うとき：19世紀科学から21世紀科学への展開」

北浦 和夫（京都大学 福井謙一記念研究センター）　11:30–12:30
「The Group Molecular Orbital Method For Large Molecular Systems」

– 昼食 –　12:30–13:50

幾原 雄一（東京大学 大学院工学研究科）　13:50–14:50
「原子直視STEM法の新展開と材料科学への応用」

「福井謙一奨励賞」表彰式（Ceremony of Kenichi Fukui Encouragement Award）　15:00–15:30
ポスターセッション（Poster Session）　15:30–17:20
懇親会（Banquet）　17:30–19:00

平成30年2月2日㊎
会場：京都大学 福井謙一記念研究センター
2018.2.2　Fukui Institute for Fundamental Chemistry (FIFC), Kyoto University

京都大学福井謙一記念研究センター
〒606-8103　京都市左京区高野西開町34-4
お申し込みは下記ホームページをご参照ください
問合せ先：西本佳央／E-mail: sympo2017@fukui.kyoto-u.ac.jp
事務室／Tel: 075-711-7708　Fax: 075-781-4757
http://www.fukui.kyoto-u.ac.jp

第15回 京都大学 福井謙一記念研究センターシンポジウム

プログラム

日時　2018年2月2日（金）　10:00~19:00
場所　京都大学 福井謙一記念研究センター

開会式 (Opening)： 3階大会議室

[開会の辞]　田中 勝久（京都大学 福井謙一記念研究センター長）	10:00 – 10:05
[ご 挨 拶]　北村 隆行（京都大学 工学研究科長）	10:05 – 10:15

講演会 (Lecture Session) ： 3階大会議室

- 佐々 真一（京都大学 大学院理学研究科）　10:15 – 11:15
  「気液転移と熱伝導が出会うとき：１９世紀科学から２１世紀科学への展開」
  座長：古賀 毅（京大院工）

- 北浦 和夫（京都大学 福井謙一記念研究センター）　11:30 – 12:30
  「The Group Molecular Orbital Method For Large Molecular Systems」
  座長：永瀬 茂（福井センター）

— 昼食 —

- 幾原 雄一（東京大学 大学院工学系研究科）　13:50 – 14:50
  「原子直視 STEM 法の新展開と材料科学への応用」
  座長：田中 功（京大院工）

「福井謙一奨励賞」表彰式 (Ceremony of Kenichi Fukui Encouragement Award)： 3階大会議室　15:00 – 15:30

受賞者：**越智 正之**（大阪大学 大学院理学研究科）
「第一原理波動関数理論の固体への展開：量子化学と固体電子論の融合」

ポスターセッション (Poster Session) ： 3階大会議室　15:30 – 17:20

懇親会 (Banquet) ： 1階多目的ルーム　17:30 – 19:00

ポスターリスト (3 階大会議室 15:30～17:20)

- ✓ 番号が奇数の方は前半（15:30–16:25）、番号が偶数の方は後半（16:25–17:20）には、ポスターボードの前で発表するようにしてください。
- ✓ Authors with odd and even poster numbers should be present at the poster during the first half (15:30–16:25) and the second half (16:25–17:30) of the session, respectively.

1. **遷移金属錯体の内殻イオン化・内殻励起スペクトルに関する理論的研究**
   ○中谷 直輝（首都大院理工）

2. **Random matrix theory in proteogenesis**
   ○山中 雅則（日大理工）

3. **Stereoselective isomerization of eugenol to trans-isoeugenol catalyzed by Ni(0) phosphines: experimental and theoretical studies**
   (Chemistry Department, Faculty of Mathematics and Natural Sciences, Institut Teknologi Bandung[1], ITbM[2]) Yessi Permana[1], ○Arifin[2], Leo Saputra[1], Nunik Gustini[1], Stephan Irle[2], Aep Patah[1], and Muhamad A. Martoprawiro[1]

4. **高次三重項状態からの逆系間交差を利用した新規有機 EL 素子の設計指針**
   ○佐藤 徹[1,2]、林 里香[3]、春田 直毅[1]、夫 勇進[4,5]（京大院工[1]、京大 ESICB[2]、京大工[3]、山形大院理工[4]、JST さきがけ[5]）

5. **福井謙一生誕百年記念事業のご紹介とフロンティア軌道に関連した展示物の準備**
   ○西本 佳央（京大福井セ）

6. **Deformable swimmers in Poiseuille flow**
   ○Mitsusuke Tarama (FIFC)

7. **The difference between the heat-induced forces of the Soret effect and the adiabatic piston problem**
   ○Masato Itami[1] and Shin-ichi Sasa[2] (FIFC[1], Dept. of Phys. Kyoto Univ.[2])

8. **Cell Colony Growth**
   ○Simon K. Schnyder[1], John J. Molina[2], and Ryoichi Yamamoto[2] (FIFC[1], Grad. School of Eng., Kyoto Univ.[2])

9. **理論的観点から見た凝集誘起発光**

〇鈴木 聡、諸熊 奎治（京大福井セ）

10. **結晶・溶媒中における五配位四角錐型コバルトサレン錯体の混合原子価電子状態と吸収スペクトル**

〇青野 信治、中垣 雅之、榊 茂好（京大福井セ）

11. **Theoretical Study on the Mechanism of Phoshoranide-Trihydroborate Reaction with Methyl Iodide**

〇Akhilesh Kumar Sharma[1], Miho Isegawa[1,2], Keiji Morokuma[1], N. J. O'Brien[3], and Naokazu Kano[3] (FIFC[1], Kyushu Univ.[2], Univ. of Tokyo[3])

12. **The potential energy surfaces of emission decay of a type of platinum(II) cyclometalated complexes**

〇Xuefeng Ren and Keiji Morokuma (FIFC)

13. **ルイス塩基安定化シリレン分子を用いた Si-H 結合の可逆的酸化的付加/還元的脱離反応の機構解明と制御**

〇中垣 雅之[1]、Antoine Baceiredo[2]、加藤 剛[2]、榊 茂好[1]（京大福井セ[1]、トゥールーズ大ヘテロ化研[2]）

14. **Theoretical Understanding of Segregation Behavior and Electronic Structure of 55 and 147-atom PtTc and PtRe Nanoclusters**

〇Jing Lu[1], Kazuya Ishimura[2], and Shigeyoshi Sakaki[1] (FIFC[1], IMS[2])

15. **How to control Ar-NO_2 bond activation and Ar-NO_2 bond formation**

〇Rong-Lin Zhong[1], Masahiro Nagaoka[2], Myuto Kashihara[2], Yoshiaki Nakao[2], and Shigeyoshi Sakaki[1] (FIFC[1], Grad. School. of Eng. Kyoto Univ.[2])

16. **Theoretical Study on C_4-Hydrocarbon Adsorption and Separation by a Soft Porous Coordination Polymer**

〇 Jia-Jia Zheng[1,2], Shinpei Kusaka[2], Ryotaro Matsuda[2], Susumu Kitagawa[2], and Shigeyoshi Sakaki[1] (FIFC[1], KUIAS-iCeMS, Kyoto Univ.[2])

17. **Photocatalytic cycle of water splitting with small manganese oxides and water clusters as source of oxygen molecules**

〇Kentaro Yamamoto and Kazuo Takatsuka (FIFC)

18. Flux analysis on nonadiabatic chemical dynamics

○Rei Matsuzaki and Kazuo Takatsuka (FIFC)

19. CaO-SiO2 融液におけるソレー効果解明への分子動力学計算によるアプローチ

○清水 雅弘、下間 靖彦、三浦 清貴（京大院工）

20. メチル化ポリロタキサン水溶液の熱誘起ゲル化に関する理論的研究

○小島 広之、古賀 毅（京大院工）

21. 円盤状粒子/高分子混合ネットワークの構造と力学物性に関する分子シミュレーション

○古谷 勉、古賀 毅（京大院工）

22. 会合性高分子のゲル化の分子シミュレーション：分子内会合と分子間会合の競合

○柴田 基樹、古谷 勉、古賀 毅（京大院工）

23. D-B-A 型分子の電子カップリングに対する架橋部分の影響の評価

○由本 美香[1]、中農 浩史[2,3]、佐藤 啓文[2,3]（京大工[1]、京大院工[2]、京大 ESICB[3]）

24. 電極－電解液界面における酸化還元反応を扱うための新規方法論開発

○松三 勇介[1]、中農 浩史[1,2]、佐藤 啓文[1,2]（京大院工[1]、京大 ESICB[2]）

25. 分子センシングに向けた酸化インジウムスズと金粒子アレイにおける表面増強赤外吸収

○鎌倉 涼介[1]、村井 俊介[1,2]、藤田 晃司[1]、田中 勝久[1]（京大院工[1]、JST さきがけ[2]）

26. 層状ペロブスカイト酸化物における間接型強誘電性

○吉田 傑[1]、藤田 晃司[1]、赤松 寛文[2]、Olivier Hernandez[3]、Arnab Sen Gupta[4]、Alexandra S. Gibbs[5]、辻 涼介[1]、Venkatraman Gopalan[4]、田中 勝久[1]（京大院工[1]、九大院工[2]、レンヌ第一大[3]、ペンシルバニア州立大[4]、ラザフォード・アップルトン研[5]）

27. Theoretical Study on Substrate and Inhibitor of HIV-1 protease

○Masahiko Taguchi, Masahiro Kaneso, and Shigehiko Hayashi (Grad. Sch. of Sci. Kyoto Univ.)

28. 光誘起チャネルロドプシンに関する理論研究

○成 せい[1]、神谷 基司[1]、吉田 紀生[2]、林 重彦[1]（京大院理[1]、九大院理[2]）

29. アルキルπピレン液体発光特性の理論的研究

○山本 裕生[1]、中西 尚志[2]、林 重彦[1]（京大院理[1]、NIMS[2]）

30. **コアシェル型混合金属微粒子 $Cu_{32}Ru_6$ による NO-CO 反応の理論研究～Cu_{38} との比較**
○高木 望[1]、石村 和也[2]、福田 良一[1]、江原 正博[1,2]、榊 茂好[1,3]（京大 ESICB[1]、分子研[2]、京大福井セ[3]）

31. **遷移金属担体の埋め込みクラスターモデルの構築**
○松井 正冬[1]、榊 茂好[1,2]（京大 ESICB[1]、京大福井セ[2]）

32. **溶媒和自由エネルギーの新しい表式とタンパク質の構造安定性への適用**
○丸山 豊[1]、光武 亜代理[2]（理研 AICS[1]、慶應大理工[2]）

33. **Optimizing conical intersections by particle-particle random phase and Tamm-Dancoff approximations**
○嶺澤 範行（理研 AICS）

34. **シクロオクタテトラエンを導入した一次元共役縮環系の構造と電子状態の理論研究**
○西垣 佑亮、高椋 章太、山根 将暉、當波 孝凱、岸 亮平、中野 雅由（阪大院基礎工）

35. **ペンタセン二量体における三次非線形光学特性のスピン状態及び分子配向依存性についての理論研究**
○當波 孝凱、永海 貴識、山根 正暉、岸 亮平、中野 雅由（阪大院基礎工）

36. **Push-pull-biphenyl (PPB) の開殻性及び電荷移動性のねじれ角依存性に関する理論研究**
○北野 奨実[1]、山根 正暉[1]、當波 孝凱[1]、岸 亮平[1]、平尾 泰一[2]、久保 孝史[2]、中野 雅由[1]（阪大院基礎工[1]、阪大院理[2]）

37. **スマネン縮合アセンのシングレットフィッションについての理論研究**
○渡邊 健一郎[1]、永海 貴識[1]、當波 孝凱[1]、伊藤 聡一[2]、中野 雅由[1]（阪大院基礎工[1]、分子研[2]）

38. **螺旋骨格を有する開殻分子の非線形光学物性および分子アクチュエーター機能**
○高椋 章太、中野 雅由（阪大院基礎工）

39. **Pyridinium *N*-phenoxide betaine とその誘導体の開殻性と非線形光学特性の理論研究**
○渡部 晃希[1]、北野 奨実[1]、山根 正暉[1]、當波 孝凱[1]、清水 章弘[1]、吉田 潤一[2]、岸 亮平[1]、中野 雅由[1]（阪大院基礎工[1]、京大院工[2]）

40. テリレンのシングレットフィッションにおける分子間相互作用に関する理論研究

○永海 貴識[1]、伊藤 聡一[2]、久保 孝史[3]、中野 雅由[1,4]（阪大院基礎工[1]、分子研[2]、阪大院理[3]、阪大 CSRN[4]）

41. Mn(III)ダイマー錯体の分子内磁気的相互作用に関する理論研究

○北河 康隆[1]、加知 千裕[2]、宮坂 等[3]、中野 雅由[1]（阪大院基礎工[1]、東邦大理[2]、東北大金研[3]）

42. ナノベルト系の一重項開殻性と第二超分極率の理論研究

○山根 正暉、岸 亮平、中野 雅由（阪大院基礎工）

43. Ab initio free-energy calculations on reactions of carbon dioxide with aqueous amine compounds

○Yoshiyuki Kubota[1] and Tomáš Bučko[2,3] (Kansai Electric Power Co.[1], Comenius Univ. Bratislava[2], Slovak Acad. Sci.[3])

44. 不斉希土類 *N,N'*－ジオキシド誘導体を触媒とするマイケル付加反応の立体選択性発現機構の解明

○宮崎 文[1]、畑中 美穂[1,2,3]（奈良先端大物質創成[1]、奈良先端大研究推進・データセンター[2]、JST さきがけ[3]）

45. 不斉トリアゾリウム塩を触媒とする開環アルキル化における立体選択性発現機構の解明

○鎌田 安奈[1]、畑中 美穂[1,2,3]（奈良先端大物質創成[1]、奈良先端大研究推進・データセンター[2]、JST さきがけ[3]）

46. Theoretical study on palladium(0)-catalyzed intramolecular cyclization: formation of δ-lactam

○Takayoshi Yoshimura[1], Yohei Ogiwara[2], Norio Sakai[2], and Miho Hatanaka[1,3] (NAIST[1], Tokyo Univ. of Science[2], JST Presto[3])

47. 2Fe–2S ferredoxin 活性中心の電子状態と水素結合に関する理論研究

○江良 伊織、名取 圭紀、寺本 玲奈、青木 笙悟、多田 隼人、北河 康隆、中野 雅由（阪大基礎工）

48. クロムおよびモリブデン二核錯体の単分子電気伝導性に関する理論研究

○多田 隼人、名取 圭紀、寺本 玲奈、青木 笙悟、江良 伊織、北河 康隆、中野 雅由（阪大基礎工）

49. ビス（ジピリナト）錯体における中心金属イオン種がフロンティア軌道に与える影響についての理論研究

○青木 笙悟、名取 圭紀、北河 康隆、中野 雅由（阪大基礎工）

５．福井センターセミナー　ポスター・プログラム

第15回
福井センターセミナー
The 15th Fukui Center Seminar

2017年5月25日(木) 15:00–17:20

京都大学福井謙一記念研究センター1F 多目的室　(Room: 1F 106)
http://www.fukui.kyoto-u.ac.jp/
〒606-8103　京都市左京区高野西開町34-4（℡075-711-7708)
(at FIFC, Kyoto Univ. on May, 25 (Thur.), 2017)

15:00–15:40　Yoshio Nishimoto (FIFC)

“Analytic Derivatives with Fractional Occupation Number”

15:40–16:20　Mitsusuke Tarama (FIFC)

“Nonlinear Dynamics of Active Deformable Particles: From Liquid Droplets to Biological Cells”

Break (10 min.)

16:30–17:20　Dmitri G. Fedorov (AIST)

“Large Scale Quantum-Mechanical Calculations with the Fragment Molecular Orbital Method”

多数の方のご来場を歓迎いたします
We welcome all of you to join.

京都大学福井謙一記念研究センター　年報　2017

2019 年 2 月発行

発行人　田 中 勝 久

編　者　田 中 勝 久

発行所　京都大学福井謙一記念研究センター
（京都市左京区高野西開町 34-4）

印刷所　株式会社 エヌジーピー
（京都市右京区太秦森ヶ東町 21-10）